Development of Local Correlation Methods for the Calculation of Molecular Magnetic Properties

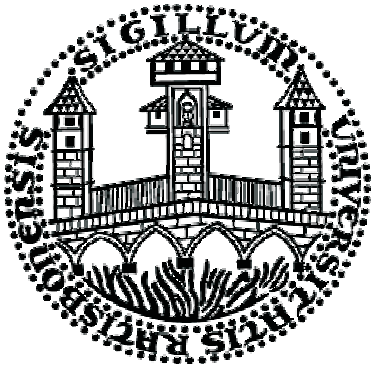

Dissertation

zur Erlangung des Doktorgrades der Naturwissenschaften (Dr. rer. nat.)
der Fakultät
- Chemie und Pharmazie -
der Universität Regensburg

vorgelegt von

Stefan Loibl

aus Niederwinkling

im Jahr 2014

Promotionsgesuch eingereicht am:	20.03.2014
Tag des Kolloquiums:	09.05.2014
Diese Arbeit wurde angeleitet von:	Prof. Dr. Martin Schütz

Prüfungsausschuss	
Vorsitzender:	Prof. Dr. Manfred Scheer
Erstgutachter:	Prof. Dr. Martin Schütz
Zweitgutachter:	Prof. Dr. Alexander Auer
Drittprüfer:	Prof. Dr. Bernhard Dick

Für meine Eltern

Die Ergebnisse dieser Arbeit sind bereits veröffentlicht worden:

Kapitel 3

Stefan Loibl and Martin Schütz

"NMR shielding tensors for density fitted local second-order Møller-Plesset perturbation theory using gauge including atomic orbitals"

The Journal of Chemical Physics

137, 084107 (2012), doi: 10.1063/1.4744102

Kapitel 4 und 5

Stefan Loibl and Martin Schütz

"Magnetizability and rotational *g* tensors for density fitted local second-order Møller-Plesset perturbation theory using gauge-including atomic orbitals"

The Journal of Chemical Physics

141, 024108 (2014), doi: 10.1063/1.4884959

Danksagung

An dieser Stelle möchte ich mich bei allen bedanken, die zum Entstehen dieser Arbeit beigetragen haben:

Prof. Dr. Martin Schütz für die Möglichkeit, dieses interessante und anspruchsvolle Thema zu bearbeiten, und seine stete Förderung meiner wissenschaftlichen Arbeit,

Prof. Dr. Alexander Auer für seine Bereitschaft die Rolle des Zweitgutachters zu übernehmen,

Dr. Denis Usvyat für seine stete Hilfsbereitschaft, wissenschaftliche Probleme und Unklarheiten zu diskutieren,

Klaus Ziereis für seine prompte und unkomplizierte Hilfe in technischen Dingen,

Katrin Ledermüller und *Gero Wälz* für viele angenehme Stunden im gemeinsamen Büro und in der Freizeit,

meinen Kollegen *Thomas Merz*, *Oliver Masur*, *Matthias Hinreiner*, *David David* und *Martin Christlmaier* sowie ehemals *Dr. Marco Lorenz* für viele nette und anregende Gespräche.

Ganz besonders bedanken möchte ich mich bei meinen Eltern *Maria* und *Karl*, die mir mein Studium und die anschließende Promotion ermöglicht haben und bei meiner Frau *Elisabeth* für Ihre stets liebevolle Unterstützung und Motivation.

Publications and Presentations

Publications

S. Loibl and M. Schütz
"Magnetizability and rotational g tensors for density fitted local second-order Møller-Plesset perturbation theory using gauge-including atomic orbitals"
The Journal of Chemical Physics, **141**, 024108 (2014), doi: 10.1063/1.4884959

S. Loibl and M. Schütz
"NMR shielding tensors for density fitted local second-order Møller-Plesset perturbation theory using gauge including atomic orbitals."
The Journal of Chemical Physics, **137**, 084107 (2012), doi: 10.1063/1.4744102

S. Loibl, F.R. Manby, and M. Schütz
"Density fitted, local Hartree-Fock treatment of NMR chemical shifts using London atomic orbitals"
Molecular Physics, **108**, 477 (2010), doi: 10.1080/00268970903580133

D. Kats, D. Usvyat, **S. Loibl**, T. Merz, M. Schütz "Comment on 'Minimax approximation for the decomposition of energy denominators in Laplace-transformed Møller-Plesset perturbation theories' "
The Journal of Chemical Physics, **130**, 127101 (2009), doi: 10.1063/1.3092982

Poster Presentations

S. Loibl and M. Schütz
"Efficient Chemical Shieldings at the Level of Density Fitted Local MP2"
48th Symposium on Theoretical Chemistry, Karlsruhe, 09/2012

S. Loibl and M. Schütz
"Accurate Chemical Shieldings for Large Molecules: the GIAO-DF-LMP2 Method"
47th Symposium on Theoretical Chemistry, Münster, 09/2011

S. Loibl, F.R. Manby, and M. Schütz
"Chemical Shieldings at the Level of GIAO-DF-HF"
First Principles Quantum Chemistry, an international conference in honour of Hans-Joachim Werner's 60th birthday, Bad Herrenalb, 04/2010

Table of Contents

1 OUTLINE **4**

2 BACKGROUND **7**

2.1 Molecular Electronic Hamiltonian 7
2.2 The Gauge Origin Problem 10
2.3 Local Approximation 15
2.4 Density Fitting Approximation 17
2.5 Lagrangian Techniques for Second Derivatives 19
2.6 Notation 23

3 THE DF-LMP2 SHIELDING TENSOR **26**

3.1 Introduction 27
3.2 NMR Shielding Tensor Theory 29
3.3 Unperturbed LMP2 Density Matrix 31
3.3.1 LMP2 Lagrangian and Hylleraas functional 31
3.3.2 Z-vector equations 34
3.4 Perturbed Density Matrix 37
3.4.1 Perturbed MO coefficients 37
3.4.2 Perturbed LMP2 density matrix 40
3.4.3 Perturbed Z-vector equations 41
3.5 Detailed Working Equations 41
3.5.1 Unperturbed Z-CPL equations 42
3.5.2 Perturbed Z-CPL equations 43
3.5.3 Perturbed Z-CPHF equations 44
3.5.4 Working equations in PAO basis 48

3.6 Accuracy and Performance 52
3.7 Conclusions 64

4 MAGNETIZABILITY TENSORS 65
4.1 Introduction 65
4.2 Magnetizabilities at the Level of DF-HF 69
4.2.1 Variation of orbitals by a perturbation 69
4.2.2 Formal expressions for the HF magnetizability tensors 70
4.2.3 Density fitting for HF magnetizabilities 72
4.2.4 Accuracy of the density fitting approximation 76
4.3 Magnetizabilities at the Level of DF-LMP2 80
4.3.1 LMP2 gradient with respect to the magnetic field . . 82
4.3.2 Generalized energy weighted density matrix 86
4.3.3 Second derivative of the LMP2 Lagrangian 89
4.3.4 Density fitting for LMP2 magnetizabilities 94
4.3.5 Frozen-core approximation 99
4.4 Accuracy and Performance 103
4.4.1 Method error of LMP2 magnetizabilities 103
4.4.2 Local approximation 104
4.4.3 Density fitting approximation 110
4.4.4 Performance of the program 111
4.5 Required GIAO Integrals 114
4.5.1 Derivatives of two-index integrals 114
4.5.2 The Gaussian Product Theorem 120
4.5.3 Derivatives of three-index integrals 122
4.6 Conclusions 123

5 ROTATIONAL *G* TENSORS 125
5.1 Introduction 125
5.2 Connection to Magnetizability Tensors 126

5.3 Accuracy and Performance 132
5.3.1 Local approximation 132
5.3.2 Method errors of HF and LMP2 rotational g tensors . 136
5.3.3 Density fitting approximation 137
5.3.4 Additional computational cost 139
5.4 Conclusions 139

6 SUMMARY **141**

A SUPPLEMENTARY DATA FOR CHAPTER 4 **144**

B SUPPLEMENTARY DATA FOR CHAPTER 5 **149**

C GLOSSARY **156**

BIBLIOGRAPHY **157**

Chapter 1

OUTLINE

Magnetic resonance techniques play a key role in the experimental understanding of matter in modern material sciences, physics and chemistry. By virtue of nuclear magnetic resonance (NMR) spectroscopy detailed structural informations of molecules [1], solid state [2], and even biomolecules [3] can be obtained. Electron paramagnetic resonance (EPR) spectroscopy allows for the investigation of molecules with unpaired electrons such as radicals or molecules in triplet states [4].
However, the detailed analysis of experimental NMR spectral data for complex molecular systems is often very complicated and can greatly benefit from theoretical calculations. These can provide insight into NMR chemical shift data of all active nuclei in a molecule and put proposed intermediates and structures to a test. Furthermore, experimental data can be verified by calculations [5].
Over the last decades molecular electronic structure theory has developed a number of methods to accurately calculate energies and molecular properties like excitation energies [6], dipole moments, or vibrational frequencies [7–9] even for large molecules [10–22]. The calculation of molecular magnetic properties, especially NMR shielding tensors, has long been hampered by the high computational cost and the gauge origin problem which arises from the incompleteness of the basis in which the wave function is

expanded. This makes the results dependent on the choice of an arbitrary gauge origin and slows down the convergence of the results to the basis set limit [5]. This problem has widely been solved by using explicitly field-dependent basis functions (gauge-including atomic orbitals, abbreviated GIAOs or also London atomic orbitals) which were put forward by F. London in the context of magnetizabilities in 1937 [23].

The unfavorably high scaling behavior of wave function based methods for the calculation of molecular magnetic properties is more involved. Numerous electron correlation methods have been proposed and implemented (one should especially note the role of J. Gauss) [24–32], yet, all of them are restricted to small or tiny molecules. Based on preliminary results by J. Gauss and H.-J. Werner [33] the first efficient implementation of NMR shielding tensors at the level of local second-order Møller-Plesset perturbation theory (LMP2), which is the simplest electron correlation method [10, 15, 34], has been developed [35] and is presented in this thesis. The new method employs GIAOs as atomic orbital (AO) basis functions and is combined with the density fitting (DF) approximation [36–41] to further improve the efficiency of the program.

Molecular magnetizabilities connect by definition the induced magnetic moment in a molecule and the applied magnetic flux density $\mathbf{B}$ and describe the energy correction due to the interaction of the induced magnetic moment with the external field [42, 43]. Magnetizability tensors can be calculated by generalizing the program for NMR shielding tensors. Hence, as a second step in this work the existing GIAO-DF-LMP2 program for NMR shielding tensors was extended so that it can also calculate magnetizabilities. However, magnetizabilities are not easily accessible through experiments and often only solid state or liquid phase data is available which complicates the comparison with calculated (gas-phase) data [44, 45].

In contrast, rotational g tensors can be measured with high accuracy by molecular beam [46] and microwave spectroscopy [47]. They describe the shift of the rotational energy levels through the (Zeeman) interaction of

the external magnetic field with the magnetic moment caused by the rotation of the molecule. Rotational g tensors and the paramagnetic part of magnetizabilities are closely related [47, 48] and thus GIAO-DF-LMP2 magnetizability tensors can be used to calculate rotational g tensors.
In this work the first efficient implementations of NMR shielding tensors, magnetizability tensors, and rotational g tensors at the level of density fitted local second-order Møller-Plesset perturbation theory is presented which employs gauge-including atomic orbitals as AO basis functions. The program was implemented in the framework of the `MOLPRO` quantum chemistry package [49, 50]. The accuracy of the method is demonstrated by test calculations on small and medium-sized molecules. Special attention is paid to the influence of the density fitting and local approximation. Furthermore, the efficiency of the program is shown by calculations on large molecular systems.
In the following Chapter 2 the most important principles and concepts are presented which are necessary to understand the calculation of magnetic properties in the framework of local correlation methods. Chapter 3 presents the formalism for NMR shielding tensors at the level of density fitted local second-order Møller-Plesset perturbation theory with gauge-including atomic orbitals (GIAO-DF-LMP2). Calculations show the accuracy of the results and the performance of the method. In Chapter 4 the formalism for the calculation of magnetizability tensors at the level of density fitted Hartree-Fock with gauge-including atomic orbitals (GIAO-DF-HF) and at the level of GIAO-DF-LMP2 is presented. Chapter 5 highlights the close connection between magnetizability tensors and rotational g tensors through rotational London atomic orbitals. In both chapters calculations show the influence of the fitting basis set and of the local approximation on the accuracy of the results. Investigations on larger systems demonstrate the efficiency of the program.

Chapter 2

BACKGROUND

The following sources were used for this chapter: the description of the molecular electronic Hamiltonian in the presence of an external magnetic field (Section 2.1) is based on and partly taken from the review by T. Helgaker, M. Jaszuński, and K. Ruud [51]. Section 2.2 about the gauge origin problem is based on the latter review [51] and is partly taken from my diploma thesis [52]. The basic concepts of local correlation methods (Section 2.3) and of the density fitting approximation (Section 2.4) are taken from my diploma thesis [52] and a talk by my supervisor at a conference in Mariapfarr [53] and slightly adapted. Furthermore, I'd like to acknowledge the work of Prof. Werner about Lagrangian techniques for gradients [54] which was used for Section 2.5. Section 2.6 which describes the notation is taken from the publication about GIAO-DF-LMP2 NMR shielding tensors [35]. For the sake of readability, these sources will not be cited individually again throughout the chapter.

2.1 Molecular Electronic Hamiltonian

The molecular electronic Hamiltonian in the presence of an external homogeneous magnetic field $\mathbf{B}$ and the magnetic moments $\mathbf{M}_K$ of the nuclei K

can be written as

$$H(\mathbf{B},\mathbf{M}) = \frac{1}{2}\sum_i \pi_i^2 - \sum_{iK}\frac{Z_K}{r_{iK}} + \frac{1}{2}\sum_{i\neq j} r_{ij}^{-1} + \frac{1}{2}\sum_{K\neq L}\frac{Z_K Z_L}{R_{KL}} - \sum_i \mathbf{m}_i \cdot \mathbf{B}^{\text{tot}}(\mathbf{r}_i) - \sum_K \mathbf{M}_K \cdot \mathbf{B}^{\text{tot}}(\mathbf{R}_K) + \sum_{K>L} (\mathbf{M}_K)^T \mathbf{D}_{KL}\mathbf{M}_L. \quad (2.1)$$

In Eq. (2.1) the charges of the nuclei, Z_K, the distance operators between two electrons i and j, r_{ij}, between electron i and nucleus K, r_{iK}, and between two nuclei K and L, R_{KL}, the position vector of nucleus K, $\mathbf{R}_K$, and the classic dipolar interactions $\mathbf{D}_{KL}$, which describe the direct couplings of the nuclear magnetic dipole moments, have been introduced. The permanent magnetic moment of electron i is connected to its spin $\mathbf{s}_i$,

$$\mathbf{m}_i = -g\mu_B \mathbf{s}_i \quad (2.2)$$

with the electron g factor and the Bohr magneton,

$$\mu_B = \frac{e\hbar}{2m_e c}, \quad (2.3)$$

which equals $\alpha/2$ in atomic units, where α is the fine structure constant. The kinetic momentum operator π_i,

$$\pi_i = -i\nabla_i + \frac{1}{c}\mathbf{A}^{\text{tot}}(\mathbf{r}_i), \quad (2.4)$$

does not only contain the generalized momentum operator, but also contributions from the total magnetic field vector potential, where $\mathbf{r}_i$ is the position vector of electron i. The vector potential $\mathbf{A}^{\text{tot}}$ is related to the magnetic field $\mathbf{B}^{\text{tot}}$ through

$$\mathbf{B}^{\text{tot}}(\mathbf{r}_i) = \nabla_i \times \mathbf{A}^{\text{tot}}(\mathbf{r}_i), \quad (2.5)$$

which fulfills the Maxwell equation,

$$\nabla_i \cdot \mathbf{B}^{\text{tot}}(\mathbf{r}_i) = 0, \quad (2.6)$$

by exploiting the mathematical relation for a vector potential $\vec{V}$,

$$\nabla \cdot \left(\nabla \times \vec{V} \right) = \mathrm{div} \left(\mathrm{rot}\, \vec{V} \right) = 0. \tag{2.7}$$

For molecules the magnetic vector potential $\mathbf{A}^{\mathrm{tot}}$ and the related magnetic field $\mathbf{B}^{\mathrm{tot}}$ have two contributions: one from the external magnetic field and a second one arising from the magnetic dipole moment of each nucleus

$$\mathbf{A}^{\mathrm{tot}}(\mathbf{r}_i) = \mathbf{A}_O(\mathbf{r}_i) + \sum_K \mathbf{A}_K(\mathbf{r}_i), \tag{2.8}$$

$$\mathbf{B}^{\mathrm{tot}}(\mathbf{r}_i) = \mathbf{B} + \sum_K \mathbf{B}_K(\mathbf{r}_i). \tag{2.9}$$

For a homogeneous external magnetic field the associated vector potential may be written as

$$\mathbf{A}_O(\mathbf{r}_i) = \frac{1}{2} \mathbf{B} \times (\mathbf{r}_i - \mathbf{R}_O). \tag{2.10}$$

The subscript O of the vector potential indicates the gauge origin, i.e., the position $\mathbf{R}_O$ at which it vanishes. The magnetic field $\mathbf{B}$ is independent of the choice of the gauge origin $\mathbf{R}_O$. With the exception of atoms there is no unique or natural choice for the gauge origin, which leads to the so-called gauge origin problem. The implications of this will be discussed in the next section.

The contribution from the nuclear magnetic dipole moments $\mathbf{M}_K$ can be written as

$$\mathbf{A}_K(\mathbf{r}_i) = \frac{\mathbf{M}_K \times \mathbf{r}_{iK}}{r_{iK}^3}, \tag{2.11}$$

where $\mathbf{r}_{iK}$ is the vector pointing from nucleus K to electron i. For this term there is a preferred gauge origin, the position of the nucleus. Therefore, the term causes no further problems in the following discussion of the gauge invariance.

In this thesis magnetic vector potentials are chosen to be divergence free,

$$\nabla \cdot \mathbf{A} = 0, \tag{2.12}$$

which corresponds to the so-called Coulomb gauge.

2.2 The Gauge Origin Problem

As mentioned in Section 2.1 the choice of the gauge origin for the magnetic vector potential $\mathbf{A}^{\text{tot}}$ and hence the molecular electronic Hamiltonian, Eq. (2.1), is not unique. Different choices of the gauge origin are connected by gauge origin transformations with a scalar function f,

$$\mathbf{A}_{O'}(\mathbf{r}) = \mathbf{A}_O(\mathbf{r}) - \mathbf{A}_O(\mathbf{R}_{O'}) = \mathbf{A}_O(\mathbf{r}) + \nabla f \tag{2.13}$$

with

$$f(\mathbf{r}) = -\mathbf{A}_O(\mathbf{R}_{O'}) \cdot \mathbf{r}. \tag{2.14}$$

Since there is a preferred gauge origin for the contributions from the nuclear magnetic dipole moments to the magnetic vector potential (as defined in Eq. 2.11) these terms do not cause any difficulties. For this reason they will be dropped in the following discussion.
Plugging the gauge transformed potential, as shown in Eq. (2.13), into the kinetic momentum operator Eq. (2.4) constitutes a unitary transformation,

$$\begin{aligned}\pi' &= -i\nabla + \frac{1}{c}\left[\mathbf{A}_O(\mathbf{r}) + \nabla f\right] \\ &= \exp\left(-\frac{i}{c}f\right)\left[-i\nabla + \frac{1}{c}\mathbf{A}_O(\mathbf{r})\right]\exp\left(\frac{i}{c}f\right) \\ &= \exp\left(-\frac{i}{c}f\right)\pi\exp\left(\frac{i}{c}f\right).\end{aligned} \tag{2.15}$$

This also induces a unitary transformation to the corresponding Hamilton operator,

$$\begin{aligned}H' = H(\mathbf{A}_{O'}) &= \frac{1}{2}\left[\exp\left(-\frac{i}{c}f\right)\pi\exp\left(\frac{i}{c}f\right)\right]^2 \\ &= \exp\left(-\frac{i}{c}f\right)H(\mathbf{A}_O)\exp\left(\frac{i}{c}f\right).\end{aligned} \tag{2.16}$$

Observables like the density or the energy must not be affected by gauge transformations, which is achieved by multiplying the wave function with a compensating phase factor,

$$\psi'(\mathbf{r}) = \exp\left(-\frac{i}{c}f\right)\psi(\mathbf{r}). \tag{2.17}$$

Gauge invariance of the energy is ensured,

$$\begin{aligned}\langle\psi'|H'|\psi'\rangle &= \left\langle\psi\left|\exp\left(\frac{i}{c}f\right)\exp\left(-\frac{i}{c}f\right)H\exp\left(\frac{i}{c}f\right)\exp\left(-\frac{i}{c}f\right)\right|\psi\right\rangle \\ &= \langle\psi|H|\psi\rangle\,, \end{aligned} \tag{2.18}$$

and the same state is still described by the gauge transformed wave function,

$$|\psi'(\mathbf{r})|^2 = \left[\exp\left(-\frac{i}{c}f\right)\psi\right]^*\left[\exp\left(-\frac{i}{c}f\right)\psi\right] = |\psi(\mathbf{r})|^2. \tag{2.19}$$

The scalar transformation function for the shift of the gauge origin from $\mathbf{R}_O$ to $\mathbf{R}_{O'}$ can be written as

$$f(\mathbf{r}) = \frac{1}{2}\mathbf{B}\times(\mathbf{R}_O - \mathbf{R}_{O'})\cdot\mathbf{r} = \mathbf{A}_{O'}(\mathbf{R}_O)\cdot\mathbf{r} \tag{2.20}$$

and the corresponding wave function as

$$\psi_{O'}(\mathbf{r}) = \exp\left(-\frac{i}{c}\mathbf{A}_{O'}(\mathbf{R}_O)\cdot\mathbf{r}\right)\psi_O(\mathbf{r})\,. \tag{2.21}$$

The gauge transformation relations above only hold for exact wave functions, for approximate wave functions gauge invariance cannot be assured. The finite space of basis functions from which the wave function is constructed might not be able to reproduce the gauge transformations correctly. Hence, calculations with finite wave functions will always depend on the choice of the gauge origin.

This has severe implications since the obtained results then depend on the choice of the gauge origin. In order to reproduce results the employed gauge origin has to be reported. The quality of the results might crucially depend on the choice of the gauge origin. Furthermore, it is not clear how to choose the gauge origin (except for atoms). In the case of atoms there is a preferred, or natural, gauge origin which is the atom itself.

This can be rationalized by the following consideration: in the absence of a perturbation a one-electron atomic system is described by the approximate wave function χ_{lm} which is centered on nucleus N; this wave function is an eigenfunction of the effective Hamiltonian H_0 of the one-electron atomic

system and the angular momentum operator relative to nucleus N along the z-axis, L_z^N,

$$H_0\chi_{lm} = E_0\chi_{lm}, \tag{2.22}$$

$$L_z^N\chi_{lm} = m_l\chi_{lm}. \tag{2.23}$$

If one now applies an external magnetic field $\mathbf{B}$ and chooses the gauge origin on nucleus N,

$$\mathbf{A}_N(\mathbf{r}) = \frac{1}{2}\mathbf{B}\times(\mathbf{r}-\mathbf{R}_N), \tag{2.24}$$

perturbational analysis shows that the unperturbed wave function χ_{lm} is correct to first order,

$$\left(H_0 + \frac{1}{2c}BL_Z^N + O\left(B^2\right)\right)\chi_{lm} = \left(E_0 + \frac{1}{2c}m_lB + O\left(B^2\right)\right)\chi_{lm}. \tag{2.25}$$

On the other hand, if one locates the gauge origin at some other randomly chosen place $\mathbf{R}_L$,

$$\mathbf{A}_L(\mathbf{r}) = \frac{1}{2}\mathbf{B}\times(\mathbf{r}-\mathbf{R}_L), \tag{2.26}$$

the unperturbed wave function is no eigenfunction of the angular momentum operator relative to L and thus only correct to zeroth order in the magnetic field,

$$\left(H_0 + \frac{1}{2c}BL_Z^L + O\left(B^2\right)\right)\chi_{lm} = \left(E_0 + O\left(B\right)\right)\chi_{lm}. \tag{2.27}$$

After identifying the center of atom N as preferred gauge origin one can ensure gauge origin independence by multiplying the unperturbed wave function with a phase factor which shifts the gauge origin from $\mathbf{R}_N$ to the global origin $\mathbf{R}_O$,

$$\omega_{lm}(\mathbf{A}_O) = \exp\left(-\frac{i}{c}\mathbf{A}_O\left(\mathbf{R}_N\right)\cdot\mathbf{r}\right)\chi_{lm}. \tag{2.28}$$

This is also valid for atoms with more than one electron. Furthermore, the energy expectation value is gauge origin independent,

$$E\left(\mathbf{B}\right) = \left\langle\omega_{lm}\left(\mathbf{A}_O\right)\left|H\left(\mathbf{A}_O\right)\right|\omega_{lm}\left(\mathbf{A}_O\right)\right\rangle. \tag{2.29}$$

The ansatz is gauge origin independent by construction and can easily be generalized to systems with more than one atom. For every atom in a molecule the natural gauge origin is the atom itself, however, it is not possible to locate the gauge origin at all atoms at once. This difficulty can be circumvented by multiplying each atomic orbital (AO) basis function χ centered at a specific atom M with a complex phase factor which shifts the gauge origin from the center of the atom, $\mathbf{R}_M$, to a global gauge origin,

$$\omega_\mu(\mathbf{r}_M, \mathbf{A}_O(\mathbf{R}_M)) = \exp\left(-\frac{i}{c}\mathbf{A}_O(\mathbf{R}_M)\cdot\mathbf{r}\right)\chi_\mu(\mathbf{r}_M). \tag{2.30}$$

These explicitly field-dependent AO basis functions are referred to as gauge-including atomic orbitals (GIAOs) or London atomic orbitals [23]. In the limit of zero magnetic field strength they reduce to ordinary Gaussian basis functions.

The IGLO (individual gauge for localized orbitals) approach [55, 56] uses local phase factors for the molecular orbitals (MOs) instead of AOs. Core orbitals and lone pairs have their gauge origin located at the corresponding nucleus, for valence orbitals the center of charge of the corresponding orbital is used. Clearly, this requires the localization of the orbitals prior to the calculation of the properties, as for delocalized orbitals no obvious gauge origin exists. In the local approach two-electron integrals can be approximated by completeness relations [57].

Woliński et al. pointed out that the IGLO approach has several disadvantages in comparison to the GIAO approach [58]:

- For the IGLO approach another approximation is introduced by the closure relation.
- The IGLO approach is more sensitive to the basis set quality.
- The IGLO approach has difficulties for systems with largely delocalized electrons.
- The IGLO approach cannot be generalized straightforwardly for correlated methods as it is possible for the GIAO approach.

Integrals of GIAOs are independent of the choice of the gauge origin. This can be easily shown for most integrals like the perturbed overlap or the derivative of the three-index integrals, e.g.,

$$\begin{aligned} S_{\mu\nu}^{B_\alpha} &= \frac{\partial}{\partial B_\alpha} \left\langle \omega_\mu(\mathbf{A}_O(\mathbf{R}_M)) | \omega_\nu(\mathbf{A}_O(\mathbf{R}_N)) \right\rangle \\ &= \frac{i}{2c} \left\langle \omega_\mu(\mathbf{A}_O(\mathbf{R}_M)) \left| ((\mathbf{R}_M - \mathbf{R}_O) \times \mathbf{r})_\alpha \right| \omega_\nu(\mathbf{A}_O(\mathbf{R}_N)) \right\rangle \\ &\quad - \frac{i}{2c} \left\langle \omega_\mu(\mathbf{A}_O(\mathbf{R}_M)) \left| ((\mathbf{R}_N - \mathbf{R}_O) \times \mathbf{r})_\alpha \right| \omega_\nu(\mathbf{A}_O(\mathbf{R}_N)) \right\rangle \\ &= \frac{i}{2c} \left\langle \mu \left| (\mathbf{R}_{MN} \times \mathbf{r})_\alpha \right| \nu \right\rangle . \end{aligned} \tag{2.31}$$

The vector $\mathbf{R}_{MN}$ is the difference between the vectors pointing from the origin to $\mathbf{R}_M$ and $\mathbf{R}_N$,

$$\mathbf{R}_{MN} = \mathbf{R}_M - \mathbf{R}_N. \tag{2.32}$$

However, it is not so obvious for integrals involving the kinetic term $\mathbf{T}$ of the one-electron core Hamiltonian [59],

$$\begin{aligned} T_{\mu\nu} &= \left\langle \omega_\mu(\mathbf{A}_O(\mathbf{R}_M)) \left| \frac{1}{2}\pi^2 \right| \omega_\nu(\mathbf{A}_O(\mathbf{R}_N)) \right\rangle \\ &= \left\langle \chi_\mu \left| \exp\left(\frac{i}{c}\mathbf{A}_O(\mathbf{R}_M) \cdot \mathbf{r}\right) \frac{1}{2} \left(-i\nabla + \frac{1}{c}\mathbf{A}^{\text{tot}}(\mathbf{r})\right)^2 \exp\left(-\frac{i}{c}\mathbf{A}_O(\mathbf{R}_N) \cdot \mathbf{r}\right) \right| \chi_\nu \right\rangle . \end{aligned} \tag{2.33}$$

In order to bring both exponential factors to the left of the differential operator ∇ the commutator

$$\begin{aligned} &\left[-i\nabla + \frac{1}{c}\mathbf{A}^{\text{tot}}(\mathbf{r}) \,; \exp\left(-\frac{i}{c}\mathbf{A}_O(\mathbf{R}_N) \cdot \mathbf{r}\right) \right] \\ &= -\frac{1}{c} \exp\left(-\frac{i}{c}\mathbf{A}_O(\mathbf{R}_N) \cdot \mathbf{r}\right) \mathbf{A}_O(\mathbf{R}_N) \end{aligned} \tag{2.34}$$

has to be applied twice. This yields

$$T_{\mu\nu} = \left\langle \chi_\mu \left| \exp\left(\frac{i}{c}\mathbf{A}_{MN} \cdot \mathbf{r}\right) \frac{1}{2} \left(-i\nabla + \frac{1}{c}\left[\mathbf{A}(\mathbf{r}) - \mathbf{A}_O(\mathbf{R}_N)\right]\right)^2 \right| \chi_\nu \right\rangle \tag{2.35}$$

with the potentials

$$\mathbf{A}_{MN} = \mathbf{A}_O(\mathbf{R}_M) - \mathbf{A}_O(\mathbf{R}_N) = \frac{1}{2}\mathbf{B} \times \mathbf{R}_{MN}, \tag{2.36}$$

$$\mathbf{A}(\mathbf{r}) - \mathbf{A}_O(\mathbf{R}_N) = \frac{1}{2}\mathbf{B} \times \mathbf{r}_N + \sum_K \frac{\mathbf{M}_K \times \mathbf{r}_K}{r_K^3}, \tag{2.37}$$

which are independent of the gauge origin $\mathbf{R}_O$.
The integral can then be rewritten as

$$T_{\mu\nu} = \left\langle \chi_\mu \left| \exp\left(\frac{i}{c}\mathbf{A}_{MN} \cdot \mathbf{r}\right) \frac{1}{2}\pi_N^2 \right| \chi_\nu \right\rangle \tag{2.38}$$

with the kinetic momentum operator π_N

$$\pi_N = -i\nabla + \frac{1}{c}\left(\frac{1}{2}\mathbf{B} \times \mathbf{r}_N + \sum_K \frac{\mathbf{M}_K \times \mathbf{r}_K}{r_K^3}\right). \tag{2.39}$$

The subscript N on the kinetic momentum operator indicates that the vector potential is calculated relative to nucleus N. This is particularly important for the first and second derivatives of the core Hamiltonian with respect to the magnetic field.

2.3 Local Approximation

Correlated electronic structure theory methods like coupled-cluster (CC) or second-order Møller-Plesset perturbation theory (MP2) show unfavorably high computational scaling behavior with the molecular system size. This is caused by the use of canonical orbitals which diagonalize the Fock matrix. However, canonical basis functions are delocalized over the whole molecule whereas the (dispersive) interaction between electrons is short-range and decays $\propto r^{-6}$ in non-metallic systems. In order to avoid that all orbitals have to be considered in a calculation, as it is inevitably the case for canonical orbitals, a local basis is introduced which helps exploit the fast decay behavior of dynamic electron correlation.
Local correlation methods make use of the short-range nature of the electron-electron interaction by spatial considerations to greatly reduce the number

of excited configuration state functions. Electron pairs with an interorbital distance beyond a certain threshold are neglected. Furthermore, excitations are restricted to orbital- or pair-specific subspaces of the virtual spaces (domains) [60].

There are several localization methods; the Pulay ansatz [61, 62] uses localized molecular orbitals (LMOs) for the occupied space. These are generated from canonical MOs which are obtained as a solution of a Hartree-Fock calculation:

$$|\phi_i^{loc}\rangle = \sum_{\bar{k}} |\phi_{\bar{k}}^{can}\rangle W_{\bar{k}i} \qquad \text{with} \qquad \mathbf{W}\mathbf{W}^\dagger = \mathbf{1}. \tag{2.40}$$

Different choices are possible for the unitary transformation matrix $\mathbf{W}$, the most widely used are Pipek-Mezey [63] and Boys [64, 65] localization. Pipek-Mezey maximizes the sum of the Mulliken atomic charges, i.e., it minimizes the net number of atoms on which the LMO is localized, whereas the Boys method maximizes the distance between orbital centroids [66]. In this work the Pipek-Mezey localization procedure is used.

The LMO coefficient matrix $\mathbf{L}$ can be represented as

$$\mathbf{L} = \bar{\mathbf{C}}_\mathbf{o}\mathbf{W}, \tag{2.41}$$

where $\bar{\mathbf{C}}_\mathbf{o}$ is the occupied part of the canonical MO coefficient matrix. The corresponding LMOs still form an orthogonal basis due to the unitary nature of the transformation matrix $\mathbf{W}$. The localization matrix is specified by

$$\mathbf{W} = \bar{\mathbf{C}}_\mathbf{o}^\dagger \mathbf{S}\mathbf{L}. \tag{2.42}$$

Instead of localizing the canonical virtual orbitals, which turns out to be difficult and to provide poor results for the diffuse virtual MOs, the AOs χ_μ are projected onto the virtual space [10] in the Pulay ansatz:

$$|\phi_r\rangle = \left(1 - \sum_{i=1}^{n_{occ}} |\phi_i\rangle\langle\phi_i|\right) |\chi_\mu\rangle|_{\mu=r} = P|\chi_\mu\rangle|_{\mu=r}. \tag{2.43}$$

The projected atomic orbitals (PAOs) coefficient matrix can be written as

$$P_{\mu r} = \left[\mathbf{C}_\mathbf{v}\mathbf{C}_\mathbf{v}^\dagger\mathbf{S}\right]_{\mu r} = [\mathbf{C}_\mathbf{v}\mathbf{Q}]_{\mu r} \tag{2.44}$$

with the transformation matrix

$$Q_{ar} = \left[\mathbf{C}_\mathbf{v}^\dagger \mathbf{S}\right]_{ar} \tag{2.45}$$

connecting virtual canonical and PAO orbitals; $\mathbf{C_v}$ is the coefficient matrix of the virtual canonical orbitals. The PAOs which are modified AOs turn out to be a natural and reasonable choice to describe the virtual space. They are still orthogonal to the LMOs but are no longer orthonormal with metric

$$\mathbf{S}^{\mathrm{PAO}} = \mathbf{P}^\dagger \mathbf{S} \mathbf{P} = \mathbf{Q}^\dagger \mathbf{Q}. \tag{2.46}$$

The PAOs span exactly the same space as the virtual orbitals but form a redundant basis.
In local MP2 for magnetic properties excitations can be restricted to subspaces of the PAO basis, so-called domains. Furthermore, the number of doubly excited amplitudes can be reduced by spatial considerations: electron pairs with an interorbital distance beyond 15 bohrs are neglected.

2.4 Density Fitting Approximation

The transformation of four-index two-electron integrals from the atomic orbital (AO) basis to the molecular orbital (MO) basis is an unfavorably expensive step:

$$(mn|pq) = \sum_{\mu\nu\rho\sigma} C^*_{\mu m} C_{\nu n} C^*_{\rho p} C_{\sigma q} (\mu\nu|\rho\sigma) \tag{2.47}$$

with the four-index electron repulsion integrals in chemists' notation

$$\begin{aligned}(mn|pq) &= \int d\mathbf{r}_1 \int d\mathbf{r}_2 \phi^*_m(\mathbf{r}_1)\phi_n(\mathbf{r}_1) r_{12}^{-1} \phi^*_p(\mathbf{r}_2)\phi_q(\mathbf{r}_2) \\ &= \int d\mathbf{r}_1 \int d\mathbf{r}_2 \rho_{mn}(\mathbf{r}_1) r_{12}^{-1} \rho_{pq}(\mathbf{r}_2).\end{aligned} \tag{2.48}$$

In order to reduce the computational effort the one-particle orbital product densities $\rho_{pq}(\mathbf{r}) = \phi^*_p(\mathbf{r})\phi_q(\mathbf{r})$ are replaced by approximate densities $\tilde{\rho}_{pq}(\mathbf{r})$

which are expanded in an auxiliary (fitting) basis $\Xi_P(\mathbf{r})$:

$$\rho_{pq}(\mathbf{r}) = \phi_p^*(\mathbf{r})\phi_q(\mathbf{r}) \approx \tilde{\rho}_{pq}(\mathbf{r}) = \sum_P c_{pq}^P \Xi_P(\mathbf{r}). \tag{2.49}$$

The required fitting coefficients c_{pq}^P are obtained by minimizing the error functional Δ_w,

$$\Delta_w = \int d\mathbf{r}_1 \int d\mathbf{r}_2 [\rho_{pq} - \tilde{\rho}_{pq}](\mathbf{r}_1) w_{12} [\rho_{pq} - \tilde{\rho}_{pq}](\mathbf{r}_2), \tag{2.50}$$

where w_{12} is an appropriate weight operator. Inserting the expansion of the approximate densities (2.49) into the error functional (2.50) yields

$$\Delta_w = (\rho_{pq}|w_{12}|\rho_{pq}) - 2\sum_P c_{pq}^P (P|w_{12}|\rho_{pq}) + \sum_{PQ} c_{pq}^P (P|w_{12}|Q) c_{pq}^Q. \tag{2.51}$$

Minimizing Δ_w with respect to c_{pq}^P determines the values of the fitting coefficients,

$$\frac{\partial \Delta_w}{\partial c_{pq}^P} = -2(P|w_{12}|\rho_{pq}) + 2\sum_Q (P|w_{12}|Q) c_{pq}^Q = 0. \tag{2.52}$$

If the weight operator is chosen as $w_{12} = r_{12}^{-1}$ the self repulsion of the residual $\rho_{pq} - \tilde{\rho}_{pq}$ is minimized. The fitting coefficients are then the solution of the linear equation system

$$\sum_Q (P|Q) c_{pq}^Q = (P|pq) \Rightarrow c_{pq}^Q = \sum_P (pq|P) J_{PQ}^{-1}, \tag{2.53}$$

where

$$J_{PQ} = (P|Q) = \int d\mathbf{r}_1 \int d\mathbf{r}_2 \Xi_P(\mathbf{r}_1) r_{12}^{-1} \Xi_Q(\mathbf{r}_2), \tag{2.54}$$

$$(P|pq) = \int d\mathbf{r}_1 \int d\mathbf{r}_2 \Xi_p(\mathbf{r}_1) r_{12}^{-1} \phi_p^*(\mathbf{r}_2) \phi_q(\mathbf{r}_2). \tag{2.55}$$

It can be ensured that the error introduced by the DF approximation for the integral $(mn|pq)$ is second order with respect to the fitting coefficients by using Dunlap's robust formula [67]:

$$(mn|pq) = (\rho_{mn}|\rho_{pq}) = (\rho_{mn}|\tilde{\rho}_{pq}) + (\tilde{\rho}_{mn}|\rho_{pq}) - (\tilde{\rho}_{mn}|\tilde{\rho}_{pq}). \tag{2.56}$$

If the same fitting basis is used for all product densities and the fitting coefficients are given by Eq. (2.53) all three terms in the robust formula, Eq. (2.56), are identical. It simplifies to

$$(mn|pq) = \sum_{PQ} (mn|P) J^{-1}_{PQ} (Q|pq). \tag{2.57}$$

The transformation from AO to MO basis in the conventional formalism (see Eq. 2.47) is a four-index step which scales $O(N^5)$. In comparison, the transformation of the three-index electron repulsion integrals (ERIs) is a two-index transformation step which scales $O(N^4)$,

$$(Q|pq) = \sum_{\mu\nu} C^*_{\mu p} C_{\nu q} (Q|\mu\nu). \tag{2.58}$$

The assembly step in Eq. (2.57) still scales $O(N^5)$ but with a significantly lower prefactor than the conventional transformation. In practical calculations the scaling behavior can be drastically improved by using localized orbitals in combination with prescreening techniques.

As outlined for GIAO-DF-HF [68] ordinary Gaussians are used as fitting functions (FFs) for the calculation of magnetic properties because GIAOs as FFs would inevitably violate gauge origin independence. Since for a given FF there is naturally no complex conjugate corresponding to the same electron the origin dependence (on $\mathbf{R}_O$) would not cancel in the three-index ERIs. An alternative natural choice are ordinary Gaussian basis functions, implying that the GIAO orbital product densities are fitted at zero field strength, i.e., at $\mathbf{B} = 0$. In the present implementation no local restrictions to the fitting basis (fit domains [14, 15]) have been introduced.

2.5 Lagrangian Techniques for Second Derivatives

NMR shielding tensors, magnetizability tensors, and rotational g tensors can be calculated as second derivatives of the energy. Formal expressions

for their calculation can be obtained by differentiating the energy in the presence of a perturbation twice and subsequently considering the obtained expressions in the limit of zero perturbation strength. This means the derivatives with respect to a perturbation q are taken at a reference point $q = 0$, for which the (unperturbed) wave function with its parameters was optimized. For the sake of simplicity the subscript $q = 0$ will be omitted in the rest of this section. The perturbation q, for which the first derivative of the energy will be considered, is the nuclear magnetic dipole moment for NMR shielding tensors, the external magnetic field for magnetizabilities and the total rotational angular momentum for rotational g tensors.

In general, the energy is not variational with respect to all wave function parameters: e.g., the MP2 wave function is not variational with respect to the molecular orbital coefficients. For variational wave functions there is a $(2n+1)$ rule [66], i.e., for the derivative of order $(2n+1)$ the wave function parameters of order n are required. However, for non-variational wave functions the derivative of order n requires the wave function parameters of order n. In order to account for this difficulty it is advantageous to set up a Lagrangian which has the same energy as the non-variational wave function but is variational with respect to all wave function parameters. For this Lagrangian the $(2n+1)$ rule is again valid.

One can formulate the derivatives in a symmetric way so that an even stricter $(2n+2)$ rule is valid for the Lagrange multipliers. However, this would require the calculation of the responses of both perturbations for second derivatives [69] which is disadvantageous for NMR shielding tensors. Hence, this scheme is not applied in this work.

In a general notation all variational parameters of the wave function are collected in a vector $\mathbf{t}$ and all non-variational parameters in a vector $\mathbf{c}$, i.e.,

$$\frac{\partial E(\mathbf{t}, \mathbf{c})}{\partial t_i} = 0, \tag{2.59}$$

$$\frac{\partial E(\mathbf{t}, \mathbf{c})}{\partial c_i} := y_i \neq 0. \tag{2.60}$$

The Lagrangian can be constructed from the energy by adding the (vector of the n) stationary conditions $\mathbf{g}$ of the non-variational wave function parameters $\mathbf{c}$,

$$\mathcal{L} = E(\mathbf{t}, \mathbf{c}) + \sum_k z_k g_k(\mathbf{c}) \tag{2.61}$$

with the Lagrange multipliers $\mathbf{z}$ and

$$\mathbf{g}(\mathbf{c}) = 0. \tag{2.62}$$

The stationary conditions must be fulfilled for any value of the perturbation q, hence,

$$\left(\frac{\partial g_i(\mathbf{c})}{\partial q}\right) = g_i^q(\mathbf{c}) = 0, \tag{2.63}$$

which can be split into different contributions,

$$g_i^q(\mathbf{c}) = g_i^{(q)}(\mathbf{c}) + \left[\sum_k \frac{\partial g_i(\mathbf{c})}{\partial c_k} c_k^q\right]. \tag{2.64}$$

The superscript (q) with the first term on the right-hand side of Eq. (2.64) indicates that this quantity has been evaluated with perturbed AO integrals which depend explicitly on the perturbation, e.g., the derivatives of the integrals or explicitly field-dependent basis functions (such as GIAOs), and are independent of the response of the non-variational wave function parameters, $\mathbf{c}^q$ (see, e.g., Eq. 2.78). The second term on the right-hand side of Eq. (2.64) contains all the contributions which arise from derivatives of the non-variational wave function parameters.

Since the Lagrangian has to be stationary with respect to $\mathbf{t}$, $\mathbf{c}$, and $\mathbf{z}$, differentiation yields the stationary conditions,

$$\frac{\partial \mathcal{L}}{\partial t_i} = 0, \tag{2.65}$$

$$\frac{\partial \mathcal{L}}{\partial z_i} = g_i(\mathbf{c}) = 0, \tag{2.66}$$

$$\frac{\partial \mathcal{L}}{\partial c_i} = y_i + \sum_k z_k \left(\frac{\partial g_k(\mathbf{c})}{\partial c_i}\right) = 0. \tag{2.67}$$

Equations (2.65) and (2.66) are the stationary conditions of the wave functions parameters **t** and **c**, whereas Eq. (2.67) determines the Lagrange multipliers and is called the Z-vector equation.
If the above Eqs. (2.65)–(2.67) are fulfilled the Lagrangian is variational with respect to all wave function parameters. Then the gradient of the energy with respect to a perturbation q can be written as

$$\begin{aligned} E^q = \mathcal{L}^q &= \mathcal{L}^{(q)} + \sum_l \left(\frac{\partial \mathcal{L}}{\partial t_l} t_l^q + \frac{\partial \mathcal{L}}{\partial c_l} c_l^q + \frac{\partial \mathcal{L}}{\partial z_l} z_l^q \right) \\ &= \mathcal{L}^{(q)} = E^{(q)} + \sum_k z_k g_k^{(q)}(\mathbf{c}), \end{aligned} \tag{2.68}$$

where only derivative integrals and derivatives of AO basis functions contribute. The responses of the wave functions parameters, e.g., perturbed MO coefficients or perturbed amplitudes, are not required for the calculation of the gradient.
Differentiating the gradient for perturbation q, Eq. (2.68), with respect to another perturbation r (at the expansion point $r = 0$) yields

$$\begin{aligned} E^{q,r} = \mathcal{L}^{q,r} &= \mathcal{L}^{(q,r)} + \sum_l \left(\frac{\partial \mathcal{L}^{(q)}}{\partial t_l} t_l^r + \frac{\partial \mathcal{L}^{(q)}}{\partial c_l} c_l^r + \frac{\partial \mathcal{L}^{(q)}}{\partial z_l} z_l^r \right) \\ &= E^{(q,r)} + \sum_k z_k g_k^{(q,r)}(\mathbf{c}) \\ &\quad + \sum_l \frac{\partial E^{(q)}}{\partial t_l} t_l^r + \sum_l \left[\frac{\partial E^{(q)}}{\partial c_l} + \sum_k z_k \frac{\partial g_k^{(q)}(\mathbf{c})}{\partial c_l} \right] c_l^r \\ &\quad + \sum_l g_l^{(q)}(\mathbf{c}) z_l^r. \end{aligned} \tag{2.69}$$

For the properties presented in this work the second perturbation r is the external magnetic field. As one can see from Eq. (2.69) the calculation of the derivative (or response) of the wave function parameters and of the Lagrange multipliers can no longer be avoided for second derivatives (in contrast to the gradient). The equations which determine the response quantities are obtained by differentiating the stationary conditions Eqs. (2.65)–(2.67) with respect to the perturbation r. The stationary

conditions have to be fulfilled for any value of the perturbation r. Hence, the derivative with respect to the perturbation has to be zero,

$$\frac{\partial}{\partial r}\frac{\partial \mathcal{L}}{\partial t_i} = 0, \tag{2.70}$$

$$\frac{\partial}{\partial r}\frac{\partial \mathcal{L}}{\partial c_i} = 0, \tag{2.71}$$

$$\frac{\partial}{\partial r}\frac{\partial \mathcal{L}}{\partial z_i} = 0. \tag{2.72}$$

By evaluating the terms above and taking into account that $\mathcal{L}$ is linear in the Lagrange multipliers $\mathbf{z}$ and $\partial^2\mathcal{L}/\partial t_i \partial z_k = 0$ one obtains the coupled equation system

$$\sum_k \begin{pmatrix} \frac{\partial^2 \mathcal{L}}{\partial t_i \partial t_k} & \frac{\partial^2 \mathcal{L}}{\partial t_i \partial c_k} & 0 \\ \frac{\partial^2 \mathcal{L}}{\partial c_i \partial t_k} & \frac{\partial^2 \mathcal{L}}{\partial c_i \partial c_k} & \frac{\partial^2 \mathcal{L}}{\partial c_i \partial z_k} \\ 0 & \frac{\partial^2 \mathcal{L}}{\partial z_i \partial c_k} & 0 \end{pmatrix} \begin{pmatrix} t_k^r \\ c_k^r \\ z_k^r \end{pmatrix} = - \begin{pmatrix} \frac{\partial \mathcal{L}^{(r)}}{\partial t_i} \\ \frac{\partial \mathcal{L}^{(r)}}{\partial c_i} \\ \frac{\partial \mathcal{L}^{(r)}}{\partial z_i} \end{pmatrix}. \tag{2.73}$$

First, the response equations for the non-variational wave functions parameters $\mathbf{c}$ have to be solved since these are independent of the other response quantities. Subsequently the response equations for the variational wave function parameters $\mathbf{t}$ and finally the equations for the response of the Lagrange multipliers $\mathbf{z}$ can be solved.

2.6 Notation

Molecular orbitals (MOs) for the calculation of NMR shielding tensors and magnetizabilities are expanded in the non-orthonormal basis of the gauge-including atomic orbitals $\{\omega_\mu\}$, MOs for rotational g tensors are expanded in the non-orthonormal basis of rotational London atomic orbitals (see Chapter 5). The AO basis has the metric $S_{\mu\nu} = \left\langle \omega_\mu | \omega_\nu \right\rangle$,

$$\phi_p = \sum_\mu C_{\mu p} \omega_\mu, \tag{2.74}$$

$$\left\langle \phi_p | \phi_q \right\rangle = \delta_{pq}. \tag{2.75}$$

Greek letters $\mu, \nu, \ldots$ label atomic orbitals.
In this thesis occupied orbitals are assumed to be localized using the Pipek-Mezey procedure [63] and are denoted by indices i, j, k, l; as already mentioned in Section 2.3 canonical occupied orbitals are decorated with an additional bar on top, i.e., $\bar{i}, \bar{j}, \bar{k}, \bar{l}$. Matrices referring to canonical occupied quantities are decorated with an additional bar on top as well. The rectangular submatrix of the coefficient matrix $\mathbf{C}$ referring to the localized molecular orbitals (LMOs) is denoted by $\mathbf{L}$. The submatrix which refers to the occupied canonical MOs is denoted by $\bar{\mathbf{C}}_\mathbf{o}$.
The canonical virtual orbitals are denoted by indices a, b, c, d and the coefficient submatrix by $\mathbf{C}_\mathbf{v}$. The MO coefficient matrix $\mathbf{C}$ (comprising both occupied and virtual orbitals) mentioned above thus consists of the two submatrices $\mathbf{L}$ and $\mathbf{C}_\mathbf{v}$, spliced together as $\mathbf{C} = (\mathbf{L}|\mathbf{C}_\mathbf{v})$. Analogously, the matrix $\bar{\mathbf{C}}$ is assembled from the two submatrices $\bar{\mathbf{C}}_\mathbf{o}$ and $\mathbf{C}_\mathbf{v}$ as $\bar{\mathbf{C}} = (\bar{\mathbf{C}}_\mathbf{o}|\mathbf{C}_\mathbf{v})$, i.e., the occupied block $\mathbf{L}$ in $\mathbf{C}$ referring to LMOs is substituted by $\bar{\mathbf{C}}_\mathbf{o}$ which in turn refers to canonical occupied orbitals. General MOs (occupied or virtual) are denoted by m, n, p, q.
In the approach presented in this thesis the virtual space is spanned by a redundant set of projected atomic orbitals (PAOs, see Section 2.3). PAOs are denoted by indices r, s, t, u in the following.
Fitting functions (FFs) for density fitting are denoted by indices P, Q with their respective Coulomb metric $J_{PQ} = (P|Q)$ and the three-index electron repulsion integrals (ERIs) $(\mu\nu|P)$.
Superscripted q or r indicates the partial derivative of a quantity with respect to the perturbation taken at the reference point, $q = 0$, respectively, $r = 0$, e.g.,

$$I^q = \left(\frac{\partial I}{\partial q}\right)_{q=0}, \tag{2.76}$$

or for second derivatives

$$I^{q,r} = \left(\frac{\partial^2 I}{\partial q \partial r}\right)_{q,r=0}. \tag{2.77}$$

Superscripted (q) or (r) means that the quantity was evaluated with perturbed AO integrals but unperturbed MO coefficients, e.g.,

$$h_{mn}^{(q)} = \sum_{\mu\nu} C_{\mu m}^{*} C_{\nu n} \left(\frac{\partial h_{\mu\nu}}{\partial q} \right)_{q=0} . \tag{2.78}$$

Greek indices $\alpha, \beta, \ldots$ denote Cartesian components of the corresponding perturbation.

In this work general electronic interaction matrices for a density matrix $\mathbf{d}$ are used,

$$g(\mathbf{d})_{pq} = \sum_{mn} d_{mn} \left[(pq|mn) - \frac{1}{2}(pn|mq) \right]. \tag{2.79}$$

They can also be written in an equivalent way with the density matrix in AO basis,

$$g(\mathbf{D})_{pq} = \sum_{\mu\nu} D_{\mu\nu} \left[(pq|\mu\nu) - \frac{1}{2}(p\nu|\mu q) \right] \tag{2.80}$$

with

$$D_{\mu\nu} = \sum_{mn} C_{\mu m}^{*} d_{mn} C_{\nu n}. \tag{2.81}$$

Furthermore, the following perturbed general electronic interaction matrices for a density matrix are used:

$$\left(\frac{\partial g(\mathbf{d})}{\partial B_\alpha} \right)_{pq} = \sum_{mn} d_{mn} \left[\frac{\partial (pq|mn)}{\partial B_\alpha} - \frac{1}{2} \frac{\partial (pn|mq)}{\partial B_\alpha} \right], \tag{2.82}$$

$$\left[g(\mathbf{d}) \right]_{pq}^{(B_\alpha)} = \sum_{mn} d_{mn} \left[(pq|mn)^{(B_\alpha)} - \frac{1}{2}(pn|mq)^{(B_\alpha)} \right], \tag{2.83}$$

$$g\left(\mathbf{d}^{B_\alpha} \right)_{pq} = \sum_{mn} d_{mn}^{B_\alpha} \left[(pq|mn) - \frac{1}{2}(pn|mq) \right]. \tag{2.84}$$

Chapter 3

THE DF-LMP2 SHIELDING TENSOR

The formalism and results which are presented in this chapter were already published in "*The Journal of Chemical Physics*" with my supervisor Prof. Schütz as co-author [35]. Since then, a few minor programming errors concerning mainly the treatment of frozen-core orbitals have been identified and fixed. The influence of those error fixes on the calculated NMR shielding tensors and shifts was investigated for a number of medium-sized molecules, e.g., coronene and glycine chains of different lengths. The deviations were found to be small, i.e., in the range of 10^{-2} ppm for ^{1}H-shieldings; for this reason the systems for which results are presented in this chapter were not recalculated. Instead the results published in Ref. [35] are presented.
This chapter is taken completely from the above mentioned publication [35], only minor changes were made to the original publication in "*The Journal of Chemical Physics*".

3.1 Introduction

The reliable prediction of nuclear magnetic resonance (NMR) shielding tensors and chemical shifts from ab-initio calculations has emerged as a versatile tool to support experimental NMR spectroscopy. Yet, there are two major problems hampering the theoretical treatment of potentially interesting large molecules: (*i*) the gauge origin problem which arises from the incompleteness of the atomic orbital (AO) basis sets and (*ii*) the unfavorably high scaling behavior of correlated wave function methods.
Several methods have been proposed to overcome the gauge origin problem, among them the individual gauge for localized orbitals (IGLO) approach by Schindler and Kutzelnigg [55, 56] and the localized orbital/local origin (LORG) approach by Hansen and Bouman [70], which are both aiming at minimizing the gauge error by introducing separate gauge origins for the localized molecular orbitals. Nowadays, the method of gauge-including atomic orbitals (GIAOs or London atomic orbitals) [23, 71] is more widely used; those explicitly field-dependent basis functions ensure gauge origin independence of the results by localizing the gauge origin of each individual basis function on its own atom. The explicit dependence on the gauge origin then cancels in all integrals and renders the obtained result independent of the choice of the gauge origin [59]. A discussion of the advantages and disadvantages of GIAOs in comparisons to IGLOs for wave function based methods can be found in Refs. [58] and [72] and for a density-functional theory (DFT) implementation in Ref. [73].
For many cases the accuracy provided by Hartree-Fock (HF) or DFT calculations is sufficient. Yet, there are examples where the proper treatment of electron correlation by wave function based methods is mandatory [69]. Numerous correlation methods for NMR shielding tensors have been presented within the GIAO framework, among them multi-configurational self-consistent field (MCSCF) theory [24], Møller-Plesset perturbation theory up to fourth-order [25, 26], and coupled-cluster implementations including up to triples and quadruples excitations [27–30]. Those approaches

all bear a highly unfavorable scaling behavior; one of the simplest approaches, second-order Møller-Plesset perturbation theory (MP2), could be applied to molecules with up to 600 basis functions by exploiting non-Abelian point group symmetry in combination with a simple coarse-grain parallelization [31] and integral-direct techniques [32]. Potentially interesting larger molecules are therefore out of reach for those methods. For HF even (sub-)linear scaling for shielding calculations was reported which allows to tackle very large systems [74–76]. Recently, Maurer and Ochsenfeld presented a (sub-)linear scaling AO based MP2 approach for NMR shielding tensors [77].

Chemical shifts calculated at the level of canonical GIAO-MP2 provide nearly quantitative accuracy for molecules with small correlation effects, i.e., corrections up to 30 ppm; for larger correlation effects MP2 overestimates the correction for the shifts. In comparison to Hartree-Fock MP2 usually provides an improvement, particularly for molecules with multiple bonds involving atoms with lone pairs [78]. In a pilot implementation on top of a conventional GIAO-MP2 program Gauss and Werner showed that the calculation of NMR shielding tensors in the framework of local correlation methods might be promising [33]. They assessed the accuracy of the local approach by a number of medium-sized test systems and concluded that the effect of the local approximation on the resulting shielding constants is small, i.e., in the range of 1 ppm for ^{13}C and therefore much smaller than the inherent error of the MP2 approximation itself. This is in line with the previously observed small deviations between canonical and local methods for ground state energies [10–16], gradients, [17], and properties of excited states [18–22].

In previous work the author presented a way to introduce the density fitting (DF) approximation in the calculation of NMR shielding tensors at the level of HF [52, 68]. It was shown that ordinary Gaussians can be employed as fitting functions for the orbital product densities in the electron repulsion integrals, which corresponds to density fitting at zero magnetic

field strength. The use of GIAOs as fitting functions, on the other hand, would not work and inevitably violate the gauge origin independence. In this chapter the first efficient implementation of NMR shielding tensors at the level of local MP2 in combination with DF, i.e., the GIAO-DF-LMP2 method is presented. It has been implemented in the MOLPRO program package [49, 50].

In Sections 3.2–3.5 the formalism for GIAO-DF-LMP2 NMR shielding tensors and detailed working equations are derived from the LMP2 Lagrangian by taking the mixed second derivative with respect to the external magnetic field and the magnetic moment of each nucleus. Essentially, the DF-LMP2 gradient of Ref. [17] interpreted as the derivative with respect to the magnetic moment of each nucleus, is differentiated a second time with respect to the external magnetic field. Localized molecular orbitals (LMOs) and projected atomic orbitals (PAOs) are employed to span occupied and virtual spaces, respectively. The "short-sightedness" of dynamic electron correlation is exploited (*i*) by restricting the LMO pair list and (*ii*) by allowing only excitations from LMO pairs into pair specific subspaces of the virtual space spanned by the PAOs of those few atoms near the corresponding LMO pair (pair domains).

In Section 3.6 the accuracy of the local approximation and the influence of the fitting basis set are investigated. Additionally, test calculations on large molecular systems are presented, like the photodamaged cyclobutane pyrimidine dimer lesion with adjacent nucleobases in the native intrahelical DNA double strand and its repaired analogue (296 valence electrons, 2636 AO basis functions) whose intermolecular interactions have been studied before [79, 80].

3.2 NMR Shielding Tensor Theory

The NMR shielding tensor of nucleus Z can be written as the mixed second derivative with respect to the external magnetic field $\mathbf{B}$ and the magnetic

moment $\mathbf{M}_Z$ of nucleus Z,

$$\begin{aligned}\sigma^Z_{\beta\alpha} &= \left[\frac{d^2E}{dB_\alpha dM_{Z\beta}}\right]_{\mathbf{B},\mathbf{M}_Z=\mathbf{0}} \\ &= \left[\sum_{\mu\nu} D_{\mu\nu}\frac{\partial^2 h_{\mu\nu}}{\partial B_\alpha \partial M_{Z\beta}} + \sum_{\mu\nu}\frac{\partial D_{\mu\nu}}{\partial B_\alpha}\frac{\partial h_{\mu\nu}}{\partial M_{Z\beta}}\right]_{\mathbf{B},\mathbf{M}_Z=\mathbf{0}},\end{aligned} \tag{3.1}$$

where $\mathbf{D}$ and $\mathbf{D}^{B_\alpha}$ denote the unperturbed and perturbed density matrices of the chosen method, in this case of DF-LMP2. The indices α and β denote the directions of the external magnetic field and of the magnetic moment of nucleus Z, respectively. Detailed expressions for the derivatives of the one-electron part of the Hamiltonian in AO basis, $\mathbf{h}$, can be found, e.g., in Ref. [68].

The (isotropic) shielding constant can be calculated as the arithmetic mean of the diagonal elements of the shielding tensor,

$$\sigma^Z_{iso} = \frac{1}{3}\left(\sigma^Z_{xx} + \sigma^Z_{yy} + \sigma^Z_{zz}\right). \tag{3.2}$$

The chemical shift δ of nucleus Z for a reference compound (typically tetramethylsilane, TMS, for ^{1}H and ^{13}C measurements) is obtained by additionally calculating the isotropic shielding constant σ^{ref}_{iso} of the reference and taking the difference, i.e.,

$$\delta(Z) = \sigma^{ref}_{iso} - \sigma^Z_{iso}. \tag{3.3}$$

In this work expressions for the unperturbed LMP2 density matrix are obtained by considering the gradient with respect to the magnetic moment $\mathbf{M}_Z$ following the formalism presented for the DF-LMP2 gradient [17] (see Section 3.3). Subsequently, the equations for the unperturbed density matrix can be differentiated with respect to the three components of the external magnetic field $\mathbf{B}$ to obtain the equations for the perturbed density matrices.

As a solution to the gauge origin problem the GIAO ansatz is employed, which uses explicitly field-dependent basis functions ω_μ, i.e.,

$$\omega_\mu(\mathbf{r}_M, \mathbf{A}_O(\mathbf{R}_M)) = \exp\left(-\frac{i}{c}\mathbf{A}_O(\mathbf{R}_M)\cdot\mathbf{r}\right)\chi_\mu(\mathbf{r}_M), \tag{3.4}$$

where $\mathbf{A}_O(\mathbf{R}_M)$ is the vector potential with gauge origin O,

$$\mathbf{A}_O(\mathbf{R}_M) = \frac{1}{2}\mathbf{B} \times (\mathbf{R}_M - \mathbf{R}_O) = \frac{1}{2}\mathbf{B} \times \mathbf{R}_{MO}, \tag{3.5}$$

and $\chi_\mu(\mathbf{r}_M)$ the field-independent basis functions. $\mathbf{R}_M$ and $\mathbf{R}_O$ represent the position vectors of nucleus M and of the gauge origin, respectively, $\mathbf{R}_{MO}$ is their difference vector. Furthermore, $\mathbf{r}$ denotes the position vector of an electron and $\mathbf{r}_M$ the vector pointing from nucleus M to this electron. The complex phase factor in Eq. (3.4) represents the gauge transformation from the center of nucleus M to the global gauge origin $\mathbf{R}_O$. Note that in the limit of zero magnetic field strength, $\mathbf{B} = 0$, GIAOs reduce to ordinary Gaussians.

The theory for the shielding tensor at the level of GIAO-DF-LMP2 is most conveniently derived for an orthonormal set of orbitals. The transformation to the non-orthonormal set of projected atomic orbitals (PAOs) as used in local correlation methods can be carried out subsequently (see the working equations provided in Section 3.5.4).

3.3 Unperturbed LMP2 Density Matrix

3.3.1 LMP2 Lagrangian and Hylleraas functional

Derivatives at the level of LMP2 are conveniently evaluated if one starts from the LMP2 Lagrangian [17],

$$\begin{aligned}\mathcal{L}_2 = E_2 &+ \sum_{kl} z_{kl}^{\mathrm{loc}} r_{kl} + \sum_{ck} \left[z_{ck} f_{ck} + z_{kc} f_{kc} \right] \\ &+ \sum_{pq} x_{pq} \left[\mathbf{C}^\dagger \mathbf{S} \mathbf{C} - \mathbf{1} \right]_{pq},\end{aligned} \tag{3.6}$$

which is required to be stationary with respect to the LMP2 amplitudes, the molecular orbital coefficients $\mathbf{C} = (\mathbf{L}|\mathbf{C}_\mathbf{v})$, and the Lagrange multipliers. The Lagrangian includes the Hylleraas functional E_2 and the localization,

Brillouin, and orthonormality conditions with the corresponding multipliers z_{kl}^{loc}, z_{ck}, respectively, z_{kc}, and x_{pq}. In the frozen-core approximation an additional term $z_{kl_c} f_{kl_c} + z_{l_c k} f_{l_c k}$ with $k \in \{\text{valence}\}$ and $l_c \in \{\text{core}\}$ has to be considered. The additional equations which arise are explicitly given in Section 4.3.5.

The Hylleraas functional can be written as

$$\begin{aligned} E_2 &= \langle \Psi^{(0)} | \hat{H} | \Psi^{(1)} \rangle + \langle \Psi^{(1)} | \hat{H} | \Psi^{(0)} \rangle \\ &\quad + \langle \Psi^{(1)} | \hat{H}^{(0)} - E^{(0)} | \Psi^{(1)} \rangle \\ &= \sum_{cdkl} \left(\tilde{T}_{cd}^{kl} K_{cd}^{kl*} + \tilde{T}_{cd}^{kl*} K_{cd}^{kl} \right) + \sum_{pq} f_{pq} d_{pq}^{(2)}, \end{aligned} \tag{3.7}$$

where the matrix $\mathbf{K}$,

$$K_{cd}^{kl} = (ck|dl), \tag{3.8}$$

represents the two-electron exchange integrals. The LMP2 amplitudes for a given orbital pair (kl) are collected in $\mathbf{T}^{kl}$; the contravariant amplitude matrices are defined as

$$\tilde{T}_{cd}^{kl} = 2T_{cd}^{kl} - T_{cd}^{lk}. \tag{3.9}$$

The closed-shell Fock matrix in MO basis, $\mathbf{f}$, is given by

$$f_{pq} = h_{pq} + g\left(\mathbf{d}^{(\mathbf{0})}\right)_{pq} \tag{3.10}$$

with the one-electron core Hamiltonian matrix $\mathbf{h}$, the general electronic interaction matrix for a density matrix $\mathbf{d}$,

$$g\left(\mathbf{d}\right)_{pq} = \sum_{mn} d_{mn} \left[(pq|mn) - \frac{1}{2}(pn|mq) \right], \tag{3.11}$$

and the Hartree-Fock density matrix

$$d_{ij}^{(0)} = 2\delta_{ij}. \tag{3.12}$$

The LMP2 density matrix is given by

$$\begin{aligned} \left[\mathbf{d}^{(2)}\right]_{ij} &= -2 \sum_{cd} \sum_{k} \left[T_{cd}^{ik} \tilde{T}_{cd}^{jk*} \right], \\ \left[\mathbf{d}^{(2)}\right]_{ab} &= 2 \sum_{c} \sum_{kl} \left[\tilde{T}_{ac}^{kl*} T_{bc}^{kl} \right], \\ \left[\mathbf{d}^{(2)}\right]_{ia} &= \left[\mathbf{d}^{(2)}\right]_{ai} = 0 . \end{aligned} \tag{3.13}$$

Equations for the determination of the amplitudes are found by minimizing the Hylleraas functional, respectively, the Lagrangian (3.6) with respect to the amplitudes,

$$\frac{\partial \mathcal{L}_2}{\partial \tilde{T}^{ij*}_{ab}} = R^{ij}_{ab} = 0, \quad \text{for all } i \geq j,\ a,\ b \tag{3.14}$$

with the residual matrices

$$\begin{aligned} R^{ij}_{ab} = K^{ij}_{ab} &+ \sum_c \left(T^{ij}_{ac} f_{bc} + f_{ac} T^{ij}_{cb} \right) \\ &- \sum_k \left(f_{ki} T^{kj}_{ab} + f_{kj} T^{ik}_{ab} \right). \end{aligned} \tag{3.15}$$

Detailed working equations for the residual in PAO basis can be found in Section 3.5.4.

In local MP2 excitations are restricted to subspaces of PAOs (domains) [60] which are specific for each pair (ij). The corresponding amplitude matrices are denoted T^{ij}_{rs}, where r,s are restricted to the domain $[ij]$. These amplitudes can be projected back to the MO basis,

$$T^{ij}_{ab} = \sum_{rs \in [ij]} Q_{ar} T^{ij}_{rs} Q_{bs}, \tag{3.16}$$

where only for full domains the canonical amplitudes are obtained. The transformation matrix $\mathbf{Q}$ is defined in Eq. (2.45).

For the optimized amplitudes T^{ij}_{rs} the residual must vanish in the corresponding domain $[ij]$ of the PAO basis,

$$R^{ij}_{rs} = \sum_{ab} Q_{ar} R^{ij}_{ab} Q_{bs} = 0 \ \text{ for } r,s \in [ij]\,. \tag{3.17}$$

The residuals in the MO basis R^{ij}_{ab} do not vanish unless the domains span the full virtual space.

The orbital-relaxed unperturbed density matrix in AO basis $\mathbf{D}$ as needed for the shielding tensor Eq. (3.1) is given by

$$D_{\mu\nu} = \sum_{pq} C^*_{\mu p} \left[d^{(0)}_{pq} + d^{(2)}_{pq} + z_{pq} \right] C_{\nu q}. \tag{3.18}$$

Note that the Lagrange multipliers $\mathbf{z}^{\text{loc}}$ do not contribute to the unperturbed density matrix for the gradient with respect to the magnetic moment of the nucleus; for a detailed discussion of the unperturbed density matrix for the LMP2 energy gradient cf. Section II D in Ref. [17].
The presented method employs Pipek-Mezey localization [63] with its localization condition

$$r_{kl} = \sum_A \left[S^A_{kk} - S^A_{ll} \right] S^A_{kl} = 0 \quad \forall k > l \tag{3.19}$$

and the matrices $\mathbf{S}^A$,

$$S^A_{kl} = \sum_{\mu \in A} \sum_{\nu} \left[L^*_{\mu k} S_{\mu\nu} L_{\nu l} + L^*_{\nu k} S_{\nu\mu} L_{\mu l} \right], \tag{3.20}$$

where the summation over the AO index μ is restricted to basis functions centered at atom A.

3.3.2 Z-vector equations

Variations of the orbitals in the presence of a perturbation, e.g., the external magnetic field $\mathbf{B}$ can be described by the coefficient matrix

$$\mathbf{C}(\mathbf{B}) = \mathbf{C}(0)\mathbf{O}(\mathbf{B}), \tag{3.21}$$

where $\mathbf{C}(0)$ is the coefficient matrix of the optimized HF orbitals in the absence of a perturbation and the matrix $\mathbf{O}(\mathbf{B})$ describes the variation of the orbitals in the presence of the magnetic field $\mathbf{B}$, with $\mathbf{O}(0) = \mathbf{1}$.
Minimization of the Lagrangian (3.6) with respect to the (variation of the) orbitals yields the expressions for the Lagrange multipliers, the so-called Z-vector equations. The contributions can be split into individual terms

(for a more detailed discussion see Ref. [17]),

$$[\mathbf{A}]_{pq} = \left(\frac{\partial}{\partial O_{pq}} E_2\right)_{\mathbf{B}=0}, \tag{3.22}$$

$$\left[\tilde{\mathbf{A}}\,(\mathbf{z})\right]_{pq} = \left(\frac{\partial}{\partial O_{pq}} \sum_{ck} \left[z_{ck} f_{ck} + z_{kc} f_{kc}\right]\right)_{\mathbf{B}=0}, \tag{3.23}$$

$$\left[\mathbf{a}\left(\mathbf{z}^{\mathrm{loc}}\right)\right]_{pi} = \left(\frac{\partial}{\partial O_{pi}} \sum_{kl} z_{kl}^{\mathrm{loc}} r_{kl}\right)_{\mathbf{B}=0}. \tag{3.24}$$

Combining the stationary conditions $\left(\partial \mathcal{L}_2 / \partial O_{pq}\right)_{\mathbf{B}=0} = 0$ with the auxiliary conditions $\mathbf{x} = \mathbf{x}^{\dagger}$ yields the linear Z-vector equations,

$$\left(1 - \mathcal{T}_{pq}\right)\left[\mathbf{A} + \tilde{\mathbf{A}}(\mathbf{z}) + \mathbf{a}\left(\mathbf{z}^{\mathrm{loc}}\right)\right]_{pq} = 0, \tag{3.25}$$

where the operator $\mathcal{T}_{pq}$ interchanges the index pair p and q of the orbital variation matrix $\mathbf{O}$ and complex conjugates its elements. The Z-vector Eqs. (3.25) can be further decoupled into the Z-vector coupled-perturbed Hartree-Fock (Z-CPHF) equations and the Z-vector coupled-perturbed localization (Z-CPL) equations. The theory for the Z-vector equations in MO basis without density fitting was outlined earlier by Gauss and Werner [33]. This work builds on the formalism as introduced for the DF-LMP2 gradient in Ref. [17].

The Lagrange multipliers $\mathbf{z}$ are assumed to be defined in the whole MO basis with $z_{aa} = z_{ii} = 0$. The Z-CPHF equations for the determination of the virtual-occupied block of $\mathbf{z}$ take the form

$$y_{ai} + \sum_{c} f_{ca} z_{ci} - \sum_{k} z_{ak} f_{ik} + 2g(\mathbf{z})_{ia} = 0 \tag{3.26}$$

with the right-hand side

$$y_{ai} = A_{ai} - A_{ia}^{*} + \left[\mathbf{a}(\mathbf{z}^{\mathrm{loc}})\right]_{ai}, \tag{3.27}$$

where

$$A^*_{ia} = \left(\frac{\partial}{\partial O^*_{ia}} E_2\right)_{\mathbf{B}=0} = 2\left[\sum_{ckl}\left(\tilde{T}^{kl*}_{ac} K^{kl}_{ic} + \sum_{rs\rho} L^*_{\rho i} S_{\rho r} \tilde{T}^{kl}_{rs} Q_{cs} R^{kl*}_{ac}\right)\right], \tag{3.28}$$

$$A_{pi} = \left(\frac{\partial}{\partial O_{pi}} E_2\right)_{\mathbf{B}=0} = 2\left[B_{pi} + \frac{1}{2}\sum_k f_{kp} d^{(2)}_{ki} + g(\mathbf{d}^{(2)})_{ip}\right], \tag{3.29}$$

with

$$K^{kl}_{ic} = (ik|cl), \tag{3.30}$$

$$B_{pi} = \sum_k \sum_{cd} (cp|dk) \tilde{T}^{ik*}_{cd}, \tag{3.31}$$

and the contribution from the Z-CPL equations $\left[\mathbf{a}(\mathbf{z}^{\mathrm{loc}})\right]_{ai}$. The second term in Eq. (3.28) comes from the variation of the transformation matrices $\mathbf{Q}$ in the LMP2 amplitudes (for further details see Appendix B in Ref. [17]). There is no such term in Eq. (3.29) since $\mathbf{Q}$ describes the transformation from virtual MO to the PAO basis and does not contain occupied indices. Since the Lagrange multiplier $\mathbf{z}$ is a real Hermitian, i.e., symmetric quantity, the equations for the occupied-virtual block are identical to the ones for the virtual-occupied part. The occupied-virtual block of the unperturbed Lagrange multipliers is therefore given by $[\mathbf{z}]_{ia} = \left[\mathbf{z}^\dagger\right]_{ia} = [\mathbf{z}^*]_{ai} = [\mathbf{z}]_{ai}$.
The Lagrange multipliers for the localization condition $\mathbf{z}^{\mathrm{loc}}$ are determined by solving the Z-CPL equations,

$$(1 - \mathcal{T}_{ij})\left(A_{ij} + \left[\mathbf{a}\left(\mathbf{z}^{\mathrm{loc}}\right)\right]_{ij}\right) = 0, \tag{3.32}$$

$$\left[\mathbf{a}\left(\mathbf{z}^{\mathrm{loc}}\right)\right]_{pi} = \sum_{k>l} \mathcal{B}^+_{pi,kl} z^{\mathrm{loc}}_{kl}. \tag{3.33}$$

The derivation of the Z-CPL equations and the matrix elements $\mathcal{B}^+_{pi,kl}$ are given in Section 3.5.1.

3.4 Perturbed Density Matrix

The expression for the orbital-relaxed perturbed density matrix is obtained by differentiation of the equation for the unperturbed density matrix (3.18) with respect to the components of the external magnetic field **B**. This yields

$$\frac{\partial D_{\mu\nu}}{\partial B_\alpha} = [\mathbf{D}]^{B_\alpha}_{\mu\nu} = \sum_{pq} \left[C^{B_\alpha *}_{\mu p} d_{pq} C_{\nu q} + C^{*}_{\mu p} d^{B_\alpha}_{pq} C_{\nu q} + C^{*}_{\mu p} d_{pq} C^{B_\alpha}_{\nu q} \right] \tag{3.34}$$

with the perturbed density matrix $\mathbf{d}^{B_\alpha}$ and the perturbed MO coefficients $\mathbf{C}^{B_\alpha}$ to be evaluated. The perturbed density matrix has contributions from the derivatives of the HF density matrix $\mathbf{d^{(0)}}$, of the LMP2 density matrix $\mathbf{d^{(2)}}$, and of the Lagrange multipliers **z**,

$$d^{B_\alpha}_{pq} = \left(\left[\mathbf{d}^{(0)} \right]^{B_\alpha}_{pq} + \left[\mathbf{d}^{(2)} \right]^{B_\alpha}_{pq} + [\mathbf{z}]^{B_\alpha}_{pq} \right) \tag{3.35}$$

with the perturbed HF density matrix according to Ref. [68],

$$\frac{\partial D^{(0)}_{\mu\nu}}{\partial B_\alpha} = \left[\mathbf{D}^{(0)} \right]^{B_\alpha}_{\mu\nu} = 2 \sum_{k} \left[L^{B_\alpha *}_{\mu k} L_{\nu k} + L^{*}_{\mu k} L^{B_\alpha}_{\nu k} \right], \tag{3.36}$$

where $\mathbf{L}^{B_\alpha}$ are the perturbed LMO coefficients which are explicitly defined in the following subsection (see Eq. 3.38).

3.4.1 Perturbed MO coefficients

The coefficient matrix of the localized occupied orbitals in the presence of a magnetic field can generally be written as

$$\mathbf{L}(B_\alpha) = \bar{\mathbf{C}} \bar{\mathbf{U}}(B_\alpha) \mathbf{W} \mathbf{V}(B_\alpha), \tag{3.37}$$

where $\bar{\mathbf{C}} = (\bar{\mathbf{C}}_\mathbf{o} | \mathbf{C}_\mathbf{v})$ contains purely canonical HF coefficients. The matrix $\bar{\mathbf{U}}$ describes the change of the optimized canonical orbitals, **W** is the localization matrix (as defined in Eq. 2.42) and **V** describes the change of the localization matrix. The corresponding derivative with respect to the

magnetic field can be written with the derivatives of the transformation matrices, $\bar{\mathbf{U}}^{B_\alpha}$ and $\mathbf{V}^{B_\alpha}$,

$$\frac{\partial \mathbf{L}(B_\alpha)}{\partial B_\alpha} = \mathbf{L}^{B_\alpha} = \bar{\mathbf{C}}\bar{\mathbf{U}}^{B_\alpha}\mathbf{W} + \mathbf{L}\mathbf{V}^{B_\alpha}. \tag{3.38}$$

The following relations have been used to derive Eq. (3.38): $\mathbf{U}(0) = \mathbf{1}$, respectively, $\mathbf{V}(0) = \mathbf{1}$ and the connection between the localized and canonical MO coefficient matrices (see Eq. 2.41).

The transformation matrix $\bar{\mathbf{U}}^{B_\alpha}$ for occupied orbitals can be considered as the composite rectangular matrix

$$\bar{\mathbf{U}}^{B_\alpha} = \begin{pmatrix} \bar{\mathbf{U}}_{\mathbf{o}}^{B_\alpha} \\ \mathbf{U}_{\mathbf{v}}^{B_\alpha} \end{pmatrix} \tag{3.39}$$

with the $n_{occ} \times n_{occ}$ (n_{occ} number of occupied orbitals) submatrix $\bar{\mathbf{U}}_{\mathbf{o}}^{B_\alpha}$ describing the contributions from occupied orbital coefficients to the perturbed occupied orbitals coefficients and the $n_{virt} \times n_{occ}$ (n_{virt} number of virtual orbitals) submatrix $\bar{\mathbf{U}}_{\mathbf{v}}^{B_\alpha}$ describing the contributions from virtual orbital coefficients to the perturbed occupied orbital coefficients.

The submatrix $\bar{\mathbf{U}}_{\mathbf{o}}^{B_\alpha}$ can be transformed to local basis,

$$\mathbf{U}_{\mathbf{o}}^{B_\alpha} = \mathbf{W}^\dagger \bar{\mathbf{U}}_{\mathbf{o}}^{B_\alpha} \mathbf{W}. \tag{3.40}$$

Inverting Eq. (3.40) and inserting it in Eq. (3.38) yields

$$\mathbf{L}^{B_\alpha} = \mathbf{C}\mathbf{U}^{B_\alpha} + \mathbf{L}\mathbf{V}^{B_\alpha} \tag{3.41}$$

with the composite rectangular transformation matrix

$$\mathbf{U}^{B_\alpha} = \begin{pmatrix} \mathbf{U}_{\mathbf{o}}^{B_\alpha} \\ \mathbf{U}_{\mathbf{v}}^{B_\alpha} \end{pmatrix}. \tag{3.42}$$

Thus, the perturbed LMO coefficients can be written in terms of local quantities.

The occupied-occupied part of $\mathbf{U}^{B_\alpha}$ can be determined by ensuring orthonormality for the perturbed orbitals,

$$\frac{\partial}{\partial B_\alpha}\left(\frac{\partial \mathcal{L}_2}{\partial x_{pq}}\right)_{\mathbf{B}=0} = \left(\frac{\partial \left(\mathbf{C}^\dagger \mathbf{S} \mathbf{C}\right)_{pq}}{\partial B_\alpha}\right)_{\mathbf{B}=0} = 0. \tag{3.43}$$

Since $\mathbf{V}$ is a unitary matrix the derivative with respect to the magnetic field ,$\mathbf{V}^{B_\alpha}$, is an anti-Hermitian matrix and hence does not contribute to Eq. (3.43) (the two terms involving $\mathbf{V}^{B_\alpha}$ or its adjoint cancel). A possible choice for $\mathbf{U}_\mathbf{o}^{B_\alpha}$ satisfying Eq. (3.43) then is

$$U_{ij}^{B_\alpha} = -\frac{1}{2}\sum_{\mu\nu} L_{\mu i}^{*} S_{\mu\nu}^{B_\alpha} L_{\nu j} \tag{3.44}$$

with the perturbed overlap

$$S_{\mu\nu}^{B_\alpha} = \frac{i}{2c}\left\langle\mu\right|\left[(\mathbf{R}_\mathrm{M}-\mathbf{R}_\mathrm{N})\times\mathbf{r}\right]_\alpha\left|\nu\right\rangle. \tag{3.45}$$

This is only one possible choice for the occupied-occupied part of $\mathbf{U}^{B_\alpha}$. For the frozen-core approximation of magnetizabilities and rotational g tensors the core-valence and valence-core part of $\mathbf{U}^{B_\alpha}$ are chosen differently (see Section 4.3.5).

The virtual-occupied part of $\mathbf{U}^{B_\alpha}$ is obtained by ensuring that Brillouin's condition is fulfilled for the perturbed orbitals,

$$\frac{\partial}{\partial B_\alpha}\left(\frac{\partial\mathcal{L}_2}{\partial z_{ai}}\right)_{\mathbf{B}=0} = \left(\frac{\partial f_{ai}}{\partial B_\alpha}\right)_{\mathbf{B}=0} = 0, \tag{3.46}$$

yielding the coupled-perturbed Hartree-Fock (CPHF) equations [81–83],

$$\begin{aligned} 0 = &\sum_c f_{ac}U_{ci}^{B_\alpha} - \sum_k f_{ik}U_{ak}^{B_\alpha} - \sum_k f_{ik}S_{ak}^{B_\alpha} \\ &+ g\left(\left[\mathbf{d}^{(0)}\right]^{B_\alpha}\right)_{ai} - \left(h_{ai}^{(B_\alpha)} + \left[g\left(\mathbf{d}^{(0)}\right)\right]_{ai}^{(B_\alpha)}\right). \end{aligned} \tag{3.47}$$

Additionally, the response of the localization criterion has to be considered for local MP2, ensuring that the derivative of the localization condition Eq. (3.19) with respect to the magnetic field is still fulfilled,

$$\frac{\partial}{\partial B_\alpha}\left(\frac{\partial\mathcal{L}_2}{\partial z_{ij}^{\mathrm{loc}}}\right)_{\mathbf{B}=0} = \left(\frac{\partial r_{ij}}{\partial B_\alpha}\right)_{\mathbf{B}=0} = 0. \tag{3.48}$$

This yields the coupled-perturbed localization (CPL) equations,

$$\begin{aligned} &\sum_A \left(S_{ii}^A - S_{jj}^A\right) S_{ij}^{A,(B_\alpha)} + \sum_{kl} \mathcal{B}_{kl,ij}^{-} V_{kl}^{B_\alpha} \\ &+ \sum_{ck} \mathcal{B}_{ck,ij}^{-} U_{ck}^{B_\alpha} - \frac{1}{2}\sum_{kl} \mathcal{B}_{kl,ij}^{-} S_{kl}^{(B_\alpha)} = 0, \end{aligned} \tag{3.49}$$

where

$$S_{ij}^{A,(B_\alpha)} = \sum_{\mu\in A}\sum_{\nu}\left[L_{\mu i}^{*} S_{\mu\nu}^{B_\alpha} L_{\nu j} + L_{\nu i}^{*} S_{\nu\mu}^{B_\alpha} L_{\mu j}\right]. \tag{3.50}$$

One needs to solve the CPHF equations beforehand, as the solution $\mathbf{U}^{B_\alpha}$ is required for the right-hand side. The matrices $\mathcal{B}^{-}$ are defined explicitly in Section 3.5.2.

3.4.2 Perturbed LMP2 density matrix

The perturbed LMP2 density matrix as the derivative of Eq. (3.13) with respect to the magnetic field can be written as

$$\begin{aligned}
\left[\mathbf{d}^{(2)}\right]_{ij}^{B_\alpha} &= -2\sum_{cd}\sum_{k}\left[\frac{\partial T_{cd}^{ik}}{\partial B_\alpha}\tilde{T}_{cd}^{jk*} + T_{cd}^{ik}\frac{\partial \tilde{T}_{cd}^{jk*}}{\partial B_\alpha}\right], \\
\left[\mathbf{d}^{(2)}\right]_{ab}^{B_\alpha} &= 2\sum_{c}\sum_{kl}\left[\frac{\partial \tilde{T}_{ac}^{kl*}}{\partial B_\alpha}T_{bc}^{kl} + \tilde{T}_{ac}^{kl*}\frac{\partial T_{bc}^{kl}}{\partial B_\alpha}\right], \\
\left[\mathbf{d}^{(2)}\right]_{ia}^{B_\alpha} &= \left[\mathbf{d}^{(2)}\right]_{ai}^{B_\alpha} \;=\; 0\,,
\end{aligned} \tag{3.51}$$

which requires the perturbed LMP2 amplitudes $\partial\mathbf{T}^{ij}/\partial B_\alpha$.
The stationary conditions of the Hylleraas functional also have to be fulfilled in the presence of a magnetic field, i.e., for the perturbed amplitudes, hence

$$\frac{\partial}{\partial B_\alpha}\left(\frac{\partial \mathcal{L}_2}{\partial \tilde{T}_{ab}^{ij*}}\right)_{\mathbf{B}=0} = \left(\frac{\partial R_{ab}^{ij}}{\partial B_\alpha}\right)_{\mathbf{B}=0} = 0 \tag{3.52}$$

for all $i \geq j,\ a,\ b$.
Solving Eq. (3.52) for the perturbed amplitudes in combination with the transformation of the electron repulsion integrals (ERIs) from AO to MO basis to obtain the perturbed exchange matrix is one of the main bottlenecks in canonical GIAO-MP2 implementations. It is entirely removed by virtue of the local approach and density fitting techniques. The explicit working equations for the perturbed residual $\partial\mathbf{R}^{ij}/\partial B_\alpha$ in PAO basis are given in Section 3.5.4. The corresponding equations for the non-DF case can be found in the GIAO-LMP2 publication by Gauss and Werner [33].

3.4.3 Perturbed Z-vector equations

The response of the Lagrange multipliers $\mathbf{z}$ and $\mathbf{z}^{\text{loc}}$ is obtained from the first-order Z-vector equations, i.e., the derivatives of the Z-CPHF Eqs. (3.26) and Z-CPL Eqs. (3.32) with respect to the magnetic field. The perturbed Z-vector equations in MO basis without density fitting can be found in Ref. [33]. For the perturbed Z-CPHF equations one obtains

$$\sum_c f_{ca} z_{ci}^{B_\alpha} - \sum_k z_{ak}^{B_\alpha} f_{ik} + 2g(\mathbf{z}^{B_\alpha})_{ia} = -\frac{\partial Y_{ai}}{\partial B_\alpha} \tag{3.53}$$

with the right-hand side

$$\frac{\partial Y_{ai}}{\partial B_\alpha} = \frac{\partial y_{ai}}{\partial B_\alpha} + \sum_c \frac{\partial f_{ca}}{\partial B_\alpha} z_{ci} - \sum_k z_{ak} \frac{\partial f_{ik}}{\partial B_\alpha} + 2\frac{\partial g(\mathbf{z})_{ia}}{\partial B_\alpha}, \tag{3.54}$$

where y_{ai} is defined in Eq. (3.27). All terms contributing to the perturbed Z-CPHF equations are given in detail in Section 3.5.3, respectively, the corresponding working equations in PAO basis in Section 3.5.4.

The perturbed Lagrange multipliers for the localization $\partial \mathbf{z}^{\text{loc}} / \partial B_\alpha$ are obtained by differentiation of the Z-CPL Eqs. (3.32) with respect to the magnetic field,

$$\frac{\partial}{\partial B_\alpha} \left[(1 - \mathcal{T}_{ij}) \left(A_{ij} + \left[\mathbf{a}\left(\mathbf{z}^{\text{loc}}\right) \right]_{ij} \right) \right] = 0 \tag{3.55}$$

with the derivative

$$\left[\frac{\partial \mathbf{a}(\mathbf{z}^{\text{loc}})}{\partial B_\alpha} \right]_{pi} = \sum_{k>l} \left(\mathcal{B}^-_{pi,kl} \frac{\partial z_{kl}^{\text{loc}}}{\partial B_\alpha} + \frac{\partial \mathcal{B}^+_{pi,kl}}{\partial B_\alpha} z_{kl}^{\text{loc}} \right). \tag{3.56}$$

Detailed equations and the definitions of the coefficient matrices $\mathcal{B}^-$ and $\partial \mathcal{B}^+ / \partial B_\alpha$ in Eq. (3.56) are given in Section 3.5.2.

Equation (3.56) also gives a contribution to the right-hand side of the perturbed Z-CPHF Eqs. (3.54).

3.5 Detailed Working Equations

In this section detailed working equations for the unperturbed and perturbed Z-CPL equations and for the equations in PAO basis are provided.

3.5.1 Unperturbed Z-CPL equations

The contribution from the localization condition r_{kl} to the Lagrangian (3.6) can be rewritten if one exploits the antihermiticity of the localization condition and of the Lagrange multipliers $\mathbf{z}^{\mathrm{loc}}$,

$$\sum_{kl} z_{kl}^{\mathrm{loc}} r_{kl} = \sum_{k>l} \left[z_{kl}^{\mathrm{loc}} r_{kl} + z_{kl}^{\mathrm{loc}*} r_{kl}^{*} \right] \tag{3.57}$$

with the localization condition

$$r_{kl} = \sum_{A} \left(S_{kk}^{A} - S_{ll}^{A} \right) S_{kl}^{A} = 0 \quad \forall k > l. \tag{3.58}$$

Differentiating Eq. (3.57) with respect to variations of the orbitals yields

$$\begin{aligned} \left[\mathbf{a}\left(\mathbf{z}^{\mathrm{loc}} \right) \right]_{pi} &= \left(\frac{\partial}{\partial O_{pi}} \sum_{k>l} \left[z_{kl}^{\mathrm{loc}} r_{kl} + z_{kl}^{\mathrm{loc}*} r_{kl}^{*} \right] \right)_{\mathbf{B}=0} \\ &= \sum_{k>l} \left[\mathcal{B}_{pi}^{kl} z_{kl}^{\mathrm{loc}} + \mathcal{B}_{pi}^{(kl)^{*}} z_{kl}^{\mathrm{loc}*} \right] \end{aligned} \tag{3.59}$$

with the coefficient matrices

$$\begin{aligned} \mathcal{B}_{pi}^{kl} = \left(\frac{\partial r_{kl}}{\partial O_{pi}} \right)_{\mathbf{B}=0} &= \sum_{A} \Big[\left(S_{kp}^{A} \delta_{ki} - S_{lp}^{A} \delta_{li} \right) S_{kl}^{A} \\ &\quad + \left(S_{kk}^{A} - S_{ll}^{A} \right) S_{kp}^{A} \delta_{il} \Big], \end{aligned} \tag{3.60}$$

$$\begin{aligned} \mathcal{B}_{pi}^{(kl)^{*}} = \left(\frac{\partial r_{kl}^{*}}{\partial O_{pi}} \right)_{\mathbf{B}=0} &= \sum_{A} \Big[\left(S_{pk}^{A*} \delta_{ik} - S_{pl}^{A*} \delta_{il} \right) S_{kl}^{A*} \\ &\quad + \left(S_{kk}^{A*} - S_{ll}^{A*} \right) S_{pl}^{A*} \delta_{ki} \Big]. \end{aligned} \tag{3.61}$$

For the unperturbed Lagrange multipliers $\mathbf{z}^{\mathrm{loc}}$, which are real quantities, Eq. (3.59) can be further simplified:

$$\begin{aligned} &\sum_{k>l} \left[\mathcal{B}_{pi}^{kl} z_{kl}^{\mathrm{loc}} + \mathcal{B}_{pi}^{(kl)^{*}} z_{kl}^{\mathrm{loc}*} \right] \\ &= \sum_{k>l} \left[\mathcal{B}_{pi}^{kl} + \mathcal{B}_{pi}^{(kl)^{*}} \right] z_{kl}^{\mathrm{loc}} = \sum_{k>l} \mathcal{B}_{pi,kl}^{+} z_{kl}^{\mathrm{loc}} \end{aligned} \tag{3.62}$$

with the coefficient matrix

$$\mathcal{B}_{pi,kl}^{+} = \mathcal{B}_{pi}^{kl} + \mathcal{B}_{pi}^{(kl)^{*}}. \tag{3.63}$$

For given indices p and i the matrix $\left[\mathcal{B}^{+}{}_{pi}\right]_{kl}$ is antisymmetric, respectively, anti-Hermitian with respect to k and l.
For the diamagnetic part one has to solve the Z-CPL equations to obtain the Lagrange multipliers $\mathbf{z}^{\mathrm{loc}}$,

$$(1-\mathcal{T}_{ij})\left(A_{ij}+\left[\mathbf{a}\left(\mathbf{z}^{\mathrm{loc}}\right)\right]_{ij}\right)=0, \tag{3.64}$$

or more explicitly

$$A_{ij}-A^{*}_{ji}+\sum_{k>l}\left(\mathcal{B}^{+}_{ij,kl}-\mathcal{B}^{+}_{(ji)^{*},kl}\right)z^{\mathrm{loc}}_{kl}=0 \tag{3.65}$$

with the coefficient matrix

$$\mathcal{B}^{+}_{(ji)^{*},kl}=\left[\frac{\partial r_{kl}}{\partial O^{*}_{ji}}+\left(\frac{\partial r^{*}_{kl}}{\partial O^{*}_{ji}}\right)\right]_{\mathbf{B}=0}. \tag{3.66}$$

As a consequence of the antihermiticity of $\left[\mathcal{B}^{+}{}_{pi}\right]_{kl}$ with respect to k and l (see above) the multipliers $\mathbf{z}^{\mathrm{loc}}$ have to be antisymmetric, respectively anti-Hermitian, as well, otherwise the contraction would yield zero,

$$\left[\mathbf{z}^{\mathrm{loc}}\right]_{kl}=-\left[(\mathbf{z}^{\mathrm{loc}})^{\dagger}\right]_{kl}=-\left[(\mathbf{z}^{\mathrm{loc}})^{*}\right]_{lk}. \tag{3.67}$$

3.5.2 Perturbed Z-CPL equations

For the perturbed Z-CPL equations one finds

$$\begin{aligned}&\frac{\partial A_{ij}}{\partial B_{\alpha}}-\frac{\partial A^{*}_{ji}}{\partial B_{\alpha}}+\sum_{k>l}\left(\frac{\partial \mathcal{B}^{+}_{ij,kl}}{\partial B_{\alpha}}-\frac{\partial \mathcal{B}^{+}_{(ji)^{*},kl}}{\partial B_{\alpha}}\right)z^{\mathrm{loc}}_{kl}\\ &=\sum_{k>l}\left(\mathcal{B}^{-}_{ij,kl}-\mathcal{B}^{-}_{(ji)^{*},kl}\right)\frac{\partial z^{\mathrm{loc}}_{kl}}{\partial B_{\alpha}}.\end{aligned} \tag{3.68}$$

One arrives at Eq. (3.68) by differentiating the expressions for the unperturbed Z-CPL Eqs. (3.64) after inserting Eq. (3.59) so that proper care of complex conjugation is taken. Furthermore, one can then exploit the fact that the unperturbed Lagrange multipliers $\mathbf{z}^{\mathrm{loc}}$ are real quantities (just like

in the unperturbed Z-CPL equations) and the fact that the perturbed Lagrange multipliers $\partial \mathbf{z}^{\mathrm{loc}}/\partial B_\alpha$ are purely imaginary quantities.
Thus, the contraction of the perturbed Lagrange multipliers with the unperturbed coefficient matrices (cf. Eq. 3.59) can be further simplified to

$$\begin{aligned}
&\sum_{k>l}\left[\mathcal{B}_{ij}^{kl}\frac{\partial z_{kl}^{\mathrm{loc}}}{\partial B_\alpha}+\mathcal{B}_{ij}^{(kl)^*}\frac{\partial z_{kl}^{\mathrm{loc}*}}{\partial B_\alpha}\right]\\
&=\sum_{k>l}\left[\mathcal{B}_{ij}^{kl}-\mathcal{B}_{ij}^{(kl)^*}\right]\frac{\partial z_{kl}^{\mathrm{loc}}}{\partial B_\alpha}=\sum_{k>l}\mathcal{B}_{ij,kl}^{-}\frac{\partial z_{kl}^{\mathrm{loc}}}{\partial B_\alpha}
\end{aligned}\tag{3.69}$$

with the modified coefficient matrix

$$\mathcal{B}_{pi,kl}^{-}=\mathcal{B}_{pi}^{kl}-\mathcal{B}_{pi}^{(kl)^*}.\tag{3.70}$$

3.5.3 Perturbed Z-CPHF equations

For the contraction of the perturbed Lagrange multipliers $\mathbf{z}^{B_\alpha}$ with the ERIs one gets

$$\begin{aligned}
g\left(\mathbf{z}^{B_\alpha}\right)_{ia}&=-\frac{1}{2}\sum_{ck}\left[z_{ck}^{B_\alpha}(ik|ca)+z_{kc}^{B_\alpha}(ic|ka)\right]\\
&=-\frac{1}{2}\sum_{k}\left[(ik|\hat{ka})+(i\hat{k}|ka)\right]\\
&\overset{\mathrm{DF}}{=}-\frac{1}{2}\sum_{k}\sum_{P}\left[(\hat{ka}|P)c_{ik}^{P}+(i\hat{k}|P)c_{ka}^{P}\right],
\end{aligned}\tag{3.71}$$

where a hat denotes a contraction with the Lagrange multipliers, i.e.,

$$(ik|\hat{ka})=\sum_{c}z_{ck}^{B_\alpha}(ik|ca),\tag{3.72}$$

$$(i\hat{k}|ka)=\sum_{c}z_{kc}^{B_\alpha}(ic|ka).\tag{3.73}$$

In the last line of Eq. (3.71) fitting coefficients have been introduced,

$$c_{ik}^{P}=\sum_{Q}J_{PQ}^{-1}(Q|ik),\tag{3.74}$$

$$c_{ka}^{P}=\sum_{Q}J_{PQ}^{-1}(Q|ka).\tag{3.75}$$

Note that $\mathbf{z}^{B_\alpha}$ is a purely imaginary Hermitian quantity. Therefore, the contraction with the Coulomb integrals yields zero.
For the contraction of the unperturbed Lagrange multipliers $\mathbf{z}$ with the perturbed integrals on the right-hand side of Eq. (3.54) one finds

$$\begin{aligned}
\frac{\partial g(\mathbf{z})_{ia}}{\partial B_\alpha} &= \sum_{ck}\left(z_{ck}\left[\frac{\partial(ia|ck)}{\partial B_\alpha}-\frac{1}{2}\frac{\partial(ik|ca)}{\partial B_\alpha}\right]\right. \\
&\quad \left. + z_{kc}\left[\frac{\partial(ia|kc)}{\partial B_\alpha}-\frac{1}{2}\frac{\partial(ic|ka)}{\partial B_\alpha}\right]\right) \\
&\overset{\text{DF}}{=} \sum_P \left[c\left(\mathbf{Z}\right)\right]^P \frac{\partial(ia|P)}{\partial B_\alpha} \\
&\quad -\frac{1}{2}\sum_P\sum_{\mu\nu} Z_{\mu\nu}\frac{\partial(\mu a|P)}{\partial B_\alpha}c_{i\nu}^P \\
&\quad -\frac{1}{2}\sum_P\sum_{\mu\nu} Z_{\mu\nu}c_{\mu a}^P\frac{\partial(i\nu|P)}{\partial B_\alpha} \\
&\quad -\frac{1}{2}\sum_P\sum_{\mu\nu} \mathcal{Z}_{\mu\nu}^{B_\alpha}(\mu a|P)c_{i\nu}^P
\end{aligned} \tag{3.76}$$

with the density matrices $\mathbf{Z}$ and $\mathcal{Z}^{B_\alpha}$,

$$Z_{\mu\nu} = \sum_{ck}\left[C_{\mu c}^* z_{ck} C_{\nu k} + C_{\mu k}^* z_{kc} C_{\nu c}\right], \tag{3.77}$$

$$\begin{aligned}
\mathcal{Z}_{\mu\nu}^{B_\alpha} &= \sum_{ck}\left[\frac{\partial C_{\mu c}^*}{\partial B_\alpha} z_{ck} C_{\nu k} + C_{\mu c}^* z_{ck}\frac{\partial C_{\nu k}}{\partial B_\alpha}\right. \\
&\quad \left. + \frac{\partial C_{\mu k}^*}{\partial B_\alpha} z_{kc} C_{\nu c} + C_{\mu k}^* z_{kc}\frac{\partial C_{\nu c}}{\partial B_\alpha}\right],
\end{aligned} \tag{3.78}$$

the fitting coefficients

$$\left[c\left(\mathbf{Z}\right)\right]^P = \sum_Q\sum_{\mu\nu} Z_{\mu\nu} J_{PQ}^{-1}(Q|\mu\nu), \tag{3.79}$$

$$c_{i\nu}^P = \sum_Q J_{PQ}^{-1}(Q|i\nu), \tag{3.80}$$

$$c_{\mu a}^P = \sum_Q J_{PQ}^{-1}(Q|\mu a), \tag{3.81}$$

and the perturbed integrals

$$\frac{\partial(i\nu|P)}{\partial B_\alpha} = \sum_\mu \left(\frac{\partial C^*_{\mu i}}{\partial B_\alpha}(\mu\nu|P) + C^*_{\mu i}\frac{\partial(\mu\nu|P)}{\partial B_\alpha} \right), \tag{3.82}$$

$$\frac{\partial(\mu a|P)}{\partial B_\alpha} = \sum_\nu \left(\frac{\partial C_{\nu a}}{\partial B_\alpha}(\mu\nu|P) + C_{\nu a}\frac{\partial(\mu\nu|P)}{\partial B_\alpha} \right). \tag{3.83}$$

For the derivative of $\mathbf{y}$ (defined in Eq. 3.27) with respect to the magnetic field which occurs in the right-hand side of the perturbed Z-CPHF Eqs. (3.54) one obtains

$$\frac{\partial y_{ai}}{\partial B_\alpha} = \frac{\partial A_{ai}}{\partial B_\alpha} - \frac{\partial A^*_{ia}}{\partial B_\alpha} + \left[\frac{\partial \mathbf{a}(\mathbf{z}^{\mathrm{loc}})}{\partial B_\alpha} \right]_{ai}, \tag{3.84}$$

where

$$\begin{aligned} \frac{\partial A^*_{ia}}{\partial B_\alpha} = 2\Bigg[& \sum_c \sum_{kl} \left(\tilde{T}^{kl*}_{ac}\frac{\partial K^{kl}_{ic}}{\partial B_\alpha} + \frac{\partial \tilde{T}^{kl*}_{ac}}{\partial B_\alpha}K^{kl}_{ic} \right) \\ & + \sum_{ckl}\sum_{rs\rho} \frac{\partial}{\partial B_\alpha}\left(L^*_{\rho i} S_{\rho r} \tilde{T}^{kl}_{rs} Q_{cs} R^{kl*}_{ac} \right) \Bigg] \end{aligned} \tag{3.85}$$

and

$$\begin{aligned} \frac{\partial A_{ai}}{\partial B_\alpha} = 2\Bigg[& \frac{\partial B_{ai}}{\partial B_\alpha} + \left(\frac{\partial g(\mathbf{d}^{(2)})}{\partial B_\alpha} \right)_{ia} \\ & + \left(g\left(\left[\mathbf{d}^{(2)} \right]^{B_\alpha} \right) \right)_{ia} \Bigg] \end{aligned} \tag{3.86}$$

with the matrix $\partial\mathbf{B}/\partial B_\alpha$

$$\frac{\partial B_{ai}}{\partial B_\alpha} = \sum_{kcd} \left[\frac{\partial(ca|dk)}{\partial B_\alpha}\tilde{T}^{ik*}_{cd} + (ca|dk)\frac{\partial \tilde{T}^{ik*}_{cd}}{\partial B_\alpha} \right]. \tag{3.87}$$

Detailed equations for the quantities (3.85–3.87) in PAO basis applying density fitting are given in Section 3.5.4.

The contraction of the unperturbed LMP2 density matrix with the per-

turbed integrals in Eq. (3.86) yields

$$\begin{aligned}\left(\frac{\partial g(\mathbf{d}^{(2)})}{\partial B_\alpha}\right)_{ia} &= \sum_{pq}\left(d^{(2)}_{pq}\left[\frac{\partial(ia|pq)}{\partial B_\alpha} - \frac{1}{2}\frac{\partial(iq|pa)}{\partial B_\alpha}\right]\right)\\ &\overset{\text{DF}}{=} \sum_P \left[c\left(\mathbf{D}^{(2)}\right)\right]^P \frac{\partial(ia|P)}{\partial B_\alpha}\\ &\quad - \frac{1}{2}\sum_P\sum_{\mu\nu} D^{(2)}_{\mu\nu}\frac{\partial(\mu a|P)}{\partial B_\alpha}c^P_{i\nu}\\ &\quad - \frac{1}{2}\sum_P\sum_{\mu\nu} D^{(2)}_{\mu\nu}c^P_{\mu a}\frac{\partial(i\nu|P)}{\partial B_\alpha}\\ &\quad - \frac{1}{2}\sum_P\sum_{\mu\nu}\left[\mathcal{D}^{(2)}\right]^{B_\alpha}_{\mu\nu}(\mu a|P)c^P_{i\nu}\end{aligned} \tag{3.88}$$

with the LMP2 density matrices $\mathbf{D}$ and $\left[\mathcal{D}^{(2)}\right]^{B_\alpha}$,

$$D^{(2)}_{\mu\nu} = \sum_{pq} C^*_{\mu p} d^{(2)}_{pq} C_{\nu q}, \tag{3.89}$$

$$\left[\mathcal{D}^{(2)}\right]^{B_\alpha}_{\mu\nu} = \sum_{pq}\left[\frac{\partial C^*_{\mu p}}{\partial B_\alpha} d^{(2)}_{pq} C_{\nu q} + C^*_{\mu p} d^{(2)}_{pq}\frac{\partial C_{\nu q}}{\partial B_\alpha}\right], \tag{3.90}$$

and the fitting coefficients

$$\left[c\left(\mathbf{D}^{(2)}\right)\right]^P = \sum_Q\sum_{\mu\nu} D^{(2)}_{\mu\nu} J^{-1}_{PQ}(Q|\mu\nu). \tag{3.91}$$

Finally, the contraction of the density matrix with the ERIs in Eq. (3.86) can be written as

$$\begin{aligned}\left(g\left(\left[\mathbf{d}^{(2)}\right]^{B_\alpha}\right)\right)_{ia} &= -\frac{1}{2}\sum_{\mu\nu}\left[\mathscr{D}^{(2)}\right]^{B_\alpha}_{\mu\nu}(\mu a|i\nu)\\ &\overset{\text{DF}}{=} -\frac{1}{2}\sum_\mu \tilde{c}^P_{i\mu}(\mu a|P)\end{aligned} \tag{3.92}$$

with the density matrix

$$\left[\mathscr{D}^{(2)}\right]^{B_\alpha}_{\mu\nu} = \sum_{pq} C^*_{\mu p}\left[\mathbf{d}^{(2)}\right]^{B_\alpha}_{pq} C_{\nu q} \tag{3.93}$$

and the fitting coefficients

$$\tilde{c}_{i\mu}^{P} = \sum_{\nu} \left[\mathscr{D}^{(2)}\right]_{\mu\nu}^{B_\alpha} (i\nu|P). \tag{3.94}$$

Note that the contraction of the purely imaginary Hermitian density matrix $\left[\mathscr{D}^{(2)}\right]^{B_\alpha}$ with the Coulomb integrals in Eq. (3.92) yields zero, similar to the contraction of the perturbed Lagrange multipliers in Eq. (3.71).

3.5.4 Working equations in PAO basis

Working equations in PAO basis are derived by using the transformation matrix **Q** defined in Eq. (2.45) and the relations

$$T_{ab}^{ij} = \sum_{rs\in[ij]} Q_{ar} T_{rs}^{ij} Q_{bs}, \tag{3.95}$$

$$S_{rs} = \sum_{c} Q_{cr}^{*} Q_{cs}. \tag{3.96}$$

For the LMP2 residual matrix, Eq. (3.15), one finds

$$\begin{aligned} R_{rs}^{ij} = K_{rs}^{ij} &+ \sum_{tu} \left(S_{rt} T_{tu}^{ij} f_{su} + f_{rt} T_{tu}^{ij} S_{su} \right) \\ &- \sum_{k} \sum_{tu} \left(S_{rt} \left[f_{ki} T_{tu}^{kj} + f_{kj} T_{tu}^{ik} \right] S_{su} \right) \end{aligned} \tag{3.97}$$

and for the corresponding derivative with respect to the magnetic field

$$\begin{aligned}
\frac{\partial R_{rs}^{ij}}{\partial B_\alpha} = & \frac{\partial K_{rs}^{ij}}{\partial B_\alpha} \\
& + \sum_{tu} \left(\frac{\partial f_{rt}}{\partial B_\alpha} T_{tu}^{ij} S_{su} + f_{rt} \frac{\partial T_{tu}^{ij}}{\partial B_\alpha} S_{su} + f_{rt} T_{tu}^{ij} \frac{\partial S_{su}}{\partial B_\alpha} \right. \\
& + \frac{\partial S_{rt}}{\partial B_\alpha} T_{tu}^{ij} f_{su} + S_{rt} \frac{\partial T_{tu}^{ij}}{\partial B_\alpha} f_{su} + S_{rt} T_{tu}^{ij} \frac{\partial f_{su}}{\partial B_\alpha} \\
& - \sum_k \frac{\partial S_{rt}}{\partial B_\alpha} \left[f_{ki} T_{tu}^{kj} + f_{kj} T_{tu}^{ik} \right] S_{su} \\
& - \sum_k S_{rt} \left[\frac{\partial f_{ki}}{\partial B_\alpha} T_{tu}^{kj} + \frac{\partial f_{kj}}{\partial B_\alpha} T_{tu}^{ik} \right] S_{su} \\
& - \sum_k S_{rt} \left[f_{ki} \frac{\partial T_{tu}^{kj}}{\partial B_\alpha} + f_{kj} \frac{\partial T_{tu}^{ik}}{\partial B_\alpha} \right] S_{su} \\
& \left. - \sum_k S_{rt} \left[f_{ki} T_{tu}^{kj} + f_{kj} T_{tu}^{ik} \right] \frac{\partial S_{su}}{\partial B_\alpha} \right) = 0,
\end{aligned} \tag{3.98}$$

where the derivative of the exchange matrix in density fitting approximation can be written as

$$\frac{\partial K_{rs}^{ij}}{\partial B_\alpha} \overset{\text{DF}}{=} \sum_P \left(\frac{\partial (ri|P)}{\partial B_\alpha} c_{sj}^P + c_{ri}^P \frac{\partial (sj|P)}{\partial B_\alpha} \right) \tag{3.99}$$

with the fitting coefficients

$$c_{ri}^P = \sum_Q J_{PQ}^{-1} (Q|ri). \tag{3.100}$$

The LMP2 density matrix can be written as

$$\begin{aligned}
\left[\mathbf{d}^{(2)} \right]_{ij} &= -2 \sum_k \sum_{rstu} S_{rt} T_{tu}^{ik} S_{su} \tilde{T}_{rs}^{jk*}, \\
\left[\mathbf{d}^{(2)} \right]_{rs} &= 2 \sum_{kl} \sum_{tu} S_{ut} \tilde{T}_{ru}^{kl*} T_{st}^{kl},
\end{aligned} \tag{3.101}$$

and its derivative with respect to the magnetic field is given by

$$\begin{aligned}
\left[\mathbf{d}^{(2)}\right]_{ij}^{B_\alpha} &= -2\sum_{k}\sum_{rstu}\Bigg[\frac{\partial S_{rt}}{\partial B_\alpha}T_{tu}^{ik}S_{su}\tilde{T}_{rs}^{jk*} \\
&\quad + S_{rt}\frac{\partial T_{tu}^{ik}}{\partial B_\alpha}S_{su}\tilde{T}_{rs}^{jk*} + S_{rt}T_{tu}^{ik}\frac{\partial S_{su}}{\partial B_\alpha}\tilde{T}_{rs}^{jk*} \\
&\quad + S_{rt}T_{tu}^{ik}S_{su}\frac{\partial \tilde{T}_{rs}^{jk*}}{\partial B_\alpha}\Bigg], \\
\left[\mathbf{d}^{(2)}\right]_{rs}^{B_\alpha} &= 2\sum_{kl}\sum_{tu}\Bigg[\frac{\partial S_{ut}}{\partial B_\alpha}\tilde{T}_{ru}^{kl*}T_{st}^{kl} \\
&\quad + S_{ut}\frac{\partial \tilde{T}_{ru}^{kl*}}{\partial B_\alpha}T_{st}^{kl} + S_{ut}\tilde{T}_{ru}^{kl*}\frac{\partial T_{st}^{kl}}{\partial B_\alpha}\Bigg].
\end{aligned} \tag{3.102}$$

For the contractions of the exchange matrix with the LMP2 amplitudes on the right-hand side of the perturbed Z-CPHF equations (see Eq. 3.84 and the following ones) the quantity $\mathbf{X}^{\mathrm{K}}$ and its derivative with respect to the magnetic field $\partial\mathbf{X}^{\mathrm{K}}/\partial B_\alpha$ are defined,

$$X_{ai}^{\mathrm{K}} = \sum_{c}\sum_{kl}\tilde{T}_{ac}^{kl*}K_{ic}^{kl}, \tag{3.103}$$

$$\frac{\partial X_{ai}^{\mathrm{K}}}{\partial B_\alpha} = \sum_{c}\sum_{kl}\left(\tilde{T}_{ac}^{kl*}\frac{\partial K_{ic}^{kl}}{\partial B_\alpha} + \frac{\partial \tilde{T}_{ac}^{kl*}}{\partial B_\alpha}K_{ic}^{kl}\right). \tag{3.104}$$

These are related to the quantities in PAO basis by the transformation

$$X_{ai}^{\mathrm{K}} = \sum_{r\in[i]_{\mathrm{U}}} Q_{ar}^{*}X_{ri}^{\mathrm{K}}, \tag{3.105}$$

$$\frac{\partial X_{ai}^{\mathrm{K}}}{\partial B_\alpha} = \sum_{r\in[i]_{\mathrm{U}}}\left(Q_{ar}^{*}\frac{\partial X_{ri}^{\mathrm{K}}}{\partial B_\alpha} + \frac{\partial Q_{ar}^{*}}{\partial B_\alpha}X_{ri}^{\mathrm{K}}\right). \tag{3.106}$$

In Eqs. (3.105) and (3.106) the summation over the PAO index r is restricted to the united pair domain $[i]_{\mathrm{U}}$ which is the union of all pair domains $[ij]$ for a fixed index i.

When density fitting is employed to the matrices above one obtains

$$X^{\mathrm{K}}_{ri} = \sum_{kP} V^P_{kr}(P|ik), \tag{3.107}$$

$$\frac{\partial X^{\mathrm{K}}_{ri}}{\partial B_\alpha} = \sum_{kP}\left(\frac{\partial V^P_{kr}}{\partial B_\alpha}(P|ik) + V^P_{kr}\frac{\partial (P|ik)}{\partial B_\alpha}\right), \tag{3.108}$$

with the quantities

$$V^P_{kr} = \sum_l \sum_{s\in[kl]} \tilde{T}^{kl*}_{rs} c^P_{sl}, \tag{3.109}$$

$$\frac{\partial V^P_{kr}}{\partial B_\alpha} = \sum_l \sum_{s\in[kl]}\left(\frac{\partial \tilde{T}^{kl*}_{rs}}{\partial B_\alpha} c^P_{sl} + \tilde{T}^{kl*}_{rs}\frac{\partial c^P_{sl}}{\partial B_\alpha}\right), \tag{3.110}$$

where the perturbed fitting coefficients have been introduced,

$$\frac{\partial c^P_{sl}}{\partial B_\alpha} = \sum_Q J^{-1}_{PQ}\frac{\partial (Q|sl)}{\partial B_\alpha}. \tag{3.111}$$

The matrix $\mathbf{B}$ in Eq. (3.29) and its derivative $\partial\mathbf{B}/\partial B_\alpha$ in Eq. (3.86) are affected by density fitting as well. They are computed directly from the ERIs in AO basis,

$$B_{\nu i} = \sum_{\mu P} (\mu\nu|P) V^P_{i\mu}, \tag{3.112}$$

$$\frac{\partial B_{\nu i}}{\partial B_\alpha} = \sum_{\mu P}\left(\frac{\partial (\mu\nu|P)}{\partial B_\alpha} V^P_{i\mu} + (\mu\nu|P)\frac{\partial V^P_{i\mu}}{\partial B_\alpha}\right), \tag{3.113}$$

with

$$V^P_{i\mu} = \sum_{r\in[i]_{\mathrm{U}}} V^P_{ir} P^*_{\mu r}, \tag{3.114}$$

$$\frac{\partial V^P_{i\mu}}{\partial B_\alpha} = \sum_{r\in[i]_{\mathrm{U}}}\left(\frac{\partial V^P_{ir}}{\partial B_\alpha} P^*_{\mu r} + V^P_{ir}\frac{\partial P^*_{\mu r}}{\partial B_\alpha}\right), \tag{3.115}$$

where $P_{\mu r}$ is the PAO coefficient matrix as defined in Eq. (2.44).

3.6 Accuracy and Performance

The new GIAO-DF-LMP2 program has been implemented in the MOLPRO program package [49, 50]; the correctness of the implementation has been verified by comparing shielding tensors calculated with full domains and unrestricted pair lists to the corresponding canonical result obtained with the CFOUR program [84].

Most of the time-critical subroutines of the new GIAO-DF-LMP2 program are parallelized based on a simple shared file approach: the scratch files containing integrals, fitting coefficients, and amplitudes reside on two file systems common to all parallel threads. Input/output (I/O) operations are organized such that both file systems are in use, e.g., one for reading, the other one for writing. The I/O of course does not scale with the number of processors/cores and becomes a bottleneck beyond 8 cores, depending on the efficiency of the I/O subsystem.

As mentioned in the introduction chemical shifts at the level of MP2 usually provide an improvement over results at the level of Hartree-Fock. Figure 3.1 shows the deviations of chemical shieldings calculated at the levels of GIAO-DF-HF and GIAO-DF-LMP2 with a cc-pVQZ basis set from experimental ^{13}C gas-phase shieldings measured in the zero-pressure limit [85]. The error of the Hartree-Fock results is particularly large for molecules with large correlation effects (see Table 3.1). For this set of small to medium-sized molecules the error of the LMP2 shieldings is typically one order of magnitude smaller than the error made by Hartree-Fock. However, one should bear in mind that chemical shifts are calculated relative to a reference substance which allows for the cancellation of systematic errors. This often makes the Hartree-Fock chemical shifts surprisingly good, even for larger molecules.

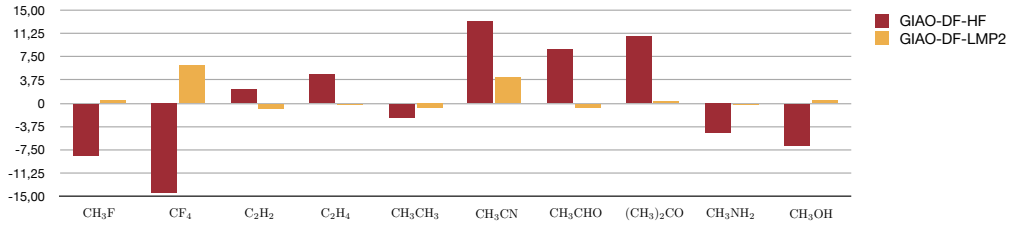

Figure 3.1: Deviation of calculated shieldings (cc-pVQZ basis set) at the levels of GIAO-DF-HF and GIAO-DF-LMP2 from experimental ^{13}C gas-phase shieldings [85] (in ppm).

This section discusses the effects of local approximation and density fitting on the calculated shieldings, i.e., the accuracy of the new GIAO-DF-LMP2 method. Furthermore, illustrating calculations on several more extended molecular systems are presented to demonstrate the efficiency and capabilities of the new program. The influence of the local approximation and of density fitting on the accuracy of the chemical shieldings was investigated by performing a series of test calculations on a set of small molecules which was already utilized previously when presenting the GIAO-DF-HF method [68]. The geometries of these test molecules were optimized at the MP2 level in the cc-pVTZ AO basis set. Core electrons were not correlated (frozen-core approximation).

Table 3.1 compiles the GIAO-DF-LMP2 ^{13}C, ^{15}N, and ^{17}O chemical shieldings of the test set calculated in the cc-pVXZ (X=D, T, and Q) AO basis sets [86–91] with the related JK- [92] and MP2-fitting basis sets [93]. Local calculations with standard domains [60] are compared to calculations with full domains (the latter are equivalent to canonical calculations, since the pair list remains untruncated for all molecules of the test set). The correlation contribution to the chemical shieldings, also included in Table 3.1, is calculated as the difference between the GIAO-DF-LMP2 full domain result and the shielding constant obtained with the GIAO-DF-HF method. The correlation contributions are modest for most of the molecules of the

test set and range up to 30 ppm. Exceptions are the ^{17}O chemical shieldings of acetone and acetaldehyde with a correlation contribution of 60–100 ppm. The deviations of the local from the full domain results are small, i.e., in the range of 1 ppm, which is much smaller than the method error of MP2 itself. As expected, the local error also becomes smaller for larger AO basis sets since a larger set provides a more flexible basis on the few centers included in a pair domain.

In order to explore the effect of pair list truncation on the shielding tensors calculations on a linear glycine chain with four monomers (1176 orbital pairs) with cc-pVXZ (X=D and T) and aug-cc-pVDZ AO basis sets and the related JK- and MP2-fitting basis were carried out. The calculations with the augmented basis set were performed with the `MOLPRO` option `cpldel=1`, i.e., the contributions of the most diffuse functions were discarded in the Pipek-Mezey localization matrices Eq. (3.20) [94]. Different thresholds for the truncation of the pair list were investigated: test calculations were performed for which pairs with an interorbital distance beyond 10, 15 (default value for local calculations in `MOLPRO`), and 20 bohrs were omitted. The results were then compared to calculations with all pairs included as a benchmark. The maximum absolute errors for the different elements are collected in Table 3.2. Even for a truncation threshold of 10 bohrs at which 441 orbital pairs are omitted the maximum absolute errors are very small, i.e., at most 0.04 ppm for ^{17}O-shieldings using cc-pVTZ basis set and 0.21 ppm for ^{17}O-shieldings using aug-cc-pVDZ basis set. By increasing the threshold to 15 bohrs the errors become negligibly small with deviations of at most 0.05 ppm for ^{17}O-shieldings using aug-cc-pVDZ basis set. Thus, the default choice to omit pairs beyond an interorbital distance of 15 bohrs is found to be well justified by the test calculations; including pairs up to greater interorbital distances (of 20 bohrs or even more) does not seem to be necessary.

Table 3.1: Error introduced by the local approximation to chemical shieldings (in ppm) at the level of GIAO-DF-LMP2: comparison of local calculations and calculations with full domains and untruncated pair lists. For all calculations the frozen-core approximation was employed.

Basis	cc-pVDZ			cc-pVTZ			cc-pVQZ		
	local	full	$\sigma_{\mathrm{MP2}}^{\mathrm{correl\ a)}}$	local	full	$\sigma_{\mathrm{MP2}}^{\mathrm{correl\ a)}}$	local	full	$\sigma_{\mathrm{MP2}}^{\mathrm{correl\ a)}}$
^{13}C-Shieldings									
C_2H_2	143.22	143.64	12.79	128.07	128.36	10.78	126.04	126.00	10.52
C_2H_4	95.02	94.87	17.88	76.58	76.70	12.95	73.03	72.97	12.57
C_2H_6	200.49	199.55	5.14	190.35	190.33	4.87	188.79	188.57	4.82
CH_3OH	159.66	158.84	0.94	145.91	145.74	-0.41	143.30	143.12	-0.85
CH_3NH_2	179.14	178.39	2.81	167.68	167.60	2.03	165.70	165.49	1.83
$CH_3\underline{C}N$	101.72	101.42	21.09	81.50	81.77	16.89	77.67	77.71	16.66
$(CH_3)_2\underline{C}O$	23.58	23.54	29.43	1.52	1.62	19.52	-4.89	-4.91	18.45
$CH_3\underline{C}HO$	32.02	31.91	27.62	8.52	8.54	18.59	2.52	2.50	17.32
CO_2	90.79	90.78	21.77	68.86	69.09	17.65	66.08	66.17	17.10
$Si(CH_3)_4$	208.98	207.19	5.77	197.50	196.83	4.59	195.82	195.32	4.34
CH_3F	141.88	141.57	0.72	126.41	126.17	-1.45	123.67	123.53	-2.23
^{15}N-Shieldings									
CH_3CN	44.41	44.29	68.12	16.12	16.13	60.87	13.67	13.89	61.76
CH_3NH_2	273.99	273.12	9.14	265.29	265.06	10.70	264.02	263.53	11.49
NH_3	290.53	290.04	11.77	281.79	282.54	13.37	279.27	279.39	13.88
^{17}O-Shieldings									
CH_3OH	362.43	360.74	8.22	355.34	354.95	11.38	354.74	354.38	12.57
$(CH_3)_2CO$	-243.71	-244.78	77.44	-277.14	-276.88	57.94	-274.02	-273.79	62.43
CH_3CHO	-252.04	-252.30	101.23	-286.36	-286.25	79.80	-282.29	-282.21	84.51
CO_2	258.87	258.54	31.82	239.70	240.13	26.07	240.50	240.59	26.00
H_2O	362.86	362.56	15.40	351.45	352.16	17.26	348.46	348.83	18.09

a) Correlation effects covered by MP2 calculated as the difference between the GIAO-DF-LMP2 result for full domains including all pairs and the GIAO-DF-HF result.

Table 3.2: Influence of the threshold for omitting orbital pairs on chemical shieldings (in ppm). The maximum absolute errors (MaxAE) relative to calculations with all 1176 orbital pairs included are provided. For all calculations the frozen-core approximation was employed.

Basis	cc-pVDZ			aug-cc-pVDZ			cc-pVTZ		
Threshold / bohr	10	15	20	10	15	20	10	15	20
Number of omitted pairs	441	252	116	441	252	116	441	252	116
MaxAE ^{1}H-Shieldings	0.00	0.00	0.00	0.01	0.01	0.00	0.01	0.00	0.00
MaxAE ^{13}C-Shieldings	0.01	0.00	0.00	0.11	0.03	0.00	0.01	0.01	0.00
MaxAE ^{15}N-Shieldings	0.02	0.00	0.00	0.06	0.02	0.01	0.02	0.01	0.01
MaxAE ^{17}O-Shieldings	0.01	0.00	0.00	0.21	0.05	0.03	0.04	0.02	0.00

Table 3.3 compares the GIAO-DF-LMP2 ^{13}C, ^{15}N, and ^{17}O chemical shieldings of the test set for different fitting basis sets. The calculations in the cc-pVXZ (X=D, T, and Q) AO basis sets were carried out employing the JK- and MP2-fitting sets related to the cc-pVXZ, cc-pV(X+1)Z, and cc-pV(X+2)Z (where available) AO basis sets. The latter can be considered as the reference; it has been verified in the course of this work that shielding constants calculated in the cc-pVDZ AO basis with fitting sets related to cc-pVQZ are virtually identical to shielding constants calculated without DF approximation.

From a comparison of the shielding constants calculated in the same AO basis but with different fitting sets it is evident that the fitting error is negligibly small. It amounts to 0.1 ppm or less for most cases and decreases even further when increasing the size of the fitting basis set from X=D to X=T and X=Q. Slightly larger fitting errors are observed for the ^{17}O chemical shieldings of acetone and acetaldehyde (about 0.5 ppm for the cc-pVDZ calculations) which is attributed to the larger correlation effects in these two molecules. Nevertheless, increasing the cardinal number of the employed fitting set relative to that of the AO basis, e.g., using the fitting sets related to cc-pVTZ when using the cc-pVDZ AO basis seems needless. Thus, the use of ordinary Gaussians as fitting functions, which corresponds to the fitting of orbital product densities in the ERIs at zero

Table 3.3: Influence of the fitting basis set on chemical shieldings (in ppm) at the level of GIAO-DF-LMP2. For all calculations the frozen-core approximation was employed.

Basis	cc-pVDZ			cc-pVTZ			cc-pVQZ	
Fitting basis	VDZ	VTZ	VQZ	VTZ	VQZ	V5Z	VQZ	V5Z
^{13}C-Shieldings								
C_2H_2	143.22	143.25	143.25	128.07	128.08	128.08	126.04	126.05
C_2H_4	95.02	95.07	95.08	76.58	76.60	76.60	73.03	73.03
C_2H_6	200.49	200.51	200.52	190.35	190.35	190.35	188.79	188.79
CH_3OH	159.66	159.69	159.70	145.91	145.92	145.92	143.30	143.31
CH_3NH_2	179.14	179.17	179.18	167.68	167.69	167.69	165.70	165.70
$CH_3\underline{C}N$	101.72	101.76	101.76	81.50	81.51	81.51	77.67	77.67
$(CH_3)_2\underline{C}O$	23.58	23.69	23.71	1.52	1.57	1.57	-4.89	-4.88
$CH_3\underline{C}HO$	32.02	32.12	32.14	8.52	8.56	8.56	2.52	2.53
CO_2	90.79	90.82	90.82	68.86	68.87	68.87	66.08	66.08
$Si(CH_3)_4$	208.98	209.02	209.03	197.50	197.50	197.50	195.82	195.82
CH_3F	141.88	141.92	141.93	126.41	126.42	126.42	123.67	123.67
^{15}N-Shieldings								
CH_3CN	44.41	44.43	44.45	16.12	16.15	16.15	13.67	13.68
CH_3NH_2	273.99	274.02	274.02	265.29	265.31	265.30	264.02	264.02
NH_3	290.53	290.51	290.51	281.79	281.80	281.81	279.27	279.27
^{17}O-Shieldings								
CH_3OH	362.43	362.49	362.51	355.34	355.35	355.35	354.74	354.75
$(CH_3)_2CO$	-243.71	-243.36	-243.33	-277.14	-276.95	-276.93	-274.02	-273.96
CH_3CHO	-252.04	-251.66	-251.62	-286.36	-286.20	-286.17	-282.29	-282.24
CO_2	258.87	258.94	258.96	239.70	239.73	239.73	240.50	240.51
H_2O	362.86	362.83	362.83	351.45	351.46	351.46	348.46	348.49

magnetic field strength, works very well for the GIAO-DF-LMP2 method, as it does for GIAO-DF-HF [68].

In order to demonstrate the computational performance and the capabilities of the new implementation calculations on three more extended molecular systems are presented: (*i*) coronene, (*ii*) a tweezer host-guest complex 1@2 "clinching" the 1,4-dicyanobenzene guest molecule 2, and (*iii*) a photodamaged cyclobutane pyrimidine dimer (CPD) lesion with adjacent nucleobases in the native intrahelical DNA double strand and its undamaged analogue with two pyrimidines (TpT). The geometries of these three systems are displayed in Figs. 3.2 and 3.3.

Experimental chemical shifts of coronene and the 1@2 tweezer, as well

as calculations thereof at the HF level are available in the literature (see Refs. [68, 95, 96] and references therein). The 1@2 tweezer host-guest complex was first investigated by Brown et al. [96] and also used as a test case for the GIAO-DF-HF method [68]. However, to the author's knowledge, no shift calculations beyond the HF level have been carried out for these systems so far. The geometries of coronene and the 1@2 tweezer used for the present shielding calculations are the same as those in Ref. [68]. Shielding calculations in the cc-pVDZ and the cc-pVTZ AO basis with related fitting sets were carried out.

Table 3.4 compiles the calculated ^{1}H chemical shifts of coronene and the 1@2 tweezer, respectively, as well as the timings (CPU and elapsed times) for individual key steps of the calculation. These include the iterative solution of the perturbed amplitudes Eqs. (3.98) and the perturbed Z-CPHF Eqs. (3.53) (normed to ten iterations each), the construction of the related right-hand sides (Eq. 3.54 for the perturbed Z-CPHF), and the solution of the perturbed Z-CPL Eqs. (3.55). Additionally, the table provides the total time for the calculation of the unperturbed density matrix (Eq. 3.18) and of the perturbed density matrix (Eq. 3.34) added up for the three components of the magnetic field.

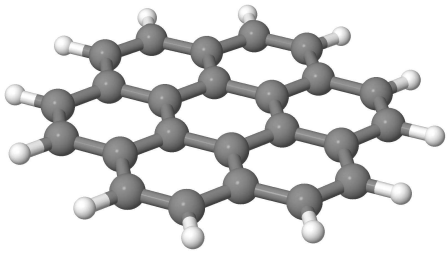

(*i*) Coronene, 36 atoms, 108 valence electrons
396/1956/1512 basis/JKfit/MP2fit functions (cc-pVDZ)
888/2256/2304 basis/JKfit/MP2fit functions (cc-pVTZ)

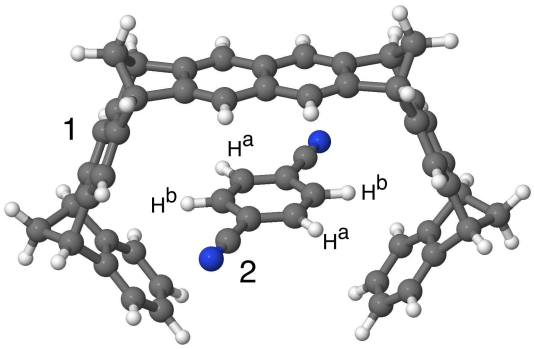

(*ii*) Tweezer host-guest complex 1@2,
with 2=1,4-dicyanobenzene,
92 atoms, 262 valence electrons
964/4748/3640 basis/JKfit/MP2fit functions (cc-pVDZ)
2184/5504/5616 basis/JKfit/MP2fit functions (cc-pVTZ)

Figure 3.2: Example molecules, (*i*) coronene and (*ii*) tweezer host-guest complex 1@2 with 1,4-dicyanobenzene as guest molecule 2.

Table 3.4: GIAO-DF-LMP2 chemical shifts (in ppm) for coronene and the 1@2 tweezer molecule using the frozen-core approximation. ^{1}H chemical shifts are relative to TMS[a)]. The CPU times (per processor) and the elapsed times measured for the individual key steps of the GIAO-DF-LMP2 calculation and the total times for the calculation of the unperturbed density matrix and the perturbed density matrix are provided. All timings of the perturbed equations are added up for the three components of the magnetic field[b)].

	cc-pVDZ	cc-pVTZ
Coronene		
H	8.5	8.8
R.H.S. of the perturbed amplitude Eqs. (3.98)		
CPU (elapsed) time / min	4 (8)	29 (34)
Iterating perturbed amplitude equations[c)]		
CPU (elapsed) time / min	10 (12)	90 (95)
R.H.S. of the perturbed Z-CPHF Eqs. (3.54)		
CPU (elapsed) time / min	19 (20)	115 (118)
Iterating perturbed Z-CPHF Eqs. (3.53)[c)]		
CPU (elapsed) time / min	5 (6)	12 (14)
Solving the perturbed Z-CPL Eqs. (3.55)		
CPU (elapsed) time / sec	2 (2)	4 (4)
Perturbed density total CPU (elapsed) time / min	37 (46)	239 (256)
Unperturbed density total CPU (elapsed) time / min	3 (4)	11 (13)
1@2 Tweezer		
H 2,3,14,15	6.1	6.3
H_{arom}(host)	6.6-7.1	6.7-7.7
$H_{bridgehead}$	3.4-3.6	3.6-3.8
H 25,28	1.8	2.0-2.2
H 26,27	1.6-1.8	1.9-2.0
R.H.S. of the perturbed amplitude Eqs. (3.98)		
CPU (elapsed) time / min	42 (73)	228 (394)
Iterating perturbed amplitude equations[c)]		
CPU (elapsed) time / min	39 (47)	330 (343)
R.H.S. of the perturbed Z-CPHF Eqs. (3.54)		
CPU (elapsed) time / min	223 (300)	956 (1645)
Iterating perturbed Z-CPHF Eqs. (3.53)[c)]		
CPU (elapsed) time / min	81 (112)	245 (898)
Solving the perturbed Z-CPL Eqs. (3.55)		
CPU (elapsed) time / min	4.0 (4.0)	4.2 (4.3)
Perturbed density total CPU (elapsed) time / min	419 (576)	1859 (3705)
Unperturbed density total CPU (elapsed) time / min	50 (61)	183 (590)

a) TMS optimized at MP2/cc-pVTZ level,
isotropic shielding constants: 31.4 (cc-pVDZ), 31.3 (cc-pVTZ).
b) Calculations were performed on 8 CPUs of an AMD Opteron 6180 SE @ 2.50 GHz.
c) Time for 10 iteration steps.

Table 3.5: GIAO-DF-LMP2 and in parentheses GIAO-DF-HF chemical shifts (in ppm) for the photodamaged cyclobutane pyrimidine dimer lesion (CPD) and its repaired analogue with pyrimidine (TpT) using the frozen-core approximation. ^{1}H chemical shifts are relative to TMS[a)]. The CPU times (per processor) and the elapsed times measured for the individual key steps of the GIAO-DF-LMP2 calculation and the total times for the calculation of the unperturbed density matrix and the perturbed density matrix are provided. All timings of the perturbed equations are added up for the three components of the magnetic field[b)].

	aVDZ	aVTZ
Photodamaged DNA (CPD)		
H_1	8.9 (9.1)	9.1 (9.2)
H_2	15.9 (16.8)	16.3 (17.2)
H_3	9.2 (9.4)	9.4 (9.6)
H_4	10.6 (11.1)	10.8 (11.3)
R.H.S. of the perturbed amplitude Eqs. (3.98)		
CPU (elapsed) time / min	84 (158)	489 (826)
Iterating perturbed amplitude equations[c)]		
CPU (elapsed) time / min	90 (102)	829 (848)
R.H.S. of the perturbed Z-CPHF Eqs. (3.54)		
CPU (elapsed) time / min	425 (978)	2051 (3420)
Iterating perturbed Z-CPHF Eqs. (3.53)[c)]		
CPU (elapsed) time / min	163 (323)	478 (1590)
Solving the perturbed Z-CPL Eqs. (3.55)		
CPU (elapsed) time / min	2.5 (2.5)	1.4 (1.8)
Perturbed density total CPU (elapsed) time / min	827 (1690)	4118 (7585)
Unperturbed density total CPU (elapsed) time / min	103 (163)	365 (1182)
repaired form TpT		
H_1	8.1 (8.2)	8.2 (8.3)
H_2	16.1 (17.0)	16.7 (17.4)
H_3	10.9 (11.0)	11.1 (11.2)
H_4	15.6 (16.2)	16.0 (16.6)
R.H.S. of the perturbed amplitude Eqs. (3.98)		
CPU (elapsed) time / min	82 (158)	511 (816)
Iterating perturbed amplitude equations[c)]		
CPU (elapsed) time / min	90 (101)	905 (957)
R.H.S. of the perturbed Z-CPHF Eqs. (3.54)		
CPU (elapsed) time / min	431 (974)	2152 (3268)
Iterating perturbed Z-CPHF Eqs. (3.53)[c)]		
CPU (elapsed) time / min	161 (317)	483 (1529)
Solving the perturbed Z-CPL Eqs. (3.55)		
CPU (elapsed) time / min	2.3 (2.3)	3.9 (6.0)
Perturbed density total CPU (elapsed) time / min	827 (1678)	4308 (7385)
Unperturbed density total CPU (elapsed) time / min	99 (177)	360 (1147)

a) TMS optimized at MP2/cc-pVTZ level,
isotropic shielding constants for GIAO-DF-HF: 31.7 (cc-pVDZ), 31.6 (cc-pVTZ),
isotropic shielding constants for GIAO-DF-LMP2: 31.4 (cc-pVDZ), 31.3 (cc-pVTZ).
b) Calculations were performed on 8 CPUs of an AMD Opteron 6180 SE @ 2.50 GHz.
c) Time for 10 iteration steps.

Table 3.5 compiles the corresponding data for the third example, the CPD lesion and the corresponding undamaged TpT analogue in the ATTA sequence of the DNA double strand. The CPD lesion is an important type of mutagenic photoproducts in DNA caused by solar irradiation in the UV spectral range and the repair of these photolesions is of major importance for the survival of organisms. The intermolecular interactions between either CPD or TpT and the adjacent nucleobases in ATTA were previously studied by means of hybrid quantum mechanics/molecular mechanics (QM/MM) and density-functional theory symmetry-adapted perturbation theory (DFT-SAPT) [79]. It turned out that the intermolecular interactions (hydrogen bonds and π-stacking) are 6 kcal/mol larger for the undamaged TpT form in ATTA than for the CPD form. This destabilization of CPD vs. TpT in the DNA strand is almost exclusively related to a weakening of the hydrogen bonds between CPD and one of its adjoining adenines. This work presents NMR chemical shift calculations for the geometry of frame A in Ref. [79], using the cc-pVXZ (X=D and T) basis sets with additional diffuse functions on O and N, i.e., for C and H the cc-pVXZ, and for O and N the aug-cc-pVXZ basis sets were used. These mixed basis sets are denoted by aVXZ (X=D and T). The related JK- and MP2-fitting basis sets were employed. It is evident from Table 3.5 that the ^{1}H chemical shift of H_4 decreases substantially from 16.0 ppm (TpT) to 10.8 ppm (CPD), whereas the shifts of the other protons participating in the hydrogen bonds are hardly affected. This observation is also well reproduced by the GIAO-DF-HF results. The reduction in the ^{1}H chemical shift is a clear sign, that the hydrogen bond involving H_4 is significantly weaker in the CPD lesion than in the TpT lesion. Generally, low field shift of a ^{1}H resonance is an indicator for a stronger hydrogen bond. The observed decrease of the ^{1}H chemical shift of H_4 thus is in line with the conclusions of Ref. [79].
In the following the timings reported in Tables 3.4 and 3.5 will be discussed: all presented calculations were performed on 8 CPUs of an AMD Opteron 6180 SE @ 2.50 GHz without exploiting point group symmetry. The largest

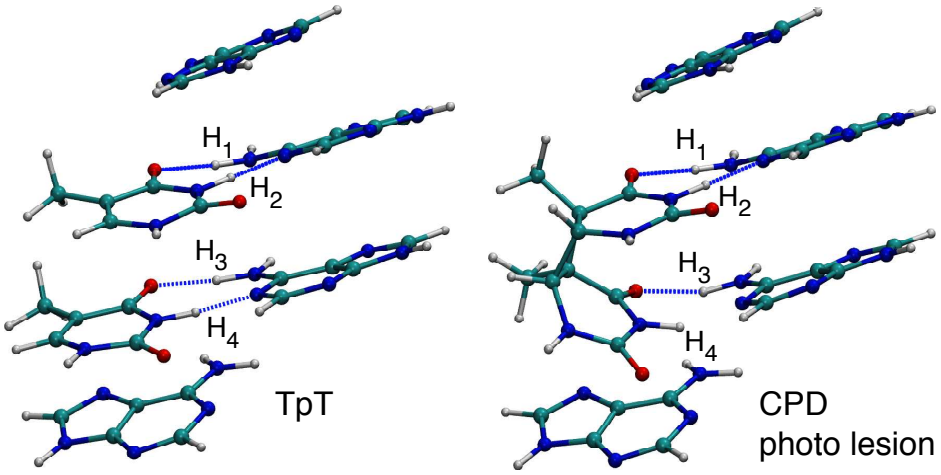

Example Molecule (*iii*): Photodamaged DNA
and its repaired analogue,
90 atoms, 296 valence electrons
1224/5244/4144 basis/JKfit/MP2fit functions (aVDZ)
2636/6242/6358 basis/JKfit/MP2fit functions (aVTZ)

Figure 3.3: Photodamaged DNA as an example molecule.

calculations carried out for TpT and CPD in the ATTA sequence involve 2636 AO basis functions and 296 correlated electrons. Evidently, solving the perturbed amplitude equations, which constitutes the computational bottleneck in canonical GIAO-MP2 calculations, becomes rather inexpensive for the local method, as expected. Furthermore, the computational cost for solving the perturbed Z-CPL equations is entirely negligible. The most expensive step, also in terms of I/O overhead, is the construction of the right-hand side of the perturbed Z-CPHF equations and the subsequent iterative solution of these equations. The reason for the massive I/O is the contraction of the unperturbed and perturbed density matrices and Lagrange multipliers with the perturbed and unperturbed ERIs (see Eqs. 3.71, 3.76, 3.88, and 3.92). This requires the repeated reading of four different sets of half-transformed integrals and four different sets of half-transformed fitting coefficients from disk for each component of the

magnetic field. Nevertheless, the presented method is quite efficient and opens the door to shielding calculations of systems like the last example, which were inaccessible for a treatment at the correlated level so far.

3.7 Conclusions

In this chapter an efficient program for the calculation of correlated NMR shielding tensors at the level of local MP2 has been presented. Gauge-including atomic orbitals (GIAOs or London atomic orbitals) are used to expand the molecular orbitals in order to eliminate the gauge origin problem (which arises from the incompleteness of the AO basis set). Density fitting is employed to factorize the electron repulsion integrals. Ordinary Gaussians can be used as fitting functions, which corresponds to density fitting at zero magnetic field strength. The fitting errors turn out to be entirely negligible. By virtue of the local ansatz the construction of the right-hand side of the perturbed amplitude equations and the subsequent iterative solution becomes rather inexpensive. The most expensive step of the present implementation also (and mainly) due to I/O overhead is the construction of the right-hand side of the perturbed Z-CPHF equations and the subsequent iterative solution of these equations. This I/O overhead is caused by many different sets of perturbed and unperturbed three-index objects which have to be read for these steps.

As already anticipated on the basis of previous work by Gauss and Werner, the accuracy of the local approximation is very good. Even with ordinary (non-extended) Boughton-Pulay domains the calculated shieldings deviate from canonical reference values only by a few tenths of a ppm. The performance of the GIAO-DF-LMP2 program is illustrated by test calculations on some extended systems; the largest thereof comprises 2636 basis functions, 90 atoms, and 296 correlated electrons. These are systems which were previously not accessible for shielding calculations at a correlated level.

Chapter 4

MAGNETIZABILITY TENSORS

4.1 Introduction

The last decades have seen an increasing demand for theoretical tools to accurately predict experimentally accessible quantities. Some of the most versatile tools are based on molecular magnetic properties like nuclear magnetic resonance (NMR) and electron paramagnetic resonance (EPR) spectroscopy for which many highly accurate and efficient ab-initio methods have been developed. Besides this there are numerous other magnetic properties like the molecular magnetizability tensor and the closely related rotational g tensor, which arises from the coupling of molecular rotational motion to electronic motion [47, 48, 97]. Rotational g tensors are discussed in detail in Chapter 5. The accurate treatment of magnetic properties is complicated by two major issues: (*i*) the gauge origin problem for approximate wave functions and (*ii*) the unfavorably high scaling behavior of correlated wave function methods and especially their derivatives.
Calculations of molecular magnetic properties with ordinary atomic orbital (AO) basis sets are hampered by slow convergence towards the basis set limit and the dependence of the results on the choice of an arbitrary gauge origin. This implies that the quality might crucially depend on the choice of the gauge origin and that the specific choice would have to be

reported for reproducible results [51]. The most common way to overcome this problem is by employing gauge-including atomic orbitals (GIAOs or London atomic orbitals) [23]. This ansatz was proposed by F. London in the context of molecular magnetizabilities: ordinary (Gaussian) AO basis functions are multiplied with a phase factor which shifts the gauge origin from the center of the atom where the function is located to a global origin. GIAOs ensure fast convergence to the basis set limit [69, 98] particularly for magnetizabilities [99], the second-order response of the system with respect to the externally applied magnetic field. Furthermore, the explicit dependence on the gauge origin cancels in integral expressions (including integrals involving the kinetic energy operator [59]), rendering the results gauge origin independent by construction.

In the case of frequency-dependent magnetic perturbations gauge origin independence can be ensured by the use of time-dependent GIAOs [100, 101]. Implementations of time-dependent GIAOs in the framework of density-functional theory (DFT) for static and dynamic magnetizabilities and optical rotations have been reported in Refs. [101] and [102]. The presented methods therein employ Slater-type orbitals and density fitting.

As an alternative to GIAOs, Schindler and Kutzelnigg proposed the individual gauge for localized orbitals (IGLO) approach [55, 56] which attempts to tackle the gauge origin problem by introducing separate gauge origins for localized molecular orbitals (LMOs). Furthermore, Lazzeretti et al. proposed the "continuous transformation of the origin of the current density" (CTOCD) method to overcome the gauge origin problem [103]. This approach has been implemented for magnetizabilities and NMR shielding tensors at the level of Hartree-Fock [104]. Furthermore, CTOCD NMR shielding tensors were reported at the levels of multi-configurational self-consistent field (MCSCF) theory, the second-order polarization propagator approximation (SOPPA), and SOPPA with coupled-cluster singles and doubles amplitudes (SOPPA(CCSD)) [105].

The GIAO ansatz has been used in a variety of approaches: in the late

1950s Hameka calculated the magnetic susceptibility and nuclear magnetic shielding constant of H_2 [106–108]. The first implementation of a Hartree-Fock program for nuclear magnetic shieldings was presented by Ditchfield [71], the implementation of a really efficient program was later achieved by Woliński, Hinton, and Pulay [58]. The first implementation of magnetizabilities at the level of Hartree-Fock was presented by Ruud et al. [72]. The calculation of nuclear magnetic shielding tensors in the GIAO framework has been implemented for a multitude of electron correlation methods, among them MCSCF theory [24], Møller-Plesset perturbation theory up to fourth-order [25, 26] and coupled-cluster implementations including up to triples and quadruples excitations [27–30].
Electron correlation methods for magnetizabilities within the GIAO framework have been reported for density-functional theory [109], MCSCF theory [110], and coupled-cluster (CC) theory [111]. Bishop et al. presented a second-order Møller-Plesset perturbation theory (MP2) implementation for magnetizabilities and rotational g tensors which ensured gauge invariance through sum rules applied to a gauge-dependent calculation using ordinary AO basis functions [112]. It has been shown that the correlation contributions to magnetizabilities of (organic) molecules are modest, i.e., in the range of a few percent, and molecules with large electron correlation contributions in the energy like CO and N_2 show modest correlation contributions to the magnetizability tensors (in the range of 5–8 %) [44, 111, 112]. However, ozone shows significantly greater contributions from electron correlation [111]. Other exceptions are the first row hydrides BeH^-, BH and CH^+ for which Sauer et al. showed that the consideration of electron correlation effects is important [113].
The above mentioned canonical electron correlation methods for NMR shielding constants and magnetizabilities all show an unfavorably high scaling behavior of the computational complexity which keeps many larger and potentially interesting molecules out of reach. In previous works S. Loibl et al. presented efficient methods for the calculation of NMR shield-

ing tensors at the levels of density fitted (local) HF and density fitted local MP2 (LMP2) employing GIAOs [35, 68]. The errors introduced by the local approximation are small, i.e., in the range of 1 ppm for ^{13}C chemical shieldings. The magnitude of the deviations are in good agreement with the quality of ground state energies [10–16], gradients [17], and properties of excited states [18–22] in the local approximation. Furthermore, the MP2 approximation for NMR chemical shifts provides nearly quantitative accuracy for molecules with small correlation effects up to 30 ppm, but overestimates the effects for molecules with large correlation contributions. Overall, MP2 provides usually significantly better results than HF shift calculations, especially for molecules with multiple bonds involving atoms with lone pairs [78].

In this work magnetizabilities and rotational g tensors are presented at the level of LMP2 employing GIAOs as basis functions in combination with density fitting (DF). The approach is based on the GIAO-DF-LMP2 method for NMR shielding tensors (see Chapter 3). It was shown by Loibl and Schütz how to introduce density fitting for the NMR shielding tensors at the levels of Hartree-Fock [68] and LMP2 [35]. Ordinary Gaussians can be employed as fitting functions for the orbital product densities in the electron repulsion integrals which corresponds to fitting in the limit of zero magnetic field strength in which the NMR shielding tensor as well as magnetizabilities and rotational g tensors are evaluated. GIAOs as fitting functions would inevitably violate gauge origin independence (for details see Sections 2.2 and 2.4).

In Section 4.2 the formalism for magnetizabilities at the level of DF-HF is derived. Furthermore, terms which involve density fitting, i.e., the contraction of electron repulsion integrals with density matrices are shown in detail. Section 4.3 shows the formalism for magnetizabilities at the level of DF-LMP2. Since this is similar to the formalism for DF-LMP2 NMR shielding tensors (see Chapter 3) repetitions are avoided to a great extent and extra attention is paid to the differences in the formalisms of the two

quantities. Section 4.4 shows test calculations which assess the accuracy and performance of the new program. Finally, AO derivative integrals which have not yet appeared for the NMR shielding tensors are presented in Section 4.5. Their implementation based on the Obara-Saika recurrence scheme [114] is described in detail.

4.2 Magnetizabilities at the Level of DF-HF

The derivation of the formalism for the HF gradient is based on lecture notes by Prof. Werner [54].

4.2.1 Variation of orbitals by a perturbation

The variation of the molecular orbital (MO) coefficients $\mathbf{C}$ in the presence of a perturbation, in this case the magnetic field $\mathbf{B}$, can be described by an orbital rotation matrix $\mathbf{O}$, i.e.,

$$\mathbf{C}(\mathbf{B}) = \mathbf{C}(0)\mathbf{O}(\mathbf{B}) = \mathbf{C}\mathbf{O}(\mathbf{B}), \tag{4.1}$$

where $\mathbf{C}(0) \equiv \mathbf{C}$ are the optimized HF MO coefficients in the absence of a perturbation. In the limit of no perturbation the orbital variation matrix reduces to unity, i.e., $\mathbf{O}(0)=\mathbf{1}$.
The orthonormality condition must also be fulfilled in the presence of a perturbation. Differentiating the orthonormality condition,

$$\mathbf{O}^\dagger\mathbf{C}^\dagger\mathbf{S}\mathbf{C}\mathbf{O} = \mathbf{1}, \tag{4.2}$$

with respect to the perturbation yields

$$\mathbf{O}^{B_\alpha\dagger} + \mathbf{O}^{B_\alpha} = -\mathbf{C}^\dagger\mathbf{S}^{B_\alpha}\mathbf{C}, \tag{4.3}$$

where the derivative of the AO overlap matrix with respect to the magnetic field, $\mathbf{S}^{B_\alpha}$ (see Eq. 4.140), has been introduced.

4.2.2 Formal expressions for the HF magnetizability tensors

The HF magnetizability tensor ξ^{HF} is defined as the second derivative of the HF energy, respectively, the HF Lagrangian with respect to the external magnetic field **B**,

$$\xi^{\mathrm{HF}}_{\alpha\beta} = -\left[\frac{d^2 E_{\mathrm{HF}}}{dB_\alpha dB_\beta}\right]_{\mathbf{B}=0} = -\left[\frac{d^2 \mathcal{L}_{\mathrm{HF}}}{dB_\alpha dB_\beta}\right]_{\mathbf{B}=0}. \tag{4.4}$$

For a rigorous derivation of the formalism it is convenient to start from the HF Lagrangian $\mathcal{L}_{\mathrm{HF}}$,

$$\mathcal{L}_{\mathrm{HF}} = E_{\mathrm{HF}} - 2\sum_{kl} x_{kl}\left[\left(\mathbf{O}^\dagger\mathbf{C}^\dagger\mathbf{S}\mathbf{C}\mathbf{O}\right)_{kl} - \delta_{kl}\right], \tag{4.5}$$

where the constraint of the orthonormality condition of the MOs is explicitly taken care of (with the corresponding multipliers x_{kl}).
The HF energy is given by

$$E_{\mathrm{HF}} = \sum_{\mu\nu} D^{(0)}_{\mu\nu} h_{\mu\nu} + \frac{1}{2}\sum_{\mu\nu\rho\sigma} D^{(0)}_{\mu\nu} D^{(0)}_{\rho\sigma}\left[(\mu\nu|\rho\sigma) - \frac{1}{2}(\mu\sigma|\rho\nu)\right] \tag{4.6}$$

with the HF density matrix in AO basis

$$D^{(0)}_{\mu\nu} = 2\sum_{k} L^*_{\mu k} L_{\nu k} \tag{4.7}$$

and the local MO coefficient matrix **L**.
The Lagrange multipliers **x** can be determined by differentiation of the Lagrangian with respect to the orbital variation matrix:

$$\left(\frac{\partial \mathcal{L}}{\partial O_{ij}}\right)_{\mathbf{B}=0} = 2(f_{ji} - x_{ij}) = 0, \tag{4.8}$$

$$\left(\frac{\partial \mathcal{L}}{\partial O_{ai}}\right)_{\mathbf{B}=0} = 2f_{ia} = 0, \tag{4.9}$$

which yields

$$x_{ij} = f_{ji}, \tag{4.10}$$

$$f_{ia} = 0. \tag{4.11}$$

In the limit of zero magnetic field strength the orbital rotation matrix reduces to unity and the Lagrangian, Eq. (4.5), can be simplified to

$$\mathcal{L}_{\mathrm{HF}} = E_{\mathrm{HF}} - 2\sum_{kl} f_{lk}\left[\left(\mathbf{L}^{\dagger}\mathbf{S}\mathbf{L}\right)_{kl} - \delta_{kl}\right]. \tag{4.12}$$

Following the formalism outlined in Section 2.5 the first derivative with respect to the magnetic field can be written as

$$\left(\frac{\partial E_{\mathrm{HF}}}{\partial B_\beta}\right)_{\mathbf{B}=0} = \left(\frac{\partial \mathcal{L}_{\mathrm{HF}}}{\partial B_\beta}\right)_{\mathbf{B}=0} = E_{\mathrm{HF}}^{(B_\beta)} - 2\sum_{kl} f_{lk}\left(\mathbf{L}^{\dagger}\mathbf{S}^{B_\beta}\mathbf{L}\right)_{kl}, \tag{4.13}$$

where only derivatives of the integrals are considered in $E^{\mathrm{HF}(B_\beta)}$, but no derivatives of MO coefficient or density matrices, i.e.,

$$E_{\mathrm{HF}}^{(B_\beta)} = \sum_{\mu\nu} D^{(0)}_{\mu\nu}\frac{\partial h_{\mu\nu}}{\partial B_\beta} + \frac{1}{2}\sum_{\mu\nu\rho\sigma} D^{(0)}_{\mu\nu}D^{(0)}_{\rho\sigma}\frac{\partial}{\partial B_\beta}\left[(\mu\nu|\rho\sigma) - \frac{1}{2}(\mu\sigma|\rho\nu)\right]. \tag{4.14}$$

Note that in Eqs. (4.12) and (4.13) only the occupied part of the MO coefficient matrix, **L**, contributes to the constraint.

In order to calculate magnetizabilities one needs the second derivative of the Lagrangian: this requires to determine the response of the orbital rotation matrix **O** and of the Lagrange multipliers. The former is obtained by differentiating the HF Lagrangian twice, once with respect to the Lagrange multipliers and once with respect to the magnetic field. This yields the derivative of the orthonormality condition (see Eq. 4.3) which can be used to calculate the symmetric part of the response quantity $\mathbf{O}^{B_\alpha}$.

The response equations for the Lagrange multipliers give rise to the so-called coupled-perturbed Hartree-Fock (CPHF) equations [81–83] which ensure that Brillouin's theorem is fulfilled for any value of the perturbation. Their solution contributes to the virtual-occupied block of $\mathbf{O}^{B_\beta}$. The CPHF equations are explicitly provided in Eq. (3.47) for LMP2 shielding tensors. They are identical to the CPHF equations for HF and LMP2 magnetizabilities, respectively, rotational g tensors.

The HF magnetizability tensor, Eq. (4.4), as the second derivative of the

HF energy with respect to the magnetic field, can then be written as

$$\begin{aligned}\xi^{\mathrm{HF}}_{\alpha\beta} = &-\sum_{\mu\nu}\left(D^{(0)}_{\mu\nu}\frac{\partial^2 h_{\mu\nu}}{\partial B_\alpha \partial B_\beta} + \frac{\partial D^{(0)}_{\mu\nu}}{\partial B_\alpha}\frac{\partial h_{\mu\nu}}{\partial B_\beta}\right)\\ &-\frac{1}{2}\sum_{\mu\nu\rho\sigma}\left(D^{(0)}_{\mu\nu}\frac{\partial D^{(0)}_{\rho\sigma}}{\partial B_\alpha} + \frac{\partial D^{(0)}_{\mu\nu}}{\partial B_\alpha}D^{(0)}_{\rho\sigma}\right)\frac{\partial}{\partial B_\beta}\left[(\mu\nu|\rho\sigma) - \frac{1}{2}(\mu\sigma|\rho\nu)\right]\\ &-\frac{1}{2}\sum_{\mu\nu\rho\sigma}D^{(0)}_{\mu\nu}D^{(0)}_{\rho\sigma}\frac{\partial^2}{\partial B_\alpha \partial B_\beta}\left[(\mu\nu|\rho\sigma) - \frac{1}{2}(\mu\sigma|\rho\nu)\right]\\ &-\sum_{\mu\nu}\left[X^{(0)}_{\mu\nu}\frac{\partial^2 S_{\mu\nu}}{\partial B_\alpha \partial B_\beta} + \frac{\partial X^{(0)}_{\mu\nu}}{\partial B_\alpha}\frac{\partial S_{\mu\nu}}{\partial B_\beta}\right]\Bigg|_{\mathbf{B}=0}\end{aligned} \tag{4.15}$$

with the perturbed HF density matrix

$$\frac{D^{(0)}_{\mu\nu}}{\partial B_\alpha} = \left[\mathbf{D}^{(0)}\right]^{B_\alpha}_{\mu\nu} = 2\sum_k\left[\frac{\partial L^*_{\mu k}}{\partial B_\alpha}L_{\nu k} + L^*_{\mu k}\frac{\partial L_{\nu k}}{\partial B_\alpha}\right], \tag{4.16}$$

the first and second derivatives of the AO overlap matrix $\mathbf{S}$ with respect to the magnetic field, and the HF energy weighted density matrix $\mathbf{X}^{(0)}$,

$$X^{(0)}_{\mu\nu} = -2\sum_{kl}L^*_{\mu k}f_{lk}L_{\nu l} \tag{4.17}$$

with the elements f_{lk} of the occupied-occupied block of the Fock matrix in MO basis.

The corresponding derivative of Eq. (4.17) is then given by

$$\frac{\partial X^{(0)}_{\mu\nu}}{\partial B_\alpha} = \left[\mathbf{X}^{(0)}\right]^{B_\alpha}_{\mu\nu} = -2\sum_{kl}\left[\frac{\partial L^*_{\mu k}}{\partial B_\alpha}f_{lk}L_{\nu l} + L^*_{\mu k}\frac{\partial f_{lk}}{\partial B_\alpha}L_{\nu l} + L^*_{\mu k}f_{lk}\frac{\partial L_{\nu l}}{\partial B_\alpha}\right]. \tag{4.18}$$

4.2.3 Density fitting for HF magnetizabilities

Density fitting for electron repulsion integrals (ERIs) can be introduced in the same way as for NMR shielding tensors. As mentioned before, magnetizabilities are calculated in the limit of zero magnetic field strength in which GIAOs reduce to ordinary Gaussians which are employed as fitting functions. If GIAOs were used as fitting functions the explicit dependence

on the magnetic field would not cancel in the ERIs since there is no complex conjugate for the fitting function. By employing density fitting the first derivative of the ERIs with respect to the magnetic field (see second line in Eq. 4.15) can be written as

$$\frac{\partial(\mu\nu|\rho\sigma)}{\partial B_\beta} = \sum_{PQ}\left[\frac{\partial(\mu\nu|P)}{\partial B_\beta}J^{-1}_{PQ}(Q|\rho\sigma) + (\mu\nu|P)J^{-1}_{PQ}\frac{\partial(Q|\rho\sigma)}{\partial B_\beta}\right] \tag{4.19}$$

with the Coulomb metric of the auxiliary functions $J_{PQ} = (P|Q)$. The derivative of the three-index quantity is given by

$$\frac{\partial(\mu\nu|P)}{\partial B_\beta} = \frac{i}{2c}\left(\mu\nu\left|\frac{1}{r_{12}}\left(\mathbf{R}_{MN}\times\mathbf{r}_1\right)_\beta\right|P\right). \tag{4.20}$$

Using the quantities above the second line of Eq. (4.15) can be rewritten as

$$\frac{1}{2}\sum_{\mu\nu\rho\sigma}\left(D^{(0)}_{\mu\nu}\frac{\partial D^{(0)}_{\rho\sigma}}{\partial B_\alpha} + \frac{\partial D^{(0)}_{\mu\nu}}{\partial B_\alpha}D^{(0)}_{\rho\sigma}\right)\frac{\partial}{\partial B_\beta}\left[(\mu\nu|\rho\sigma) - \frac{1}{2}(\mu\sigma|\rho\nu)\right] \tag{4.21}$$

$$= \sum_{\mu\nu\rho\sigma}\frac{\partial D^{(0)}_{\mu\nu}}{\partial B_\alpha}D^{(0)}_{\rho\sigma}\frac{\partial}{\partial B_\beta}\left[(\mu\nu|\rho\sigma) - \frac{1}{2}(\mu\sigma|\rho\nu)\right] \tag{4.22}$$

$$= \sum_{\mu\nu P}\frac{\partial D^{(0)}_{\mu\nu}}{\partial B_\alpha}\frac{\partial(\mu\nu|P)}{\partial B_\beta}c^P$$

$$- \frac{1}{2}\sum_{\mu\nu\rho\sigma}\sum_{PQ}\frac{\partial D^{(0)}_{\mu\nu}}{\partial B_\alpha}D^{(0)}_{\rho\sigma}\left[\frac{\partial(\mu\sigma|P)}{\partial B_\beta}J^{-1}_{PQ}(Q|\rho\nu) + (\mu\sigma|P)J^{-1}_{PQ}\frac{\partial(Q|\rho\nu)}{\partial B_\beta}\right] \tag{4.23}$$

with the fitting coefficient

$$c^P = \sum_{\mu\nu}\sum_{Q}D^{(0)}_{\mu\nu}(\mu\nu|Q)J^{-1}_{PQ}. \tag{4.24}$$

Note that there are no contributions from the Coulomb-type contractions of the symmetric unperturbed density matrix with the antisymmetric perturbed ERIs and of the antisymmetric perturbed density matrix with the symmetric unperturbed ERIs in Eq. (4.22).

Equation (4.23) can be further simplified by using the definitions of the

unperturbed and perturbed HF density matrix, Eqs. (4.7) and (4.16),

$$\begin{aligned}
&\frac{1}{2}\sum_{\mu\nu\rho\sigma}\left(D^{(0)}_{\mu\nu}\frac{\partial D^{(0)}_{\rho\sigma}}{\partial B_\alpha}+\frac{\partial D^{(0)}_{\mu\nu}}{\partial B_\alpha}D^{(0)}_{\rho\sigma}\right)\frac{\partial}{\partial B_\beta}\left[(\mu\nu|\rho\sigma)-\frac{1}{2}(\mu\sigma|\rho\nu)\right]\\
&=4\left(\sum_{kP}(k\tilde{k}|P)^{(B_\beta)}c^P-\sum_{kl}\sum_{PQ}\left[(\tilde{k}l|P)^{(B_\beta)}J^{-1}_{PQ}(Q|lk)+(kl|P)^{(B_\beta)}J^{-1}_{PQ}(Q|l\tilde{k})\right]\right)\\
&=4\sum_k\left[g(\mathbf{D}^{(0)})\right]^{(B_\beta)}_{\tilde{k}k},
\end{aligned}\tag{4.25}$$

where $\tilde{k}$ denotes the transformation with a perturbed MO coefficient, i.e.,

$$\phi_{\tilde{k}}=\sum_\mu\frac{\partial L_{\mu k}}{\partial B_\alpha}\omega_\mu. \tag{4.26}$$

The quantity $\left[g\left(\mathbf{D}^{(0)}\right)\right]^{(B_\beta)}_{\tilde{k}k}$ in Eq. (4.25) can easily be evaluated from the corresponding half-transformed quantity $\left[g\left(\mathbf{D}^{(0)}\right)\right]^{(B_\beta)}_{\mu k}$ which has to be calculated for the CPHF Eqs. (3.47) anyway (see also Eq. 26 in Ref. [68]). Analogously, one finds for the second derivative of the ERIs with respect to the magnetic field (as it appears in the third line of Eq. 4.15)

$$\begin{aligned}
\frac{\partial^2(\mu\nu|\rho\sigma)}{\partial B_\alpha\partial B_\beta}=\sum_{PQ}\Bigg[&\frac{\partial^2(\mu\nu|P)}{\partial B_\alpha\partial B_\beta}J^{-1}_{PQ}(Q|\rho\sigma)+(\mu\nu|P)J^{-1}_{PQ}\frac{\partial^2(Q|\rho\sigma)}{\partial B_\alpha\partial B_\beta}\\
&+\frac{\partial(\mu\nu|P)}{\partial B_\alpha}J^{-1}_{PQ}\frac{\partial(Q|\rho\sigma)}{\partial B_\beta}+\frac{\partial(\mu\nu|P)}{\partial B_\beta}J^{-1}_{PQ}\frac{\partial(Q|\rho\sigma)}{\partial B_\alpha}\Bigg]
\end{aligned}\tag{4.27}$$

with the second derivative of the three-index quantity

$$\frac{\partial^2(\mu\nu|P)}{\partial B_\alpha\partial B_\beta}=-\frac{1}{4c^2}\left(\mu\nu\left|\frac{1}{r_{12}}\left(\mathbf{R}_{MN}\times\mathbf{r}_1\right)_\alpha\left(\mathbf{R}_{MN}\times\mathbf{r}_1\right)_\beta\right|P\right). \tag{4.28}$$

The third line of Eq. (4.15) can be rewritten by plugging in Eq. (4.27) and adding up identical terms as

$$\begin{aligned}
&\frac{1}{2}\sum_{\mu\nu\rho\sigma} D^{(0)}_{\mu\nu} D^{(0)}_{\rho\sigma} \frac{\partial^2}{\partial B_\alpha \partial B_\beta}\left[(\mu\nu|\rho\sigma) - \frac{1}{2}(\mu\sigma|\rho\nu)\right] \\
&= \sum_{\mu\nu}\sum_{P} D^{(0)}_{\mu\nu} \frac{\partial^2 (\mu\nu|P)}{\partial B_\alpha \partial B_\beta} c^P \\
&\quad - 2\sum_{kl}\sum_{PQ}\left((kl|P)^{(B_\alpha,B_\beta)} J^{-1}_{PQ}(Q|lk) + (kl|P)^{(B_\alpha)} J^{-1}_{PQ}(Q|lk)^{(B_\beta)}\right) \\
&= \sum_{\mu\nu}\sum_{P} D^{(0)}_{\mu\nu} \frac{\partial^2 (\mu\nu|P)}{\partial B_\alpha \partial B_\beta} c^P - 2\sum_{kl}\sum_{P}\left((kl|P)^{(B_\alpha,B_\beta)} c^P_{lk} + (kl|P)^{(B_\alpha)} c^{P,(B_\beta)}_{lk}\right) \qquad (4.29)
\end{aligned}$$

with the fitting coefficients

$$c^P_{lk} = \sum_{Q} J^{-1}_{PQ}(Q|lk), \qquad (4.30)$$

$$c^{P,(B_\beta)}_{lk} = \sum_{Q}\sum_{\mu\nu} J^{-1}_{PQ} \frac{\partial (Q|\mu\nu)}{\partial B_\beta} L^*_{\mu l} L_{\nu k}. \qquad (4.31)$$

4.2.4 Accuracy of the density fitting approximation

Tables 4.1 and 4.2 show the influence of the auxiliary fitting basis set on the accuracy of HF magnetizabilities. The calculations were carried out for a benchmark set of 28 small molecules which was originally proposed by Lutnæs et al. [45]. The geometries were taken from the supplementary material of Ref. [45], the calculations were carried out using Dunning's cc-pVXZ and aug-cc-pVXZ (AVXZ) AO basis sets for X=D, T, and Q [86–91, 115]. The JK-fitting basis sets of Weigend [92] related to the cc-pVXZ, cc-pV(X+1)Z, and cc-pV(X+2)Z AO basis set, respectively, the augmented analogues, were used where available. The reference values were taken from the supplementary material of Ref. [45]. These were calculated with a conventional, non-DF program using the `DALTON` quantum chemistry package [116].

The tables in this chapter show isotropic magnetizabilities $\bar{\xi}$, which are calculated as ⅓ of the sum of the diagonal elements of the magnetizability tensor [112],

$$\bar{\xi} = \frac{1}{3}\left(\xi_{xx} + \xi_{yy} + \xi_{zz}\right). \tag{4.32}$$

The deviations from conventional calculations are small, i.e., in the range of $0.1 \cdot 10^{-30}\,\mathrm{JT}^{-2}$ or less. This is even true without increasing the cardinal number of the JK-fitting basis set relative to the AO basis set for both, augmented and non-augmented basis sets. The fitting errors for the cc-pVDZ AO basis set with the cc-pVDZ JK-fitting basis set and for the aug-cc-pVDZ AO basis set with the aug-cc-pVDZ JK-fitting basis set are slightly larger compared to the other results. This might be explained by the rather small AO basis set which causes only a crude description of the wave function. Additionally, the small JK-fitting basis set is not flexible enough to reproduce the product densities occurring in the ERIs. For larger AO basis sets in combination with the nominally in size related fitting basis sets the fitting error becomes smaller: for the cc-pVQZ AO basis set deviations between cc-pVQZ and cc-pV5Z JK-fitting basis sets are (with the exception of ozone) $0.01 \cdot 10^{-30}\,\mathrm{JT}^{-2}$. The fitting error for ozone is larger than for the

other molecules of the test set probably due to the fact that HF cannot be considered an appropriate method for the calculation of O_3. This makes it difficult for the density fitting approximation to accurately fit the density. LiH and LiF were calculated with the cc-pVXZ basis sets for Li published in 2011 [115] which differ from the AO basis sets used for the reference calculations. Test calculations for these two molecules with the basis sets of Ref. [115] were carried out with `CFOUR` [84]: the difference of the results between the non-DF program and the DF-HF program of `MOLPRO` is in the range of $0.01 \cdot 10^{-30}\,\mathrm{JT}^{-2}$ which is in good agreement with the deviations found for the other molecules of the test set.

The results are in perfect agreement with the findings when introducing density fitting for NMR shielding tensors (see Section 3.6 as well as Refs. [35] and [68]). It can be concluded that it is valid to use ordinary Gaussians as fitting functions for the calculation of magnetizabilities at the level of Hartree-Fock. Since magnetizabilities are calculated in the limit of zero magnetic field strength (see Eq. 4.4) the orbital product densities of GIAOs reduce to products of ordinary Gaussians and can be fitted with Gaussians as auxiliary functions.

Table 4.1: Influence of the fitting basis set on isotropic magnetizabilities at the level of GIAO-DF-HF. The ΔVXZ values are provided as the difference between the VXZ value and the value with the largest fitting basis set available for this AO basis, e.g., ΔVDZ=VDZ-VQZ. All magnetizability values are provided in SI units (10^{-30} JT^{-2}).

Basis	VDZ				VTZ				VQZ		
Fitting basis	ΔVDZ	ΔVTZ	VQZ	Ref.[a)]	ΔVTZ	ΔVQZ	V5Z	Ref.[a)]	ΔVQZ	V5Z	Ref.[a)]
AlF	-0.03	-0.01	-399.93	-399.9	0.00	0.00	-400.95	-400.9	0.00	-399.63	-399.6
C_2H_4	-0.02	0.00	-348.69	-348.7	-0.03	0.00	-352.07	-352.1	-0.01	-353.19	-353.2
C_3H_4	-0.03	-0.01	-481.09	-481.1	-0.01	0.00	-479.01	-479.0	0.00	-478.16	-478.2
CH_2O	-0.01	0.00	-134.05	-134.0	-0.01	0.00	-137.49	-137.5	0.00	-138.62	-138.6
CH_3F	-0.02	-0.01	-314.56	-314.6	-0.02	0.00	-315.72	-315.7	0.00	-316.63	-316.6
CH_4	0.01	0.01	-311.94	-311.9	0.00	0.00	-314.33	-314.3	0.00	-313.81	-313.8
CO	0.01	0.00	-199.35	-199.4	0.01	0.00	-203.05	-203.0	0.00	-203.85	-203.9
FCCH	-0.06	-0.01	-459.30	-459.3	-0.02	-0.01	-454.54	-454.5	-0.01	-453.31	-453.3
$FC^{15}N$	-0.05	-0.02	-381.59	-381.6	-0.01	0.00	-378.65	-378.7	0.00	-378.28	-378.3
H_2C_2O	0.00	0.00	-440.69	-440.7	0.01	0.00	-435.60	-435.6	0.01	-433.87	-433.9
H_2O	0.00	0.01	-218.90	-218.9	0.00	0.00	-225.34	-225.3	0.00	-228.21	-228.2
H_2S	-0.02	0.00	-453.12	-453.1	0.01	0.00	-453.52	-453.5	0.00	-453.51	-453.5
H_4C_2O	0.02	0.01	-544.40	-544.4	-0.01	0.00	-543.55	-543.6	-0.01	-543.68	-543.7
$HC^{15}N$	-0.01	0.00	-275.60	-275.6	0.00	0.00	-278.44	-278.4	0.00	-279.46	-279.5
HCP	-0.04	-0.01	-504.54	-504.6	-0.01	0.00	-507.15	-507.1	0.00	-509.86	-509.9
HF	0.00	0.00	-164.22	-164.2	0.00	0.00	-168.80	-168.8	0.00	-170.89	-170.9
HFCO	-0.05	-0.01	-309.08	-309.1	-0.02	-0.01	-310.29	-310.3	-0.01	-310.88	-310.9
HOF	-0.03	-0.01	-244.71	-244.7	-0.02	-0.01	-245.30	-245.3	0.00	-244.80	-244.8
LiF	0.00	0.00	-201.49	-200.5	0.00	0.00	-192.99	-193.2	-0.01	-191.38	-191.4
LiH	0.00	0.00	-133.02	-133.1	0.00	0.00	-126.47	-126.4	-0.01	-125.58	-125.6
$^{15}N_2$	0.02	0.01	-193.07	-193.1	0.01	0.00	-199.41	-199.4	0.00	-201.04	-201.0
N_2O	0.01	-0.01	-352.10	-352.1	0.00	0.00	-346.89	-346.9	0.00	-344.49	-344.5
NH_3	0.00	0.00	-274.85	-274.9	0.00	0.00	-282.15	-282.2	0.00	-284.75	-284.8
O_3	-0.10	0.12	694.81	694.8	0.03	-0.02	602.94	603.0	-0.03	588.05	588.1
OCS	0.01	-0.01	-610.08	-610.1	-0.01	0.00	-600.94	-600.9	0.00	-599.02	-599.0
OF_2	-0.08	-0.04	-275.29	-275.3	-0.05	-0.01	-273.45	-273.4	-0.01	-271.97	-272.0
PN	0.15	0.03	-288.41	-288.4	0.02	0.00	-296.69	-296.7	0.01	-301.20	-301.2
SO_2	0.09	0.01	-292.43	-292.4	0.08	0.00	-300.96	-301.0	0.01	-301.64	-301.6

a) Reference values are taken from conventional HF calculations as provided in Ref. [45].

Table 4.2: Influence of the fitting basis set on isotropic magnetizabilities at the level of GIAO-DF-HF for augmented basis sets. The ΔAVXZ values are provided as the difference between the AVXZ value and the value with the largest fitting basis set available for this AO basis, e.g., ΔAVDZ=AVDZ-AVQZ. All magnetizability values are provided in SI units (10^{-30} JT^{-2}).

Basis	AVDZ				AVTZ				AVQZ		
Fitting basis	ΔAVDZ	ΔAVTZ	AVQZ	Ref.[a)]	ΔAVTZ	ΔAVQZ	AV5Z	Ref.[a)]	ΔAVQZ	AV5Z	Ref.[a)]
AlF	-0.03	-0.01	-402.53	-402.5	-0.01	0.00	-401.03	-401.0	0.00	-399.91	-399.9
C_2H_4	-0.02	0.00	-358.42	-358.4	-0.02	-0.01	-355.06	-355.1	0.00	-354.73	-354.7
C_3H_4	-0.03	0.00	-481.44	-481.4	0.00	0.00	-478.33	-478.3	0.00	-478.03	-478.0
CH_2O	-0.02	-0.01	-141.21	-141.2	-0.01	0.00	-139.72	-139.7	0.00	-139.47	-139.5
CH_3F	-0.03	-0.01	-319.71	-319.7	-0.01	0.00	-318.60	-318.6	0.00	-318.04	-318.0
CH_4	0.01	0.01	-315.46	-315.5	0.00	0.00	-314.11	-314.1	0.00	-313.76	-313.8
CO	0.02	0.01	-207.30	-207.3	0.01	0.00	-204.95	-205.0	0.00	-204.50	-204.5
FCCH	-0.07	-0.01	-455.47	-455.5	-0.01	0.00	-452.94	-452.9	0.00	-452.19	-452.2
$FC^{15}N$	-0.04	0.00	-382.03	-382.0	0.00	0.00	-378.65	-378.7	0.00	-378.02	-378.0
H_2C_2O	0.01	0.01	-436.24	-436.2	0.00	0.00	-433.22	-433.2	0.00	-432.65	-432.7
H_2O	0.00	0.00	-232.01	-232.0	0.00	0.00	-231.45	-231.4	0.00	-231.28	-231.3
H_2S	-0.02	-0.01	-462.44	-462.4	0.01	0.00	-456.52	-456.5	0.00	-454.66	-454.6
H_4C_2O	0.01	0.00	-549.73	-549.7	0.00	0.00	-545.26	-545.3	0.00	-544.81	-544.8
$HC^{15}N$	0.00	0.00	-282.90	-282.9	0.00	0.00	-280.51	-280.5	0.00	-280.10	-280.1
HCP	-0.03	0.00	-517.25	-517.3	0.00	0.00	-512.49	-512.5	0.00	-511.79	-511.8
HF	0.00	0.00	-174.09	-174.1	0.00	0.00	-172.89	-172.9	0.00	-172.67	-172.7
HFCO	-0.05	-0.01	-315.11	-315.1	-0.01	0.00	-312.12	-312.1	0.00	-311.50	-311.5
HOF	-0.04	0.00	-245.43	-245.4	0.00	0.00	-244.91	-244.9	0.00	-244.58	-244.6
LiF	0.00	0.00	-194.97	-195.0	0.00	0.00	-191.36	-191.3	0.00	-190.93	-190.9
LiH	0.00	0.00	-129.25	-129.3	0.00	0.00	-125.79	-125.7	0.00	-125.32	-125.3
$^{15}N_2$	0.02	0.01	-204.33	-204.3	0.01	0.00	-203.10	-203.1	0.00	-202.82	-202.8
N_2O	0.02	0.01	-346.65	-346.7	0.00	0.00	-343.15	-343.2	0.00	-342.78	-342.8
NH_3	0.00	0.00	-287.88	-287.9	0.00	0.00	-287.56	-287.6	0.00	-287.45	-287.5
O_3	-0.43	0.11	588.91	588.9	0.04	0.01	581.63	581.7	0.01	581.09	581.1
OCS	0.02	0.00	-605.13	-605.1	-0.01	0.00	-598.87	-598.9	0.00	-597.91	-597.9
OF_2	-0.09	-0.02	-271.12	-271.1	-0.01	0.00	-271.88	-271.9	0.00	-271.53	-271.5
PN	0.12	0.01	-306.26	-306.3	0.03	0.00	-302.34	-302.3	0.01	-302.81	-302.8
SO_2	0.03	0.00	-304.95	-305.0	0.08	0.01	-304.00	-304.0	0.01	-302.67	-302.7

a) Reference values are taken from conventional HF calculations as provided in Ref. [45].

4.3 Magnetizabilities at the Level of DF-LMP2

The LMP2 magnetizability tensor ξ^{LMP2} is defined as the second derivative of the LMP2 energy E_2, respectively, of the LMP2 Lagrangian $\mathcal{L}_2$ with respect to the external magnetic field $\mathbf{B}$,

$$\xi^{\mathrm{LMP2}}_{\alpha\beta} = -\left[\frac{d^2 E_2}{dB_\alpha dB_\beta}\right]_{\mathbf{B}=0} = -\left[\frac{d^2 \mathcal{L}_2}{dB_\alpha dB_\beta}\right]_{\mathbf{B}=0}. \tag{4.33}$$

The LMP2 Lagrangian can be written as [17, 35]

$$\begin{aligned}\mathcal{L}_2 = E_2 &+ \sum_{kl} z^{\mathrm{loc}}_{kl} r_{kl} + \sum_{ck} \left[z_{ck} f_{ck} + z_{kc} f_{kc}\right] \\ &+ \sum_{pq} x_{pq} \left[\mathbf{C}^\dagger \mathbf{S} \mathbf{C} - \mathbf{1}\right]_{pq}.\end{aligned} \tag{4.34}$$

It is stationary with respect to the LMP2 amplitudes through the Hylleraas functional E_2 and with respect to the molecular orbital coefficients $\mathbf{C}$. In the case of LMP2 one has to ensure stationarity with respect to orbital rotations through Brillouin's condition $f_{ck} = 0$, respectively, $f_{kc} = 0$ with the corresponding Lagrange multipliers $\mathbf{z}$. Furthermore, the orthonormality condition of the MOs has to be fulfilled for any value of the perturbation. This is ensured by adding $\mathbf{C}^\dagger\mathbf{S}\mathbf{C}$ with the corresponding Lagrange multipliers $\mathbf{x}$ as a constraint. Finally, the LMP2 energy is no longer invariant with respect to rotations within the occupied space; this is caused by the neglect of very distant pairs and restrictions of excitations to pair domains [54]. Stationarity with respect to these (occupied-occupied) rotations is obtained by enforcing the localization condition $r_{kl} = 0$ with the multipliers $\mathbf{z}^{\mathrm{loc}}$.
In the frozen-core approximation an additional term $z_{kl_c} f_{kl_c} + z_{l_c k} f_{l_c k}$ with $k \in \{\text{valence}\}$ and $l_c \in \{\text{core}\}$ has to be included in the Lagrangian. The additional equations which arise are explicitly given in Section 4.3.5.
The here presented formalism for the calculation of magnetizabilities at the level of density fitted LMP2 is based on the DF-LMP2 gradient for nuclear displacements [17]. The idea is to reinterpret the gradient expressions in Ref. [17] with the external magnetic field as a perturbation and to differentiate the expressions a second time with respect to the magnetic field. This

is closely related to the formalism for NMR shielding tensors for which the gradient with respect to the magnetic moment of the corresponding nucleus is considered and then differentiated a second time with respect to the magnetic field. Hence, NMR shielding tensors and magnetizabilities require the same perturbed wave function parameters which are differentiated with respect to the magnetic field. In contrast to NMR shielding tensors, magnetizabilities have contributions from the unperturbed and perturbed generalized energy weighted density matrix and the unperturbed and perturbed two-particle density matrix (cf. Eqs. 3.1 and 4.76). These additional terms in the expression for the magnetizability tensor are caused by the fact that the overlap and electron repulsion integrals depend explicitly on the external magnetic field (through the GIAOs) whereas they do not explicitly depend on the nuclear magnetic dipole moment.
The Hylleraas functional is stationary with respect to the LMP2 amplitudes and can be written as

$$\begin{aligned} E_2 &= \langle \Psi^{(0)} | \hat{H} | \Psi^{(1)} \rangle + \langle \Psi^{(1)} | \hat{H} | \Psi^{(0)} \rangle \\ &\quad + \langle \Psi^{(1)} | \hat{H}^{(0)} - E^{(0)} | \Psi^{(1)} \rangle \\ &= \sum_{cdkl} \left(\tilde{T}^{kl}_{cd} K^{kl*}_{cd} + \tilde{T}^{kl*}_{cd} K^{kl}_{cd} \right) + \sum_{pq} f_{pq} d^{(2)}_{pq} \end{aligned} \tag{4.35}$$

with the two-electron exchange matrix $\mathbf{K}$,

$$K^{kl}_{cd} = (ck|dl). \tag{4.36}$$

The LMP2 amplitudes for a given orbital pair (kl) are collected in $\mathbf{T}^{kl}$; the contravariant amplitude matrices are defined as

$$\tilde{T}^{kl}_{ab} = 2T^{kl}_{ab} - T^{lk}_{ab}. \tag{4.37}$$

The closed-shell Fock matrix in MO basis, $\mathbf{f}$, is given by

$$f_{pq} = h_{pq} + g\left(\mathbf{d}^{(\mathbf{0})}\right)_{pq} \tag{4.38}$$

with the one-electron core Hamiltonian in MO basis, $\mathbf{h}$, the general electronic interaction matrix for a density $\mathbf{d}$,

$$g\left(\mathbf{d}\right)_{pq} = \sum_{mn} d_{mn} \left[(pq|mn) - \frac{1}{2}(pn|mq) \right], \tag{4.39}$$

and the Hartree-Fock density matrix

$$d_{ij}^{(0)} = 2\delta_{ij}. \tag{4.40}$$

The LMP2 density matrix is given by

$$\begin{aligned}
\left[\mathbf{d}^{(2)}\right]_{ij} &= -2\sum_{cd}\sum_{k}\left[T_{cd}^{ik}\tilde{T}_{cd}^{jk*}\right], \\
\left[\mathbf{d}^{(2)}\right]_{ab} &= 2\sum_{c}\sum_{kl}\left[\tilde{T}_{ac}^{kl*}T_{bc}^{kl}\right], \\
\left[\mathbf{d}^{(2)}\right]_{ia} &= \left[\mathbf{d}^{(2)}\right]_{ai} = 0\,.
\end{aligned} \tag{4.41}$$

In this work Pipek-Mezey localization is employed with its localization condition [63]

$$r_{kl} = \sum_{A}\left[S_{kk}^{A} - S_{ll}^{A}\right]S_{kl}^{A} = 0 \qquad \forall k > l \tag{4.42}$$

and the matrices $\mathbf{S}^{A}$,

$$S_{kl}^{A} = \sum_{\mu\in A}\sum_{\nu}\left[L_{\mu k}^{*}S_{\mu\nu}L_{\nu l} + L_{\nu k}^{*}S_{\nu\mu}L_{\mu l}\right], \tag{4.43}$$

where the summation over the AO index μ is restricted to basis functions centered at atom A.

4.3.1 LMP2 gradient with respect to the magnetic field

The formalism presented in this and the following subsections follows the ideas of the DF-LMP2 gradient with respect to nuclear displacements [17] but considers the external magnetic field as a perturbation instead. The GIAO basis functions depend explicitly on the perturbation, however, the fitting functions are independent of the perturbation (in contrast to the formalism for nuclear displacements, cf. Eq. 49 in Ref. [17]). Ref. [17] will not be cited individually again throughout this section.

In order to obtain the stationary conditions which yield the Lagrange multipliers one has to differentiate the Lagrangian with respect to the non-variational parameters, in this case the (local) MO coefficients. The LMP2

Lagrangian is not differentiated directly with respect to the MO coefficients but instead with respect to the orbital rotation matrix which yields the Z-vector equations.
As outlined in Section 4.2.1 the orbital rotation matrix **O** formally describes the change of the MO coefficient matrix in the presence of a perturbation. The derivative of the Lagrangian with respect to the orbital rotation parameters can be split into individual terms as follows,

$$\left(\frac{\partial \mathcal{L}_2}{\partial O_{pq}}\right)_{\mathbf{B}=0} = \left[\mathbf{A} + \tilde{\mathbf{A}}\left(\mathbf{z}\right) + \mathbf{a}\left(\mathbf{z}^{\mathrm{loc}}\right) + \mathbf{x}\right]_{pq} \tag{4.44}$$

with

$$[\mathbf{A}]_{pq} = \left(\frac{\partial}{\partial O_{pq}} E_2\right)_{\mathbf{B}=0}, \tag{4.45}$$

$$\left[\tilde{\mathbf{A}}\left(\mathbf{z}\right)\right]_{pq} = \left(\frac{\partial}{\partial O_{pq}} \sum_{ck} \left[z_{ck} f_{ck} + z_{kc} f_{kc}\right]\right)_{\mathbf{B}=0}, \tag{4.46}$$

$$\left[\mathbf{a}\left(\mathbf{z}^{\mathrm{loc}}\right)\right]_{pi} = \left(\frac{\partial}{\partial O_{pi}} \sum_{kl} z_{kl}^{\mathrm{loc}} r_{kl}\right)_{\mathbf{B}=0}. \tag{4.47}$$

Combining the stationary conditions $\left(\partial \mathcal{L}_2 / \partial O_{pq}\right)_{\mathbf{B}=0} = 0$ with the auxiliary conditions $\mathbf{x} = \mathbf{x}^{\dagger}$ gives the linear Z-vector equations,

$$\left(1 - \mathcal{T}_{pq}\right)\left[\mathbf{A} + \tilde{\mathbf{A}}(\mathbf{z}) + \mathbf{a}\left(\mathbf{z}^{\mathrm{loc}}\right)\right]_{pq} = 0, \tag{4.48}$$

where $\mathcal{T}_{pq}$ interchanges p and q and complex conjugates the index pair. The Z-vector Eqs. (4.48) can be further decoupled into the Z-vector coupled-perturbed Hartree-Fock (Z-CPHF) and Z-vector coupled-perturbed localization (Z-CPL) equations.
The Lagrange multipliers **x** can be calculated accordingly as

$$x_{pq} = -\frac{1}{2}\left(1 + \mathcal{T}_{pq}\right)\left[\mathbf{A} + \tilde{\mathbf{A}}(\mathbf{z}) + \mathbf{a}\left(\mathbf{z}^{\mathrm{loc}}\right)\right]_{pq}. \tag{4.49}$$

The Lagrange multipliers **z** are assumed to be defined in the whole MO basis with $z_{aa} = z_{ii} = 0$. The Z-CPHF equations for the determination of the

virtual-occupied block of $\mathbf{z}$ take the form

$$y_{ai} + \sum_c f_{ca} z_{ci} - \sum_k z_{ak} f_{ik} + 2g(\mathbf{z})_{ia} = 0 \tag{4.50}$$

with the right-hand side

$$y_{ai} = A_{ai} - A^*_{ia} + \left[\mathbf{a}(\mathbf{z}^{\mathrm{loc}})\right]_{ai}, \tag{4.51}$$

where

$$\begin{aligned} A^*_{ia} &= \left(\frac{\partial}{\partial O^*_{ia}} E_2\right)_{\mathbf{B}=0} \\ &= 2\left[\sum_{ckl}\left(\tilde{T}^{kl*}_{ac} K^{kl}_{ic} + \sum_{rs\rho} L^*_{\rho i} S_{\rho r} \tilde{T}^{kl}_{rs} Q_{cs} R^{kl*}_{ac}\right)\right], \end{aligned} \tag{4.52}$$

$$\begin{aligned} A_{pi} &= \left(\frac{\partial}{\partial O_{pi}} E_2\right)_{\mathbf{B}=0} \\ &= 2\left[B_{pi} + \frac{1}{2}\sum_k f_{kp} d^{(2)}_{ki} + g(\mathbf{d}^{(2)})_{ip}\right], \end{aligned} \tag{4.53}$$

$$\begin{aligned} A_{ab} = 2\Bigg[&\sum_{ckl}\left(R^{kl*}_{ac}\tilde{T}^{kl}_{bc} + \tilde{T}^{kl*}_{ac} R^{kl}_{bc}\right) + \sum_{cjkl} f_{kl}\left(T^{lj*}_{ca}\tilde{T}^{kj}_{cb} + T^{lj*}_{ac}\tilde{T}^{kj}_{bc}\right) \\ &- \sum_{klcd} f_{cd} T^{kl*}_{ca}\tilde{T}^{kl}_{db}\Bigg], \end{aligned} \tag{4.54}$$

with

$$K^{kl}_{ic} = (ik|cl), \tag{4.55}$$

$$B_{pi} = \sum_k \sum_{cd} (cp|dk)\tilde{T}^{ik*}_{cd}, \tag{4.56}$$

and the contribution from the Z-CPL equations $\left[\mathbf{a}(\mathbf{z}^{\mathrm{loc}})\right]_{ai}$. The LMP2 residual matrix $\mathbf{R}^{kl}$ is defined in Eq. (3.14). The second term in Eq. (4.52) comes from the variation of the transformation matrices $\mathbf{Q}$ (see Eq. 2.45) in the LMP2 amplitudes (for further details see Appendix B in Ref. [17]). There is no such term in Eq. (4.53) since $\mathbf{Q}$ describes the transformation from virtual MO to the PAO basis and does not contain occupied indices.

Since the Lagrange multiplier $\mathbf{z}$ is a real Hermitian, i.e., symmetric quantity, the equations for the occupied-virtual block are identical to the ones for the virtual-occupied part. The occupied-virtual block of the unperturbed Lagrange multipliers is therefore given by $[\mathbf{z}]_{ia} = \left[\mathbf{z}^{\dagger}\right]_{ia} = [\mathbf{z}^{*}]_{ai} = [\mathbf{z}]_{ai}$.
The Lagrange multipliers for the localization condition $\mathbf{z}^{\mathrm{loc}}$ are determined by solving the Z-CPL equations,

$$(1 - \mathcal{T}_{ij})\left(A_{ij} + \left[\mathbf{a}\left(\mathbf{z}^{\mathrm{loc}}\right)\right]_{ij}\right) = 0, \tag{4.57}$$

$$\left[\mathbf{a}\left(\mathbf{z}^{\mathrm{loc}}\right)\right]_{pi} = \sum_{k>l} \mathcal{B}^{+}_{pi,kl} z^{\mathrm{loc}}_{kl}. \tag{4.58}$$

The quantity $\mathcal{B}^{+}$ is defined in detail in Section 3.5.1.
Following the general theory for derivatives of the Lagrangian (as outlined in Section 2.5) the gradient of the LMP2 energy with respect to the magnetic field is given by

$$\begin{aligned} E_2^{B_\beta} = \mathcal{L}_2^{B_\beta} = E_2^{(B_\beta)} + \sum_{kl} z^{\mathrm{loc}}_{kl} r_{kl}^{(B_\beta)} + \sum_{ck}\left[z_{ck} f_{ck}^{(B_\beta)} + z_{kc} f_{kc}^{(B_\beta)}\right] \\ + \sum_{pq} x_{pq}\left[\mathbf{C}^{\dagger}\mathbf{S}^{B_\beta}\mathbf{C}\right]_{pq}. \end{aligned} \tag{4.59}$$

For computational convenience the gradient expression (4.59) can be rearranged, collecting all terms which involve the perturbed AO overlap matrix $\mathbf{S}^{B_\beta}$ in the matrix $\mathbf{X}^{(2)}$ (this quantity is defined in detail in Section 4.3.2),

$$\begin{aligned} E_2^{B_\beta} = \sum_{cdkl}\left(\tilde{T}^{kl}_{cd} K^{kl,(B_\beta)*}_{cd} + \tilde{T}^{kl*}_{cd} K^{kl,(B_\beta)}_{cd}\right) \\ + \sum_{pq} f_{pq}^{(B_\beta)}\left[d^{(2)}_{pq} + z_{pq}\right] + \sum_{\mu\nu} X^{(2)}_{\mu\nu} S^{B_\beta}_{\mu\nu}. \end{aligned} \tag{4.60}$$

By adding the HF magnetic field gradient, Eq. (4.13), and splitting up the contribution from the perturbed Fock matrix into one-electron and two-electron contributions one finally obtains

$$E^{B_\beta}_{\mathrm{HF}} + E^{B_\beta}_2 = \sum_{\mu\nu}\left[D_{\mu\nu} h^{B_\beta}_{\mu\nu} + X_{\mu\nu} S^{B_\beta}_{\mu\nu}\right] + \sum_{\mu\nu\rho\sigma} \Gamma_{\mu\nu\rho\sigma}\left(\mu\nu|\rho\sigma\right)^{B_\beta}, \tag{4.61}$$

where the following one- and two-particle density matrices have been introduced,

$$D_{\mu\nu} = \sum_{pq} C^*_{\mu p} \left[d^{(0)}_{pq} + d^{(2)}_{pq} + z_{pq} \right] C_{\nu q}, \tag{4.62}$$

$$X_{\mu\nu} = X^{(0)}_{\mu\nu} + X^{(2)}_{\mu\nu}, \tag{4.63}$$

$$\Gamma_{\mu\nu\rho\sigma} = \Gamma^{\text{nonsep}}_{\mu\nu\rho\sigma} + \Gamma^{\text{sep}}_{\mu\nu\rho\sigma}, \tag{4.64}$$

$$\Gamma^{\text{nonsep}}_{\mu\nu\rho\sigma} = \sum_{cdkl} \left[\tilde{T}^{kl}_{cd} L^*_{\mu k} C_{\nu c} L^*_{\rho l} C_{\sigma d} + \tilde{T}^{kl*}_{cd} C^*_{\mu c} L_{\nu k} C^*_{\rho d} L_{\sigma l} \right], \tag{4.65}$$

$$\Gamma^{\text{sep}}_{\mu\nu\rho\sigma} = \bar{D}_{\mu\nu} D^{(0)}_{\rho\sigma} - \frac{1}{2} \bar{D}_{\mu\sigma} D^{(0)}_{\rho\nu}, \tag{4.66}$$

with

$$\bar{D}_{\mu\nu} = D_{\mu\nu} - \frac{1}{2} D^{(0)}_{\mu\nu}. \tag{4.67}$$

The HF density matrix $\mathbf{D}^{(0)}$ is defined in Eq. (4.7) and the HF energy weighted density matrix $\mathbf{X}^{(0)}$ in Eq. (4.17). The two-particle density matrix can be split into a separable part Γ^{sep} and into a non-separable part Γ^{nonsep}. The LMP2 generalized energy weighted density matrix $\mathbf{X}^{(2)}$ is treated in depth in the following subsection.

4.3.2 Generalized energy weighted density matrix

The generalized energy weighted density matrix $\mathbf{X}$ contains contributions from the derivatives of the localization condition and of the Hylleraas functional with respect to the AO overlap matrix, from the LMP2 Lagrange multipliers $\mathbf{x}$, which can be calculated according to Eq. (4.49), and from the HF energy weighted density matrix $\mathbf{X}^{(0)}$ (see Eq. 4.17).
The contributions from the derivative of the localization condition, Eq. (4.42),

with respect to the AO overlap matrix can be written as

$$\begin{aligned}\sum_{kl}\left(\frac{\partial r_{kl}}{\partial S_{\mu\nu}}\right)z_{kl}^{\mathrm{loc}} &= \sum_{k>l}\left[\left(\frac{\partial r_{kl}}{\partial S_{\mu\nu}}\right)z_{kl}^{\mathrm{loc}}+\left(\frac{\partial r_{kl}^{*}}{\partial S_{\mu\nu}}\right)z_{kl}^{\mathrm{loc}*}\right]\\ &= \sum_{k>l}\left[\left(L_{\mu k}^{*}L_{\nu k}-L_{\mu l}^{*}L_{\nu l}\right)\left(\delta_{\mu\in A}+\delta_{\nu\in A}\right)\right]\left[S_{kl}^{A}z_{kl}^{\mathrm{loc}}+S_{kl}^{A*}z_{kl}^{\mathrm{loc}*}\right]\\ &\quad+\sum_{k>l}\left[\left(S_{kk}^{A}-S_{ll}^{A}\right)L_{\mu k}^{*}L_{\nu l}\left(\delta_{\mu\in A}+\delta_{\nu\in A}\right)\right]z_{kl}^{\mathrm{loc}}\\ &\quad+\sum_{k>l}\left[\left(S_{kk}^{A*}-S_{ll}^{A*}\right)L_{\mu l}^{*}L_{\nu k}\left(\delta_{\mu\in A}+\delta_{\nu\in A}\right)\right]z_{kl}^{\mathrm{loc}*}. \end{aligned}\tag{4.68}$$

The Hylleraas functional depends on the AO overlap matrix through the amplitudes. For the derivative of the Hylleraas functional with respect to the AO overlap matrix one finds

$$\begin{aligned}\left(\frac{\partial E_2}{\partial S_{\mu\nu}}\right) &= \sum_{klab}\left[\left(\frac{\partial E_2}{\partial \tilde{T}_{ab}^{kl}}\right)\left(\frac{\partial \tilde{T}_{ab}^{kl}}{\partial S_{\mu\nu}}\right)+\left(\frac{\partial E_2}{\partial \tilde{T}_{ab}^{kl*}}\right)\left(\frac{\partial \tilde{T}_{ab}^{kl*}}{\partial S_{\mu\nu}}\right)\right]\\ &= \sum_{klab}\left[R_{ab}^{kl*}\left(\frac{\partial \tilde{T}_{ab}^{kl}}{\partial S_{\mu\nu}}\right)+R_{ab}^{kl}\left(\frac{\partial \tilde{T}_{ab}^{kl*}}{\partial S_{\mu\nu}}\right)\right]\\ &= \sum_{pq}\left[C_{\mu p}^{*}\tilde{x}_{pq}C_{\nu q}\right]\end{aligned}\tag{4.69}$$

with the matrix $\tilde{\mathbf{x}}$,

$$\begin{aligned}\tilde{x}_{ab} &= 2\sum_{klc}\left[R_{ac}^{kl*}\tilde{T}_{bc}^{kl}+\tilde{T}_{ac}^{kl*}R_{bc}^{kl}\right],\\ \tilde{x}_{ai} &= 2\sum_{klbrs\sigma}L_{\sigma i}^{*}S_{\sigma r}\tilde{T}_{rs}^{kl}Q_{bs}R_{ab}^{kl*},\\ \tilde{x}_{ia} &= 2\sum_{klbrs\sigma}L_{\sigma i}S_{\sigma r}^{*}\tilde{T}_{rs}^{kl*}Q_{bs}^{*}R_{ab}^{kl},\\ \tilde{x}_{ij} &= 0.\end{aligned}\tag{4.70}$$

Taking into account the contributions from the derivative of the localization condition with respect to the AO overlap matrix, Eq. (4.68), yields in total for $\mathbf{X}^{(2)}$,

$$X_{\mu\nu}^{(2)} = \sum_{pq}\left[C_{\mu p}^{*}(x_{pq}+\tilde{x}_{pq})C_{\nu q}\right]+\sum_{kl}\left(\frac{\partial r_{kl}}{\partial S_{\mu\nu}}\right)z_{kl}^{\mathrm{loc}}.\tag{4.71}$$

The virtual-virtual block of $\tilde{\mathbf{x}}$ cancels with corresponding terms in the virtual-virtual block of $\mathbf{A}$ (see Eq. 4.54) when the Lagrange multipliers $\mathbf{x}$ are calculated according to Eq. (4.49).
Since the generalized energy weighted density matrix is contracted with the Hermitian perturbed AO overlap matrix (see Eq. 4.60) one can apply the permutation operator $\mathcal{T}$ to symmetrize and complex conjugate the contributions from the virtual-occupied block of $\mathbf{x}^{\text{tot}} = \tilde{\mathbf{x}} + \mathbf{x}$,

$$\begin{aligned} E_2^{B_\beta} &\leftarrow \sum_{\mu\nu}\sum_{ai}\left[C^*_{\mu a}\left[\mathbf{x}^{\text{tot}}\right]_{ai} L_{\nu i} + L^*_{\mu i}\left[\mathbf{x}^{\text{tot}}\right]_{ia} C_{\nu a}\right] S^{B_\beta}_{\mu\nu} \\ &= \sum_{\mu\nu}\sum_{ai}\frac{1}{2}(1+\mathcal{T}_{\mu\nu})\left[C^*_{\mu a}\left[\mathbf{x}^{\text{tot}}\right]_{ai} L_{\nu i} + L^*_{\mu i}\left[\mathbf{x}^{\text{tot}}\right]_{ia} C_{\nu a}\right] S^{B_\beta}_{\mu\nu} \\ &= \sum_{\mu\nu}\sum_{ai}\frac{1}{2}(1+\mathcal{T}_{\mu\nu})\left[C^*_{\mu a}([\mathbf{x}^{\text{tot}}]_{ai} + \left[\mathbf{x}^{\text{tot},\dagger}\right]_{ai})L_{\nu i}\right] S^{B_\beta}_{\mu\nu}. \end{aligned} \tag{4.72}$$

The expressions for the virtual-occupied block of the matrix $\mathbf{x}^{\text{tot}}$,

$$\begin{aligned} [\mathbf{x}^{\text{tot}}]_{ai} + \left[\mathbf{x}^{\text{tot},\dagger}\right]_{ai} &= [\mathbf{x}]_{ai} + \left[\mathbf{x}^{\dagger}\right]_{ai} + [\tilde{\mathbf{x}}]_{ai} + \left[\tilde{\mathbf{x}}^{\dagger}\right]_{ai} \\ &= -\Bigg[A_{ai} + A^*_{ia} + \sum_c f_{ca} z_{ci} + \sum_k z_{ak} f_{ik} \\ &\quad + 2g(\mathbf{z})_{ia} + \left[\mathbf{a}\left(\mathbf{z}^{\text{loc}}\right)_{ai}\right] \\ &\quad - 4\sum_{klbrs\sigma} L^*_{\sigma i} S_{\sigma r} \tilde{T}^{kl}_{rs} Q_{bs} R^{kl*}_{ab}\Bigg], \end{aligned} \tag{4.73}$$

can be further simplified by adding the Z-CPHF Eqs. (4.50),

$$\begin{aligned} &[\mathbf{x}^{\text{tot}}]_{ai} + \left[\mathbf{x}^{\text{tot},\dagger}\right]_{ai} \\ &= -\left[2A^*_{ia} + 2\sum_k z_{ak} f_{ik} - 4\sum_{klbrs\sigma} L^*_{\sigma i} S_{\sigma r} \tilde{T}^{kl}_{rs} Q_{bs} R^{kl*}_{ab}\right] \\ &= -\sum_k\left[4\sum_{cl}\tilde{T}^{kl*}_{ac} K^{kl}_{ic} + 2z_{ak} f_{ik}\right]. \end{aligned} \tag{4.74}$$

Summing up all contributions the generalized energy weighted density matrix in AO basis can be written as

$$\begin{aligned}
X_{\mu\nu} &= X^{(0)}_{\mu\nu} + X^{(2)}_{\mu\nu} \\
&= \sum_{ij}\left[-L^*_{\mu i}\left(2f_{ji} + \frac{1}{2}\left(A_{ij} + A^*_{ji}\right) + 2g\left(\mathbf{z}\right)_{ji}\right)L_{\nu j}\right] \\
&\quad - \sum_{acikl} C^*_{\mu a}\left[4\tilde{T}^{kl*}_{ac}K^{kl}_{ic} + 2z_{ak}f_{ik}\right]L_{\nu i} \\
&\quad + 2\sum_{ab} C^*_{\mu a}\left[\sum_{cdkl} f_{cd}T^{kl*}_{ca}\tilde{T}^{kl}_{db}\right]C_{\nu b} \\
&\quad - 2\sum_{ab} C^*_{\mu a}\left[\sum_{cjkl} f_{kl}\left(T^{lj*}_{ca}\tilde{T}^{kj}_{cb} + T^{lj*}_{ac}\tilde{T}^{kj}_{bc}\right)\right]C_{\nu b} \\
&\quad + \sum_{ij}\left[\left(\frac{\partial r_{ij}}{\partial S_{\mu\nu}}\right)z^{\mathrm{loc}}_{ij} - \frac{1}{2}L^*_{\mu i}\left[\left[\mathbf{a}\left(\mathbf{z}^{\mathrm{loc}}\right)\right]_{ij} + \left[\mathbf{a}\left(\mathbf{z}^{\mathrm{loc}}\right)^*_{ji}\right]\right]L_{\nu j}\right].
\end{aligned} \tag{4.75}$$

4.3.3 Second derivative of the LMP2 Lagrangian

For the calculation of LMP2 magnetizabilities the LMP2 magnetic field gradient has to be differentiated a second time with respect to the magnetic field. Starting from the gradient expression Eq. (4.61) one obtains for the LMP2 magnetizability tensor (including the HF contribution)

$$\begin{aligned}
\xi^{\mathrm{LMP2}}_{\alpha\beta} &= -\sum_{\mu\nu}\left[\frac{\partial D_{\mu\nu}}{\partial B_\alpha}\frac{\partial h_{\mu\nu}}{\partial B_\beta} + D_{\mu\nu}\frac{\partial^2 h_{\mu\nu}}{\partial B_\alpha \partial B_\beta}\right] \\
&\quad - \sum_{\mu\nu}\left[\frac{\partial X_{\mu\nu}}{\partial B_\alpha}\frac{\partial S_{\mu\nu}}{\partial B_\beta} + X_{\mu\nu}\frac{\partial^2 S_{\mu\nu}}{\partial B_\alpha \partial B_\beta}\right] \\
&\quad - \sum_{\mu\nu\rho\sigma}\left[\frac{\partial \Gamma_{\mu\nu\rho\sigma}}{\partial B_\alpha}\frac{\partial(\mu\nu|\rho\sigma)}{\partial B_\beta} + \Gamma_{\mu\nu\rho\sigma}\frac{\partial^2(\mu\nu|\rho\sigma)}{\partial B_\alpha \partial B_\beta}\right]\Bigg|_{\mathbf{B}=0}
\end{aligned} \tag{4.76}$$

with the orbital-relaxed perturbed density matrix

$$\frac{\partial D_{\mu\nu}}{\partial B_\alpha} = \sum_{pq}\left[C^{B_\alpha *}_{\mu p}d_{pq}C_{\nu q} + C^*_{\mu p}d^{B_\alpha}_{pq}C_{\nu q} + C^*_{\mu p}d_{pq}C^{B_\alpha}_{\nu q}\right] \tag{4.77}$$

and the perturbed MO coefficient matrix $\mathbf{C}^{B_\alpha}$ as well as the perturbed density matrix $\mathbf{d}^{B_\alpha}$ to be evaluated. The latter contains contributions from the derivatives of the HF density matrix $\mathbf{d}^{(0)}$, of the LMP2 density matrix $\mathbf{d}^{(2)}$, and of the Lagrange multipliers $\mathbf{z}$,

$$d_{pq}^{B_\alpha} = \left(\left[\mathbf{d}^{(0)} \right]_{pq}^{B_\alpha} + \left[\mathbf{d}^{(2)} \right]_{pq}^{B_\alpha} + \left[\mathbf{z} \right]_{pq}^{B_\alpha} \right) \tag{4.78}$$

with the perturbed HF density matrix in AO basis according to Ref. [68],

$$\frac{D_{\mu\nu}^{(0)}}{\partial B_\alpha} = \left[\mathbf{D}^{(0)} \right]_{\mu\nu}^{B_\alpha} = 2 \sum_k \left[L_{\mu k}^{B_\alpha *} L_{\nu k} + L_{\mu k}^{*} L_{\nu k}^{B_\alpha} \right], \tag{4.79}$$

where $\mathbf{L}^{B_\alpha}$ are the perturbed LMO coefficients for which explicit expressions are given in Section 3.4.1.

First, the response of the non-variational parameters which are the (localized) MO coefficients has to be calculated (see Section 2.5). In order to ensure that the LMP2 Lagrangian is variational with respect to the MO coefficients for any value of the perturbation the first derivatives of the stationary conditions with respect to the external magnetic field must be zero, i.e.,

$$\frac{\partial}{\partial B_\alpha} \left(\frac{\partial \mathcal{L}_2}{\partial x_{pq}} \right)_{\mathbf{B}=0} = \left(\frac{\partial \left(\mathbf{C}^\dagger \mathbf{S} \mathbf{C} \right)_{pq}}{\partial B_\alpha} \right)_{\mathbf{B}=0} = 0, \tag{4.80}$$

$$\frac{\partial}{\partial B_\alpha} \left(\frac{\partial \mathcal{L}_2}{\partial z_{ai}} \right)_{\mathbf{B}=0} = \left(\frac{\partial f_{ai}}{\partial B_\alpha} \right)_{\mathbf{B}=0} = 0, \tag{4.81}$$

$$\frac{\partial}{\partial B_\alpha} \left(\frac{\partial \mathcal{L}_2}{\partial z_{ij}^{\mathrm{loc}}} \right)_{\mathbf{B}=0} = \left(\frac{\partial r_{ij}}{\partial B_\alpha} \right)_{\mathbf{B}=0} = 0. \tag{4.82}$$

These equations yield, in the following order, the conditions for the orthonormality of the perturbed MO coefficients, the coupled-perturbed Hartree-Fock (CPHF) equations, and the coupled-perturbed localization equations (CPL equations, for details see Section 3.4.1). Their solutions provide the perturbed LMO coefficients. Note that the CPL equations do not have to be solved in the case of HF, conventional MP2, or untruncated LMP2 (i.e., with full lists and full pair domains) in order to obtain

the perturbed MO coefficients.

With the perturbed LMO coefficients available the perturbed LMP2 amplitudes can be calculated in the orbital-relaxed case. The stationary conditions of the Hylleraas functional have to be fulfilled in the presence of a magnetic field, i.e.,

$$\frac{\partial}{\partial B_\alpha}\left(\frac{\partial E_2}{\partial \tilde{T}^{ij}_{ab}}\right)_{\mathbf{B}=0} = \left(\frac{\partial R^{ij}_{ab}}{\partial B_\alpha}\right)_{\mathbf{B}=0} = 0. \tag{4.83}$$

The explicit equations for the perturbed residual in PAO basis are given in Section 3.5.4.

The perturbed LMP2 amplitudes can then be used to build the perturbed LMP2 density matrix,

$$\begin{aligned}
\left[\mathbf{d}^{(2)}\right]^{B_\alpha}_{ij} &= -2\sum_{cd}\sum_{k}\left[\frac{\partial T^{ik}_{cd}}{\partial B_\alpha}\tilde{T}^{jk*}_{cd} + T^{ik}_{cd}\frac{\partial \tilde{T}^{jk*}_{cd}}{\partial B_\alpha}\right], \\
\left[\mathbf{d}^{(2)}\right]^{B_\alpha}_{ab} &= 2\sum_{c}\sum_{kl}\left[\frac{\partial \tilde{T}^{kl*}_{ac}}{\partial B_\alpha}T^{kl}_{bc} + \tilde{T}^{kl*}_{ac}\frac{\partial T^{kl}_{bc}}{\partial B_\alpha}\right], \\
\left[\mathbf{d}^{(2)}\right]^{B_\alpha}_{ia} &= \left[\mathbf{d}^{(2)}\right]^{B_\alpha}_{ai} \;=\; 0\,.
\end{aligned} \tag{4.84}$$

The response of the Lagrange multipliers $\mathbf{z}$ and $\mathbf{z}^{\mathrm{loc}}$ is obtained from the first-order Z-vector equations, i.e., the derivatives of the Z-CPHF Eqs. (4.50) and Z-CPL Eqs. (4.57) with respect to the magnetic field. The perturbed Lagrange multipliers $\mathbf{z}^{B_\alpha}$ are needed for the orbital-relaxed perturbed density matrix, Eq. (4.78); the perturbed multipliers of the localization condition, $\partial\mathbf{z}^{\mathrm{loc}}/\partial B_\alpha$, enter the right-hand side of the perturbed Z-CPHF Eqs. (4.85) and the perturbed generalized energy weighted density matrix $\partial\mathbf{X}/\partial B_\alpha$ (see Eq. 4.89). The perturbed Z-vector equations in MO basis without density fitting can be found in Ref. [33].

For the perturbed Z-CPHF equations one obtains

$$\sum_{c} f_{ca} z^{B_\alpha}_{ci} - \sum_{k} z^{B_\alpha}_{ak} f_{ik} + 2g(\mathbf{z}^{B_\alpha})_{ia} = -\frac{\partial Y_{ai}}{\partial B_\alpha} \tag{4.85}$$

with the right-hand side

$$\frac{\partial Y_{ai}}{\partial B_\alpha} = \frac{\partial y_{ai}}{\partial B_\alpha} + \sum_c \frac{\partial f_{ca}}{\partial B_\alpha} z_{ci} - \sum_k z_{ak} \frac{\partial f_{ik}}{\partial B_\alpha} + 2\frac{\partial g(\mathbf{z})_{ia}}{\partial B_\alpha}, \tag{4.86}$$

where y_{ai} is defined in Eq. (4.51). All terms contributing to the perturbed Z-CPHF equations are given in detail in Section 3.5.3.
The perturbed Z-CPL equations can be written as

$$\frac{\partial}{\partial B_\alpha}\left[(1-\mathcal{T}_{ij})\left(A_{ij} + \left[\mathbf{a}\left(\mathbf{z}^{\mathrm{loc}}\right)\right]_{ij}\right)\right] = 0 \tag{4.87}$$

with the derivative

$$\left[\frac{\partial \mathbf{a}(\mathbf{z}^{\mathrm{loc}})}{\partial B_\alpha}\right]_{pi} = \sum_{k>l}\left(\mathcal{B}^-_{pi,kl}\frac{\partial z^{\mathrm{loc}}_{kl}}{\partial B_\alpha} + \frac{\partial \mathcal{B}^+_{pi,kl}}{\partial B_\alpha} z^{\mathrm{loc}}_{kl}\right). \tag{4.88}$$

Detailed equations and the definitions of the coefficient matrices $\mathcal{B}^-$ and $\partial\mathcal{B}^+/\partial B_\alpha$ in Eq. (4.88) are given in Section 3.5.2.
Since the virtual-occupied part of the quantity defined in Eq. (4.88) gives a contribution to the right-hand side of the perturbed Z-CPHF Eqs. (4.85) the perturbed Z-CPL equations have to be solved beforehand.
The derivative of the generalized energy weighted density matrix, which is required for the calculation of magnetizabilities in Eq. (4.76), can be obtained by differentiation of the unperturbed quantity defined in Eq. (4.75)

with respect to the magnetic field,

$$
\begin{aligned}
\frac{\partial X_{\mu\nu}}{\partial B_\alpha} &= X_{\mu\nu}^{B_\alpha} = X_{\mu\nu}^{(0),B_\alpha} + X_{\mu\nu}^{(2),B_\alpha} \\
&= \sum_{ij}\left[-\left(2f_{ji} + \frac{1}{2}\left(A_{ij} + A_{ji}^*\right) + 2g\left(\mathbf{z}\right)_{ji}\right)\right]\left[L_{\mu i}^{B_\alpha *} L_{\nu j} + L_{\mu i}^* L_{\nu j}^{B_\alpha}\right] \\
&\quad - \sum_{ij}\left[L_{\mu i}^*\left(2\frac{\partial f_{ji}}{\partial B_\alpha} + \frac{1}{2}\left(\frac{\partial A_{ij}}{\partial B_\alpha} + \frac{\partial A_{ji}^*}{\partial B_\alpha}\right) + 2\frac{\partial g\left(\mathbf{z}\right)_{ji}}{\partial B_\alpha} + 2g\left(\mathbf{z}^{B_\alpha}\right)_{ji}\right) L_{\nu j}\right] \\
&\quad - \sum_{acikl}\left[4\tilde{T}_{ac}^{kl*} K_{ic}^{kl} + 2z_{ak} f_{ik}\right]\left[C_{\mu a}^{B_\alpha *} L_{\nu i} + C_{\mu a}^* L_{\nu i}^{B_\alpha}\right] \\
&\quad - \sum_{acikl} C_{\mu a}^*\left[4\left(\frac{\partial \tilde{T}_{ac}^{kl*}}{\partial B_\alpha} K_{ic}^{kl} + \tilde{T}_{ac}^{kl*}\frac{\partial K_{ic}^{kl}}{\partial B_\alpha}\right) + 2\left(\frac{\partial z_{ak}}{\partial B_\alpha} f_{ik} + z_{ak}\frac{\partial f_{ik}}{\partial B_\alpha}\right)\right] L_{\nu i} \\
&\quad + 2\sum_{abcdkl}\left[f_{cd} T_{ca}^{kl*} \tilde{T}_{db}^{kl}\right]\left[C_{\mu a}^{B_\alpha *} C_{\nu b} + C_{\mu a}^* C_{\nu b}^{B_\alpha}\right] \\
&\quad + 2\sum_{abcdkl} C_{\mu a}^*\left[\frac{\partial f_{cd}}{\partial B_\alpha} T_{ca}^{kl*} \tilde{T}_{db}^{kl} + f_{cd}\frac{\partial T_{ca}^{kl*}}{\partial B_\alpha}\tilde{T}_{db}^{kl} + f_{cd} T_{ca}^{kl*}\frac{\partial \tilde{T}_{db}^{kl}}{\partial B_\alpha}\right] C_{\nu b} \\
&\quad - 2\sum_{ab}\left[\sum_{cjkl} f_{kl}\left(T_{ca}^{lj*}\tilde{T}_{cb}^{kj} + T_{ac}^{lj*}\tilde{T}_{bc}^{kj}\right)\right]\left[C_{\mu a}^{B_\alpha *} C_{\nu b} + C_{\mu a}^* C_{\nu b}^{B_\alpha}\right] \\
&\quad - 2\sum_{ab} C_{\mu a}^*\left[\sum_{cjkl}\frac{\partial f_{kl}}{\partial B_\alpha}\left(T_{ca}^{lj*}\tilde{T}_{cb}^{kj} + T_{ac}^{lj*}\tilde{T}_{bc}^{kj}\right)\right] C_{\nu b} \\
&\quad - 2\sum_{ab} C_{\mu a}^*\left[\sum_{cjkl} f_{kl}\left(\frac{\partial T_{ca}^{lj*}}{\partial B_\alpha}\tilde{T}_{cb}^{kj} + T_{ca}^{lj*}\frac{\partial \tilde{T}_{cb}^{kj}}{\partial B_\alpha} + T_{ac}^{lj*}\frac{\partial \tilde{T}_{bc}^{kj}}{\partial B_\alpha} + \frac{\partial T_{ac}^{lj*}}{\partial B_\alpha}\tilde{T}_{bc}^{kj}\right)\right] C_{\nu b} \\
&\quad + \sum_{ij}\frac{\partial}{\partial B_\alpha}\left[\left(\frac{\partial r_{ij}}{\partial S_{\mu\nu}}\right) z_{ij}^{\mathrm{loc}}\right] \\
&\quad - \frac{1}{2}\sum_{ij}\left[\left[\mathbf{a}\left(\mathbf{z}^{\mathrm{loc}}\right)\right]_{ij} + \left[\mathbf{a}\left(\mathbf{z}^{\mathrm{loc}}\right)^*_{ji}\right]\right]\left[L_{\mu i}^{B_\alpha *} L_{\nu j} + L_{\mu i}^* L_{\nu j}^{B_\alpha}\right] \\
&\quad - \frac{1}{2}\sum_{ij} L_{\mu i}^*\left[\left[\frac{\partial \mathbf{a}\left(\mathbf{z}^{\mathrm{loc}}\right)}{\partial B_\alpha}\right]_{ij} + \left[\frac{\partial \mathbf{a}\left(\mathbf{z}^{\mathrm{loc}}\right)^*}{\partial B_\alpha}\right]_{ji}\right] L_{\nu j}. \qquad (4.89)
\end{aligned}
$$

Finally, the derivative of the effective second-order density matrix $\mathbf{\Gamma}$ which is defined in Eq. (4.64) can be written as

$$\frac{\partial \Gamma_{\mu\nu\rho\sigma}}{\partial B_\alpha} = \Gamma^{B_\alpha}_{\mu\nu\rho\sigma} = \Gamma^{\mathrm{nonsep},B_\alpha}_{\mu\nu\rho\sigma} + \Gamma^{\mathrm{sep},B_\alpha}_{\mu\nu\rho\sigma}, \tag{4.90}$$

$$\begin{aligned}
\Gamma^{\mathrm{nonsep},B_\alpha}_{\mu\nu\rho\sigma} = \sum_{cdkl} \Bigg[& \frac{\partial \tilde{T}^{kl}_{cd}}{\partial B_\alpha} L^*_{\mu k} C_{\nu c} L^*_{\rho l} C_{\sigma d} + \tilde{T}^{kl}_{cd} \frac{\partial L^*_{\mu k}}{\partial B_\alpha} C_{\nu c} L^*_{\rho l} C_{\sigma d} \\
& + \tilde{T}^{kl}_{cd} L^*_{\mu k} \frac{\partial C_{\nu c}}{\partial B_\alpha} L^*_{\rho l} C_{\sigma d} + \tilde{T}^{kl}_{cd} L^*_{\mu k} C_{\nu c} \frac{\partial L^*_{\rho l}}{\partial B_\alpha} C_{\sigma d} \\
& + \tilde{T}^{kl}_{cd} L^*_{\mu k} C_{\nu c} L^*_{\rho l} \frac{\partial C_{\sigma d}}{\partial B_\alpha} + \frac{\partial \tilde{T}^{kl*}_{cd}}{\partial B_\alpha} C^*_{\mu c} L_{\nu k} C^*_{\rho d} L_{\sigma l} \\
& + \tilde{T}^{kl*}_{cd} \frac{\partial C^*_{\mu c}}{\partial B_\alpha} L_{\nu k} C^*_{\rho d} L_{\sigma l} + \tilde{T}^{kl*}_{cd} C^*_{\mu c} \frac{\partial L_{\nu k}}{\partial B_\alpha} C^*_{\rho d} L_{\sigma l} \\
& + \tilde{T}^{kl*}_{cd} C^*_{\mu c} L_{\nu k} \frac{\partial C^*_{\rho d}}{\partial B_\alpha} L_{\sigma l} + \tilde{T}^{kl*}_{cd} C^*_{\mu c} L_{\nu k} C^*_{\rho d} \frac{\partial L_{\sigma l}}{\partial B_\alpha} \Bigg],
\end{aligned} \tag{4.91}$$

$$\begin{aligned}
\Gamma^{\mathrm{sep},B_\alpha}_{\mu\nu\rho\sigma} = & \frac{\partial \bar{D}_{\mu\nu}}{\partial B_\alpha} D^{(0)}_{\rho\sigma} + \bar{D}_{\mu\nu} \frac{\partial D^{(0)}_{\rho\sigma}}{\partial B_\alpha} \\
& - \frac{1}{2} \left[\frac{\partial \bar{D}_{\mu\sigma}}{\partial B_\alpha} D^{(0)}_{\rho\nu} + \bar{D}_{\mu\sigma} \frac{\partial D^{(0)}_{\rho\nu}}{\partial B_\alpha} \right].
\end{aligned} \tag{4.92}$$

4.3.4 Density fitting for LMP2 magnetizabilities

The density fitting (DF) approximation can be applied to the derivatives of the four-index electron repulsion integrals (ERIs) in the magnetizability tensor, Eq. (4.76),

$$\frac{\partial (\mu\nu|\rho\sigma)}{\partial B_\beta} = \sum_P \left[\frac{\partial (\mu\nu|P)}{\partial B_\beta} c^P_{\rho\sigma} + c^P_{\mu\nu} \frac{\partial (P|\rho\sigma)}{\partial B_\beta} \right]. \tag{4.93}$$

Applying the DF approximation to the contraction of the separable part of the perturbed two-electron density matrix with the derivative of the ERIs

with respect to the magnetic field one obtains

$$\begin{aligned}
&\sum_{\mu\nu\rho\sigma}\left[\frac{\partial\bar{D}_{\mu\nu}}{\partial B_\alpha}D^{(0)}_{\rho\sigma}+\bar{D}_{\mu\nu}\frac{\partial D^{(0)}_{\rho\sigma}}{\partial B_\alpha}-\frac{1}{2}\frac{\partial\bar{D}_{\mu\sigma}}{\partial B_\alpha}D^{(0)}_{\rho\nu}-\frac{1}{2}\bar{D}_{\mu\sigma}\frac{\partial D^{(0)}_{\rho\nu}}{\partial B_\alpha}\right]\frac{\partial(\mu\nu|\rho\sigma)}{\partial B_\beta}\\
&=\sum_{\mu\nu P}\frac{\partial(\mu\nu|P)}{\partial B_\beta}\left[\frac{\partial\bar{D}_{\mu\nu}}{\partial B_\alpha}\left[c(\mathbf{D}^{(0)})\right]^P+\frac{\partial D^{(0)}_{\mu\nu}}{\partial B_\alpha}\left[c(\bar{\mathbf{D}})\right]^P\right]\\
&\quad-2\sum_{\mu\nu\sigma kP}\frac{\partial(\mu\nu|P)}{\partial B_\beta}\left[\frac{\partial\bar{D}_{\mu\sigma}}{\partial B_\alpha}L_{\nu k}c^P_{k\sigma}+\sum_\rho\left(\bar{D}_{\mu\sigma}L_{\nu k}\frac{\partial L^*_{\rho k}}{\partial B_\alpha}c^P_{\rho\sigma}+\bar{D}_{\mu\sigma}\frac{\partial L_{\nu k}}{\partial B_\alpha}c^P_{k\sigma}\right)\right],
\end{aligned}\tag{4.94}$$

where fitting coefficients (FCs) $[c(\mathbf{D})]^P$ for a general density matrix $\mathbf{D}$ have been introduced,

$$[c(\mathbf{D})]^P=\sum_{\mu\nu}\sum_Q D_{\mu\nu}(\mu\nu|Q)J^{-1}_{PQ}.\tag{4.95}$$

The second derivative of the ERIs with respect to the magnetic field can be written as

$$\begin{aligned}
\frac{\partial^2(\mu\nu|\rho\sigma)}{\partial B_\alpha\partial B_\beta}=\sum_P\Bigg[&\frac{\partial^2(\mu\nu|P)}{\partial B_\alpha\partial B_\beta}c^P_{\rho\sigma}+\frac{\partial(\mu\nu|P)}{\partial B_\alpha}\frac{\partial c^P_{\rho\sigma}}{\partial B_\beta}\\
&+\frac{\partial c^P_{\mu\nu}}{\partial B_\beta}\frac{\partial(P|\rho\sigma)}{\partial B_\alpha}+c^P_{\mu\nu}\frac{\partial^2(P|\rho\sigma)}{\partial B_\alpha\partial B_\beta}\Bigg]
\end{aligned}\tag{4.96}$$

with the unperturbed and perturbed FCs

$$c^P_{\mu\nu}=\sum_Q J^{-1}_{PQ}(Q|\mu\nu),\tag{4.97}$$

$$\frac{\partial c^P_{\mu\nu}}{\partial B_\beta}=\sum_Q J^{-1}_{PQ}\frac{\partial(Q|\mu\nu)}{\partial B_\beta}.\tag{4.98}$$

By applying the DF approximation to the contraction of the separable part of the unperturbed two-electron density matrix with the second derivative

of the ERIs with respect to the magnetic field one obtains

$$\sum_{\mu\nu\rho\sigma}\left[\bar{D}_{\mu\nu}D^{(0)}_{\rho\sigma}-\frac{1}{2}\bar{D}_{\mu\sigma}D^{(0)}_{\rho\nu}\right]\frac{\partial^2(\mu\nu|\rho\sigma)}{\partial B_\alpha\partial B_\beta}$$
$$=\sum_{\mu\nu P}\frac{\partial^2(\mu\nu|P)}{\partial B_\alpha\partial B_\beta}\left[\bar{D}_{\mu\nu}\left[c(\mathbf{D}^{(0)})\right]^P+D^{(0)}_{\mu\nu}\left[c(\bar{\mathbf{D}})\right]^P-2\sum_{\sigma k}\bar{D}_{\mu\sigma}L_{\nu k}c^P_{k\sigma}\right]$$
$$-\sum_{\mu\sigma kP}\bar{D}_{\mu\sigma}\left[c^{P,(B_\beta)}_{\mu k}(P|k\sigma)^{(B_\alpha)}+c^{P,(B_\alpha)}_{\mu k}(P|k\sigma)^{(B_\beta)}\right] \tag{4.99}$$
$$=\sum_{\mu\nu P}\frac{\partial^2(\mu\nu|P)}{\partial B_\alpha\partial B_\beta}\left[\bar{D}_{\mu\nu}\left[c(\mathbf{D}^{(0)})\right]^P+D^{(0)}_{\mu\nu}\left[c(\bar{\mathbf{D}})\right]^P-2\sum_{\sigma k}\bar{D}_{\mu\sigma}L_{\nu k}c^P_{k\sigma}\right]$$
$$-2\sum_{\mu\sigma kP}\bar{D}_{\mu\sigma}\left[c^{P,(B_\beta)}_{\mu k}(P|k\sigma)^{(B_\alpha)}\right] \tag{4.100}$$

with the unperturbed and perturbed half-transformed fitting coefficients,

$$c^P_{\mu k}=\sum_{\nu Q}J^{-1}_{PQ}(Q|\mu\nu)L_{\nu k}, \tag{4.101}$$
$$c^{P,(B_\beta)}_{\mu k}=\sum_{\nu Q}J^{-1}_{PQ}\frac{\partial(Q|\mu\nu)}{\partial B_\beta}L_{\nu k}, \tag{4.102}$$

and the perturbed half-transformed three-index ERIs

$$(P|k\sigma)^{(B_\beta)}=\sum_{\rho}\frac{\partial(P|\rho\sigma)}{\partial B_\beta}L^*_{\rho k}. \tag{4.103}$$

Note that there are no contributions from the Coulomb-type contractions of the symmetric unperturbed density matrices with the purely imaginary and thus antisymmetric first derivatives of the three-index-ERIs $(\mu\nu|P)$; only exchange-type contractions are generally non-zero (see the second line of Eqs. 4.99 and 4.100).

The contributions from the non-separable part of the unperturbed two-electron density matrix to the gradient (see Eqs. 4.65 and 4.61) and from the non-separable part of the unperturbed and perturbed two-electron density matrices to the magnetizability tensor (see Eqs. 4.65, 4.91, and 4.76) can be

calculated via conveniently chosen intermediates.
For the gradient the contribution in PAO basis can be written as

$$\begin{aligned} E_2^{B_\beta} &\leftarrow \sum_{\mu\nu\rho\sigma} \Gamma^{\text{nonsep}}_{\mu\nu\rho\sigma} (\mu\nu|\rho\sigma)^{B_\beta} \\ &= \sum_{\mu\nu\rho\sigma} \sum_{kl} \sum_{rs\in[kl]} \Big[\tilde{T}^{kl}_{rs} L^*_{\mu k} P_{\nu r} L^*_{\rho l} P_{\sigma s} \\ &\quad + \tilde{T}^{kl*}_{rs} P^*_{\mu r} L_{\nu k} P^*_{\rho s} L_{\sigma l} \Big] (\mu\nu|\rho\sigma)^{B_\beta} \\ &\overset{\text{DF}}{=} 2 \sum_{\mu\nu kP} \sum_{r\in[k]_\text{U}} (\mu\nu|P)^{B_\beta} \Big[V^{P*}_{kr} L^*_{\mu k} P_{\nu r} + V^P_{kr} P^*_{\mu r} L_{\nu k} \Big] \\ &= 2 \sum_{\mu\nu P} (\mu\nu|P)^{B_\beta} \Big[V^{P*}_{\mu\nu} + V^P_{\nu\mu} \Big]. \end{aligned} \tag{4.104}$$

The three-index quantity V^P_{kr} was already introduced for NMR shielding tensors (see Eq. 3.109),

$$V^P_{kr} = \sum_l \sum_{s\in[kl]} \tilde{T}^{kl*}_{rs} c^P_{sl}, \tag{4.105}$$

$$V^{P*}_{kr} = \sum_l \sum_{s\in[kl]} \tilde{T}^{kl}_{rs} c^P_{ls}, \tag{4.106}$$

and can be transformed step by step to AO basis,

$$V^P_{k\mu} = \sum_{r\in[k]_\text{U}} V^P_{kr} P^*_{\mu r}, \tag{4.107}$$

$$V^{P*}_{k\nu} = \sum_{r\in[k]_\text{U}} V^{P*}_{kr} P_{\nu r}, \tag{4.108}$$

and

$$V^P_{\nu\mu} = \sum_k L_{\nu k} V^P_{k\mu}, \tag{4.109}$$

$$V^{P*}_{\mu\nu} = \sum_k L^*_{\mu k} V^{P*}_{k\nu}. \tag{4.110}$$

The contribution from the non-separable part to the magnetizability tensor,

$$\xi^{\text{LMP2}}_{\alpha\beta} \leftarrow \sum_{\mu\nu\rho\sigma} \left[\frac{\partial \Gamma^{\text{nonsep}}_{\mu\nu\rho\sigma}}{\partial B_\alpha} \frac{\partial (\mu\nu|\rho\sigma)}{\partial B_\beta} + \Gamma^{\text{nonsep}}_{\mu\nu\rho\sigma} \frac{\partial^2 (\mu\nu|\rho\sigma)}{\partial B_\alpha \partial B_\beta} \right], \tag{4.111}$$

is obtained in DF approximation by differentiating Eq. (4.104) a second time with respect to the magnetic field,

$$\xi_{\alpha\beta}^{\mathrm{LMP2}} \leftarrow 2\sum_{\mu\nu P}\frac{\partial^2(\mu\nu|P)}{\partial B_\alpha \partial B_\beta}\left[V_{\mu\nu}^{P*}+V_{\nu\mu}^{P}\right] + 2\sum_{\mu\nu P}\frac{\partial(\mu\nu|P)}{\partial B_\beta}\left[\frac{\partial V_{\mu\nu}^{P*}}{\partial B_\alpha}+\frac{\partial V_{\nu\mu}^{P}}{\partial B_\alpha}\right]. \tag{4.112}$$

The perturbed quantities are defined in analogy to the unperturbed Eqs. (4.109) and (4.110) as

$$\frac{\partial V_{\nu\mu}^{P}}{\partial B_\alpha} = \sum_k\left[\frac{\partial L_{\nu k}}{\partial B_\alpha}V_{k\mu}^{P}+L_{\nu k}\frac{\partial V_{k\mu}^{P}}{\partial B_\alpha}\right], \tag{4.113}$$

$$\frac{\partial V_{\mu\nu}^{P*}}{\partial B_\alpha} = \sum_k\left[\frac{\partial L_{\mu k}^{*}}{\partial B_\alpha}V_{k\nu}^{P*}+L_{\mu k}^{*}\frac{\partial V_{k\nu}^{P*}}{\partial B_\alpha}\right], \tag{4.114}$$

with the perturbed half-transformed quantities,

$$\frac{\partial V_{k\mu}^{P}}{\partial B_\alpha} = \sum_{r\in[k]_{\mathrm{U}}}\left[\frac{\partial V_{kr}^{P}}{\partial B_\alpha}P_{\mu r}^{*}+V_{kr}^{P}\frac{\partial P_{\mu r}^{*}}{\partial B_\alpha}\right], \tag{4.115}$$

$$\frac{\partial V_{k\nu}^{P*}}{\partial B_\alpha} = \sum_{r\in[k]_{\mathrm{U}}}\left[\frac{\partial V_{kr}^{P*}}{\partial B_\alpha}P_{\nu r}+V_{kr}^{P*}\frac{\partial P_{\nu r}}{\partial B_\alpha}\right], \tag{4.116}$$

and the perturbed quantities in MO basis,

$$\frac{\partial V_{kr}^{P}}{\partial B_\alpha} = \sum_l\sum_{s\in[kl]}\left[\frac{\partial \tilde{T}_{rs}^{kl*}}{\partial B_\alpha}c_{sl}^{P}+\tilde{T}_{rs}^{kl*}\frac{\partial c_{sl}^{P}}{\partial B_\alpha}\right], \tag{4.117}$$

$$\frac{\partial V_{kr}^{P*}}{\partial B_\alpha} = \sum_l\sum_{s\in[kl]}\left[\frac{\partial \tilde{T}_{rs}^{kl}}{\partial B_\alpha}c_{ls}^{P}+\tilde{T}_{rs}^{kl}\frac{\partial c_{ls}^{P}}{\partial B_\alpha}\right], \tag{4.118}$$

with the perturbed fitting coefficients

$$\frac{\partial c_{sl}^{P}}{\partial B_\alpha} = \sum_Q J_{PQ}^{-1}\frac{\partial(Q|sl)}{\partial B_\alpha}. \tag{4.119}$$

The unperturbed quantities defined in Eqs. (4.105)–(4.110) and the perturbed quantities, Eqs. (4.113)–(4.118), are required to build two further

perturbed quantities: (*i*) $\partial\mathbf{B}/\partial B_\alpha$, which is the derivative of Eq. (4.56), and is required for the right-hand side of the perturbed Z-CPHF Eqs. (4.85),

$$\frac{\partial B_{\nu k}}{\partial B_\alpha} = \sum_{\mu P}\left(\frac{\partial(\mu\nu|P)}{\partial B_\alpha}V^P_{k\mu} + (\mu\nu|P)\frac{\partial V^P_{k\mu}}{\partial B_\alpha}\right), \tag{4.120}$$

and (*ii*) the quantity $\partial X^{\mathrm{K}}/\partial B_\alpha$ which is required for the perturbed generalized energy weighted LMP2 density matrix Eq. (4.89),

$$\begin{aligned}\frac{\partial X^{\mathrm{K}}_{ri}}{\partial B_\alpha} &= \sum_{kls}\left(\frac{\partial \tilde{T}^{kl*}_{rs}}{\partial B_\alpha}K^{kl}_{is} + \tilde{T}^{kl*}_{rs}\frac{\partial K^{kl}_{is}}{\partial B_\alpha}\right)\\ &= \sum_{kP}\left(\frac{\partial V^P_{kr}}{\partial B_\alpha}(P|ik) + V^P_{kr}\frac{\partial(P|ik)}{\partial B_\alpha}\right).\end{aligned} \tag{4.121}$$

In the program the following quantity is evaluated

$$\frac{\partial X^{\mathrm{K}}_{r\mu}}{\partial B_\alpha} = \sum_{kP}\left(\frac{\partial V^P_{kr}}{\partial B_\alpha}(P|\mu k) + V^P_{kr}\frac{\partial(P|\mu k)}{\partial B_\alpha}\right), \tag{4.122}$$

which is then transformed to MO basis in the following way:

$$\frac{\partial X^{\mathrm{K}}_{ri}}{\partial B_\alpha} = \sum_{\mu}\left(\frac{\partial X^{\mathrm{K}}_{r\mu}}{\partial B_\alpha}L^*_{\mu i} + X^{\mathrm{K}}_{r\mu}\frac{\partial L^*_{\mu i}}{\partial B_\alpha}\right). \tag{4.123}$$

4.3.5 Frozen-core approximation

The frozen-core approximation is taken into account by adding an additional term $z_{kl_c}f_{kl_c} + z_{l_ck}f_{l_ck}$ with $k \in \{\text{valence, local}\}$ and $l_c \in \{\text{core, canonical}\}$ to the LMP2 Lagrangian,

$$\mathcal{L}_2 \leftarrow \sum_{kl_c}\left[z_{kl_c}f_{kl_c} + z_{l_ck}f_{l_ck}\right]. \tag{4.124}$$

In this subsection the subscript c denotes core orbitals. The Lagrange multipliers for the frozen-core approximation are defined in the whole basis of occupied and core orbitals with $z_{ii} = z_{i_ci_c} = 0$ as elements of the

Hermitian matrix **z**.
The derivative of f_{kl_c} with respect to the magnetic field,

$$\frac{\partial f_{kl_c}}{\partial B_\alpha} = \sum_{\mu\nu} \left[L^{B_\alpha *}_{\mu k} C_{\nu l_c} f_{\mu\nu} + L_{\mu k} C^{B_\alpha}_{\nu l_c} f_{\mu\nu} + L_{\mu k} C_{\nu l_c} f^{B_\alpha}_{\mu\nu} \right], \tag{4.125}$$

is generally non-zero with the choice of perturbed orbital coefficients as defined in Section 3.4.1. As outlined by Gauss et al. in the context of CCSD(T) NMR shielding tensors [27] an alternative choice for the occupied-occupied block of the orbital rotation matrix is possible which zeroes the occupied-occupied block of the perturbed Fock matrix in MO basis. This approach was adopted in this work: only the valence-core and core-valence part of the orbital rotation matrix were modified such that the derivative of the Fock matrix in MO basis as defined in Eq. (4.125) equals zero by construction.
As outlined in more detail in Section 3.4.1 and Ref. [68] the orbital rotation matrix has to fulfill the following condition

$$U^{B_\alpha}_{kl_c} + U^{B_\alpha *}_{l_c k} = -S^{(B_\alpha)}_{kl_c} \tag{4.126}$$

which makes the explicit form of $\mathbf{U}^{B_\alpha}$ non-unique. For the NMR shielding tensors in Ref. [35] and Chapter 3 the following scheme had been used

$$U^{B_\alpha}_{kl_c} = -\frac{1}{2} L^*_{\mu k} S^{B_\alpha}_{\mu\nu} C_{\nu l_c}. \tag{4.127}$$

Following the idea outlined above $\mathbf{U}^{B_\alpha}$ is chosen differently; it is most convenient to first calculate $\mathbf{U}^{B_\alpha}$ in canonical basis,

$$U^{B_\alpha}_{\bar{k}l_c} = \frac{-f^{(B_\alpha)}_{\bar{k}l_c} + \epsilon_{l_c} S^{(B_\alpha)}_{\bar{k}l_c}}{\epsilon_{\bar{k}} - \epsilon_{l_c}}, \tag{4.128}$$

which can then be transformed to local basis with the localization matrix (as defined in Eq. 2.42).
For the derivatives of the additional condition, Eq. (4.124), with respect to

the variation of the orbitals one finds

$$\begin{aligned}\left[\tilde{\mathbf{A}}'(\mathbf{z})\right]_{ij_c} &= \left(\frac{\partial}{\partial O_{ij_c}} \sum_{kl_c} \left[z_{kl_c} f_{kl_c} + z_{l_c k} f_{l_c k}\right]\right)_{\mathbf{B}=0} \\ &= \sum_{k} z_{kj_c} f_{ki} \\ &\quad + \sum_{kl_c} z_{kl_c} \left[(kl_c|j_c i) - \frac{1}{2}(ki|j_c l_c)\right] \\ &\quad + \sum_{kl_c} z_{l_c k} \left[(l_c k|j_c i) - \frac{1}{2}(l_c i|j_c k)\right] \end{aligned} \tag{4.129}$$

and

$$\begin{aligned}\left[\tilde{\mathbf{A}}'(\mathbf{z})\right]^*_{j_c i} &= \left(\frac{\partial}{\partial O^*_{j_c i}} \sum_{kl_c} \left[z_{kl_c} f_{kl_c} + z_{l_c k} f_{l_c k}\right]\right)_{\mathbf{B}=0} \\ &= \sum_{l_c} z_{il_c} f_{j_c l_c} \\ &\quad + \sum_{kl_c} z_{kl_c} \left[(kl_c|j_c i) - \frac{1}{2}(ki|j_c l_c)\right] \\ &\quad + \sum_{kl_c} z_{l_c k} \left[(l_c k|j_c i) - \frac{1}{2}(l_c i|j_c k)\right]. \end{aligned} \tag{4.130}$$

The linear Z-vector equations for the valence-core part take the form (similar to Eq. 4.48)

$$\left(1 - \mathcal{T}_{ij_c}\right)\left[\mathbf{A} + \tilde{\mathbf{A}}(\mathbf{z}) + \tilde{\mathbf{A}}'(\mathbf{z}) + \mathbf{a}\left(\mathbf{z}^{\mathrm{loc}}\right)\right]_{ij_c} = 0. \tag{4.131}$$

The derivatives of Brillouin's condition with respect to O_{ij_c} and $O^*_{j_c i}$, $\tilde{\mathbf{A}}_{ij_c}$ and $\left[\tilde{\mathbf{A}}\right]^*_{j_c i}$, are zero. Furthermore, the derivative of the localization condition with respect to O_{ij_c}, $\left[\mathbf{a}\left(\mathbf{z}^{\mathrm{loc}}\right)\right]_{ij_c}$, is zero because the localization condition is only defined in the valence space. There is solely a contribution from the derivative of the localization condition with respect to $O^*_{j_c i}$ which corresponds to contributions from core orbitals to valence orbitals through orbital rotations. The contributions from the contractions of the Lagrange multipliers with the two-electron integrals also cancel each other

(see Eqs. 4.129 and 4.130), yielding

$$\left(1 - \mathcal{T}_{ij_c}\right)\left[\mathbf{A} + \tilde{\mathbf{A}}'(\mathbf{z})\right]_{ij_c} - \left[\mathbf{a}\left(\mathbf{z}^{\mathrm{loc}}\right)\right]^*_{j_c i} = 0 \tag{4.132}$$

or more explicitly

$$\left[A_{ij_c} - A^*_{j_c i} + \sum_k z_{kj_c} f_{ki} - \sum_{l_c} z_{il_c} f_{j_c l_c} - \left[\mathbf{a}\left(\mathbf{z}^{\mathrm{loc}}\right)\right]^*_{j_c i}\right] = 0. \tag{4.133}$$

The derivatives of the Hylleraas functional with respect to orbital rotations can be written as

$$A_{ij_c} = 2g\left(\mathbf{d}^{(2)}\right)_{j_c i}, \tag{4.134}$$

$$A^*_{j_c i} = 2\left[\sum_k \sum_{cd} (j_c c|kd)\tilde{T}^{ik}_{cd} + g\left(\mathbf{d}^{(2)}\right)_{j_c i}\right], \tag{4.135}$$

so that one finally obtains

$$A_{ij_c} - A^*_{j_c i} = -2\sum_k \sum_{cd} (j_c c|kd)\tilde{T}^{ik}_{cd}. \tag{4.136}$$

Transformation to canonical basis finally yields the working equations,

$$z_{\bar{i}j_c} = -\frac{A_{\bar{i}j_c} - A^*_{j_c\bar{i}} - \left[\mathbf{a}\left(\mathbf{z}^{\mathrm{loc}}\right)\right]^*_{j_c\bar{i}}}{\epsilon_{\bar{i}} - \epsilon_{j_c}}. \tag{4.137}$$

Differentiating Eq. (4.137) with respect to the magnetic field yields the perturbed Lagrange multipliers for the frozen-core contribution,

$$\begin{aligned} z^{B_\alpha}_{\bar{i}j_c} = &-\left[\frac{\partial(A_{\bar{i}j_c} - A^*_{j_c\bar{i}} - \left[\mathbf{a}\left(\mathbf{z}^{\mathrm{loc}}\right)\right]^*_{j_c\bar{i}})}{\partial B_\alpha}\right] \cdot \left(\epsilon_{\bar{i}} - \epsilon_{j_c}\right)^{-1} \\ &-\left[\sum_{\bar{k}} z_{\bar{k}j_c}\frac{\partial f_{\bar{k}\bar{i}}}{\partial B_\alpha} - \sum_{l_c} z_{\bar{i}l_c}\frac{\partial f_{j_c l_c}}{\partial B_\alpha}\right] \cdot \left(\epsilon_{\bar{i}} - \epsilon_{j_c}\right)^{-1}. \end{aligned} \tag{4.138}$$

4.4 Accuracy and Performance

4.4.1 Method error of LMP2 magnetizabilities

Table 4.3 compares results of isotropic magnetizabilities calculated with HF, LMP2, and LMP2 with full lists and full domains ("LMP2 full") to CCSD(T) / aug-cc-pCV[TQ]Z benchmark values of Ref. [45]. Since ozone is a multireference case it was excluded from the calculation of the statistical measures in Table 4.3. In the course of this work the influence of the frozen-core approximation was investigated and found to be small, for this reason only LMP2 calculations with frozen-core approximation are provided.
For HF and LMP2 root mean square values of the deviation from the benchmark values are in the range of 10–15 $\cdot 10^{-30}\,\mathrm{J T^{-2}}$, mean absolute percentage errors (MAPE) are in the range of 3–5 %. MAPE for a set of n_{Mol} molecules is calculated as

$$\mathrm{MAPE} = \frac{1}{n_{\mathrm{Mol}}} \sum_{i=1}^{n_{\mathrm{Mol}}} \left| \frac{\bar{\xi}_i^{\mathrm{local}} - \bar{\xi}_i^{\mathrm{full}}}{\bar{\xi}_i^{\mathrm{full}}} \right| \cdot 100\,\%. \tag{4.139}$$

For both methods the error becomes smaller for larger AO basis sets. However for LMP2, augmented basis sets show larger deviations from the benchmark values than non-augmented ones. In contrast, HF magnetizabilities calculated with augmented basis sets show an improvement in accuracy over non-augmented basis sets.
Magnetizabilities of closed-shell molecules are dominated by the diamagnetic contributions and show only little to modest correlation contributions in the range of a few percent [44, 111, 112]. For this reason HF magnetizabilities provide nearly the same accuracy as LMP2 calculations for the molecules of the benchmark set. Hence, in order to reach an accuracy significantly higher than Hartree-Fock for magnetizabilities, it appears that rather large basis sets and correlation methods beyond MP2 are required. Furthermore, one can see from the provided LMP2 and LMP2 full results that the local error is small. The accuracy of the local approximation is discussed in detail in Section 4.4.2.

Table 4.3: Deviation of isotropic magnetizabilities calculated at the levels of HF, LMP2, and LMP2 with full domains and full lists (LMP2 full) from CCSD(T) / aug-cc-pCV[TQ]Z benchmark values [45]. Root mean square (R.M.S.) value of the deviation, the absolute value of the maximum absolute error (MaxAE), the absolute value of the maximum relative error (MaxRE), and the mean absolute percentage error (MAPE) are provided. For all LMP2 calculations the frozen-core approximation was employed.
R.M.S. deviation and MaxAE are provided in SI units (10^{-30} JT^{-2}).

Method	Basis	R.M.S. deviation	MaxAE	MaxRE	MAPE
HF	cc-pVDZ	14.0	28.3	11.4 %	4.0 %
	cc-pVTZ	11.0	26.5	10.7 %	3.0 %
	cc-pVQZ	10.5	27.0	10.1 %	2.8 %
	aug-cc-pVDZ	12.0	26.3	10.9 %	3.0 %
	aug-cc-pVTZ	10.5	26.9	10.0 %	2.7 %
	aug-cc-pVQZ	10.3	27.2	10.0 %	2.7 %
LMP2	cc-pVDZ	14.6	31.6	11.6 %	4.0 %
	cc-pVTZ	10.3	30.3	11.1 %	2.5 %
	cc-pVQZ	9.8	30.7	11.3 %	2.2 %
	aug-cc-pVDZ	18.7	43.3	14.1 %	5.2 %
	aug-cc-pVTZ	11.8	29.2	10.7 %	3.0 %
	aug-cc-pVQZ	10.5	30.3	11.2 %	2.6 %
LMP2 full	cc-pVDZ	14.5	31.6	11.6 %	4.0 %
	cc-pVTZ	10.4	30.3	11.1 %	2.5 %
	cc-pVQZ	9.8	30.7	11.3 %	2.2 %
	aug-cc-pVDZ	18.7	43.2	14.0 %	5.1 %
	aug-cc-pVTZ	11.8	29.3	10.8 %	3.0 %
	aug-cc-pVQZ	10.5	30.4	11.2 %	2.6 %

4.4.2 Local approximation

Tables A.1 and A.2 in Appendix A show the influence of the local approximation on isotropic magnetizabilities. Additionally, it is illustrated in Figs. 4.1 and 4.2. As for DF-HF magnetizablities the benchmark set of 28 small molecules by Lutnæs et al. [45] was investigated. One of the benchmark molecules is ozone which is a multireference case: the description by HF and MP2 cannot be considered correct. The geometries were taken from the supplementary material of Ref. [45], the calculations were carried

out using Dunning's cc-pVXZ and aug-cc-pVXZ AO basis sets [86–91, 115] for X=D, T, and Q with the related JK- [92] and MP2-fitting basis sets [93] of Weigend. For Li the cc-pVXZ and aug-cc-pVXZ AO basis sets published in 2011 were used [115]. Local calculations with standard domains [60] are compared to calculations with full domains (the latter are equivalent to canonical calculations, since the pair list remains untruncated for all molecules of the test set). Electron pairs with an interorbital distance beyond 15 bohrs are omitted. The correlation contribution to the isotropic magnetizabilities, also included in Tables A.1 and A.2, is calculated as the difference between the GIAO-DF-LMP2 full domain result and the isotropic magnetizability obtained with the GIAO-DF-HF method. The correlation contributions to isotropic magnetizabilities are only small to modest: for most molecules of the benchmark set correlation accounts for only a few percent. Exceptions are the molecules OF_2, PN, and SO_2 for which the contributions are in the range of 10–15 %. Clearly, MP2 fails to calculate the magnetizabilities for ozone: Luetnæs et al. report magnetizability values in the range of $120 \cdot 10^{-30}\,\mathrm{JT}^{-2}$ for CCSD(T) calculations using Dunning's cc-pVXZ basis sets (X=D, T, and Q) [45], whereas the MP2 results for the calculations with full domains are in the range from $-891 \cdot 10^{-30}\,\mathrm{JT}^{-2}$ for cc-pVDZ to $-628 \cdot 10^{-30}\,\mathrm{JT}^{-2}$ for cc-pVQZ.

The error introduced by the local approximation is small: for calculations with cc-pVDZ AO basis set the error is (with the exception of ozone) in the range of $1 \cdot 10^{-30}\,\mathrm{JT}^{-2}$ or below. For larger AO basis sets the error is in most cases even smaller. This can be rationalized as follows: a larger set provides a more flexible basis for the description on the few centers included in the pair domain. However, for non-augmented basis sets, the local error of AlF, LiF, and NH_3 gets larger when the size of the AO basis set is increased. For augmented basis sets one finds particularly large local errors for aug-cc-pVDZ (e.g., $-1.83 \cdot 10^{-30}\,\mathrm{JT}^{-2}$ for H_4C_2O). For larger basis sets the local error becomes rapidly smaller; this is also reflected by the root mean square values of the local error in Tables 4.4 and 4.5 which are

well below $1 \cdot 10^{-30}\,\mathrm{JT}^{-2}$. Although the absolute local error is small it can make a significant contribution to the correlation part, since the latter itself is small (see also Section 4.4.1).

Table 4.4: Deviation of isotropic magnetizabilities calculated within the local approximation from full calculations for cc-pVXZ (X=D, T, and Q) AO basis sets. Root mean square (R.M.S.) value of the local error, mean absolute percentage error (MAPE), the absolute value of the maximum relative error (MaxRE), the absolute value of the maximum absolute error (MaxAE), and root mean square value of the correlation contribution are provided. For all calculations the frozen-core approximation was employed. All R.M.S. values and MaxAE are provided in SI units ($10^{-30}\,\mathrm{JT}^{-2}$).

Basis	cc-pVDZ		cc-pVTZ		cc-pVQZ	
Molecules	excl. O_3	all	excl. O_3	all	excl. O_3	all
R.M.S. local error	0.51	0.95	0.38	0.81	0.33	0.37
MAPE	0.1 %	0.1 %	0.1 %	0.1 %	0.1 %	0.1 %
MaxRE	0.3 %	0.5 %	0.3 %	0.6 %	0.3 %	0.3 %
MaxAE	1.34	4.27	0.95	3.82	1.07	1.07
R.M.S. correlation contribution	14.11	300.19	10.61	237.61	10.36	230.22

Table 4.5: Deviation of isotropic magnetizabilities calculated within the local approximation from full calculations for aug-cc-pVXZ (X=D, T, and Q) AO basis sets. Root mean square (R.M.S.) value of the local error, mean absolute percentage error (MAPE), the absolute value of the maximum relative error (MaxRE), the absolute value of the maximum absolute error (MaxAE), and root mean square value of the correlation contribution are provided. For all calculations the frozen-core approximation was employed. All R.M.S. values and MaxAE are provided in SI units ($10^{-30}\,\mathrm{JT}^{-2}$).

Basis	aug-cc-pVDZ		aug-cc-pVTZ		aug-cc-pVQZ	
Molecules	excl. O_3	all	excl. O_3	all	excl. O_3	all
R.M.S. local error	0.80	0.81	0.30	0.93	0.12	0.83
MAPE	0.2 %	0.2 %	0.1 %	0.1 %	0.03 %	0.05 %
MaxRE	0.5 %	0.5 %	0.2 %	0.7 %	0.1 %	0.7 %
MaxAE	1.83	1.83	0.74	4.66	0.33	4.33
R.M.S. correlation contribution	15.38	248.50	11.43	235.45	10.80	233.53

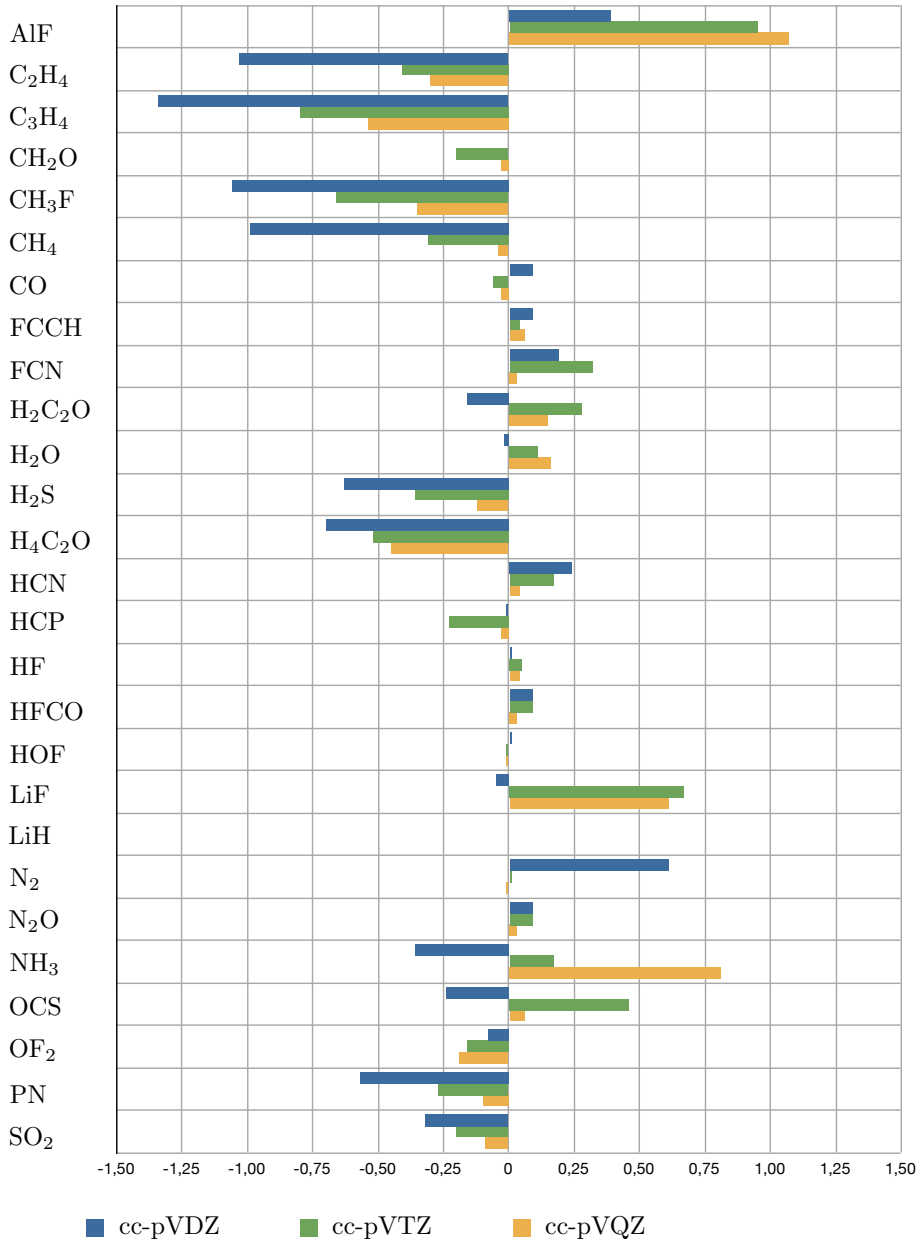

Figure 4.1: Deviation of isotropic magnetizabilities calculated in the local approximation from results calculated with full domains and full lists for GIAO-DF-LMP2. The values $\bar{\xi}^{\text{local}}$-$\bar{\xi}^{\text{full}}$ are provided. Calculations were done in the frozen-core approximation using the cc-pVXZ basis sets (X=D, T, and Q). All results are provided in SI units (10^{-30} JT^{-2}).

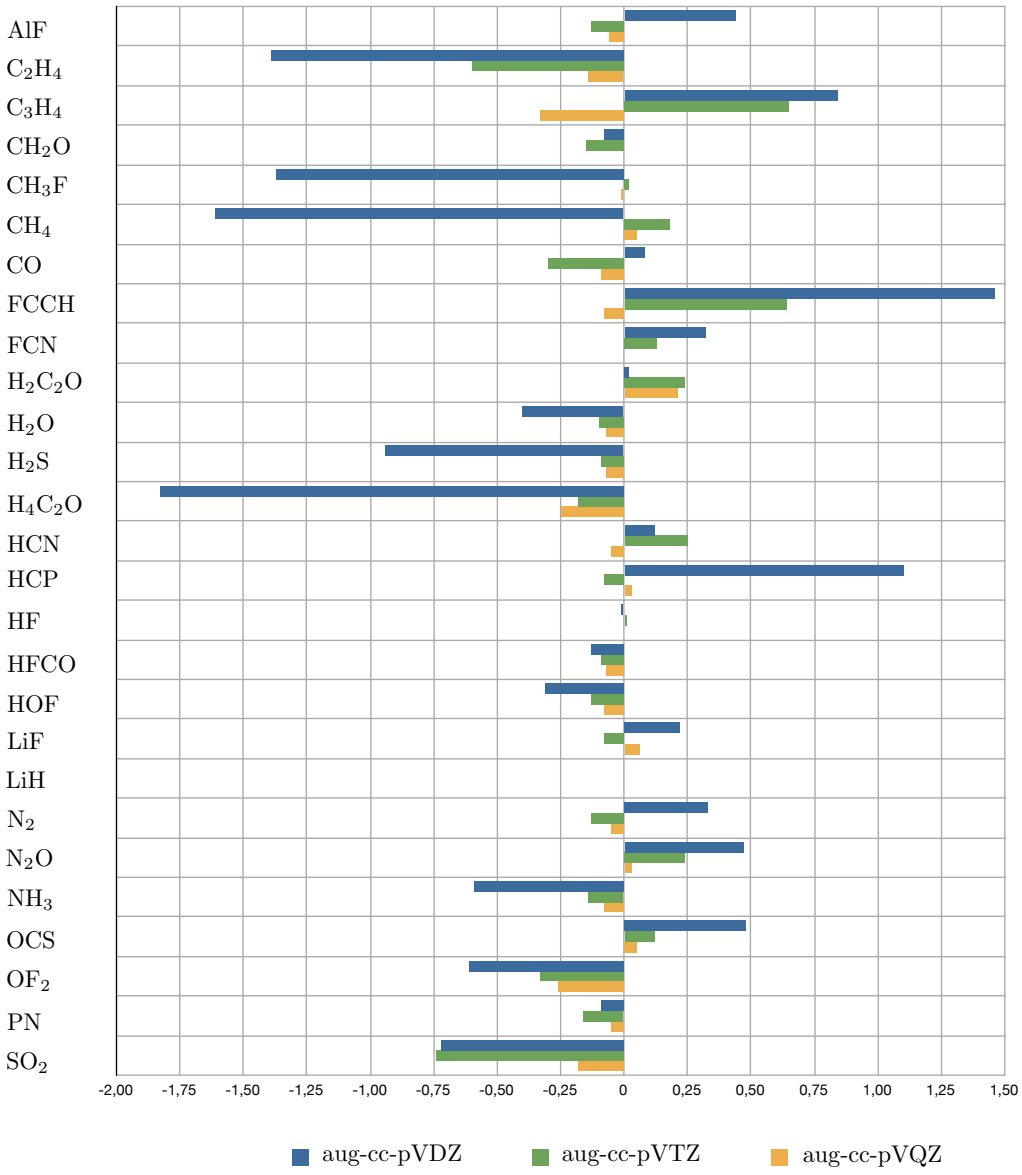

Figure 4.2: Deviation of isotropic magnetizabilities calculated in the local approximation from results calculated with full domains and full lists for GIAO-DF-LMP2 with augmented basis sets. The values $\bar{\xi}^{\text{local}}$-$\bar{\xi}^{\text{full}}$ are provided. Calculations were done in the frozen-core approximation using the aug-cc-pVXZ basis sets (X=D, T, and Q). All results are provided in SI units (10^{-30} JT^{-2}).

In order to assess the accuracy of the LMP2 method and of the local approximation additional calculations were performed for medium-sized test molecules with cc-pVXZ (X=D and T) and the augmented aug-cc-pVXZ (X=D and T) AO basis sets using the nominally in size related fitting basis sets. Table 4.6 shows the results for HF and LMP2 calculations with standard Boughton-Pulay domains and with full domains and full pair lists for cc-pVXZ (X=D and T) AO basis sets, as well as the results for HF and LMP2 calculations with standard Boughton-Pulay domains, extended domains (extended by one shell of neighboring atoms, `MOLPRO` command `iext=1` [94]), and with full domains and full pair lists for aug-cc-pVXZ (X=D and T) AO basis sets. For the calculations of the medium-sized molecules with augmented basis sets the contributions of the most diffuse functions were discarded in the Pipek-Mezey localization matrices Eq. (4.43) (`MOLPRO` command `cpldel=1` [94]).

For non-augmented basis sets the local approximation works well. Relative errors with respect to the total magnetizability tensor are in the range of 1 %. However, one has to bear in mind that magnetizabilities show only little correlation contribution. This means that the relative error with respect to the correlation contribution can be in the range of nearly 50 % for the calculations with cc-pVDZ basis set; for cc-pVTZ the errors are smaller. For aug-cc-pVDZ calculations with standard Boughton-Pulay domains LMP2 results show rather large deviations from the "full" results, particularly for 1-phenylpyrrole and p-cresol. For aug-cc-pVTZ calculations the local errors with Boughton-Pulay domains are considerably smaller and show good agreement with the results of the full domain calculations (except for DMABN). However, it appears necessary to use extended domains for the calculation of magnetizabilities with augmented basis sets in order to ensure small local errors.

Table 4.6: Isotropic magnetizabilities for a set of medium-sized molecules. Results for HF calculations (HF), LMP2 calculations with Boughton-Pulay domains (BP), with extended domains (ext. dom.) and with full domains and full pair lists (full) are provided for cc-pVXZ and aug-cc-pVXZ (X=D and T) AO basis sets. For all LMP2 calculations the frozen-core approximation was employed. All results are provided in SI units (10^{-30} JT^{-2}).

Basis	cc-pVDZ			aug-cc-pVDZ			
Method	HF	BP	full	HF	BP	ext. dom.	full
DMABN	-1725.81	-1722.80	-1717.29	-1720.55	-1710.76	-1709.82	-1707.82
Phloretic acid	-1783.17	-1773.86	-1763.93	-1773.33	-1768.27	-1758.93	-1759.48
1-Phenylpyrrole	-1760.75	-1754.75	-1742.30	-1750.13	-1740.42	-1722.78	-1726.51
trans-Urocanic acid	-1307.82	-1322.84	-1320.28	-1296.33	-1314.74	-1311.31	-1313.05
p-Cresol	-1304.46	-1293.80	-1283.74	-1294.58	-1291.71	-1274.29	-1271.02
Basis	cc-pVTZ			aug-cc-pVTZ			
Method	HF	BP	full	HF	BP	ext. dom.	full
DMABN	-1708.36	-1691.66	-1687.65	-1701.95	-1630.35	-1667.91	-1687.15
Phloretic acid	-1765.05	-1739.48	-1732.66	-1758.69	-1726.79	-1734.30	-1727.62
1-Phenylpyrrole	-1739.56	-1713.76	-1704.70	-1736.58	-1709.30	-1708.73	-1703.16
trans-Urocanic acid	-1284.82	-1286.38	-1283.33	-1279.47	-1277.52	-1279.84	1281.93
p-Cresol	-1288.88	-1266.99	-1260.26	-1281.58	-1251.33	-1251.08	-1248.15

4.4.3 Density fitting approximation

Tables A.3 and A.4 compile the influence of the auxiliary fitting basis set on isotropic magnetizabilities. The same benchmark set of molecules as for the effects of the local approximation was investigated. The calculations were carried out using Dunning's cc-pVXZ and aug-cc-pVXZ (AVXZ) AO basis sets for X=D, T, and Q. For Li the AO basis sets published in 2011 were used [115]. The JK- [92] and MP2-fitting basis sets [93] of Weigend related to the cc-pVXZ, cc-pV(X+1)Z, and cc-pV(X+2)Z AO basis sets, respectively, the augmented analogues, were used if available. It has been verified in the course of this work that magnetizabilities calculated in the cc-pVDZ AO basis set with cc-pVQZ fitting basis set employing full domains and full lists are virtually identical to the canonical MP2 results obtained by `CFOUR` [84]. Comparing the results for a chosen AO basis set and different fitting basis sets shows that the fitting error is very small, i.e., in the range

of $0.1 \cdot 10^{-30}\,\mathrm{JT}^{-2}$. Augmented basis sets show even smaller errors than non-augmented ones. Deviations for ozone are larger and in the range of $3 \cdot 10^{-30}\,\mathrm{JT}^{-2}$. It is evident that density fitting with ordinary Gaussians works very well for magnetizabilities, as it does for NMR shielding tensors.

4.4.4 Performance of the program

The performance of the program was investigated by calculations on two larger molecular systems, (*i*) coronene and (*ii*) the tweezer host-guest complex 1@2 "clinching" the 1,4-dicyanobenzene as guest molecule 2 (see Fig. 3.2). These molecules were already used for NMR shielding tensors at the levels of GIAO-DF-HF and GIAO-DF-LMP2. For the host-guest complex the same geometry as in Ref. [68] was used. The molecules were then aligned in the principal axis system.
The calculations were performed on 8 CPUs of an AMD Opteron 6180 SE @ 2.50 GHz without exploiting point group symmetry. The key steps of the magnetizability program were parallelized based on a shared file approach in the same way as the program for the NMR shielding tensors (see Section 3.6). The timings of some key steps are provided in Tables 4.7 and 4.8. The calculation of magnetizabilities takes longer than the calculation of NMR shielding tensors by roughly a factor of 1.5. The calculation of coronene with cc-pVTZ AO basis (888 basis functions) took about 7 hours, the 1@2 tweezer molecule with cc-pVTZ AO basis (2184 basis functions) required about 5.5 days. The additional computational cost is caused by the terms in the second and especially in the third line of Eq. (4.76) which are not required for shielding constants. These terms involve the contractions of the unperturbed and perturbed energy weighted density matrices with the derivatives of the overlap matrix and the contraction of the unperturbed and perturbed two-particle density matrices with the derivatives of the ERIs (see the timings for Eqs. 4.100, 4.94, 4.113, 4.120, 4.122, and 4.112 in the tables). The calculation of rotational g tensors from magnetizabilities

requires only one additional set of two-index AO integrals (Eq. 5.28) and a nuclear contribution (Eq. 5.27): both terms are computationally cheap and the computational effort can be neglected.

Table 4.7: GIAO-DF-LMP2 isotropic magnetizabilities (in 10^{-30} JT^{-2}) and rotational g tensors for coronene using the frozen-core approximation. The CPU times (per processor) and the elapsed times measured for the individual key steps of the GIAO-DF-LMP2 calculation and the total times for the calculation of the unperturbed density matrix, the perturbed density matrix are provided. All timings of the perturbed equations are added up for the three components of the magnetic field[a].

	cc-pVDZ	cc-pVTZ
Coronene		
Magnetizability	-4496.4	-4406.7
Rotational g tensor	-0.0182	-0.0190
	-0.0182	-0.0190
	0.0285	0.0283
Number of valence electrons	108	108
Number of AO basis functions	396	888
Number of JKfit basis functions	1956	2256
Number of MP2fit basis functions	1512	2304
Building Eqs. (4.100) and (4.94)		
CPU (elapsed) time / min	3 (3)	11 (11)
Building Eqs. (4.113), (4.120), (4.122), and (4.112)		
CPU (elapsed) time / min	2 (2)	11 (12)
R.H.S. of the perturbed amplitude Eqs. (4.83)		
CPU (elapsed) time / min	4 (4)	28 (30)
Iterating perturbed amplitude equations[b]		
CPU (elapsed) time / min	10 (10)	91 (92)
R.H.S. of the perturbed Z-CPHF Eqs. (4.86)		
CPU (elapsed) time / min	29 (32)	139 (151)
Iterating perturbed Z-CPHF Eqs. (4.85)[b]		
CPU (elapsed) time / min	5 (7)	13 (17)
Solving the perturbed Z-CPL Eqs. (4.87)		
and building Eqs. (4.88), (4.68) and its derivative		
CPU (elapsed) time / sec	6 (6)	8 (9)
Unperturbed LMP2 density total CPU (elapsed) time / min	3 (4)	11 (13)
Perturbed LMP2 density total CPU (elapsed) time / min	53 (58)	288 (311)
Time for HF magnetizability		
CPU (elapsed) time / min	12 (12)	27 (28)
Total CPU (elapsed) time / min	74 (81)	368 (394)

a) Calculations were performed on 8 CPUs of an AMD Opteron 6180 SE @ 2.50 GHz.
b) Time for 10 iteration steps.

Table 4.8: GIAO-DF-LMP2 isotropic magnetizabilities (in 10^{-30} JT^{-2}) and rotational g tensors for the 1@2 tweezer molecule using the frozen-core approximation. The CPU times (per processor) and the elapsed times measured for the individual key steps of the GIAO-DF-LMP2 calculation and the total times for the calculation of the unperturbed density matrix and the perturbed density matrix are provided. All timings of the perturbed equations are added up for the three components of the magnetic field[a].

1@2 Tweezer		
Magnetizability	-8158.2	-7944.1
Rotational g tensor	-0.0010	-0.0009
	-0.0032	-0.0033
	-0.0017	-0.0020
Number of valence electrons	262	262
Number of AO basis functions	964	2184
Number of JKfit basis functions	4748	5504
Number of MP2fit basis functions	3640	5616
Building Eqs. (4.100) and (4.94)		
CPU (elapsed) time / min	146 (161)	661 (696)
Building Eqs. (4.113), (4.120), (4.122), and (4.112)		
CPU (elapsed) time / min	47 (50)	193 (207)
R.H.S. of the perturbed amplitude Eqs. (4.83)		
CPU (elapsed) time / min	43 (65)	207 (362)
Iterating perturbed amplitude equations[b]		
CPU (elapsed) time / min	42 (42)	328 (331)
R.H.S. of the perturbed Z-CPHF Eqs. (4.86)		
CPU (elapsed) time / min	342 (947)	1297 (2725)
Iterating perturbed Z-CPHF Eqs. (4.85)[b]		
CPU (elapsed) time / min	85 (171)	243 (825)
Solving the perturbed Z-CPL Eqs. (4.87)		
and building Eqs. (4.88), (4.68) and its derivative		
CPU (elapsed) time / min	7 (7)	7 (7)
Unperturbed density total CPU (elapsed) time / min	53 (74)	181 (508)
Perturbed density total CPU (elapsed) time / min	774 (1551)	3197 (5737)
Time for HF magnetizability		
CPU (elapsed) time / min	339 (409)	731 (1214)
Total CPU (elapsed) time / min	1295 (2166)	4545 (7923)

a) Calculations were performed on 8 CPUs of an AMD Opteron 6180 SE @ 2.50 GHz.
b) Time for 10 iteration steps.

4.5 Required GIAO Integrals

4.5.1 Derivatives of two-index integrals

Derivatives of the AO overlap matrix with respect to the magnetic field can be conveniently derived for GIAOs as basis functions. The first derivative is given by

$$S_{\mu\nu}^{B_\beta} = \frac{i}{2c} \left\langle \mu \left| (\mathbf{R}_{MN} \times \mathbf{r})_\beta \right| \nu \right\rangle , \tag{4.140}$$

where the vectors $\mathbf{R}_M$ and $\mathbf{R}_N$ point from the origin to the center of the AO basis functions ω_μ, respectively, ω_ν. Their difference vector $\mathbf{R}_M - \mathbf{R}_N$ is denoted by $\mathbf{R}_{MN}$. The vector $\mathbf{r}$ is the position vector of an electron.
The second derivative of the AO overlap matrix with respect to the magnetic field can be written as

$$\frac{\partial^2 S_{\mu\nu}}{\partial B_\alpha \partial B_\beta} = -\frac{1}{4c^2} \left\langle \mu \left| (\mathbf{R}_{MN} \times \mathbf{r})_\alpha \, (\mathbf{R}_{MN} \times \mathbf{r})_\beta \right| \nu \right\rangle . \tag{4.141}$$

The first derivative of the one-electron core Hamiltonian with respect to the magnetic field is given by

$$\frac{\partial h_{\mu\nu}}{\partial B_\beta} = \frac{i}{2c} \left\langle \mu \left| (\mathbf{R}_{MN} \times \mathbf{r})_\beta \, h - (\mathbf{r}_N \times \nabla)_\beta \right| \nu \right\rangle , \tag{4.142}$$

where the vector $\mathbf{r}_N$ is pointing from the center of the ket-side AO basis function ω_ν to the electron.
The second derivative of the one-electron core Hamiltonian with respect to the magnetic field can be written as

$$\begin{aligned} \frac{\partial^2 h_{\mu\nu}}{\partial B_\alpha B_\beta} = \frac{1}{4c^2} \Bigg[& \left\langle \mu \left| (\mathbf{R}_{MN} \times \mathbf{r})_\alpha \, (\mathbf{r}_N \times \nabla)_\beta + (\mathbf{R}_{MN} \times \mathbf{r})_\beta \, (\mathbf{r}_N \times \nabla)_\alpha \right| \nu \right\rangle \\ & + \left\langle \mu \left| \delta_{\alpha\beta} \, (\mathbf{r}_N \cdot \mathbf{r}_N) - (\mathbf{r}_N)_\alpha \cdot (\mathbf{r}_N)_\beta \right| \nu \right\rangle \\ & - \left\langle \mu \left| (\mathbf{R}_{MN} \times \mathbf{r})_\alpha \, (\mathbf{R}_{MN} \times \mathbf{r})_\beta \, h \right| \nu \right\rangle \Bigg] . \end{aligned} \tag{4.143}$$

Integrals (4.140) and (4.142) were already implemented in the context of Hartree-Fock NMR shielding tensors [52, 68], the second derivative of the

overlap integral, Eq. (4.141), and of the core Hamiltonian, Eq. (4.143), were programmed in the course of this work. The expressions for the calculation of the integrals are based on the recurrence scheme for primitive Cartesian Gaussian basis functions by Obara and Saika [114]. The corresponding program routines generate the integrals for all Cartesian primitives, i.e., non-contracted basis functions which are then contracted to the common atomic orbitals.

The following basics of the Obara-Saika scheme and the presentation of the implementation is based on my diploma thesis (see Chapter 4 in Ref. [52]). An unnormalized Cartesian Gaussian function with its origin at **R** can be written as [114]

$$\chi(\mathbf{r};\alpha,\mathbf{n},\mathbf{R}) = (x-R_x)^{n_x}\left(y-R_y\right)^{n_y}(z-R_z)^{n_z}\exp\left(-\alpha(\mathbf{r}-\mathbf{R})^2\right), \qquad (4.144)$$

where $\mathbf{r} = (x, y, z)$ is the electron coordinate, α the orbital exponent and $\mathbf{n}$ the angular momentum index, a set of non-negative integers related to the angular momentum. The normalization constant of the function is then given by

$$\xi(\alpha,\mathbf{n}) = \left(\frac{2\alpha}{\pi}\right)^{3/4}(4\alpha)^{(n_x+n_y+n_z)/2}\left[(2n_x-1)!!(2n_y-1)!!(2n_z-1)!!\right]^{-1/2}, \qquad (4.145)$$

where the double factorial is defined for positive integers as

$$k!! = \begin{cases} k\cdot(k-2)\cdot(k-4)\cdot\ldots\cdot 2 & \text{if } k \text{ is even} \\ k\cdot(k-2)\cdot(k-4)\cdot\ldots\cdot 1 & \text{if } k \text{ is odd.} \end{cases} \qquad (4.146)$$

If one defines the sum of the components of $\mathbf{n}$ as l,

$$l = n_x + n_y + n_z, \qquad (4.147)$$

then this l is closely related to the angular momentum. Functions with l equal to $0, 1, 2, \ldots$ are referred to as $s, p, d, \ldots$ functions. A set of functions located at **R** with the same angular momentum l and orbital exponent α is called a shell, the functions constituting the shell are its components. A shell with angular momentum l has $(l+1)(l+2)/2$ components.

The single component of the s-shell has the angular momentum index $\mathbf{n} = (0, 0, 0)$, whereas the i-th component of the p-shell corresponds to the angular momentum index $\mathbf{n} = \mathbf{1}_i = (\delta_{ix}, \delta_{iy}, \delta_{iz})$.
Differentiation of a Cartesian Gaussian function yields

$$\frac{\partial}{\partial R_i}\chi(\mathbf{r}; \alpha, \mathbf{n}, \mathbf{R}) = 2\alpha\chi(\mathbf{r}; \alpha, \mathbf{n} + \mathbf{1}_i, \mathbf{R}) - n_i\chi(\mathbf{r}; \alpha, \mathbf{n} - \mathbf{1}_i, \mathbf{R}). \tag{4.148}$$

Therefore, the functions with the angular momentum index incremented and decremented by 1 are required for the calculation of the derivative with respect to a spatial coordinate. The Cartesian Gaussian functions depend on the coordinate of the nucleus in the form $r_i - R_i$, i.e., differentiation with respect to R_i can be expressed by differentiation with respect to r_i:

$$\frac{\partial}{\partial R_i}\chi(\mathbf{r}; \alpha, \mathbf{n}, \mathbf{R}) = -\frac{\partial}{\partial r_i}\chi(\mathbf{r}; \alpha, \mathbf{n}, \mathbf{R}). \tag{4.149}$$

In the following, the explicit expressions for the calculation of the integrals (4.141) and (4.143) will be shown. For the sake of simplicity the following notation will be used:

- **M** and **N** are the centers of μ and ν, i.e., $\mathbf{M} := \mathbf{R}_M$, $\mathbf{N} := \mathbf{R}_N$.
- **CM** is the center of mass of the molecule, i.e., $\mathbf{CM} := \mathbf{R}_{CM}$.
- M_α, N_α, and CM_α are the Cartesian components of **M**, **N**, and **CM**.
- n_α is the angular momentum of ν in Cartesian direction α.
- α_n is the orbital exponent of ν.
- α, β, γ denote the Cartesian components (of the perturbation) and permute cyclically.

The second derivative of the overlap integrals with respect to the magnetic field can be written more explicitly as

$$\begin{aligned}
\frac{\partial^2 S_{\mu\nu}}{\partial B_\alpha \partial B_\beta} &= -\frac{1}{4c^2}\left\langle \mu \left| (\mathbf{R}_{MN} \times \mathbf{r})_\alpha \left((\mathbf{R}_{MN} \times \mathbf{r})_\beta \right| \nu \right\rangle \right. \\
&= -\frac{1}{4c^2}\Bigg[\left\langle \mu \left| \left(M_\beta - N_\beta\right)\left(M_\gamma - N_\gamma\right) \cdot \gamma \cdot \alpha \right| \nu \right\rangle \\
&\quad - \left\langle \mu \left| \left(M_\beta - N_\beta\right)\left(M_\alpha - N_\alpha\right) \cdot \gamma \cdot \gamma \right| \nu \right\rangle \\
&\quad - \left\langle \mu \left| \left(M_\gamma - N_\gamma\right)^2 \cdot \beta \cdot \alpha \right| \nu \right\rangle \\
&\quad + \left\langle \mu \left| \left(M_\gamma - N_\gamma\right)\left(M_\alpha - N_\alpha\right) \cdot \beta \cdot \gamma \right| \nu \right\rangle \Bigg] \\
&= -\frac{1}{4c^2}\Bigg[\left(M_\beta - N_\beta\right)\left(M_\gamma - N_\gamma\right) \left\langle \mu \left| \gamma \cdot \alpha \right| \nu \right\rangle \\
&\quad - \left(M_\beta - N_\beta\right)\left(M_\alpha - N_\alpha\right) \left\langle \mu \left| \gamma \cdot \gamma \right| \nu \right\rangle \\
&\quad - \left(M_\gamma - N_\gamma\right)^2 \left\langle \mu \left| \beta \cdot \alpha \right| \nu \right\rangle \\
&\quad + \left(M_\gamma - N_\gamma\right)\left(M_\alpha - N_\alpha\right) \cdot \left\langle \mu \left| \beta \cdot \gamma \right| \nu \right\rangle \Bigg].
\end{aligned} \tag{4.150}$$

Equation (4.150) shows that the second derivative of the overlap integrals can be written as a sum of quadrupole moment integrals multiplied with the differences of the centers of the functions. The implementation of quadrupole moment integrals was based on the `MOLPRO` routine for dipole moment integrals, `basis_shell_DM`, by using the following relation:

$$\left\langle \mu \left| \gamma \cdot \alpha \right| \nu \right\rangle = \left\langle \mu + \mathbf{1}_\gamma \left| \alpha \right| \nu \right\rangle + M_\gamma \left\langle \mu \left| \alpha \right| \nu \right\rangle . \tag{4.151}$$

The individual terms of the second derivative of the one-electron core Hamiltonian with respect to the magnetic field will be discussed separately. The last term of Eq. (4.143) can be derived conveniently from an integral which already appears in the first derivative of the Hamiltonian with respect to the magnetic field, Eq. (4.142). In analogy to Eq. (4.150) one

finds

$$\begin{aligned}
&\left\langle \mu \left| (\mathbf{R}_{MN} \times \mathbf{r})_\alpha \, (\mathbf{R}_{MN} \times \mathbf{r})_\beta \, h \right| \nu \right\rangle \\
&= \Big[\left(M_\beta - N_\beta\right) \left(M_\gamma - N_\gamma\right) \left\langle \mu \left| \gamma \cdot \alpha \cdot h \right| \nu \right\rangle \\
&\quad - \left(M_\beta - N_\beta\right) \left(M_\alpha - N_\alpha\right) \left\langle \mu \left| \gamma \cdot \gamma \cdot h \right| \nu \right\rangle \\
&\quad - \left(M_\gamma - N_\gamma\right)^2 \left\langle \mu \left| \beta \cdot \alpha \cdot h \right| \nu \right\rangle \\
&\quad + \left(M_\gamma - N_\gamma\right) \left(M_\alpha - N_\alpha\right) \cdot \left\langle \mu \left| \beta \cdot \gamma \cdot h \right| \nu \right\rangle \Big]. \qquad (4.152)
\end{aligned}$$

The integral can be further decomposed by the following relation,

$$\begin{aligned}
&\left\langle \mu \left| \gamma \cdot \alpha \cdot h \right| \nu \right\rangle \\
&= \left\langle \mu + \mathbf{1}_\gamma \left| \alpha \cdot h \right| \nu \right\rangle + M_\gamma \left\langle \mu \left| \alpha \cdot h \right| \nu \right\rangle, \qquad (4.153)
\end{aligned}$$

where the integrals over the dipole moment operator times the one-electron core Hamiltonian in the second line of Eq. (4.153) are available in the `MOLPRO` routine `basis_giao_shell_dm_h0`.
For the second term of Eq. (4.143),

$$\left\langle \mu \left| \delta_{\alpha\beta} \left(\mathbf{r}_N \cdot \mathbf{r}_N\right) - \left(\mathbf{r}_N\right)_\alpha \cdot \left(\mathbf{r}_N\right)_\beta \right| \nu \right\rangle, \qquad (4.154)$$

it is useful to distinguish between two cases: (*i*) when the differentiation is carried out twice with respect to the same components of the magnetic field, and (*ii*) when the two components differ. For differentiation with respect to the same components (which is considered to be α) one finds

$$\begin{aligned}
&\left\langle \mu \left| (\beta - N_\beta)(\beta - N_\beta) + (\gamma - N_\gamma)(\gamma - N_\gamma) \right| \nu \right\rangle \\
&= \left\langle \mu | \nu + \mathbf{1}_\beta + \mathbf{1}_\beta \right\rangle + \left\langle \mu | \nu + \mathbf{1}_\gamma + \mathbf{1}_\gamma \right\rangle, \qquad (4.155)
\end{aligned}$$

which means that these integrals can be calculated directly from overlap integrals by incrementing the angular momentum on the ket-side.
For differentiation with respect to different components of the magnetic field one finds

$$- \left\langle \mu \left| (\alpha - N_\alpha)(\beta - N_\beta) \right| \nu \right\rangle = - \left\langle \mu | \nu + \mathbf{1}_\alpha + \mathbf{1}_\beta \right\rangle, \qquad (4.156)$$

which is again an overlap integral for which the angular momentum on the ket-side has been incremented.
The first term of Eq. (4.143),

$$\left\langle \mu \left| (\mathbf{R}_{MN} \times \mathbf{r})_\alpha \, (\mathbf{r}_N \times \nabla)_\beta + (\mathbf{R}_{MN} \times \mathbf{r})_\beta \, (\mathbf{r}_N \times \nabla)_\alpha \right| \nu \right\rangle , \tag{4.157}$$

is more involved than the other two terms; for this consideration only the first term of Eq. (4.157) will be discussed. The second term can be programmed analogously by swapping the indices of the perturbations. One then finds

$$\begin{aligned} &\left\langle \mu \left| (\mathbf{R}_{MN} \times \mathbf{r})_\alpha \, (\mathbf{r}_N \times \nabla)_\beta \right| \nu \right\rangle \\ &= \left\langle \mu \left| \Big((M_\beta - N_\beta)\gamma - (M_\gamma - N_\gamma)\beta \Big) \left((\gamma - N_\gamma) \frac{\partial}{\partial \alpha} - (\alpha - N_\alpha) \frac{\partial}{\partial \gamma} \right) \right| \nu \right\rangle , \end{aligned} \tag{4.158}$$

which yields the following individual terms:

$$\begin{aligned} &\left\langle \mu \left| (\mathbf{R}_{MN} \times \mathbf{r})_\alpha \, (\mathbf{r}_N \times \nabla)_\beta \right| \nu \right\rangle \\ &= (M_\beta - N_\beta) \left[\left\langle \mu \left| \gamma\gamma \frac{\partial}{\partial \alpha} \right| \nu \right\rangle - N_\gamma \left\langle \mu \left| \gamma \frac{\partial}{\partial \alpha} \right| \nu \right\rangle \right] \\ &\quad - (M_\beta - N_\beta) \left[\left\langle \mu \left| \gamma\alpha \frac{\partial}{\partial \gamma} \right| \nu \right\rangle - N_\alpha \left\langle \mu \left| \gamma \frac{\partial}{\partial \gamma} \right| \nu \right\rangle \right] \\ &\quad - (M_\gamma - N_\gamma) \left[\left\langle \mu \left| \beta\gamma \frac{\partial}{\partial \alpha} \right| \nu \right\rangle - N_\gamma \left\langle \mu \left| \beta \frac{\partial}{\partial \alpha} \right| \nu \right\rangle \right] \\ &\quad + (M_\gamma - N_\gamma) \left[\left\langle \mu \left| \beta\alpha \frac{\partial}{\partial \gamma} \right| \nu \right\rangle - N_\alpha \left\langle \mu \left| \beta \frac{\partial}{\partial \gamma} \right| \nu \right\rangle \right] . \end{aligned} \tag{4.159}$$

In order to program this expression one must consider two principle terms which can be derived from dipole moment and quadrupole moment integrals by applying the differentiation relation Eq. (4.148):

$$\left\langle \mu \left| \beta \frac{\partial}{\partial \alpha} \right| \nu \right\rangle = n_\alpha \left\langle \mu \left| \beta \right| \nu - \mathbf{1}_\alpha \right\rangle - 2\alpha_n \left\langle \mu \left| \beta \right| \nu + \mathbf{1}_\alpha \right\rangle \tag{4.160}$$

and

$$\left\langle \mu \left| \beta\gamma \frac{\partial}{\partial \alpha} \right| \nu \right\rangle = n_\alpha \left\langle \mu \left| \beta\gamma \right| \nu - \mathbf{1}_\alpha \right\rangle - 2\alpha_n \left\langle \mu \left| \beta\gamma \right| \nu + \mathbf{1}_\alpha \right\rangle . \tag{4.161}$$

Hence, one needs the dipole moment and quadrupole moment integrals with the angular momentum on the ket-side incremented, respectively, decremented by 1.

For the calculation of rotational g tensors (see Chapter 5) another set of integrals is required, which appears in the diamagnetic part of the magnetizability evaluated with the center of mass of the molecule, $\mathbf{R}_{CM}$, as gauge origin,

$$\left\langle \mu \left| \delta_{\alpha\beta} \left(\mathbf{r}_{CM} \cdot \mathbf{r}_{CM} \right) - \left(\mathbf{r}_{CM} \right)_{\alpha} \cdot \left(\mathbf{r}_{CM} \right)_{\beta} \right| \nu \right\rangle , \tag{4.162}$$

where $\mathbf{r}_{CM}$ is the vector pointing from the center of mass to the electron. Like before, it is useful to distinguish between two cases: (*i*) when the same components of the perturbation are considered, and (*ii*) when the two components differ. For the same components one finds

$$\begin{aligned} &\left\langle \mu \left| (\beta - CM_{\beta})(\beta - CM_{\beta}) + (\gamma - CM_{\gamma})(\gamma - CM_{\gamma}) \right| \nu \right\rangle \\ &= \left\langle \mu | \nu + \mathbf{1}_{\beta} + \mathbf{1}_{\beta} \right\rangle + 2(N_{\beta} - CM_{\beta}) \left\langle \mu | \nu + \mathbf{1}_{\beta} \right\rangle + (N_{\beta} - CM_{\beta})^2 \left\langle \mu | \nu \right\rangle \\ &\quad + \left\langle \mu | \nu + \mathbf{1}_{\gamma} + \mathbf{1}_{\gamma} \right\rangle + 2(N_{\gamma} - CM_{\gamma}) \left\langle \mu | \nu + \mathbf{1}_{\gamma} \right\rangle + (N_{\gamma} - CM_{\gamma})^2 \left\langle \mu | \nu \right\rangle \end{aligned} \tag{4.163}$$

and for different components

$$\begin{aligned} &- \left\langle \mu \left| (\alpha - CM_{\alpha})(\beta - CM_{\beta}) \right| \nu \right\rangle \\ &= - \left\langle \mu | \nu + \mathbf{1}_{\alpha} + \mathbf{1}_{\beta} \right\rangle - (N_{\alpha} - CM_{\alpha}) \left\langle \mu | \nu + \mathbf{1}_{\beta} \right\rangle \\ &\quad - (N_{\beta} - CM_{\beta}) \left\langle \mu | \nu + \mathbf{1}_{\alpha} \right\rangle - (N_{\alpha} - CM_{\alpha})(N_{\beta} - CM_{\beta}) \left\langle \mu | \nu \right\rangle . \end{aligned} \tag{4.164}$$

These integrals can be obtained directly from overlap integrals by incrementing the angular momentum on the ket-side and multiplying them with the corresponding differences of the center of the function and the center of mass.

4.5.2 The Gaussian Product Theorem

The Gaussian Product Theorem (GPT) states that a product of two Cartesian Gaussian functions can be expressed as a linear combination of Cartesian Gaussian functions. The resulting function is centered on the connection line between the original centers. Thus, a product of two Gaussians

located on two different centers **A** and **B** with arbitrary angular momentum can be written as [52, 117]

$$\begin{aligned}\chi_{\mathbf{A}}\chi_{\mathbf{B}} &= \chi_1(\mathbf{r}_1;\alpha_1,\mathbf{n}_1,\mathbf{A})\chi_2(\mathbf{r}_2;\alpha_2,\mathbf{n}_2,\mathbf{B}) \\ &= \exp\left[-\frac{\alpha_1\alpha_2}{\gamma}\left(\mathbf{A}-\mathbf{B}\right)^2\right]\times \\ &\left[\sum_{n_{P_x}=0}^{n_{1x}+n_{2x}} \mathbf{T}^{A_x,B_x}_{n_{1x},n_{2x},n_{P_x}}\left(x-\mathrm{P}_x\right)^{n_{P_x}} e^{-\gamma(x-\mathrm{P}_x)^2}\right]\times \\ &\left[\sum_{n_{P_y}=0}^{n_{1y}+n_{2y}} \mathbf{T}^{A_y,B_y}_{n_{1y},n_{2y},n_{P_y}}\left(y-\mathrm{P}_y\right)^{n_{P_y}} e^{-\gamma\left(y-\mathrm{P}_y\right)^2}\right]\times \\ &\left[\sum_{n_{P_z}=0}^{n_{1z}+n_{2z}} \mathbf{T}^{A_z,B_z}_{n_{1z},n_{2z},n_{P_z}}\left(z-\mathrm{P}_z\right)^{n_{P_z}} e^{-\gamma(z-\mathrm{P}_z)^2}\right],\end{aligned} \tag{4.165}$$

where γ, **P** and **T** are given by

$$\gamma = \alpha_1 + \alpha_2, \tag{4.166}$$

$$\mathbf{P} = \frac{\alpha_1\mathbf{A}+\alpha_2\mathbf{B}}{\gamma}, \tag{4.167}$$

$$\mathbf{T}^{A_x,B_x}_{l_1,l_2,k} = \sum_{i=0}^{l_1}\sum_{j=0}^{l_2}\delta_{(i+j),k}\left(\mathbf{P}-\mathbf{A}\right)_x^{l_1-i}\binom{l_1}{i}\left(\mathbf{P}-\mathbf{B}\right)_x^{l_2-j}\binom{l_2}{j}. \tag{4.168}$$

Considering two 1-s orbitals ϕ_1, ϕ_2 located at **A** and **B** one finds

$$\begin{aligned}\phi_1\phi_2 &= e^{-\alpha_1(\mathbf{r}-\mathbf{A})^2}e^{-\alpha_2(\mathbf{r}-\mathbf{B})^2} \\ &= \exp\left[-\frac{\alpha_1\alpha_2}{\alpha_1+\alpha_2}\left(\mathbf{A}-\mathbf{B}\right)\right]\exp\left[-\gamma\left(\mathbf{r}-\mathbf{P}\right)^2\right].\end{aligned} \tag{4.169}$$

The definition of the GPT in Eq. (4.165) can be rewritten more compactly in terms of the transformation matrix **T**,

$$\chi_A\chi_B = \sum_{\mathbf{n}_P} T^{\mathbf{A},\mathbf{B}}_{\mathbf{n}_1,\mathbf{n}_2,\mathbf{n}_P}\chi_{\mathbf{P}}(\mathbf{r}_P;\gamma,\mathbf{n}_P,\mathbf{P}), \tag{4.170}$$

where we have introduced

$$\mathbf{T}^{\mathbf{A},\mathbf{B}}_{\mathbf{n}_1,\mathbf{n}_2,\mathbf{n}_P} = \mathbf{T}^{A_x,B_x}_{n_{1x},n_{2x},n_{P_x}}\mathbf{T}^{A_y,B_y}_{n_{1y},n_{2y},n_{P_y}}\mathbf{T}^{A_z,B_z}_{n_{1z},n_{2z},n_{P_z}}, \tag{4.171}$$

$$\begin{aligned}\chi_{\mathbf{P}}(\mathbf{r}_P;\gamma,\mathbf{n}_P,\mathbf{P}) &= \left(x-\mathrm{P}_x\right)^{n_{P_x}}\left(y-\mathrm{P}_y\right)^{n_{P_y}}\left(z-\mathrm{P}_z\right)^{n_{P_z}}\times \\ &\exp\left[-\gamma\left(\mathbf{r}-\mathbf{P}\right)^2\right].\end{aligned} \tag{4.172}$$

4.5.3 Derivatives of three-index integrals

The second derivative of the three-index electron repulsion integrals with respect to the external magnetic field, as they appear in the calculation of magnetizabilities (see e.g., Sections 4.2.3 and 4.3.4), can be written as

$$\begin{aligned}
\frac{\partial^2(\mu\nu|Q)}{\partial B_\alpha \partial B_\beta} &= -\frac{1}{4c^2}\left(\mu\nu\left|\frac{1}{r_{12}}\left((\mathbf{R}_M-\mathbf{R}_N)\times\mathbf{r_1}\right)_\alpha\left((\mathbf{R}_M-\mathbf{R}_N)\times\mathbf{r_1}\right)_\beta\right|Q\right)\\
&= -\frac{1}{4c^2}\Bigg[\left(\mu\nu\left|\frac{1}{r_{12}}\left(M_\beta-N_\beta\right)\left(M_\gamma-N_\gamma\right)\cdot\gamma\cdot\alpha\right|Q\right)\\
&\quad-\left(\mu\nu\left|\frac{1}{r_{12}}\left(M_\beta-N_\beta\right)\left(M_\alpha-N_\alpha\right)\cdot\gamma\cdot\gamma\right|Q\right)\\
&\quad-\left(\mu\nu\left|\frac{1}{r_{12}}\left(M_\gamma-N_\gamma\right)^2\cdot\beta\cdot\alpha\right|Q\right)\\
&\quad+\left(\mu\nu\left|\frac{1}{r_{12}}\left(M_\gamma-N_\gamma\right)\left(M_\alpha-N_\alpha\right)\cdot\beta\cdot\gamma\right|Q\right)\Bigg]\\
&= -\frac{1}{4c^2}\Bigg[\left(M_\beta-N_\beta\right)\left(M_\gamma-N_\gamma\right)\left(\mu\nu\left|\frac{\gamma\cdot\alpha}{r_{12}}\right|Q\right)\\
&\quad-\left(M_\beta-N_\beta\right)\left(M_\alpha-N_\alpha\right)\left(\mu\nu\left|\frac{\gamma\cdot\gamma}{r_{12}}\right|Q\right)\\
&\quad-\left(M_\gamma-N_\gamma\right)^2\left(\mu\nu\left|\frac{\beta\cdot\alpha}{r_{12}}\right|Q\right)\\
&\quad+\left(M_\gamma-N_\gamma\right)\left(M_\alpha-N_\alpha\right)\left(\mu\nu\left|\frac{\beta\cdot\gamma}{r_{12}}\right|Q\right)\Bigg].
\end{aligned} \tag{4.173}$$

Exploiting the Gaussian Product Theorem for this integral yields

$$\left(\mu\nu\left|\frac{\gamma\cdot\alpha}{r_{12}}\right|Q\right)=\sum_{\mathbf{n}_A}T^{\mathbf{M},\mathbf{N}}_{\mathbf{n}_\mu,\mathbf{n}_\nu,\mathbf{n}_A}\left(A\left|\frac{\gamma\cdot\alpha}{r_{12}}\right|Q\right). \tag{4.174}$$

The `MOLPRO` routine `basis_shell_QM_J` creates the required two-index integrals based on the integrals $(A\,|^{\alpha}/_{r_{12}}|\,Q)$ from the routine `basis_shell_DM_J` according to the following formula:

$$\left(A\left|\frac{\gamma\cdot\alpha}{r_{12}}\right|Q\right)=\left(A+\mathbf{1}_\gamma\left|\frac{\alpha}{r_{12}}\right|Q\right)+R_{A,\gamma}\left(A\left|\frac{\alpha}{r_{12}}\right|Q\right). \tag{4.175}$$

Note that A and Q are both ordinary Gaussian functions; A is defined in Eq. (4.172), whereas Q is a fitting function. $R_{A,\gamma}$ is the γ Cartesian component of the position vector of function A. The fitting functions have to be ordinary Gaussians as gauge invariance would be violated otherwise. There is no complex conjugate for the fitting function Q which would cancel the explicit gauge origin dependence of GIAOs.

4.6 Conclusions

In this chapter magnetizabilities at the levels of DF-HF and DF-LMP2 have been presented. Gauge-including atomic orbitals are used to overcome the gauge origin problem and ordinary Gaussians are employed as fitting functions. This approach for density fitting (DF) was already employed for NMR shielding tensors and also works very well for magnetizabilities. The DF errors are negligibly small for augmented and non-augmented basis sets for HF and LMP2. The results were obtained by test calculations on a benchmark set of 28 small molecules.

Furthermore, the accuracy of the local approximation for magnetizabilities at the level of DF-LMP2 was evaluated. Calculations on a benchmark set and on several medium-sized molecules show that the correlation contribution is small for closed-shell molecules (smaller than for other properties like NMR shielding tensors). Comparison with full-domain calculations indicate that for non-augmented basis sets standard Boughton-Pulay domains are sufficient. For augmented basis sets it appears reasonable to extend the domains by one shell of neighboring atoms.

Electron correlation effects are generally small for magnetizabilities of closed-shell molecules, and the MP2 method itself, overestimating correlation, does not provide a significant improvement in accuracy over Hartree-Fock. It appears necessary to use rather large basis sets and higher order methods for an improvement on Hartree-Fock magnetizabilities.

The performance of the program was tested for two larger molecular sys-

tems. The largest investigated system was the 1@2 tweezer molecule with cc-pVTZ AO basis (2184 basis functions). Calculations of magnetizabilities take roughly 1.5 half times longer than NMR shielding tensor calculations. The extra computational cost is mainly caused by the contraction of (unperturbed and perturbed) two-particle density matrices with the derivatives of the electron repulsion integrals. Overall, most computational time is spent for the calculation of the right-hand side of the perturbed Z-CPHF equations and their subsequent iterative solution (as it is also the case for DF-LMP2 NMR shielding tensors).

Chapter 5

ROTATIONAL G TENSORS

5.1 Introduction

The rotation of a molecule in an external magnetic field induces a molecular magnetic moment which leads to the rotational Zeeman effect [42]. The resulting shift of the rotational energy levels and hence the strength of the Zeeman interaction can be described by rotational g tensors [97]. Rotational g tensors and the paramagnetic part of magnetizability tensors are formally closely related [47, 48]. In contrast to magnetizabilities [44], rotational g tensors are experimentally accessible with high accuracy by molecular beam [46] and microwave spectroscopy [47]. The connection between the two aforementioned quantities can be shown in an elegant manner by introducing rotational London orbitals, which can be considered as a generalization of GIAOs to rotating molecules. This ansatz was put forward by Gauss, Ruud, and Helgaker in Ref. [97]. Along the same lines, spin-rotation constants are connected to NMR shielding tensors [97]. Yet, it should be mentioned at this point that these connections only hold in a non-relativistic framework, as recent relativistic four component calculations of spin-rotation constants indicate [118–120].
This chapter, in particular the following Section 5.2, will closely follow the aforementioned publication by Gauss et al. [97] to outline the formalism of

rotational g tensors and show their connection to magnetizabilities. For the sake of readability Ref. [97] will not be cited individually again throughout Section 5.2.
Helgaker et al. provided a good overview of the development and of current methods for the calculation of rotational g tensors (see Ref. [42] and references therein): they mention the work of Sauer et al. in which he presented a number of calculations for mainly small molecular systems within the second-order polarization propagator approximation (SOPPA) [121–123] and the SOPPA(CCSD) [124–127] method. They also point out the above mentioned formalism of rotational London orbitals which brought larger molecules within reach of high-level correlation methods. Amongst others Ruud et al. presented results for their MCSCF implementation [128] and Gauss et al. showed results for their coupled-cluster implementation up to arbitrary excitation levels [111].

5.2 Connection to Magnetizability Tensors

The shift of the rotational energy levels in the presence of an external magnetic field **B** can be written as

$$\Delta E = -\frac{\mu_N}{\hbar}\mathbf{B}g\mathbf{J}. \tag{5.1}$$

In the above equation μ_N is the nuclear magneton,

$$\mu_N = \frac{e\hbar}{2M_p c} \tag{5.2}$$

with the mass of the proton, M_p. The nuclear magneton equals $\alpha/2M_p$ in atomic units. Furthermore, **J** is the total rotational angular momentum, and g the rotational g tensor,

$$g = -\frac{\hbar}{\mu_N}\left[\frac{d^2E}{d\mathbf{B}d\mathbf{J}}\right]_{\mathbf{B},\mathbf{J}=0}. \tag{5.3}$$

Since rotational g tensors arise from the rotation of a molecule in an external magnetic field the center of mass is chosen as the origin of the coordinate system for the considerations in this chapter. In the following, detailed expressions for the derivative in Eq. (5.3) will be presented.
For the calculation of rotational g tensors the coupling of electronic and rotational motion has to be included in the Hamiltonian. Following Flygare [47, 48] this contribution, which is linear in the total rotational angular momentum, is given by the following first-order term

$$h^{(1)} = -\mathbf{I}^{-1}\mathbf{J}\mathbf{l}, \tag{5.4}$$

where $\mathbf{I}$ is the inertia tensor of the molecule and $\mathbf{l}$ is the angular momentum operator with respect to the center of mass as origin.
As outlined in Section 2.1 the total magnetic vector potential $\mathbf{A}^{\text{tot}}$ has contributions from the external magnetic field and the magnetic dipole moments $\mathbf{M}_K$ of each nucleus,

$$\mathbf{A}^{\text{tot}}(\mathbf{r}) = \frac{1}{2}\mathbf{B} \times (\mathbf{r} - \mathbf{R}_O) + \sum_K \frac{\mathbf{M}_K \times \mathbf{r}_K}{r_K^3}. \tag{5.5}$$

In this equation $\mathbf{R}_O$ denotes the arbitrary gauge origin.
Additionally, the kinetic part of the Hamiltonian has to be modified such that it contains the square of the kinetic momentum operator,

$$h = \frac{1}{2}\left(-i\nabla + \frac{1}{c}\mathbf{A}^{\text{tot}}(\mathbf{r})\right)^2. \tag{5.6}$$

Following Gauss et al. this leads to the following first-order correction to the Hamiltonian from the external magnetic field:

$$h^{(1)} = \frac{1}{2c}\mathbf{B} \cdot \mathbf{l}_O. \tag{5.7}$$

The subscript O indicates that the angular momentum operator has been defined with the gauge origin as origin, i.e.,

$$\mathbf{l}_O = -i\,(\mathbf{r} - \mathbf{R}_O) \times \nabla. \tag{5.8}$$

There is an additional second-order contribution to the Hamiltonian which arises from the rotating gauge origin (for more details see Citation 13 in Ref. [97]),

$$h^{(2)} = \frac{1}{2c}\mathbf{B}\left[(\mathbf{r}\cdot\mathbf{R}_O)\,\mathbf{1} - \mathbf{r}\mathbf{R}_O\right]\mathbf{I}^{-1}\mathbf{J}. \tag{5.9}$$

Expanding the Hamiltonian in the first- and mixed second-order terms with respect to the external magnetic field and the total rotational angular momentum yields

$$h = h^{(0)} + \left(\frac{\partial h}{\partial \mathbf{J}}\right)_{\mathbf{J}=0}\mathbf{J} + \left(\frac{\partial h}{\partial \mathbf{B}}\right)_{\mathbf{B}=0}\mathbf{B} + \mathbf{B}\left(\frac{\partial^2 h}{\partial \mathbf{J}\partial \mathbf{B}}\right)_{\mathbf{B},\mathbf{J}=0}\mathbf{J} + \ldots \tag{5.10}$$

with the derivatives

$$\left(\frac{\partial h}{\partial \mathbf{J}}\right)_{\mathbf{J}=0} = -\mathbf{l}\mathbf{I}^{-1}, \tag{5.11}$$

$$\left(\frac{\partial h}{\partial \mathbf{B}}\right)_{\mathbf{B}=0} = \frac{1}{2c}\mathbf{l}_O, \tag{5.12}$$

$$\left(\frac{\partial^2 h}{\partial \mathbf{J}\partial \mathbf{B}}\right)_{\mathbf{B},\mathbf{J}=0} = \frac{1}{2c}\left[(\mathbf{r}\cdot\mathbf{R}_O)\,\mathbf{1} - \mathbf{r}\mathbf{R}_O\right]\mathbf{I}^{-1}. \tag{5.13}$$

Gauss et al. proposed to generalize the ansatz of London atomic orbitals,

$$\omega_\mu(\mathbf{A}_O(\mathbf{R}_M)) = \exp\left(-\frac{i}{c}\mathbf{A}_O(\mathbf{R}_M)\cdot\mathbf{r}\right)\chi_\mu \tag{5.14}$$

with

$$\mathbf{A}_O(\mathbf{R}_M) = \frac{1}{2}\mathbf{B}\times(\mathbf{R}_M - \mathbf{R}_O), \tag{5.15}$$

to rotating systems by additionally adding the vector potential due to the rotation at the center $\mathbf{R}_M$ of the corresponding basis function to the complex phase factors,

$$\mathbf{A}^{\mathbf{J}}(\mathbf{R}_M) = -\mathbf{I}^{-1}\mathbf{J}\times\mathbf{R}_M. \tag{5.16}$$

This defines rotational London orbitals as

$$\omega_\mu(\mathbf{A}_O(\mathbf{R}_M), \mathbf{A}^{\mathbf{J}}(\mathbf{R}_M)) = \exp\left(-i\left[\frac{1}{c}\mathbf{A}_O(\mathbf{R}_M) + \mathbf{A}^{\mathbf{J}}(\mathbf{R}_M)\right]\cdot\mathbf{r}\right)\chi_\mu. \tag{5.17}$$

Matrix elements of rotational London orbitals over the Hamiltonian can be obtained by exploiting the following commutator relations:

$$\begin{aligned}
&\left[-i\nabla, \exp\left(-i\left[\frac{1}{c}\mathbf{A}_O\left(\mathbf{R}_N\right) + \mathbf{A}^{\mathbf{J}}(\mathbf{R}_N)\right]\cdot\mathbf{r}\right)\right] \\
&= -\exp\left(-i\left[\frac{1}{c}\mathbf{A}_O\left(\mathbf{R}_N\right) + \mathbf{A}^{\mathbf{J}}(\mathbf{R}_N)\right]\cdot\mathbf{r}\right)\left(\frac{1}{c}\mathbf{A}_O\left(\mathbf{R}_N\right) + \mathbf{A}^{\mathbf{J}}(\mathbf{R}_N)\right),
\end{aligned} \tag{5.18}$$

$$\begin{aligned}
&\left[-i\nabla^2, \exp\left(-i\left[\frac{1}{c}\mathbf{A}_O\left(\mathbf{R}_N\right) + \mathbf{A}^{\mathbf{J}}(\mathbf{R}_N)\right]\cdot\mathbf{r}\right)\right] \\
&= -\exp\left(-i\left[\frac{1}{c}\mathbf{A}_O\left(\mathbf{R}_N\right) + \mathbf{A}^{\mathbf{J}}(\mathbf{R}_N)\right]\cdot\mathbf{r}\right)\Bigg[i\left(\frac{1}{c}\mathbf{A}_O\left(\mathbf{R}_N\right) + \mathbf{A}^{\mathbf{J}}(\mathbf{R}_N)\right)\nabla \\
&\quad + \frac{1}{2}\left(\frac{1}{c}\mathbf{A}_O\left(\mathbf{R}_N\right) + \mathbf{A}^{\mathbf{J}}(\mathbf{R}_N)\right)^2\Bigg]
\end{aligned} \tag{5.19}$$

and

$$\begin{aligned}
&\left[\mathbf{l}, \exp\left(-i\left[\frac{1}{c}\mathbf{A}_O\left(\mathbf{R}_N\right) + \mathbf{A}^{\mathbf{J}}(\mathbf{R}_N)\right]\cdot\mathbf{r}\right)\right] \\
&= -\exp\left(-i\left[\frac{1}{c}\mathbf{A}_O\left(\mathbf{R}_N\right) + \mathbf{A}^{\mathbf{J}}(\mathbf{R}_N)\right]\cdot\mathbf{r}\right)\left(\mathbf{r}\times\left(\frac{1}{c}\mathbf{A}_O\left(\mathbf{R}_N\right) + \mathbf{A}^{\mathbf{J}}(\mathbf{R}_N)\right)\right).
\end{aligned} \tag{5.20}$$

Matrix elements over the Hamiltonian defined in Eq. (5.10) can then be written as

$$\begin{aligned}
\left\langle \omega_\mu \left| h \right| \omega_\nu \right\rangle = \Bigg\langle \chi_\mu \Bigg| &\exp\left(-i\left[\frac{1}{c}\mathbf{A}_N\left(\mathbf{R}_M\right) + \mathbf{A}^{\mathbf{J}}(\mathbf{R}_{MN})\right]\cdot\mathbf{r}\right) \\
&\Bigg[-\frac{1}{2}\nabla^2 - \sum_K \frac{Z_K}{r_K} + \frac{1}{2c}\mathbf{B}\cdot\mathbf{l}_N - \mathbf{I}^{-1}\mathbf{J}\mathbf{l}_N \\
&+ \frac{1}{2c}\mathbf{B}\left[\mathbf{r}\cdot\mathbf{R}_N\mathbf{1} - \mathbf{r}\mathbf{R}_N + \mathbf{R}_N\cdot\left(\mathbf{r}-\mathbf{R}_N\right)\mathbf{1}\right. \\
&\left.-\mathbf{R}_N\left(\mathbf{r}-\mathbf{R}_N\right)\right]\mathbf{I}^{-1}\mathbf{J}\Bigg] \Bigg| \chi_\nu \Bigg\rangle \\
&+ \text{higher order terms.}
\end{aligned} \tag{5.21}$$

The differentiated integrals are then given by

$$\frac{\partial h_{\mu\nu}}{\partial B_\alpha} = \frac{i}{2c}\left\langle \mu \left| \left(\left(\mathbf{R}_M - \mathbf{R}_N\right)\times\mathbf{r}\right)_\alpha h^{(0)} - \left(\mathbf{r}_N\times\nabla\right)_\alpha \right| \nu \right\rangle, \tag{5.22}$$

$$\frac{\partial h_{\mu\nu}}{\partial J_\alpha} = -i\mathbf{I}^{-1}\left\langle \mu \left| \left(\left(\mathbf{R}_M - \mathbf{R}_N\right)\times\mathbf{r}\right)_\alpha h^{(0)} - \left(\mathbf{r}_N\times\nabla\right)_\alpha \right| \nu \right\rangle, \tag{5.23}$$

and

$$\begin{aligned}\frac{\partial^2 h_{\mu\nu}}{\partial J_\alpha B_\beta} = -\frac{1}{2c}\mathbf{I}^{-1}\Big[&\left\langle \mu \left| (\mathbf{R}_{MN}\times\mathbf{r})_\alpha (\mathbf{r}_N\times\nabla)_\beta + (\mathbf{R}_{MN}\times\mathbf{r})_\beta (\mathbf{r}_N\times\nabla)_\alpha \right| \nu \right\rangle \\ &+ \left\langle \mu \left| \delta_{\alpha\beta}(\mathbf{r}_N\cdot\mathbf{r}_N) - (\mathbf{r}_N)_\alpha\cdot(\mathbf{r}_N)_\beta \right| \nu \right\rangle \\ &- \left\langle \mu \left| \delta_{\alpha\beta}(\mathbf{r}\cdot\mathbf{r}) - (\mathbf{r})_\alpha\cdot(\mathbf{r})_\beta \right| \nu \right\rangle \\ &- \left\langle \mu \left| (\mathbf{R}_{MN}\times\mathbf{r})_\alpha (\mathbf{R}_{MN}\times\mathbf{r})_\beta h^{(0)} \right| \nu \right\rangle \Big]. \end{aligned} \tag{5.24}$$

By comparing the above Eq. (5.24) with the second derivative of the one-electron core Hamiltonian with respect to the magnetic field, Eq. (4.143), one finds that these two integrals only differ in the following term:

$$\frac{\partial^2 h_{\mu\nu}}{\partial J_\alpha B_\beta} \leftarrow \frac{1}{2c}\mathbf{I}^{-1}\left\langle \mu \left| \delta_{\alpha\beta}(\mathbf{r}\cdot\mathbf{r}) - (\mathbf{r})_\alpha\cdot(\mathbf{r})_\beta \right| \nu \right\rangle. \tag{5.25}$$

This integral appears in the diamagnetic part of the magnetizability evaluated with the center of mass as gauge origin. Note that the integral is gauge independent since it contains the position vector $\mathbf{r}$ pointing from the center of mass of the molecule to the electron. The gauge independent integrals over the second derivative of the core Hamiltonian, on the other hand, contain the position vector $\mathbf{r}_N$ which points from the center of the ket-function to the electron. The implementation of the integral is shown in Eqs. (4.162)–(4.164) in Section 4.5.

For the calculation of the rotational g tensor a nuclear contribution has to be taken into account additionally,

$$g^{\text{nuc}} = M_p \sum_K Z_K \left[(\mathbf{R}_K\cdot\mathbf{R}_K)\,\mathbf{1} - \mathbf{R}_K\mathbf{R}_K \right] \mathbf{I}^{-1}. \tag{5.26}$$

One then obtains the final expression

$$g = -4M_p c^2 \left(\xi^{\text{LAO}} - \xi^{\text{dia}}(\text{cm}) \right) \mathbf{I}^{-1} + g^{\text{nuc}}, \tag{5.27}$$

where ξ^{LAO} is the magnetizability tensor calculated with GIAOs, as defined in Eq. (4.15) for DF-HF, and in Eq. (4.76) for DF-LMP2. Furthermore, the

mass of the proton M_p and the diamagnetic part of the magnetizability tensor evaluated with the center of mass as gauge origin (see Eq. 5.25) have been introduced. The latter can be written explicitly as

$$\xi^{\text{dia}}\,(\text{cm}) = \frac{1}{4c^2} \sum_{\mu\nu} D_{\mu\nu} \left\langle \mu \left| \delta_{\alpha\beta} \left(\mathbf{r} \cdot \mathbf{r} \right) - (\mathbf{r})_\alpha \cdot (\mathbf{r})_\beta \right| \nu \right\rangle \tag{5.28}$$

with the unperturbed density matrix **D** of the chosen method in AO basis. For the definitions of the unperturbed density matrices see Eq. (4.7) in the case of DF-HF and Eqs. (4.62) and (4.41) in the case of DF-LMP2.

5.3 Accuracy and Performance

The tables in this chapter and in Appendix B provide the unique diagonal elements of the rotational g tensors. For linear molecules like AlF two elements are the same, whereas the third one equals 0. For molecules with high symmetry like CH_4 there may be only one unique value which is then provided in the table.

5.3.1 Local approximation

Tables 5.1 and 5.2 show the accuracy of the local approximation for rotational g tensors. The calculations were carried out for the benchmark set by Lutnæs et al. [45] which was also used to assess the accuracy of magnetizabilities in Chapter 4. Ozone was excluded from the calculation of the statistical measures. Average isotopic masses were used for all molecules, except for HCN, FCN, and N_2: these three molecules were calculated with the ^{15}N isotope (m(^{15}N)=15.000109 u). The molecules were aligned in the principal axis system, i.e., they were oriented such that the center of mass is the origin and the axes are the eigenvectors of the inertia tensor (`MOLPRO` command `orient,mass`, see `MOLPRO` users manual [94]). The calculations were done with Dunning's cc-pVXZ and aug-cc-pVXZ AO basis sets [86–91, 115] for X=D, T, and Q with the related JK- [92] and MP2-fitting basis sets [93]. For Li the cc-pVXZ and aug-cc-pVXZ AO basis sets published in 2011 were used [115]. The local calculations with standard domains [60] were compared to calculations with full domains. Electron pairs with an interorbital distance beyond 15 bohrs are omitted in local calculations. Since the pair list remains untruncated for all molecules of the benchmark set the calculations with full domains are equivalent to canonical calculations. The correlation contribution to rotational g tensors, also included in Tables 5.1 and 5.2, is calculated as the difference between the GIAO-DF-LMP2 full domain result and the rotational g tensor obtained with the GIAO-DF-HF method.

Table 5.1: Error introduced by the local approximation to rotational g tensors at the level of GIAO-DF-LMP2: the local error, results from calculations with full domains and untruncated pair lists, and the correlation contribution are provided. For all calculations the frozen-core approximation was employed.

Basis	cc-pVDZ			cc-pVTZ			cc-pVQZ		
	$\Delta^{\text{local a)}}$	full	$g_{\text{MP2}}^{\text{correl b)}}$	$\Delta^{\text{local a)}}$	full	$g_{\text{MP2}}^{\text{correl b)}}$	$\Delta^{\text{local a)}}$	full	$g_{\text{MP2}}^{\text{correl b)}}$
AlF	-0.0001	-0.0749	0.0074	-0.0005	-0.0751	0.0066	-0.0006	-0.0774	0.0059
C_2H_4	0.0021	0.0523	-0.0080	0.0005	0.0554	-0.0057	0.0004	0.0559	-0.0052
	-0.0002	-0.1075	0.0073	0.0000	-0.1103	0.0040	0.0001	-0.1103	0.0041
	0.0021	-0.3523	-0.0267	0.0009	-0.3609	-0.0317	0.0009	-0.3637	-0.0317
C_3H_4	0.0006	0.0624	-0.0021	0.0002	0.0620	-0.0017	0.0000	0.0616	-0.0015
	0.0011	-0.1398	-0.0017	0.0010	-0.1453	-0.0010	0.0007	-0.1468	-0.0001
	0.0004	-0.0699	0.0249	0.0003	-0.0722	0.0218	0.0003	-0.0724	0.0217
CH_2O	0.0003	-0.1015	-0.0365	0.0008	-0.1006	-0.0343	0.0002	-0.1000	-0.0334
	0.0000	-0.1982	0.0182	-0.0001	-0.2075	0.0120	-0.0001	-0.2104	0.0109
	-0.0012	-2.8341	-0.0629	-0.0004	-2.8341	-0.1162	0.0004	-2.8277	-0.1219
CH_3F	0.0009	-0.0589	-0.0075	0.0008	-0.0615	-0.0075	0.0004	-0.0620	-0.0072
	0.0040	0.2375	-0.0145	0.0019	0.2599	-0.0010	0.0008	0.2689	0.0049
CH_4	0.0047	0.3199	0.0168	0.0012	0.3312	0.0268	0.0002	0.3327	0.0293
CO	-0.0001	-0.2556	0.0264	0.0001	-0.2589	0.0221	0.0001	-0.2597	0.0217
FCCH	0.0000	-0.0005	-0.0019	0.0000	-0.0040	-0.0025	0.0000	-0.0052	-0.0027
$FC^{15}N$	-0.0001	-0.0420	0.0020	-0.0001	-0.0461	0.0004	0.0000	-0.0474	0.0000
H_2C_2O	0.0003	-0.0187	0.0033	-0.0001	-0.0212	0.0027	-0.0001	-0.0220	0.0028
	-0.0001	-0.0246	0.0009	-0.0002	-0.0303	-0.0001	0.0000	-0.0326	-0.0005
	-0.0005	-0.2791	0.1035	-0.0013	-0.2867	0.1018	-0.0014	-0.2942	0.1037
H_2O	0.0017	0.6161	-0.0134	0.0008	0.6519	-0.0049	-0.0001	0.6617	0.0004
	0.0023	0.6551	-0.0089	-0.0013	0.6735	-0.0043	-0.0012	0.6812	-0.0010
	0.0018	0.6817	-0.0146	0.0024	0.7087	-0.0075	0.0010	0.7249	0.0004
H_2S	0.0039	0.2591	0.0323	0.0018	0.2633	0.0552	0.0007	0.2623	0.0626
	0.0018	0.4204	0.0087	-0.0001	0.4261	0.0292	-0.0003	0.4260	0.0371
	0.0061	0.2496	0.0442	0.0059	0.2416	0.0788	0.0022	0.2355	0.0908
H_4C_2O	-0.0003	-0.0856	-0.0106	0.0003	-0.0903	-0.0116	0.0004	-0.0922	-0.0118
	0.0003	0.0398	-0.0007	0.0002	0.0395	0.0001	0.0002	0.0390	0.0005
	0.0008	0.0200	-0.0140	0.0004	0.0244	-0.0107	0.0002	0.0265	-0.0091
$HC^{15}N$	-0.0005	-0.0776	-0.0013	-0.0004	-0.0823	-0.0055	-0.0001	-0.0832	-0.0060
HCP	0.0001	-0.0309	-0.0011	0.0002	-0.0337	-0.0027	0.0000	-0.0336	-0.0024
HF	0.0003	0.7298	-0.0108	-0.0002	0.7509	-0.0058	-0.0001	0.7596	-0.0018
HFCO	0.0001	-0.0692	0.0045	-0.0002	-0.0729	0.0024	-0.0001	-0.0745	0.0018
	0.0000	-0.0354	-0.0013	0.0001	-0.0364	-0.0017	0.0000	-0.0370	-0.0017
	-0.0003	-0.4019	0.0121	-0.0005	-0.4075	0.0044	-0.0001	-0.4089	0.0042
HOF	0.0000	-0.0899	-0.0049	0.0001	-0.0964	-0.0075	0.0001	-0.1016	-0.0094
	0.0001	-0.0506	-0.0112	0.0002	-0.0523	-0.0117	0.0002	-0.0546	-0.0123
	0.0008	0.6713	-0.0172	-0.0007	0.6885	-0.0105	-0.0006	0.6956	-0.0061
LiF	0.0006	0.0892	-0.0019	-0.0002	0.0743	-0.0036	-0.0002	0.0714	-0.0048
LiH	0.0000	-0.5827	0.0372	0.0000	-0.6580	0.0222	0.0000	-0.6711	0.0189
$^{15}N_2$	-0.0012	-0.2587	0.0234	0.0002	-0.2543	0.0187	0.0001	-0.2518	0.0196
N_2O	0.0000	-0.0663	0.0060	0.0000	-0.0714	0.0038	0.0000	-0.0738	0.0032
NH_3	0.0031	0.5495	-0.0075	0.0009	0.5792	0.0028	-0.0031	0.5881	0.0092
	0.0038	0.4845	0.0023	0.0002	0.5148	0.0120	-0.0006	0.5208	0.0152
O_3	0.0002	-0.0733	-0.0080	0.0001	-0.0747	-0.0093	0.0000	-0.0763	-0.0101
	-0.0292	3.9709	10.6112	-0.0229	2.2549	8.2572	-0.0046	2.0816	7.9728
	-0.0012	0.0780	0.4984	-0.0015	0.0193	0.4138	-0.0005	0.0122	0.4040
OCS	0.0001	-0.0209	0.0038	0.0000	-0.0245	0.0026	-0.0001	-0.0255	0.0024
OF_2	0.0002	-0.0663	-0.0053	0.0001	-0.0665	-0.0064	0.0001	-0.0675	-0.0069
	-0.0002	-0.1691	-0.0375	0.0001	-0.1774	-0.0424	0.0002	-0.1847	-0.0459
	0.0000	-0.0492	-0.0044	0.0001	-0.0514	-0.0056	0.0000	-0.0530	-0.0064
PN	0.0005	-0.2012	0.0462	0.0003	-0.2116	0.0317	0.0001	-0.2119	0.0296
SO_2	0.0001	-0.0723	0.0034	0.0001	-0.0800	0.0023	0.0001	-0.0836	0.0016
	0.0005	-0.6032	0.1773	0.0003	-0.5837	0.1250	0.0001	-0.5706	0.1218
	0.0001	-0.1066	0.0134	0.0000	-0.1098	0.0079	0.0000	-0.1117	0.0073

a) Local error calculated as the difference between the local result and the result with full domains and untruncated pair lists.
b) Correlation effects covered by MP2 calculated as the difference between the GIAO-DF-LMP2 result for full domains including all pairs and the GIAO-DF-HF result.

Table 5.2: Error introduced by the local approximation to rotational g tensors at the level of GIAO-DF-LMP2 for augmented basis sets: the local error, results from calculations with full domains and untruncated pair lists, and the correlation contribution are provided. For all calculations the frozen-core approximation was employed.

Basis	aug-cc-pVDZ			aug-cc-pVTZ			aug-cc-pVQZ		
	$\Delta^{\text{local a)}}$	full	$g_{\text{MP2}}^{\text{correl b)}}$	$\Delta^{\text{local a)}}$	full	$g_{\text{MP2}}^{\text{correl b)}}$	$\Delta^{\text{local a)}}$	full	$g_{\text{MP2}}^{\text{correl b)}}$
AlF	-0.0002	-0.0770	0.0063	0.0001	-0.0782	0.0055	0.0000	-0.0784	0.0055
C_2H_4	0.0018	0.0549	-0.0080	0.0005	0.0548	-0.0065	0.0001	0.0562	-0.0050
	0.0000	-0.1060	0.0061	-0.0001	-0.1103	0.0038	-0.0001	-0.1100	0.0043
	0.0046	-0.3494	-0.0239	0.0018	-0.3655	-0.0322	0.0003	-0.3651	-0.0313
C_3H_4	-0.0002	0.0610	-0.0023	0.0000	0.0607	-0.0019	0.0002	0.0611	-0.0016
	-0.0005	-0.1505	-0.0024	-0.0008	-0.1490	-0.0008	0.0000	-0.1484	-0.0001
	-0.0006	-0.0679	0.0239	-0.0008	-0.0716	0.0220	0.0003	-0.0721	0.0218
CH_2O	0.0006	-0.1030	-0.0373	0.0002	-0.1011	-0.0347	0.0000	-0.0998	-0.0335
	-0.0006	-0.2079	0.0127	-0.0002	-0.2129	0.0096	-0.0001	-0.2129	0.0098
	0.0011	-2.8065	-0.0874	0.0029	-2.8307	-0.1283	0.0003	-2.8273	-0.1251
CH_3F	0.0009	-0.0640	-0.0091	0.0000	-0.0626	-0.0077	0.0001	-0.0624	-0.0074
	0.0071	0.2733	0.0034	-0.0016	0.2779	0.0081	-0.0008	0.2775	0.0094
CH_4	0.0064	0.3356	0.0273	-0.0014	0.3343	0.0299	-0.0005	0.3337	0.0303
CO	-0.0002	-0.2511	0.0277	0.0007	-0.2586	0.0227	0.0002	-0.2595	0.0220
FCCH	-0.0007	-0.0057	-0.0029	-0.0002	-0.0061	-0.0030	0.0000	-0.0061	-0.0029
$FC^{15}N$	-0.0002	-0.0472	0.0000	0.0000	-0.0482	-0.0004	-0.0001	-0.0481	-0.0002
H_2C_2O	-0.0001	-0.0227	0.0021	-0.0001	-0.0228	0.0024	-0.0001	-0.0227	0.0026
	-0.0003	-0.0347	-0.0015	-0.0002	-0.0347	-0.0011	-0.0001	-0.0346	-0.0010
	0.0045	-0.2691	0.1299	0.0006	-0.2941	0.1094	-0.0017	-0.2981	0.1059
H_2O	0.0059	0.6538	-0.0001	0.0012	0.6663	0.0026	0.0009	0.6680	0.0039
	0.0022	0.6914	0.0027	0.0004	0.6837	-0.0003	0.0004	0.6835	0.0002
	0.0070	0.7441	0.0085	0.0033	0.7415	0.0090	0.0013	0.7432	0.0110
H_2S	0.0051	0.2929	0.0523	0.0005	0.2716	0.0621	0.0000	0.2650	0.0652
	0.0008	0.4497	0.0333	-0.0015	0.4346	0.0398	-0.0001	0.4283	0.0406
	0.0120	0.2689	0.0809	0.0030	0.2445	0.0915	0.0011	0.2356	0.0954
H_4C_2O	0.0011	-0.0922	-0.0131	0.0001	-0.0926	-0.0120	0.0001	-0.0924	-0.0117
	0.0004	0.0393	0.0000	0.0002	0.0388	0.0006	0.0001	0.0391	0.0009
	0.0019	0.0265	-0.0114	-0.0004	0.0271	-0.0090	-0.0001	0.0277	-0.0083
$HC^{15}N$	-0.0003	-0.0768	-0.0025	-0.0006	-0.0826	-0.0057	0.0000	-0.0833	-0.0060
HCP	-0.0008	-0.0289	-0.0002	0.0000	-0.0334	-0.0023	-0.0001	-0.0333	-0.0020
HF	0.0015	0.7769	0.0027	0.0011	0.7627	-0.0003	0.0005	0.7644	0.0017
HFCO	-0.0001	-0.0749	0.0017	0.0000	-0.0756	0.0013	0.0000	-0.0756	0.0013
	0.0002	-0.0374	-0.0023	0.0001	-0.0376	-0.0021	0.0001	-0.0374	-0.0019
	0.0003	-0.3994	0.0122	-0.0005	-0.4089	0.0042	-0.0001	-0.4092	0.0045
HOF	0.0007	-0.1071	-0.0107	0.0002	-0.1069	-0.0117	0.0001	-0.1069	-0.0118
	0.0003	-0.0582	-0.0138	0.0002	-0.0577	-0.0136	0.0002	-0.0575	-0.0135
	0.0018	0.7052	-0.0049	0.0013	0.6977	-0.0042	0.0007	0.6980	-0.0031
LiF	-0.0001	0.0714	-0.0066	0.0002	0.0683	-0.0065	0.0000	0.0689	-0.0059
LiH	0.0000	-0.6596	0.0177	0.0000	-0.6754	0.0175	0.0000	-0.6780	0.0169
$^{15}N_2$	-0.0007	-0.2437	0.0261	0.0003	-0.2492	0.0209	0.0001	-0.2489	0.0210
N_2O	-0.0002	-0.0750	0.0028	-0.0002	-0.0763	0.0023	0.0000	-0.0760	0.0026
NH_3	0.0071	0.5819	0.0116	0.0009	0.5891	0.0116	0.0005	0.5903	0.0124
	0.0000	0.5270	0.0195	0.0003	0.5224	0.0154	0.0000	0.5238	0.0166
O_3	0.0006	-0.0800	-0.0120	0.0002	-0.0782	-0.0112	0.0001	-0.0779	-0.0110
	-0.0200	2.4978	8.3889	-0.0323	2.1348	7.9828	-0.0275	2.0806	7.9210
	0.0006	0.0323	0.4280	-0.0015	0.0134	0.4053	-0.0016	0.0112	0.4028
OCS	-0.0001	-0.0251	0.0025	-0.0001	-0.0262	0.0022	-0.0001	-0.0262	0.0022
OF_2	0.0004	-0.0692	-0.0070	0.0002	-0.0686	-0.0074	0.0002	-0.0685	-0.0075
	0.0007	-0.1952	-0.0491	0.0004	-0.1930	-0.0496	0.0002	-0.1927	-0.0498
	0.0002	-0.0547	-0.0067	0.0001	-0.0542	-0.0070	0.0001	-0.0542	-0.0071
PN	0.0002	-0.2003	0.0409	0.0002	-0.2120	0.0308	0.0001	-0.2124	0.0294
SO_2	0.0001	-0.0781	0.0008	0.0002	-0.0830	0.0010	0.0000	-0.0848	0.0011
	0.0024	-0.5893	0.1657	0.0012	-0.5773	0.1275	0.0004	-0.5685	0.1234
	0.0000	-0.1106	0.0095	0.0002	-0.1127	0.0069	0.0000	-0.1129	0.0069

a) Local error calculated as the difference between the local result and the result with full domains and untruncated pair lists.
b) Correlation effects covered by MP2 calculated as the difference between the GIAO-DF-LMP2 result for full domains including all pairs and the GIAO-DF-HF result.

Additionally, Tables 5.3 and 5.4 show statistical measures for the error of the local approximation: root mean square values of the local error, mean absolute percentage errors, maximum relative errors, maximum absolute errors, and root mean square values of the correlation contribution for cc-pVXZ and aug-cc-pVXZ AO basis sets. All values are calculated for the unique elements of the rotational g tensors. Since ozone is a multireference case and hence not accurately described by MP2 the presented errors are considered for all molecules and for the benchmark set excluding ozone.
Root mean square values of the local error are in the range of 0.0010 with slightly larger errors for cc-pVDZ and aug-cc-pVDZ. For larger AO basis sets the local errors become smaller, e.g., 0.0004 for aug-cc-pVQZ. By comparing the root mean square values of the local error and of the correlation contribution, one can see that the local errors account for about 10 % of the correlation contribution in the worst case and are in the range of 1–2 % for augmented and non-augmented VQZ basis sets. Mean absolute percentage errors (MAPEs) of local results compared to full calculations for the molecules of the benchmark set are in the range of 1 % or below for all basis sets which were investigated. MAPE for a set of n_{Mol} molecules is calculated as

$$\mathrm{MAPE} = \frac{1}{n_{\mathrm{Mol}}} \sum_{i=1}^{n_{\mathrm{Mol}}} \left| \frac{g_i^{\mathrm{local}} - g_i^{\mathrm{full}}}{g_i^{\mathrm{full}}} \right| \cdot 100\,\%. \tag{5.29}$$

For some molecules with larger correlation contributions, e.g., for the zz-component of H_4C_2O in cc-pVDZ basis, the relative error may be as large as 4.0 %. For the molecule FCCH in aug-cc-pVDZ AO basis the relative error is larger than 12 %. However, looking at the absolute value the local error is found to be only $\Delta^{\mathrm{local}} = -0.0007$. For larger AO basis sets the relative errors get smaller and are below 1 % for most molecules. This is in good agreement with the expectation that local errors become smaller for larger AO basis sets.
Overall, local errors and correlation contributions of rotational g tensors behave very similarly for augmented and non-augmented AO basis sets in case of the investigated molecules.

Table 5.3: Deviation of rotational g tensors calculated within the local approximation from full calculations for cc-pVXZ (X=D, T, and Q) AO basis sets. Root mean square (R.M.S.) value of the local error, mean absolute percentage error (MAPE), the absolute value of the maximum relative error (MaxRE), the absolute value of the maximum absolute error (MaxAE), and root mean square value of the correlation contribution are provided. For all calculations the frozen-core approximation was employed.

Basis	cc-pVDZ		cc-pVTZ		cc-pVQZ	
Molecules	excl. O_3	all	excl. O_3	all	excl. O_3	all
R.M.S. local error	0.0017	0.0043	0.0011	0.0033	0.0007	0.0009
MAPE	0.6 %	0.6 %	0.4 %	0.5 %	0.2 %	0.3 %
MaxRE	4.0 %	4.0 %	2.4 %	7.7 %	0.9 %	4.1 %
MaxAE	0.0061	0.0292	0.0059	0.0229	0.0031	0.0046
R.M.S. correlation contribution	0.0346	1.4460	0.0339	1.1256	0.0351	1.0869

Table 5.4: Deviation of rotational g tensors calculated within the local approximation from full calculations for aug-cc-pVXZ (X=D, T, and Q) AO basis sets. Root mean square (R.M.S.) value of the local error, mean absolute percentage error (MAPE), the absolute value of the maximum relative error (MaxRE), the absolute value of the maximum absolute error (MaxAE), and root mean square value of the correlation contribution are provided. For all calculations the frozen-core approximation was employed.

Basis	aug-cc-pVDZ		aug-cc-pVTZ		aug-cc-pVQZ	
Molecules	excl. O_3	all	excl. O_3	all	excl. O_3	all
R.M.S. local error	0.0030	0.0040	0.0010	0.0045	0.0004	0.0037
MAPE	1.1 %	1.1 %	0.4 %	0.6 %	0.1 %	0.4 %
MaxRE	12.3 %	12.3 %	3.3 %	11.2 %	0.6 %	14.3 %
MaxAE	0.0120	0.0200	0.0033	0.0323	0.0017	0.0275
R.M.S. correlation contribution	0.0380	1.1437	0.0366	1.0883	0.0362	1.0799

5.3.2 Method errors of HF and LMP2 rotational g tensors

Table 5.5 shows the deviations of rotational g tensors at the levels of HF, LMP2, and LMP2 with full domains and full lists ("LMP2 full") from CCSD(T) / aug-cc-pCV[TQ]Z benchmark values provided in Ref. [45]. For Hartree-Fock the root mean square values of the deviations are in the

range of 0.0300–0.0350, whereas for LMP2 the root mean square values of the deviations are roughly by a factor of ⅓ smaller than the HF values. This finding is also reproduced by the mean absolute percentage errors for HF which are about by a factor of 2 larger than for LMP2. The differences between local and full calculations are small for all investigated basis sets which is in good agreement with the results of Tables 5.3 and 5.4.

Table 5.5: Deviation of rotational g tensors calculated at the levels of HF, LMP2, and LMP2 with full domains and full lists (LMP2 full) from CCSD(T) / aug-cc-pCV[TQ]Z benchmark values [45]. Root mean square (R.M.S.) value of the deviation, the absolute value of the maximum absolute error (MaxAE), the absolute value of the maximum relative error (MaxRE), and the mean absolute percentage error (MAPE) are provided. For all LMP2 calculations the frozen-core approximation was employed.

Method	Basis	R.M.S. deviation	MaxAE	MaxRE	MAPE
HF	cc-pVDZ	0.0348	0.1817	122.6 %	13.4 %
	cc-pVTZ	0.0301	0.1462	75.8 %	10.0 %
	cc-pVQZ	0.0303	0.1583	59.7 %	9.3 %
	aug-cc-pVDZ	0.0331	0.1562	54.8 %	9.0 %
	aug-cc-pVTZ	0.0308	0.1617	50.0 %	8.6 %
	aug-cc-pVQZ	0.0305	0.1619	48.4 %	8.8 %
LMP2 local	cc-pVDZ	0.0308	0.1504	91.9 %	12.3 %
	cc-pVTZ	0.0240	0.1420	35.5 %	6.9 %
	cc-pVQZ	0.0227	0.1344	31.3 %	5.3 %
	aug-cc-pVDZ	0.0322	0.1654	49.2 %	7.2 %
	aug-cc-pVTZ	0.0240	0.1365	31.7 %	4.7 %
	aug-cc-pVQZ	0.0227	0.1302	30.3 %	4.6 %
LMP2 full	cc-pVDZ	0.0308	0.1509	91.9 %	12.3 %
	cc-pVTZ	0.0239	0.1433	35.5 %	6.9 %
	cc-pVQZ	0.0228	0.1358	31.6 %	5.4 %
	aug-cc-pVDZ	0.0305	0.1609	42.8 %	6.9 %
	aug-cc-pVTZ	0.0236	0.1359	31.6 %	4.7 %
	aug-cc-pVQZ	0.0228	0.1319	30.7 %	4.6 %

5.3.3 Density fitting approximation

The influence of the density fitting approximation on the accuracy of rotational g tensors is shown in Appendix B in Tables B.1, B.2, B.3, and B.4 for HF and in Tables B.5 and B.6 for LMP2. Ordinary Gaussians are used

as fitting functions. The calculations were carried out for the same set of benchmark molecules as in Section 5.3.1. Since the description of ozone by HF and MP2 cannot be considered correct the results for this molecule will be omitted in the following discussion. The calculations were done with Dunning's cc-pVXZ and aug-cc-pVXZ (AVXZ) AO basis sets for X=D, T, and Q. The JK- and MP2-fitting basis sets for cc-pVXZ, cc-pV(X+1)Z, and cc-pV(X+2)Z, respectively, the augmented analogues, were used as an auxiliary basis where available. The HF rotational g tensors are compared to the reference values provided in the supplementary material of Ref. [45]; these were calculated with the quantum chemistry package `Dalton` [116].
For HF calculations the error arising from density fitting is very small: the deviations from the reference values are in the range of 10^{-4} or below for augmented and non-augmented basis sets. As for NMR shielding tensors and magnetizabilities the fitting error becomes even smaller for calculations with larger AO basis sets and the corresponding fitting basis set (see Section 4.2.4 for HF magnetizability results). There are larger deviations for LiF and LiH. These can be explained by the following two reasons: (*i*) `MOLPRO` uses the new cc-pVXZ and aug-cc-pVXZ basis sets for Li published in 2011 [115] and (*ii*) the calculations were carried out with the average isotopic mass of Lithium (m(Li)=6.961 u) which differs significantly from the mass of the most abundant isotope (m(^{7}Li)=7.016 u) which is used by `DALTON`. Test calculations with `CFOUR` employing identical basis sets and isotopic masses could show that the results agree with the same accuracy as for the other molecules of the benchmark set.
For LMP2 the deviations are slightly larger: for particular cases with high correlation contributions, e.g., CH_2O within cc-pVDZ AO basis set, the results for cc-pVDZ and cc-pVQZ fitting basis sets differ in the range of 10^{-3}. For molecules with modest correlation contributions and larger AO basis sets the deviations are comparable to the deviations which were found for HF rotational g tensors, i.e., in the range of 10^{-4}. The error becomes even smaller with increasing size of the AO basis set. The fitting errors for

augmented and non-augmented basis sets are equally small.

5.3.4 Additional computational cost

For coronene and the 1@2 tweezer molecule of Section 4.4 rotational g tensors were calculated as well. The values are provided in Tables 4.7 and 4.8. The computational cost for the contraction of the density matrix with an additional integral, Eq. (5.28), and for the nuclear contribution, Eq. (5.27), are negligibly small. For the largest molecule, the 1@2 tweezer with cc-pVTZ AO basis set (2184 basis functions) it takes 5 seconds.

5.4 Conclusions

In this chapter an efficient program for rotational g tensors at the levels of DF-HF and DF-LMP2 has been presented. The calculation of rotational g tensors is based on the paramagnetic part of the magnetizability tensor: additionally, the computationally inexpensive contraction of the unperturbed density matrix with a two-index integral and a nuclear contribution have to be calculated. The connection to magnetizabilities has been formally shown by the ansatz of rotational London atomic orbitals as proposed by Gauss et al.

Density fitting has been introduced in the same way as for magnetizability tensors and NMR shielding tensors by employing ordinary Gaussians as fitting functions. The accuracy of the approach was investigated by test calculations on a benchmark set of 28 small molecules. This ansatz works also very well for rotational g tensors. The errors made are negligibly small for augmented and non-augmented basis sets at the levels of HF and LMP2 and it is not necessary to use a fitting basis set which is nominally larger than the AO basis set, i.e., cc-pVTZ fitting basis sets are sufficient for cc-pVTZ AO basis sets.

For larger AO basis sets the local error is in the range of 1 % of the rota-

tional g tensor. Moreover, comparison with CCSD(T) benchmark calculation showed that LMP2 provides an improvement over rotational g tensors calculated at the HF level.

Chapter 6

SUMMARY

In this thesis new wave function based methods for the calculation of molecular magnetic properties of large molecules have been presented, namely NMR shielding tensors, magnetizability tensors, and rotational g tensors. These new methods were developed at the level of local second-order Møller-Plesset perturbation theory (LMP2) combined with density fitting (DF) and gauge-including atomic orbitals (GIAOs).

The motivation of this work was based on preliminary investigations by J. Gauss and H.-J. Werner [33] who had shown that it appears promising to extend the local correlation scheme to NMR shielding tensors at the level of Møller-Plesset perturbation theory. They had simulated local MP2 shielding tensor calculations on top of a conventional MP2 program and had assessed that the error made by the local approximation is much smaller than the error of the MP2 method itself. Additionally, the author had developed a way to introduce density fitting to the calculation of NMR shielding tensors at the level of Hartree-Fock (HF) in the course of his diploma thesis [52, 68]: ordinary Gaussians can be used as fitting functions since the magnetic properties are calculated in the limit of zero magnetic field strength.

By combining the local correlation approach for MP2 with the density fitting approximation the first efficient implementation of a local wave func-

tion based correlation method for NMR shielding tensors was programmed within the MOLPRO quantum chemistry package [35] (see Chapter 3). This method employs (as most approaches nowadays) gauge-including atomic orbitals [23] to overcome the gauge origin problem. The accuracy of the local approach and of the density fitting approximation were investigated by calculations on a test set of small molecules. Deviations arising from the density fitting approximation are negligibly small. The error made by the local approach is as small as predicted by J. Gauss and H.-J. Werner [33]: for ^{13}C NMR chemical shieldings local results differ typically in the range of 1 ppm from results of full canonical calculations. The performance of the program was analyzed by calculations on a number of extended molecular systems, among them the cyclobutane pyrimidine dimer photolesion with its adjacent nucleobases in the native intrahelical DNA strand (ATTA sequence) and its repaired analogue. The calculation of NMR chemical shifts for this system with 90 atoms and 296 valence electrons took roughly 8 days on 8 CPUs of an AMD Opteron 6180 SE @ 2.50 GHz.

The GIAO-DF-LMP2 program and the GIAO-DF-HF program for NMR shielding tensors were extended to molecular magnetizability tensors and rotational g tensors. The calculation of these two properties requires the derivative (or response) of the wave function parameters with respect to the external magnetic field; these response quantities are also necessary for NMR shielding tensors. For this reason, it was a logical step to work out the formalism and to modify the program for NMR shielding tensors so that it is also able to calculate magnetizabilities and rotational g tensors. Rotational g tensors are closely related to the paramagnetic part of the magnetizablity tensor. The computation of rotational g tensors from a subsequent calculation of magnetizability tensors is computationally very cheap as it only requires the determination of one additional set of two-index integrals and of a nuclear contribution.

The accuracy of the density fitting approximation was evaluated for magnetizablities and rotational g tensors by calculations on a benchmark set of

small molecules [45] at the levels of Hartree-Fock and LMP2. The results are in perfect agreement with the findings for NMR shielding tensors: the error made by the density fitting approximation is negligibly small and it is sufficient to use fitting basis sets with the same cardinal number like the AO basis set. Furthermore, the validity of the local approximation was examined for magnetizability tensors and rotational g tensors within the LMP2 approach. For small molecules the deviations from full canonical calculations are in the range of $1 \cdot 10^{-30}\,\mathrm{JT}^{-2}$ for isotropic magnetizabilities and in the range of 1 % for rotational g tensors. For medium-sized and larger molecules it appears to be reasonable to use extended domains for the calculations of magnetizabilities, especially for augmented AO basis sets. Generally, isotropic magnetizabilities of closed-shell molecules show only small contributions from electron correlation, hence, the absolute error made by the local approximation is still small but the relative error may be larger than for NMR chemical shieldings or rotational g tensors.

The performance of the program was demonstrated by calculations on larger molecular systems, the largest of which had 92 atoms and 262 valence electrons. Magnetizability calculations are typically by a factor of about 1.5 slower than NMR shielding calculations which is caused by additional terms which are not required for NMR shielding tensors.

The here presented methods for molecular magnetic properties which combine density fitting and local correlation methods are a first important step towards efficient wave function based methods for magnetic properties. In future work this scheme could be extended to indirect spin-spin couplings or electronic g tensors for EPR spectra at the level of density fitted local coupled-cluster theory.

Appendix A

SUPPLEMENTARY DATA FOR CHAPTER 4

The following tables were moved from Chapter 4 to this appendix for the sake of readability. They compile the error of the local approximation and the influence of the density fitting approximation on isotropic magnetizabilities at the level of GIAO-DF-LMP2.

Table A.1: Error introduced by the local approximation to isotropic magnetizabilities at the level of GIAO-DF-LMP2: the local error, results from calculations with full domains and untruncated pair lists, and the correlation contribution are provided. For all calculations the frozen-core approximation was employed. All magnetizability values are provided in SI units (10^{-30} JT^{-2}).

Basis	cc-pVDZ			cc-pVTZ			cc-pVQZ		
	$\Delta^{\text{local a)}}$	full	$\bar{\xi}^{\text{correl b)}}_{\text{MP2}}$	$\Delta^{\text{local a)}}$	full	$\bar{\xi}^{\text{correl b)}}_{\text{MP2}}$	$\Delta^{\text{local a)}}$	full	$\bar{\xi}^{\text{correl b)}}_{\text{MP2}}$
AlF	0.39	-410.79	-10.83	0.95	-409.15	-8.20	1.07	-406.06	-6.43
C_2H_4	-1.03	-348.00	0.71	-0.41	-348.86	3.24	-0.30	-349.22	3.98
C_3H_4	-1.34	-492.13	-11.01	-0.80	-487.42	-8.40	-0.54	-485.84	-7.68
CH_2O	0.00	-130.56	3.50	-0.20	-129.88	7.62	-0.03	-130.39	8.23
CH_3F	-1.06	-311.49	3.09	-0.66	-313.22	2.52	-0.35	-314.56	2.07
CH_4	-0.99	-317.37	-5.44	-0.31	-321.21	-6.88	-0.04	-320.82	-7.01
CO	0.09	-211.96	-12.62	-0.06	-214.26	-11.22	-0.03	-214.94	-11.09
FCCH	0.09	-455.73	3.63	0.04	-449.38	5.18	0.06	-447.27	6.05
$FC^{15}N$	0.19	-380.71	0.93	0.32	-375.52	3.14	0.03	-374.37	3.91
H_2C_2O	-0.16	-446.81	-6.12	0.28	-439.54	-3.95	0.15	-437.21	-3.35
H_2O	-0.02	-220.66	-1.76	0.11	-228.62	-3.28	0.16	-232.76	-4.55
H_2S	-0.63	-457.53	-4.39	-0.36	-461.83	-8.32	-0.12	-462.96	-9.45
H_4C_2O	-0.70	-538.34	6.04	-0.52	-538.27	5.29	-0.45	-538.82	4.87
$HC^{15}N$	0.24	-275.62	-0.01	0.17	-275.53	2.91	0.04	-275.85	3.61
HCP	-0.01	-502.36	2.22	-0.23	-501.07	6.09	-0.03	-502.64	7.22
HF	0.01	-165.91	-1.69	0.05	-171.91	-3.11	0.04	-174.96	-4.07
HFCO	0.09	-312.76	-3.63	0.09	-311.88	-1.57	0.03	-312.32	-1.43
HOF	0.01	-240.18	4.56	-0.01	-241.53	3.79	-0.01	-241.08	3.72
LiF	-0.05	-212.38	-10.89	0.67	-201.56	-8.57	0.61	-198.91	-7.52
LiH	0.00	-137.70	-4.68	0.00	-128.48	-2.01	0.00	-126.59	-1.00
$^{15}N_2$	0.61	-200.74	-7.69	0.01	-205.66	-6.26	-0.01	-207.86	-6.82
N_2O	0.09	-357.00	-4.91	0.09	-349.57	-2.68	0.03	-346.84	-2.35
NH_3	-0.36	-277.32	-2.47	0.17	-286.10	-3.95	0.81	-289.81	-5.06
O_3	4.27	-892.05	-1586.76	3.82	-653.13	-1256.10	0.95	-628.99	-1217.01
OCS	-0.24	-610.52	-0.45	0.46	-598.26	2.69	0.06	-595.30	3.72
OF_2	-0.08	-255.81	19.56	-0.16	-253.77	19.73	-0.19	-251.55	20.43
PN	-0.57	-332.81	-44.55	-0.27	-326.77	-30.10	-0.10	-329.01	-27.82
SO_2	-0.32	-338.97	-46.63	-0.20	-332.13	-31.25	-0.09	-331.71	-30.08

a) Local error calculated as the difference between the local result and the result with full domains and untruncated pair lists.
b) Correlation effects covered by MP2 calculated as the difference between the GIAO-DF-LMP2 result for full domains including all pairs and the GIAO-DF-HF result.

Table A.2: Error introduced by the local approximation to isotropic magnetizabilities at the level of GIAO-DF-LMP2 for augmented basis sets: the local error, results from calculations with full domains and untruncated pair lists, and the correlation contribution are provided. For all calculations the frozen-core approximation was employed. All magnetizability values are provided in SI units (10^{-30} JT^{-2}).

Basis	aug-cc-pVDZ			aug-cc-pVTZ			aug-cc-pVQZ		
	$\Delta^{\text{local a)}}$	full	$\bar{\xi}^{\text{correl b)}}_{\text{MP2}}$	$\Delta^{\text{local a)}}$	full	$\bar{\xi}^{\text{correl b)}}_{\text{MP2}}$	$\Delta^{\text{local a)}}$	full	$\bar{\xi}^{\text{correl b)}}_{\text{MP2}}$
AlF	0.44	-414.25	-11.69	-0.13	-408.70	-7.66	-0.06	-406.29	-6.38
C_2H_4	-1.39	-360.06	-1.62	-0.60	-351.87	3.21	-0.14	-351.00	3.73
C_3H_4	0.84	-495.99	-14.52	0.65	-487.91	-9.58	-0.33	-486.07	-8.04
CH_2O	-0.08	-138.29	2.94	-0.15	-132.24	7.49	0.00	-131.47	8.00
CH_3F	-1.37	-320.95	-1.21	0.02	-318.55	0.06	-0.01	-317.24	0.80
CH_4	-1.61	-325.25	-9.80	0.18	-322.23	-8.12	0.05	-321.16	-7.40
CO	0.08	-224.26	-16.98	-0.30	-217.89	-12.95	-0.09	-216.37	-11.87
FCCH	1.46	-454.71	0.83	0.64	-448.32	4.63	-0.08	-446.24	5.95
$FC^{15}N$	0.32	-383.19	-1.12	0.13	-376.18	2.47	0.00	-374.55	3.47
H_2C_2O	0.02	-445.98	-9.75	0.24	-438.29	-5.07	0.21	-436.24	-3.59
H_2O	-0.40	-240.83	-8.82	-0.10	-239.06	-7.61	-0.07	-238.39	-7.11
H_2S	-0.94	-475.85	-13.39	-0.09	-468.20	-11.69	-0.07	-465.47	-10.81
H_4C_2O	-1.83	-550.74	-1.02	-0.18	-543.63	1.63	-0.25	-542.07	2.74
$HC^{15}N$	0.12	-285.17	-2.27	0.25	-278.43	2.08	-0.05	-276.85	3.25
HCP	1.10	-519.28	-2.00	-0.08	-507.32	5.17	0.03	-505.13	6.66
HF	-0.01	-181.04	-6.95	0.01	-178.93	-6.04	0.00	-178.39	-5.72
HFCO	-0.13	-322.72	-7.56	-0.09	-315.43	-3.30	-0.07	-313.86	-2.36
HOF	-0.31	-245.19	0.28	-0.13	-242.47	2.44	-0.08	-241.39	3.19
LiF	0.22	-204.26	-9.29	-0.08	-198.84	-7.48	0.06	-198.27	-7.34
LiH	0.00	-132.64	-3.39	0.00	-127.42	-1.63	0.00	-126.28	-0.96
$^{15}N_2$	0.33	-217.74	-13.43	-0.13	-212.25	-9.16	-0.05	-211.23	-8.41
N_2O	0.47	-354.21	-7.58	0.24	-346.42	-3.27	0.03	-345.28	-2.50
NH_3	-0.59	-297.81	-9.93	-0.14	-295.31	-7.75	-0.08	-294.57	-7.12
O_3	1.19	-700.36	-1288.84	4.66	-640.35	-1222.02	4.33	-631.07	-1212.17
OCS	0.48	-609.57	-4.46	0.12	-596.99	1.89	0.05	-594.50	3.41
OF_2	-0.61	-254.94	16.27	-0.33	-252.58	19.31	-0.26	-251.21	20.32
PN	-0.09	-351.44	-45.30	-0.16	-333.75	-31.44	-0.05	-331.49	-28.69
SO_2	-0.72	-353.93	-49.01	-0.74	-338.03	-34.11	-0.18	-334.28	-31.62

a) Local error calculated as the difference between the local result and the result with full domains and untruncated pair lists.
b) Correlation effects covered by MP2 calculated as the difference between the GIAO-DF-LMP2 result for full domains including all pairs and the GIAO-DF-HF result.

Table A.3: Influence of the fitting basis set on isotropic magnetizabilities at the level of GIAO-DF-LMP2. The ΔVXZ values are provided as the difference between the VXZ value and the value with the largest fitting basis set available for this AO basis, e.g., ΔVDZ=VDZ-VQZ. For all calculations the frozen-core approximation was employed. All magnetizability values are provided in SI units (10^{-30} JT^{-2}).

Basis	VDZ			VTZ			VQZ	
Fitting basis	ΔVDZ	ΔVTZ	VQZ	ΔVTZ	ΔVQZ	V5Z	ΔVQZ	V5Z
AlF	-0.01	0.00	-410.39	0.01	0.00	-408.21	0.00	-404.99
C_2H_4	0.12	0.01	-349.15	0.03	0.01	-349.30	0.01	-349.53
C_3H_4	0.14	0.01	-493.61	0.05	0.01	-488.27	0.01	-486.39
CH_2O	0.16	0.01	-130.72	0.05	0.01	-130.13	0.02	-130.44
CH_3F	0.04	0.00	-312.59	0.00	0.00	-313.88	0.00	-314.91
CH_4	0.06	0.02	-318.42	0.01	0.00	-321.53	0.00	-320.86
CO	0.01	0.00	-211.88	0.01	0.00	-214.33	0.01	-214.98
FCCH	0.00	-0.01	-455.64	0.00	0.00	-449.34	0.01	-447.22
$FC^{15}N$	-0.03	-0.02	-380.49	0.00	0.00	-375.20	0.00	-374.34
H_2C_2O	0.04	0.00	-447.01	0.03	0.00	-439.29	0.01	-437.07
H_2O	0.02	0.00	-220.70	0.00	0.00	-228.51	0.00	-232.60
H_2S	0.07	0.01	-458.23	0.01	-0.01	-462.20	0.00	-463.08
H_4C_2O	0.12	0.01	-539.16	-0.01	-0.01	-538.78	0.00	-539.27
$HC^{15}N$	0.00	-0.01	-275.38	0.01	0.00	-275.37	0.01	-275.82
HCP	0.05	-0.01	-502.42	0.02	0.01	-501.32	0.02	-502.69
HF	0.01	0.00	-165.91	0.00	0.00	-171.86	0.00	-174.92
HFCO	-0.02	-0.02	-312.65	0.01	0.00	-311.80	0.00	-312.29
HOF	0.02	-0.01	-240.19	-0.01	-0.01	-241.53	-0.01	-241.08
LiF	-0.01	0.00	-212.42	-0.01	-0.01	-200.88	-0.01	-198.29
LiH	0.10	0.02	-137.80	0.03	0.01	-128.51	0.01	-126.60
$^{15}N_2$	0.03	0.01	-200.16	0.02	0.00	-205.67	0.01	-207.88
N_2O	0.01	-0.01	-356.92	0.01	0.00	-349.49	0.01	-346.82
NH_3	0.03	0.01	-277.71	0.01	0.00	-285.95	0.00	-289.15
O_3	3.23	0.16	-891.01	0.88	0.15	-650.19	0.36	-628.40
OCS	0.04	0.00	-610.80	0.02	0.01	-597.82	0.02	-595.26
OF_2	0.00	-0.02	-255.89	-0.01	-0.01	-253.92	0.00	-251.74
PN	-0.01	0.00	-333.37	0.02	0.00	-327.06	0.02	-329.13
SO_2	0.11	0.00	-339.40	0.11	0.01	-332.44	0.04	-331.84

Table A.4: Influence of the fitting basis set on isotropic magnetizabilities at the level of GIAO-DF-LMP2 for augmented basis sets. The ΔAVXZ values are provided as the difference between the AVXZ value and the value with the largest fitting basis set available for this AO basis, e.g., ΔAVDZ=AVDZ-AVQZ. For all calculations the frozen-core approximation was employed. All magnetizability values are provided in SI units (10^{-30} JT^{-2}).

Basis	AVDZ			AVTZ			AVQZ	
Fitting basis	ΔAVDZ	ΔAVTZ	AVQZ	ΔAVTZ	ΔAVQZ	AV5Z	ΔAVQZ	AV5Z
AlF	-0.01	0.00	-413.80	0.01	0.00	-408.84	0.00	-406.35
C_2H_4	0.05	0.00	-361.50	0.01	0.00	-352.48	0.01	-351.15
C_3H_4	0.05	0.00	-495.20	0.01	-0.01	-487.27	0.01	-486.41
CH_2O	0.10	0.00	-138.47	0.04	0.01	-132.43	0.01	-131.48
CH_3F	0.01	0.00	-322.33	0.00	0.00	-318.53	0.00	-317.25
CH_4	0.01	0.00	-326.87	0.00	0.00	-322.05	0.00	-321.11
CO	0.02	0.01	-224.20	0.02	0.00	-218.21	0.01	-216.47
FCCH	0.00	0.00	-453.25	-0.01	-0.01	-447.67	0.02	-446.34
$FC^{15}N$	-0.03	-0.01	-382.84	0.00	0.00	-376.05	0.01	-374.56
H_2C_2O	0.01	0.00	-445.97	0.01	0.00	-438.06	0.00	-436.03
H_2O	0.00	0.00	-241.23	-0.01	0.00	-239.15	0.00	-238.46
H_2S	0.01	0.00	-476.80	0.01	0.00	-468.30	0.00	-465.54
H_4C_2O	0.04	0.00	-552.61	0.00	0.00	-543.81	0.00	-542.32
$HC^{15}N$	0.00	0.00	-285.05	0.01	0.00	-278.19	0.00	-276.90
HCP	0.01	0.00	-518.19	0.01	0.00	-507.41	0.01	-505.11
HF	0.00	0.00	-181.05	0.00	0.00	-178.92	-0.01	-178.38
HFCO	-0.01	-0.01	-322.84	0.01	0.00	-315.53	0.00	-313.93
HOF	0.00	0.00	-245.50	0.00	0.00	-242.60	0.00	-241.47
LiF	0.00	0.00	-204.04	-0.01	0.00	-198.91	0.00	-198.21
LiH	0.03	0.00	-132.67	0.01	0.00	-127.43	0.01	-126.29
$^{15}N_2$	0.02	0.00	-217.43	0.01	0.00	-212.39	0.01	-211.29
N_2O	0.04	0.00	-353.78	0.00	0.00	-346.18	0.00	-345.25
NH_3	0.00	0.00	-298.40	0.00	-0.01	-295.45	-0.01	-294.64
O_3	2.61	-0.01	-701.78	0.46	0.05	-636.15	0.13	-626.87
OCS	0.06	0.00	-609.15	0.01	0.01	-596.88	0.00	-594.45
OF_2	-0.03	-0.01	-255.52	0.01	0.00	-252.92	0.01	-251.48
PN	-0.01	0.00	-351.52	0.03	0.00	-333.94	0.02	-331.56
SO_2	0.14	0.00	-354.79	0.10	0.01	-338.87	0.04	-334.50

Appendix B

SUPPLEMENTARY DATA FOR CHAPTER 5

The following tables were moved from Chapter 5 to this appendix for the sake of readability. They compile the influence of the density fitting approximation on the accuracy of rotational g tensors at the levels of Hartree-Fock and LMP2.

Table B.1: Influence of the fitting basis set on rotational g tensors at the level of GIAO-DF-HF for cc-pVDZ and cc-pVTZ AO basis sets. The ΔVXZ values are provided as the difference between the VXZ value and the value with the largest fitting basis set available for this AO basis, e.g., ΔVDZ=VDZ-VQZ.

Basis	VDZ				VTZ			
Fitting basis	ΔVDZ	ΔVTZ	VQZ	Ref.[a)]	ΔVTZ	ΔVQZ	V5Z	Ref.[a)]
AlF	0.0001	0.0000	-0.0824	-0.0824	0.0000	0.0000	-0.0817	-0.0817
C_2H_4	0.0000	0.0000	0.0603	0.0603	0.0000	0.0000	0.0611	0.0611
	0.0000	0.0000	-0.1148	-0.1149	0.0000	0.0000	-0.1143	-0.1144
	0.0001	0.0001	-0.3257	-0.3257	0.0001	0.0000	-0.3293	-0.3293
C_3H_4	-0.0001	0.0000	0.0646	0.0646	0.0000	0.0000	0.0637	0.0637
	0.0001	0.0000	-0.1382	-0.1383	0.0000	0.0000	-0.1443	-0.1444
	0.0000	0.0000	-0.0948	-0.0949	0.0000	0.0000	-0.0940	-0.0941
CH_2O	0.0001	0.0000	-0.0651	-0.0651	0.0000	0.0000	-0.0663	-0.0663
	0.0000	0.0000	-0.2164	-0.2165	0.0000	0.0000	-0.2195	-0.2196
	-0.0001	0.0000	-2.7711	-2.7714	0.0000	0.0000	-2.7179	-2.7183
CH_3F	0.0000	0.0000	-0.0514	-0.0514	0.0000	0.0000	-0.0540	-0.0540
	0.0000	0.0000	0.2520	0.2521	0.0000	0.0000	0.2609	0.2610
CH_4	-0.0001	-0.0001	0.3032	0.3032	0.0000	0.0000	0.3044	0.3045
CO	-0.0001	0.0000	-0.2819	-0.2820	-0.0001	0.0000	-0.2809	-0.2811
FCCH	0.0000	0.0000	0.0014	0.0014	0.0000	0.0000	-0.0015	-0.0015
$FC^{15}N$	0.0000	0.0000	-0.0440	-0.0440	0.0000	0.0000	-0.0465	-0.0465
H_2C_2O	0.0000	0.0000	-0.0220	-0.0220	0.0000	0.0000	-0.0239	-0.0240
	0.0000	0.0000	-0.0255	-0.0255	0.0001	0.0000	-0.0303	-0.0303
	-0.0004	-0.0001	-0.3822	-0.3822	-0.0002	0.0000	-0.3883	-0.3883
H_2O	-0.0001	0.0000	0.6296	0.6297	0.0000	0.0000	0.6568	0.6568
	0.0000	0.0000	0.6640	0.6641	0.0000	0.0000	0.6778	0.6779
	0.0000	0.0000	0.6963	0.6964	0.0000	0.0000	0.7162	0.7163
H_2S	0.0001	0.0000	0.2267	0.2267	0.0000	0.0000	0.2081	0.2081
	0.0002	0.0000	0.4115	0.4116	0.0000	0.0000	0.3969	0.3969
	0.0001	0.0000	0.2053	0.2053	-0.0001	0.0000	0.1629	0.1628
H_4C_2O	0.0000	0.0000	-0.0750	-0.0750	0.0001	0.0001	-0.0788	-0.0788
	0.0000	0.0000	0.0405	0.0406	0.0000	0.0000	0.0394	0.0394
	0.0000	0.0000	0.0340	0.0341	0.0000	0.0000	0.0351	0.0351
$HC^{15}N$	0.0000	0.0000	-0.0763	-0.0763	0.0000	0.0000	-0.0768	-0.0768
HCP	-0.0001	0.0000	-0.0297	-0.0297	0.0000	0.0000	-0.0310	-0.0310
HF	0.0000	0.0000	0.7406	0.7407	0.0000	0.0000	0.7567	0.7568
HFCO	0.0000	0.0000	-0.0737	-0.0737	0.0000	0.0000	-0.0753	-0.0753
	0.0000	0.0000	-0.0341	-0.0341	0.0000	0.0000	-0.0347	-0.0347
	0.0000	0.0000	-0.4140	-0.4141	0.0001	0.0000	-0.4120	-0.4121
HOF	0.0001	0.0001	-0.0851	-0.0851	0.0001	0.0000	-0.0890	-0.0890
	0.0001	0.0000	-0.0395	-0.0395	0.0000	0.0000	-0.0406	-0.0406
	0.0001	0.0000	0.6884	0.6885	0.0000	0.0000	0.6990	0.6991
LiF	0.0000	0.0000	0.0911	0.0889	0.0000	0.0000	0.0779	0.0778
LiH	0.0000	0.0000	-0.6199	-0.6190	0.0000	0.0000	-0.6802	-0.6787
$^{15}N_2$	-0.0001	0.0000	-0.2820	-0.2820	0.0000	0.0000	-0.2730	-0.2730
N_2O	0.0000	0.0000	-0.0723	-0.0723	0.0000	0.0000	-0.0752	-0.0752
NH_3	0.0000	-0.0001	0.5570	0.5572	0.0000	0.0000	0.5764	0.5764
	0.0000	0.0000	0.4822	0.4823	-0.0001	0.0000	0.5029	0.5029
O_3	0.0000	0.0000	-0.0653	-0.0653	0.0000	0.0000	-0.0654	-0.0654
	0.0017	-0.0008	-6.6420	-6.6439	0.0000	0.0002	-6.0023	-6.0041
	-0.0001	0.0000	-0.4203	-0.4204	-0.0001	0.0000	-0.3944	-0.3945
OCS	0.0000	0.0000	-0.0247	-0.0247	0.0000	0.0000	-0.0271	-0.0271
OF_2	0.0000	0.0000	-0.0610	-0.0610	0.0000	0.0000	-0.0601	-0.0601
	0.0001	0.0000	-0.1317	-0.1317	0.0000	0.0000	-0.1350	-0.1350
	0.0001	0.0000	-0.0449	-0.0449	0.0000	0.0000	-0.0458	-0.0458
PN	-0.0003	-0.0001	-0.2471	-0.2472	0.0000	0.0000	-0.2433	-0.2433
SO_2	0.0000	0.0000	-0.0757	-0.0757	0.0000	0.0000	-0.0823	-0.0823
	-0.0011	-0.0001	-0.7794	-0.7804	-0.0005	0.0000	-0.7082	-0.7091
	-0.0001	0.0000	-0.1199	-0.1199	0.0000	0.0000	-0.1177	-0.1177

a) Reference values are taken from conventional HF calculations as provided in Ref. [45].

Table B.2: Influence of the fitting basis set on rotational g tensors at the level of GIAO-DF-HF for the cc-pVQZ AO basis set. The ΔVQZ values are provided as the difference between the VQZ value and the V5Z value, i.e., ΔVQZ=VQZ-V5Z.

Basis	VQZ		
Fitting basis	ΔVQZ	V5Z	Ref.[a)]
AlF	0.0000	-0.0833	-0.0833
C_2H_4	0.0001	0.0610	0.0611
	0.0000	-0.1144	-0.1145
	0.0000	-0.3320	-0.3321
C_3H_4	0.0000	0.0631	0.0631
	0.0000	-0.1467	-0.1468
	0.0000	-0.0941	-0.0941
CH_2O	0.0000	-0.0666	-0.0667
	0.0000	-0.2213	-0.2214
	0.0000	-2.7058	-2.7061
CH_3F	0.0000	-0.0548	-0.0548
	0.0000	0.2640	0.2641
CH_4	0.0000	0.3034	0.3034
CO	0.0000	-0.2814	-0.2815
FCCH	0.0001	-0.0026	-0.0025
$FC^{15}N$	0.0000	-0.0474	-0.0474
H_2C_2O	0.0000	-0.0248	-0.0248
	0.0000	-0.0321	-0.0322
	0.0000	-0.3979	-0.3979
H_2O	0.0000	0.6613	0.6613
	0.0000	0.6822	0.6823
	0.0000	0.7245	0.7246
H_2S	0.0000	0.1997	0.1996
	0.0000	0.3889	0.3889
	0.0000	0.1447	0.1446
H_4C_2O	0.0000	-0.0804	-0.0804
	0.0000	0.0385	0.0385
	0.0000	0.0356	0.0356
$HC^{15}N$	0.0000	-0.0772	-0.0772
HCP	0.0000	-0.0312	-0.0312
HF	0.0000	0.7614	0.7615
HFCO	0.0000	-0.0763	-0.0763
	0.0000	-0.0353	-0.0353
	0.0000	-0.4131	-0.4132
HOF	0.0000	-0.0922	-0.0922
	0.0000	-0.0423	-0.0423
	0.0000	0.7017	0.7018
LiF	0.0000	0.0762	0.0750
LiH	0.0000	-0.6900	-0.6908
$^{15}N_2$	0.0000	-0.2714	-0.2714
N_2O	0.0000	-0.0770	-0.0771
NH_3	0.0000	0.5789	0.5791
	0.0000	0.5056	0.5056
O_3	0.0000	-0.0662	-0.0662
	0.0002	-5.8914	-5.8923
	0.0000	-0.3918	-0.3919
OCS	0.0000	-0.0279	-0.0280
OF_2	0.0000	-0.0606	-0.0606
	0.0000	-0.1388	-0.1388
	0.0000	-0.0466	-0.0466
PN	0.0000	-0.2415	-0.2416
SO_2	0.0000	-0.0852	-0.0853
	0.0000	-0.6924	-0.6932
	0.0000	-0.1190	-0.1190

a) Reference values are taken from conventional HF calculations as provided in Ref. [45].

Table B.3: Influence of the fitting basis set on rotational g tensors at the level of GIAO-DF-HF for AVDZ and AVTZ AO basis sets. The ΔAVXZ values are provided as the difference between the AVXZ value and the value with the largest fitting basis set available for this AO basis, e.g., ΔAVDZ=AVDZ-AVQZ.

Basis	AVDZ				AVTZ			
Fitting basis	ΔAVDZ	ΔAVTZ	AVQZ	Ref.[a)]	ΔAVTZ	ΔAVQZ	AV5Z	Ref.[a)]
AlF	0.0000	0.0000	-0.0833	-0.0833	0.0000	0.0000	-0.0837	-0.0837
C_2H_4	0.0000	0.0000	0.0629	0.0629	0.0000	0.0000	0.0613	0.0613
	0.0000	0.0000	-0.1121	-0.1122	0.0000	0.0000	-0.1141	-0.1141
	0.0000	0.0000	-0.3255	-0.3256	0.0001	0.0000	-0.3334	-0.3334
C_3H_4	0.0000	0.0000	0.0633	0.0634	0.0000	0.0000	0.0626	0.0626
	0.0000	0.0000	-0.1481	-0.1482	0.0000	0.0000	-0.1482	-0.1483
	0.0000	0.0000	-0.0918	-0.0919	0.0000	0.0000	-0.0936	-0.0937
CH_2O	0.0001	0.0000	-0.0658	-0.0658	0.0000	0.0000	-0.0664	-0.0664
	0.0000	0.0000	-0.2206	-0.2207	0.0000	0.0000	-0.2225	-0.2226
	0.0000	0.0001	-2.7191	-2.7194	0.0001	0.0000	-2.7025	-2.7028
CH_3F	0.0000	0.0000	-0.0549	-0.0549	0.0000	0.0000	-0.0549	-0.0549
	0.0000	0.0000	0.2699	0.2699	0.0000	0.0000	0.2698	0.2698
CH_4	0.0000	0.0000	0.3083	0.3084	-0.0001	0.0000	0.3045	0.3045
CO	0.0000	0.0000	-0.2788	-0.2789	-0.0001	0.0000	-0.2812	-0.2814
FCCH	0.0000	0.0000	-0.0028	-0.0028	0.0000	0.0000	-0.0031	-0.0031
$FC^{15}N$	0.0000	0.0000	-0.0472	-0.0472	0.0000	0.0000	-0.0478	-0.0478
H_2C_2O	0.0000	0.0000	-0.0248	-0.0248	0.0000	0.0000	-0.0252	-0.0252
	0.0000	0.0000	-0.0332	-0.0332	0.0000	0.0000	-0.0336	-0.0336
	-0.0003	-0.0001	-0.3987	-0.3987	-0.0002	-0.0001	-0.4033	-0.4034
H_2O	-0.0001	0.0000	0.6540	0.6541	0.0001	0.0001	0.6636	0.6637
	0.0001	0.0000	0.6886	0.6887	0.0000	0.0000	0.6840	0.6841
	0.0001	0.0000	0.7355	0.7356	0.0000	0.0000	0.7325	0.7326
H_2S	0.0000	0.0000	0.2406	0.2406	0.0000	0.0000	0.2095	0.2095
	0.0002	0.0000	0.4162	0.4163	0.0000	0.0000	0.3948	0.3949
	0.0001	0.0000	0.1879	0.1879	-0.0001	0.0000	0.1531	0.1530
H_4C_2O	0.0000	0.0000	-0.0791	-0.0792	0.0000	0.0000	-0.0806	-0.0806
	0.0000	0.0000	0.0393	0.0394	0.0000	0.0000	0.0382	0.0383
	0.0000	0.0000	0.0379	0.0379	0.0000	0.0000	0.0361	0.0361
$HC^{15}N$	0.0000	0.0000	-0.0743	-0.0743	0.0000	0.0000	-0.0769	-0.0769
HCP	0.0000	0.0000	-0.0287	-0.0287	0.0000	0.0000	-0.0311	-0.0311
HF	0.0000	0.0000	0.7742	0.7743	0.0000	0.0000	0.7630	0.7631
HFCO	0.0000	0.0000	-0.0766	-0.0766	0.0000	0.0000	-0.0769	-0.0769
	0.0000	0.0000	-0.0351	-0.0351	0.0000	0.0000	-0.0355	-0.0355
	0.0000	0.0000	-0.4116	-0.4118	0.0000	0.0000	-0.4131	-0.4133
HOF	0.0000	0.0000	-0.0964	-0.0965	0.0000	0.0000	-0.0952	-0.0952
	0.0000	0.0000	-0.0444	-0.0445	0.0000	0.0000	-0.0441	-0.0441
	0.0001	0.0000	0.7100	0.7101	0.0000	0.0000	0.7019	0.7019
LiF	0.0000	0.0000	0.0780	0.0767	0.0000	0.0000	0.0748	0.0734
LiH	0.0000	0.0000	-0.6773	-0.6784	0.0000	0.0000	-0.6929	-0.6946
$^{15}N_2$	-0.0001	-0.0001	-0.2697	-0.2697	0.0000	0.0000	-0.2701	-0.2701
N_2O	0.0000	0.0000	-0.0778	-0.0778	0.0000	0.0000	-0.0786	-0.0787
NH_3	0.0000	0.0000	0.5703	0.5704	0.0000	0.0000	0.5775	0.5776
	0.0000	0.0000	0.5075	0.5076	0.0000	0.0000	0.5070	0.5071
O_3	0.0000	0.0000	-0.0680	-0.0680	0.0000	0.0000	-0.0670	-0.0670
	0.0039	-0.0007	-5.8950	-5.8967	-0.0002	-0.0001	-5.8478	-5.8496
	0.0000	0.0000	-0.3957	-0.3958	-0.0001	0.0000	-0.3918	-0.3919
OCS	0.0000	0.0000	-0.0276	-0.0276	0.0000	0.0000	-0.0284	-0.0284
OF_2	0.0000	0.0000	-0.0622	-0.0622	0.0000	0.0000	-0.0612	-0.0612
	0.0000	0.0000	-0.1461	-0.1461	0.0000	0.0000	-0.1434	-0.1435
	0.0000	0.0000	-0.0480	-0.0480	0.0000	0.0000	-0.0472	-0.0472
PN	-0.0002	0.0000	-0.2410	-0.2411	0.0000	0.0000	-0.2428	-0.2428
SO_2	0.0000	0.0000	-0.0789	-0.0789	0.0000	0.0000	-0.0840	-0.0841
	-0.0009	-0.0001	-0.7541	-0.7552	-0.0004	0.0000	-0.7044	-0.7053
	0.0000	0.0000	-0.1201	-0.1201	0.0000	0.0000	-0.1196	-0.1196

a) Reference values are taken from conventional HF calculations as provided in Ref. [45].

Table B.4: Influence of the fitting basis set on rotational g tensors at the level of GIAO-DF-HF for the AVQZ AO basis set. The ΔAVQZ values are provided as the difference between the AVQZ value and the AV5Z value, i.e., ΔAVQZ=AVQZ-AV5Z.

Basis	AVQZ		
Fitting basis	ΔAVQZ	AV5Z	Ref.[a)]
AlF	0.0000	-0.0839	-0.0839
C_2H_4	0.0000	0.0612	0.0612
	0.0000	-0.1143	-0.1143
	0.0000	-0.3338	-0.3338
C_3H_4	0.0000	0.0627	0.0627
	0.0000	-0.1483	-0.1484
	0.0000	-0.0939	-0.0940
CH_2O	0.0000	-0.0663	-0.0664
	0.0000	-0.2227	-0.2228
	0.0000	-2.7022	-2.7025
CH_3F	0.0000	-0.0550	-0.0550
	0.0000	0.2681	0.2681
CH_4	0.0000	0.3034	0.3034
CO	0.0000	-0.2815	-0.2816
FCCH	0.0000	-0.0032	-0.0032
$FC^{15}N$	0.0000	-0.0479	-0.0479
H_2C_2O	0.0000	-0.0253	-0.0253
	0.0000	-0.0336	-0.0336
	0.0000	-0.4040	-0.4040
H_2O	0.0000	0.6641	0.6642
	0.0000	0.6833	0.6834
	0.0000	0.7322	0.7323
H_2S	0.0000	0.1998	0.1998
	0.0000	0.3877	0.3877
	0.0000	0.1402	0.1401
H_4C_2O	0.0000	-0.0807	-0.0807
	0.0000	0.0382	0.0382
	0.0000	0.0360	0.0360
$HC^{15}N$	0.0000	-0.0773	-0.0773
HCP	0.0000	-0.0313	-0.0313
HF	0.0000	0.7627	0.7628
HFCO	0.0000	-0.0769	-0.0769
	0.0000	-0.0355	-0.0355
	0.0000	-0.4137	-0.4138
HOF	0.0000	-0.0951	-0.0951
	0.0000	-0.0440	-0.0440
	0.0000	0.7011	0.7011
LiF	0.0000	0.0748	0.0734
LiH	0.0000	-0.6949	-0.6962
$^{15}N_2$	0.0000	-0.2699	-0.2699
N_2O	0.0000	-0.0786	-0.0786
NH_3	0.0000	0.5779	0.5780
	0.0000	0.5072	0.5072
O_3	0.0000	-0.0669	-0.0669
	0.0000	-5.8404	-5.8421
	0.0000	-0.3916	-0.3917
OCS	0.0000	-0.0284	-0.0285
OF_2	0.0000	-0.0610	-0.0610
	0.0000	-0.1429	-0.1430
	0.0000	-0.0471	-0.0471
PN	0.0000	-0.2418	-0.2418
SO_2	0.0000	-0.0859	-0.0859
	-0.0001	-0.6918	-0.6927
	0.0000	-0.1198	-0.1199

a) Reference values are taken from conventional HF calculations as provided in Ref. [45].

Table B.5: Influence of the fitting basis set on rotational g tensors at the level of GIAO-DF-LMP2. The ΔVXZ values are provided as the difference between the VXZ value and the value with the largest fitting basis set available for this AO basis, e.g., ΔVDZ=VDZ-VQZ. For all calculations the frozen-core approximation was employed.

Basis	VDZ			VTZ			VQZ	
Fitting basis	ΔVDZ	ΔVTZ	VQZ	ΔVTZ	ΔVQZ	V5Z	ΔVQZ	V5Z
AlF	0.0000	0.0000	-0.0750	0.0000	0.0000	-0.0756	0.0000	-0.0780
C_2H_4	-0.0001	0.0000	0.0545	0.0000	0.0000	0.0559	0.0000	0.0563
	-0.0002	0.0000	-0.1075	-0.0001	0.0000	-0.1102	0.0000	-0.1102
	-0.0004	0.0000	-0.3498	-0.0001	0.0000	-0.3599	0.0000	-0.3628
C_3H_4	-0.0001	0.0000	0.0631	0.0000	0.0000	0.0622	0.0000	0.0616
	-0.0001	0.0000	-0.1386	0.0000	0.0000	-0.1443	0.0000	-0.1461
	-0.0002	-0.0001	-0.0693	-0.0001	0.0000	-0.0718	-0.0001	-0.0720
CH_2O	-0.0001	0.0000	-0.1011	0.0000	0.0000	-0.0998	0.0000	-0.0998
	-0.0001	0.0000	-0.1981	-0.0001	0.0000	-0.2075	0.0000	-0.2105
	-0.0023	-0.0001	-2.8330	-0.0008	-0.0002	-2.8337	-0.0002	-2.8271
CH_3F	0.0000	0.0000	-0.0580	0.0000	0.0000	-0.0607	0.0000	-0.0616
	-0.0002	-0.0001	0.2417	0.0000	0.0000	0.2618	-0.0001	0.2698
CH_4	-0.0003	-0.0001	0.3249	-0.0001	0.0000	0.3325	0.0000	0.3329
CO	-0.0001	0.0000	-0.2556	-0.0001	0.0000	-0.2587	0.0000	-0.2596
FCCH	0.0000	0.0000	-0.0005	0.0000	0.0000	-0.0040	0.0000	-0.0052
$FC^{15}N$	0.0000	0.0000	-0.0421	0.0000	0.0000	-0.0462	0.0000	-0.0474
H_2C_2O	0.0000	0.0000	-0.0184	0.0000	0.0000	-0.0213	-0.0001	-0.0220
	-0.0001	0.0000	-0.0246	0.0000	0.0000	-0.0305	0.0000	-0.0326
	0.0000	0.0000	-0.2796	0.0000	0.0000	-0.2880	0.0000	-0.2956
H_2O	-0.0002	0.0000	0.6180	-0.0001	0.0000	0.6528	0.0000	0.6616
	-0.0001	0.0000	0.6575	0.0000	0.0000	0.6722	-0.0001	0.6801
	-0.0001	0.0000	0.6836	0.0000	0.0001	0.7111	0.0000	0.7259
H_2S	-0.0003	0.0000	0.2633	-0.0001	0.0000	0.2652	0.0000	0.2630
	-0.0003	0.0000	0.4225	-0.0002	0.0000	0.4262	0.0000	0.4257
	-0.0007	-0.0001	0.2564	-0.0002	0.0000	0.2477	0.0000	0.2377
H_4C_2O	-0.0001	0.0000	-0.0858	0.0000	0.0000	-0.0900	0.0000	-0.0918
	-0.0001	0.0000	0.0402	0.0000	0.0000	0.0397	0.0000	0.0392
	-0.0001	0.0000	0.0209	0.0000	0.0000	0.0248	0.0000	0.0267
$HC^{15}N$	-0.0001	0.0000	-0.0780	-0.0001	0.0000	-0.0826	0.0000	-0.0833
HCP	0.0000	0.0000	-0.0308	0.0000	0.0000	-0.0335	0.0000	-0.0336
HF	-0.0001	0.0000	0.7302	-0.0001	0.0000	0.7508	0.0000	0.7595
HFCO	0.0000	0.0000	-0.0691	0.0000	0.0000	-0.0731	0.0000	-0.0746
	0.0000	0.0000	-0.0354	0.0000	0.0000	-0.0363	0.0000	-0.0370
	-0.0002	0.0000	-0.4020	0.0000	0.0000	-0.4080	-0.0001	-0.4089
HOF	-0.0001	0.0000	-0.0898	0.0000	0.0000	-0.0963	0.0000	-0.1015
	-0.0001	0.0000	-0.0504	0.0000	0.0000	-0.0521	0.0000	-0.0544
	0.0000	0.0000	0.6721	-0.0001	0.0000	0.6879	0.0000	0.6950
LiF	0.0000	0.0000	0.0898	0.0000	0.0000	0.0741	0.0000	0.0712
LiH	-0.0004	-0.0001	-0.5823	-0.0001	-0.0001	-0.6579	-0.0001	-0.6710
$^{15}N_2$	-0.0001	-0.0001	-0.2598	-0.0001	0.0000	-0.2540	0.0000	-0.2517
N_2O	0.0000	0.0000	-0.0663	0.0000	0.0000	-0.0714	0.0000	-0.0738
NH_3	-0.0003	-0.0001	0.5529	-0.0001	0.0000	0.5802	0.0000	0.5850
	-0.0001	0.0000	0.4884	0.0000	0.0000	0.5150	0.0000	0.5202
O_3	0.0000	0.0000	-0.0731	0.0000	0.0000	-0.0746	0.0000	-0.0763
	-0.0258	-0.0018	3.9675	-0.0074	-0.0013	2.2394	-0.0028	2.0798
	-0.0005	0.0000	0.0773	-0.0001	0.0000	0.0179	-0.0001	0.0118
OCS	0.0000	0.0000	-0.0208	0.0000	0.0000	-0.0245	0.0000	-0.0256
OF_2	0.0000	0.0000	-0.0661	0.0000	0.0000	-0.0664	0.0000	-0.0674
	0.0000	0.0000	-0.1693	-0.0001	0.0000	-0.1772	0.0000	-0.1845
	0.0000	0.0000	-0.0492	0.0000	0.0000	-0.0513	0.0000	-0.0530
PN	-0.0001	0.0000	-0.2006	0.0000	0.0000	-0.2113	0.0000	-0.2118
SO_2	0.0000	0.0000	-0.0722	0.0000	0.0000	-0.0799	0.0000	-0.0835
	-0.0010	-0.0002	-0.6017	-0.0004	-0.0001	-0.5830	-0.0002	-0.5703
	0.0000	0.0000	-0.1065	-0.0001	0.0000	-0.1097	0.0000	-0.1117

Table B.6: Influence of the fitting basis set on rotational g tensors at the level of GIAO-DF-LMP2 for augmented basis sets. The ΔAVXZ values are provided as the difference between the AVXZ value and the value with the largest fitting basis set available for this AO basis, e.g., ΔAVDZ=AVDZ-AVQZ. For all calculations the frozen-core approximation was employed.

Basis	AVDZ			AVTZ			AVQZ	
Fitting basis	ΔAVDZ	ΔAVTZ	AVQZ	ΔAVTZ	ΔAVQZ	AV5Z	ΔAVQZ	AV5Z
AlF	0.0000	0.0000	-0.0772	0.0000	0.0000	-0.0781	0.0000	-0.0784
C_2H_4	-0.0001	0.0000	0.0568	0.0000	0.0000	0.0553	0.0000	0.0563
	-0.0001	0.0000	-0.1059	-0.0001	0.0000	-0.1103	0.0000	-0.1101
	-0.0002	0.0000	-0.3446	0.0000	0.0000	-0.3637	0.0000	-0.3648
C_3H_4	0.0000	0.0000	0.0608	0.0000	0.0000	0.0607	0.0000	0.0613
	-0.0001	0.0000	-0.1509	-0.0001	0.0000	-0.1497	0.0000	-0.1484
	-0.0001	0.0000	-0.0684	0.0000	0.0000	-0.0724	0.0000	-0.0718
CH_2O	-0.0001	0.0000	-0.1023	0.0000	0.0000	-0.1009	0.0000	-0.0998
	0.0000	0.0000	-0.2085	-0.0001	0.0000	-0.2130	0.0000	-0.2130
	-0.0019	-0.0001	-2.8035	-0.0007	-0.0001	-2.8271	-0.0002	-2.8268
CH_3F	0.0000	0.0000	-0.0631	-0.0001	0.0000	-0.0625	0.0000	-0.0623
	-0.0001	0.0000	0.2805	-0.0001	0.0000	0.2764	0.0000	0.2767
CH_4	-0.0001	0.0000	0.3421	0.0000	0.0000	0.3329	0.0000	0.3332
CO	-0.0001	0.0000	-0.2512	-0.0001	0.0000	-0.2578	0.0000	-0.2593
FCCH	0.0000	0.0000	-0.0064	0.0000	0.0000	-0.0063	0.0000	-0.0061
$FC^{15}N$	0.0000	0.0000	-0.0474	0.0000	0.0000	-0.0482	0.0000	-0.0481
H_2C_2O	-0.0001	0.0000	-0.0227	0.0000	0.0000	-0.0229	0.0000	-0.0228
	-0.0001	0.0000	-0.0349	0.0000	0.0000	-0.0349	0.0000	-0.0347
	0.0001	-0.0001	-0.2647	0.0000	0.0000	-0.2935	0.0000	-0.2998
H_2O	0.0000	0.0000	0.6597	0.0000	0.0000	0.6675	0.0000	0.6689
	0.0000	0.0000	0.6936	0.0000	0.0000	0.6841	-0.0001	0.6840
	0.0000	0.0000	0.7511	0.0000	0.0000	0.7448	0.0000	0.7445
H_2S	0.0000	0.0000	0.2980	0.0000	0.0000	0.2721	-0.0001	0.2651
	0.0000	0.0000	0.4505	-0.0001	0.0000	0.4332	-0.0001	0.4283
	-0.0002	0.0000	0.2811	-0.0001	0.0000	0.2476	0.0000	0.2367
H_4C_2O	0.0000	0.0000	-0.0911	0.0000	0.0000	-0.0925	0.0000	-0.0923
	-0.0001	0.0000	0.0398	0.0000	0.0000	0.0390	0.0000	0.0392
	0.0000	0.0000	0.0284	0.0000	0.0000	0.0267	0.0000	0.0276
$HC^{15}N$	0.0000	0.0000	-0.0771	-0.0001	0.0000	-0.0831	0.0000	-0.0833
HCP	0.0000	0.0000	-0.0297	0.0000	0.0000	-0.0334	0.0000	-0.0334
HF	0.0000	0.0000	0.7784	0.0000	0.0000	0.7638	0.0000	0.7649
HFCO	0.0000	0.0000	-0.0750	0.0000	0.0000	-0.0756	0.0000	-0.0756
	0.0000	0.0000	-0.0372	0.0000	0.0000	-0.0375	0.0000	-0.0373
	-0.0001	0.0000	-0.3990	-0.0001	0.0000	-0.4093	0.0000	-0.4093
HOF	0.0000	0.0000	-0.1064	0.0000	0.0000	-0.1067	0.0000	-0.1068
	0.0000	0.0000	-0.0579	0.0000	0.0000	-0.0575	0.0000	-0.0573
	0.0000	0.0000	0.7070	0.0000	0.0000	0.6990	0.0000	0.6987
LiF	0.0000	0.0000	0.0713	0.0000	0.0000	0.0685	0.0000	0.0689
LiH	-0.0001	0.0000	-0.6595	-0.0001	-0.0001	-0.6753	0.0000	-0.6780
$^{15}N_2$	0.0000	0.0000	-0.2444	-0.0001	-0.0001	-0.2488	0.0000	-0.2488
N_2O	0.0000	0.0000	-0.0752	0.0000	0.0000	-0.0765	0.0000	-0.0760
NH_3	-0.0001	0.0000	0.5891	0.0000	0.0000	0.5900	0.0000	0.5908
	0.0001	0.0000	0.5269	0.0000	0.0001	0.5227	0.0000	0.5238
O_3	-0.0001	0.0000	-0.0793	0.0000	0.0000	-0.0780	0.0000	-0.0778
	-0.0209	0.0000	2.4987	-0.0036	-0.0003	2.1061	-0.0009	2.0540
	-0.0004	0.0000	0.0333	-0.0001	0.0000	0.0120	-0.0001	0.0097
OCS	0.0000	0.0000	-0.0252	0.0000	0.0000	-0.0263	0.0000	-0.0263
OF_2	0.0000	0.0000	-0.0688	0.0000	0.0000	-0.0684	0.0000	-0.0683
	0.0000	0.0000	-0.1945	0.0000	0.0000	-0.1926	0.0000	-0.1925
	0.0000	0.0000	-0.0545	0.0000	0.0000	-0.0541	0.0000	-0.0541
PN	0.0000	0.0000	-0.2001	0.0000	0.0000	-0.2118	0.0000	-0.2123
SO_2	0.0000	0.0000	-0.0780	0.0000	0.0000	-0.0828	0.0000	-0.0848
	-0.0009	-0.0001	-0.5860	-0.0004	-0.0001	-0.5757	-0.0001	-0.5680
	0.0000	0.0000	-0.1106	0.0000	0.0000	-0.1125	0.0000	-0.1129

Appendix C

GLOSSARY

α	Fine Structure Contant, $\alpha = 7.29735257 \cdot 10^{-3}$
aug-cc-pVXZ	Augmented cc-pVXZ Basis Set
AO	Atomic Orbital
AVXZ	Augmented cc-pVXZ Basis Set
c	Speed of Light
CC	Coupled-cluster
CCSD	Coupled-cluster Singles Doubles
CCSD(T)	CCSD with Perturbative Triples
cc-pVXZ	Correlation-Consistent Valence X-tuple Zeta Basis Set
CPHF	Coupled-Perturbed Hartree-Fock
CPD	Cyclobutane Pyrimidine Dimer Lesion
CPL	Coupled-Perturbed Localization
DMABN	4-(Dimethylamino)benzonitrile
DF	Density Fitting
DF-HF	Density Fitted Hartree-Fock
DF-LMP2	Density Fitted Local MP2
DNA	Deoxyribonucleic Acid
DFT	Density-Functional Theory
EPR	Electron Paramagnetic Resonance
ERI	Electron Repulsion Integral
FC	Fitting Coefficient
FF	Fitting Function
GIAO	Gauge-Including Atomic Orbital
GPT	Gaussian Product Theorem
HF	Hartree-Fock
i	Imaginary Unit

IGLO	Individual Gauge for Localized Orbitals
I/O	Input and Output
LMO	Localized Molecular Orbital
LORG	Localized Orbital / Local Origin
μ_B	Bohr Magneton
μ_N	Nuclear Magneton
MAPE	Mean Absolute Percentage Error
MaxAE	Maximum Absolute Error
MaxRE	Maximum Relative Error
MCSCF	Multi-Configurational Self-Consistent Field
MO	Molecular Orbital
MP2	Møller-Plesset Perturbation Theory in Second Order
NMR	Nuclear Magnetic Resonance
PAO	Projected Atomic Orbital
ppm	Parts per Million
R.H.S.	Right-Hand Side
R.M.S.	Root Mean Square
TMS	Tetramethylsilane
TpT	Repaired Analogue of CPD with Pyrimidine
Z-CPHF	Z-Vector Coupled-Perturbed Hartree-Fock
Z-CPL	Z-Vector Coupled-Perturbed Localization

BIBLIOGRAPHY

[1] A.E. Derome. *Modern NMR Techniques for Chemistry Research*. Pergamon Press, (1987).

[2] P. Hodgkinson. volume 72 of *Annual Reports on NMR Spectroscopy*, page 185. Academic Press, (2011).

[3] K. Wüthrich. *Nat.Struct.Biol.*, **8**, 923, (2001).

[4] M. Drescher. *Chemie in unserer Zeit*, **46**, 150, (2012).

[5] M. Kaupp, M. Bühl, and V.G. Malkin, editors. *Calculation of NMR and EPR Parameters*. Wiley-VCH, (2004).

[6] O. Christiansen, P. Jørgensen, and C. Hättig. *Int.J.Quantum Chem.*, **68**, 1, (1998).

[7] P. Pulay. *Mol.Phys.*, **17**, 197, (1969).

[8] K. Thomsen and P. Swanstrøm. *Mol.Phys.*, **26**, 735, (1973).

[9] A.P. Scott and L. Radom. *J.Phys.Chem.*, **100**, 16502, (1996).

[10] M. Schütz, G. Hetzer, and H.-J. Werner. *J. Chem. Phys.*, **111**, 5691, (1999).

[11] M. Schütz and H.-J. Werner. *J.Chem.Phys.*, **114**, 661, (2001).

[12] M. Schütz. *J.Chem.Phys.*, **113**, 9986, (2000).

[13] M. Schütz. *J.Chem.Phys.*, **116**, 8772, (2002).

[14] M. Schütz and F.R. Manby. *Phys.Chem.Chem.Phys.*, **5**, 3349, (2003).

[15] H.-J. Werner, F.R. Manby, and P.J. Knowles. *J.Chem.Phys.*, **118**, 8149, (2003).

[16] T.B. Adler, H.-J. Werner, and F.R. Manby. *J.Chem.Phys.*, **130**, 054106, (2009).

[17] M. Schütz, H.-J. Werner, R. Lindh, and F.R. Manby. *J.Chem.Phys.*, **121**, 737, (2004).

[18] D. Kats, T. Korona, and M. Schütz. *J.Chem.Phys.*, **125**, 104106, (2006).

[19] D. Kats, T. Korona, and M. Schütz. *J.Chem.Phys.*, **127**, 064107, (2007).

[20] D. Kats and M. Schütz. *J.Chem.Phys.*, **131**, 124117, (2009).

[21] K. Freundorfer, D. Kats, T. Korona, and M. Schütz. *J.Chem.Phys.*, **133**, 244110, (2010).

[22] K. Ledermüller, D. Kats, and M. Schütz. *J.Chem.Phys.*, **139**, 084111, (2013).

[23] F. London. *J.Phys.Radium*, **8**, 397, (1937).

[24] K. Ruud, T. Helgaker, R. Kobayashi, P. Jørgensen, K.L. Bak, and H.J.A. Jensen. *J.Chem.Phys.*, **100**, 8178, (1994).

[25] J. Gauss. *Chem.Phys.Lett.*, **191**, 614, (1992).

[26] J. Gauss. *Chem.Phys.Lett.*, **229**, 198, (1994).

[27] J. Gauss and J.F. Stanton. *J.Chem.Phys.*, **104**, 2574, (1996).

[28] J. Gauss and J.F. Stanton. *J.Chem.Phys.*, **102**, 251, (1995).

[29] J. Gauss. *J.Chem.Phys.*, **116**, 4773, (2002).

[30] M. Kállay and J. Gauss. *J.Chem.Phys.*, **120**, 6841, (2004).

[31] M. Kollwitz, M. Häser, and J. Gauss. *J.Chem.Phys.*, **108**, 8295, (1998).

[32] M. Kollwitz and J. Gauss. *Chem.Phys.Lett.*, **260**, 639, (1996).

[33] J. Gauss and H.-J. Werner. *Phys.Chem.Chem.Phys.*, **2**, 2083, (2000).

[34] C. Møller and M.S. Plesset. *Phys.Rev.*, **46**, 618, (1934).

[35] S. Loibl and M. Schütz. *J.Chem.Phys.*, **137**, 084107, (2012).

[36] E.J. Baerends, D.E. Ellis, and P. Ros. *Chem.Phys.*, **2**, 41, (1973).

[37] J.L. Whitten. *J.Chem.Phys.*, **58**, 4496, (1973).

[38] B.I. Dunlap, J.W.D. Connolly, and J.R. Sabin. *J.Chem.Phys.*, **71**, 3396, (1979).

[39] M. Feyereisen, G. Fitzgerald, and A. Komornicki. *Chem.Phys.Lett.*, **208**, 359, (1993).

[40] F. Weigend and M. Häser. *Theor.Chim.Acta*, **97**, 331, (1997).

[41] F. Weigend, M. Häser, H. Patzelt, and R. Ahlrichs. *Chem.Phys.Lett.*, **294**, 143, (1998).

[42] T. Helgaker, S. Coriani, P. Jørgensen, K. Kristensen, J. Olsen, and K. Ruud. *Chem.Rev.*, **112**, 543, (2012).

[43] *Green Book, IUPAC Quantities, Units and Symbols in Physical Chemistry*. Blackwell Scientific Publication, Oxford, 2nd edition edition, (1993).

[44] K. Ruud, H. Skaane, T. Helgaker, K. L. Bak, and P. Jørgensen. *J.Am.Chem.Soc.*, **116**, 10135, (1994).

[45] O. B. Lutnæs, A. M. Teale, T. Helgaker, D. J. Tozer, K. Ruud, and J. Gauss. *J.Chem.Phys.*, **131**, 144104, (2009).

[46] N.F. Ramsey. *Molecular beams*. Oxford University Press, (1956).

[47] W.H. Flygare. *Chem.Rev.*, **74**, 653, (1974).

[48] W.H. Flygare. *Molecular Structure and Dynamics*. Prentice-Hall, (1978).

[49] H.-J. Werner, P.J. Knowles, G. Knizia, F.R. Manby, and M. Schütz. *Comput.Mol.Sci.*, **2**, 242, (2012).

[50] H.-J. Werner, P.J. Knowles, G.Knizia, F.R. Manby, M. Schütz, P. Celani, T. Korona, R. Lindh, A. Mitrushenkov, G. Rauhut, K.R. Shamasundar, T.B. Adler, R.D. Amos, A. Bernhardsson, A. Berning, D.L. Cooper, M.J.O. Deegan, A.J. Dobbyn, F. Eckert, E. Goll, C. Hampel, A. Hesselmann, G. Hetzer, T. Hrenar, G. Jansen, C. Köppl, Y. Liu, A.W. Lloyd, R.A. Mata, A.J. May, S.J. McNicholas, W. Meyer, M.E. Mura, A.Nicklass, D.P. O'Neill, P. Palmieri, D. Peng, K. Pflüger, R. Pitzer, M. Reiher, T. Shiozaki, H. Stoll, A.J. Stone, R. Tarroni, T. Thorsteinsson, and M. Wang. Molpro, version 2012.1, a package of ab initio programs, (2012). see `http://www.molpro.net`.

[51] T. Helgaker, M. Jaszuński, and K. Ruud. *Chem.Rev.*, **99**, 293, (1999).

[52] S. Loibl. *Development of new Ab Initio Methods for the Calculation of Molecular Magnetic Properties*. Diplomarbeit, Regensburg, (2009).

[53] M. Schütz. Linear scaling methods in electron correlation theories. Presented in Mariapfarr, Austria, (2003).

[54] H.-J. Werner. *Methods in Quantum Chemistry: Analytical energy gradients*. Lecture Notes, unpublished, Stuttgart, (SS 2003).

[55] M. Schindler and W. Kutzelnigg. *J.Chem.Phys.*, **76**, 1919, (1982).

[56] U. Meier, C. van Wüllen, and M. Schindler. *J.Comput.Chem.*, **13**, 551, (1992).

[57] W. Kutzelnigg. *J.Mol.Struct.*, **202**, 11, (1989).

[58] K. Woliński, J. F. Hinton, and P. Pulay. *J. Am. Chem. Soc.*, **112**, 8251, (1990).

[59] T. Helgaker and P. Jørgensen. *J.Chem.Phys.*, **95**, 2595, (1991).

[60] J.W. Boughton and P. Pulay. *J.Comput.Chem.*, **14**, 736, (1993).

[61] P. Pulay. *Chem.Phys.Lett.*, **100**, 151, (1983).

[62] H.-J. Werner P. Knowles, M. Schütz. Ab initio methods for electron correlation in molecules. In J. Grotendorst, editor, *Modern Methods and Algorithms of Quantum Chemistry*, number 3 in NIC Series, page 130. John von Neumann Institute for Computing (NIC), (2000).

[63] J. Pipek and P.G. Mezey. *J.Chem.Phys.*, **90**, 4916, (1989).

[64] S.F. Boys. Localized orbitals and localized adjustment functions. In P.-O. Löwdin, editor, *Quantum Theory of Atoms, Molecules, and the Solid State: A Tribute to John C. Slater*. Academic Press, New York, (1966).

[65] S.F. Boys. *Rev.Mod.Phys.*, **32**, 296, (1960).

[66] F. Jensen. *Introduction to Computational Chemistry*. Wiley-VCH, (2007).

[67] B.I. Dunlap. *Phys.Chem.Chem.Phys.*, **2**, 2113, (2000).

[68] S. Loibl, F.R. Manby, and M. Schütz. *Mol.Phys.*, **108**, 477, (2010).

[69] J. Gauss. Molecular properties. In J. Grotendorst, editor, *Modern Methods and Algorithms of Quantum Chemistry*, number 3 in NIC Series, page 541. John von Neumann Institute for Computing (NIC), (2000).

[70] A.E. Hansen and T.D. Bouman. *J.Chem.Phys.*, **82**, 5035, (1985).

[71] R. Ditchfield. *Mol.Phys.*, **27**, 789, (1974).

[72] K. Ruud, T. Helgaker, K. L. Bak, P. Jørgensen, and H. J. A. Jensen. *J. Chem. Phys.*, **99**, 3847, (1993).

[73] C. van Wüllen. *J. Chem. Phys.*, **102**, 2806, (1995).

[74] C. Ochsenfeld, J. Kussmann, and F. Koziol. *Angew. Chem. Int. Ed.*, **43**, 4485, (2004).

[75] M. Beer and C. Ochsenfeld. *J. Chem. Phys.*, **128**, 221102, (2008).

[76] M. Beer, J. Kussmann, and C. Ochsenfeld. *J. Chem. Phys.*, **134**, 074102, (2011).

[77] M. Maurer and C. Ochsenfeld. *J. Chem. Phys.*, **138**, 174104, (2013).

[78] J. Gauss. *J. Chem. Phys.*, **99**, 3629, (1993).

[79] K. Sadeghian, M. Bocola, and M. Schütz. *Chem. Phys. Chem*, **12**, 1251, (2011).

[80] H.-J. Werner and M. Schütz. *J. Chem. Phys.*, **135**, 144116, (2011).

[81] R. M. Stevens, R. M. Pitzer, and W. N. Lipscomb. *J. Chem. Phys.*, **38**, 550, (1963).

[82] J. Gerratt and I. M. Mills. *J. Chem. Phys.*, **49**, 1719, (1968).

[83] J. A. Pople, R. Krishnan, H. B. Schlegel, and J. S. Binkley. *Int. J. Quantum Chem.*, **16**, 225 (S13), (1979).

[84] CFOUR, a quantum chemical program package written by J.F. Stanton, J. Gauss, M.E. Harding, P.G. Szalay with contributions from A. A. Auer, R. J. Bartlett, U. Benedikt, C. Berger, D. E. Bernholdt, Y. J. Bomble, L. Cheng, O. Christiansen, M. Heckert, O. Heun, C. Huber, T.-C. Jagau, D. Jonsson, J. Jusélius, K. Klein, W. J. Lauderdale, D. A. Matthews, T. Metzroth, L. A. Mück, D. P. O'Neill, D. R. Price, E. Prochnow, C. Puzzarini, K. Ruud, F. Schiffmann, W. Schwalbach, S.

Stopkowicz, A. Tajti, J. Vàzquez, F. Wang, J. D. Watts and the integral packages MOLECULE (J. Almlöf and P. R. Taylor), PROPS (P. R. Taylor), ABACUS (T. Helgaker, H. J. Aa. Jensen, P. Jørgensen, and J. Olsen) and ECP routines by A. V. Mitin and C. van Wüllen. For the current version, see `http://www.cfour.de`.

[85] A.K. Jameson and C.J. Jameson. *Chem. Phys. Lett.*, **134**, 461, (1987).

[86] T.H. Dunning, Jr. *J. Chem. Phys.*, **90**, 1007, (1989).

[87] R.A. Kendall, T.H. Dunning, Jr., and R.J. Harrison. *J. Chem. Phys.*, **96**, 6796, (1992).

[88] D.E. Woon and T.H. Dunning, Jr. *J. Chem. Phys.*, **98**, 1358, (1993).

[89] D.E. Woon and T.H. Dunning, Jr. *J. Chem. Phys.*, **100**, 2975, (1994).

[90] D.E. Woon and T.H. Dunning, Jr. *J. Chem. Phys.*, **103**, 4572, (1995).

[91] T.H. Dunning, Jr. and P.J. Hay. In H.F. Schaefer III, editor, *Methods of electronic structure theory*, volume 2. Plenum Press, (1977).

[92] F. Weigend. *Phys. Chem. Chem. Phys.*, **4**, 4285, (2002).

[93] F. Weigend, A. Köhn, and C. Hättig. *J. Chem. Phys.*, **116**, 3175, (2002).

[94] H.-J. Werner and P.J. Knowles. Molpro, users manual, version 2012.1, (2012). see `https://www.molpro.net/info/2012.1/doc/manual.pdf`.

[95] C. Ochsenfeld. *Phys. Chem. Chem. Phys.*, **2**, 2153, (2000).

[96] S.P. Brown, T. Schaller, U.P. Seelbach, F. Koziol, C. Ochsenfeld, F.G. Klärner, and H.W. Spiess. *Angew. Chem. Int. Edit.*, **40**, 717, (2001).

[97] J. Gauss, K. Ruud, and T. Helgaker. *J. Chem. Phys.*, **105**, 2804, (1996).

[98] P. Pulay, J. F. Hinton, and K. Woliński. In J. A. Tossell, editor, *Nuclear Magnetic Shieldings and Moleculare Structure*, page 243. Kluwer Academic Publishers, (1993).

[99] K. Ruud and T. Helgaker. *Chem. Phys. Lett.*, **264**, 17, (1997).

[100] J. Olsen, K. L. Bak, K. Ruud, T. Helgaker, and P. Jørgensen. *Theor. Chim. Acta*, **90**, 421, (1995).

[101] M. Krykunov and J. Autschbach. *J. Chem. Phys.*, **123**, 114103, (2005).

[102] M. Krykunov and J. Autschbach. *J. Chem. Phys.*, **126**, 024101, (2007).

[103] P. Lazzeretti, M. Malagoli, and R. Zanasi. *Chem. Phys. Lett.*, **220**, 299, (1994).

[104] S. Coriani, P. Lazzeretti, M. Malagoli, and R. Zanasi. *Theor. Chim. Acta*, **89**, 181, (1994).

[105] A. Ligabue, S. P. A. Sauer, and P. Lazzeretti. *J. Chem. Phys.*, **118**, 6830, (2003).

[106] H.F. Hameka. *Mol. Phys.*, **1**, 203, (1958).

[107] H.F. Hameka. *Z. Naturforsch., Teil A*, **14**, 599, (1959).

[108] H.F. Hameka. *Rev. Mod. Phys.*, **34**, 87, (1962).

[109] D. J. D. Wilson, C. E. Mohn, and T. Helgaker. *J. Chem. Theory Comput.*, **1**, 877, (2005).

[110] K. Ruud, T. Helgaker, K.L. Bak, P. Jørgensen, and J. Olsen. *Chem. Phys*, **195**, 157, (1995).

[111] J. Gauss, K. Ruud, and M. Kállay. *J. Chem. Phys.*, **127**, 074101, (2007).

[112] S.M. Cybulski and DM. Bishop. *J. Chem. Phys.*, **100**, 2019, (1994).

[113] S. P. A. Sauer, T. Enevoldsen, and J. Oddershede. *J. Chem. Phys.*, **98**, 9748, (1993).

[114] S. Obara and A. Saika. *J. Chem. Phys.*, **84**, 3963, (1986).

[115] B. Prascher, D. E. Woon, K.A. Peterson, T. H. Dunning, Jr., and A. K. Wilson. *Theor. Chim. Acta*, **128**, 69, (2011).

[116] Dalton, release 2.0, (2005). See `http://www.kjemi.uio.no/software/dalton/dalton.html`.

[117] Justin T. Fermann. The gaussian product theorem, (1996). See `http://www.uam.es/docencia/quimcursos/Docs/Knowledge/Fundamental_Theory/ints/node4.html`.

[118] I. A. Aucar, S. S. Gómez, M. C. Ruiz de Azúa, and C. G. Giribet. *J. Chem. Phys.*, **136**, 204119, (2012).

[119] E. Malkin, S. Komorovsky, M. Repisky, TB. Demissie, and K. Ruud. *J. Phys. Chem. Lett.*, **4**, 459, (2013).

[120] Y. Xiao and W. Liu. *J. Chem. Phys.*, **138**, 134104, (2013).

[121] S. P. A. Sauer, V. Špirko, and J. Oddershede. *Chem. Phys*, **153**, 189, (1991).

[122] S. P. A. Sauer, J. Oddershede, and J. Geertsen. *Mol. Phys.*, **76**, 445, (1992).

[123] S.P.A. Sauer and J.F. Ogilvie. *J. Phys. Chem.*, **98**, 8617, (1994).

[124] S.P.A. Sauer. *Chem. Phys. Lett.*, **260**, 271, (1996).

[125] J.F. Ogilvie, J. Oddershede, and S.P.A. Sauer. *Adv. Chem. Phys.*, **111**, 475, (2000).

[126] S.P.A. Sauer. *Adv. Quantum Chem.*, **48**, 469, (2005).

[127] S.P.A. Sauer. *J.Chem.Phys.*, **133**, 171101, (2010).

[128] K. Ruud, T. Helgaker, and P. Jørgensen. *J. Chem. Phys.*, **107**, 10599, (1997).